Investigations of the Thermal Properties of Human and Animal Tissues

Gavin Hamilton

Department of Physics and Astronomy
University of Glasgow

Presented for the degree of Doctor of Philosophy
to the University of Glasgow
September 1998

This thesis is dedicated to:

My Mum and Dad.

Declaration.

This thesis has been composed by the undersigned. It has not been accepted in any previous application for a degree. The work of which it is a record has been done by myself, unless indicated otherwise in the text. I further state that no part of this has already been or is being concurrently submitted for any such degree or qualification at any other university.

Gavin Hamilton.

Acknowledgements.

This work was carried out whilst I was a student in the Department of Physics and Astronomy at the University of Glasgow, and in receipt of a research studentship grant as part of the Robertson Trust award for the development of microwave thermography.

The author would also like to express his sincere appreciation of the following people:

Dr D.V. Land, my supervisor and initiator of this research, who constructed the experimental probes, sent us to some nice conferences in pleasant locations, and provided helpful advice.

Dr Andrew James Gorton and Dr Patrick Charles Harrison, who I have suffered in tandem with, and who proved to be good colleagues and damn fine friends.

Alan And Gavin of the Royal Infirmary Mortuary, and Robert and Patricia of the Western Infirmary Mortuary, who were so helpful in providing the specimens of human tissue.

Dr H. Ward, my second supervisor.

Alan Seath and all the technical staff associated with the group.

My brothers Stuart and Andrew, and my twin sister Gail, for all their encouragement.

Mr Glen, my physics teacher in school, who started me down this long path.

Shirley, a good drinking buddy.

All the other people who have kept me going through the years, either in person or through e-mail.

Finally, special thanks must go to my mum and dad, who have provided support and encouragement throughout the years.

Table of Contents.

Summary.

Definitions.

Summary.

The work presented in this thesis was carried as part of a project to improve the analysis of clinical data obtained by microwave thermography. For microwave thermography measurements to be usefully interpreted for detecting thermal anomalies in the human body at depths of up to several centimetres, the thermal and microwave dielectric properties of tissues must be known. This thesis is mainly concerned with the measurement and interpretation of the values of the thermal conductivity and diffusivity of human and animal tissues.

The thermal properties of biological tissue are required, in conjunction with a bio-heat equation, to allow the formation of computational models to simulate the temperature distribution inside the human body. These computational models are also useful in the analysis of tomographic temperature measurements, and are essential to ensure accurate heating in hyperthermia. The Pennes conventional bio-heat equation has proven to be successful in analysing the data produced by microwave thermography.

The thermal properties of biological soft tissue are dependant on the tissue water content. Water is a major constituent of most soft biological tissues, and it has a higher thermal conductivity and thermal diffusivity than any other constituent of biological tissue. The thermal properties of biological tissue can be modelled using a mixture equation, which describes the behaviour of a two phase system in terms of the thermal properties of the individual constituents and their relative volume fractions. This allows the variation of the thermal properties of biological tissue with water content to be analysed.

A self-heating thermistor probe system was used in this study to measure the *in-vitro* thermal conductivity and thermal diffusivity of a wide variety of human and animal tissues. The system was calibrated using glycerol and agar-gelled water since the thermal behaviour of these materials and mixtures of these materials was well known. The calibration data was examined to determine the accuracy of the calibration and to determine if there was a relationship between the observed thermal conductivity and thermal diffusivity which was generated by the measurement system.

The thermal conductivity and thermal diffusivity of a wide range of human and animal tissues was measured. In collaboration with a colleague, the microwave complex

permittivity of tissue samples was also measured to investigate the relationship between the thermal and dielectric properties. The water content of the tissue samples was measured by dehydration.

First the results were analysed by tissue type. The distribution of measurements of the thermal conductivity, diffusivity, and water content were examined for each of the individual tissue types. The measured values for these three quantities were compared against each other to try to establish relationships between the quantities. The measured properties were also compared to values for the same tissues collected from published work. There was little literature data available for some of the tissue types, and that which was available showed considerable differences in the thermal properties quoted.

The measured values collected from animal tissues where compared to those from human tissue of the same type. Generally the human tissue had higher water content, possibly due to the blood in the animal tissues being drained. This usually gave human tissue higher thermal conductivity and thermal diffusivity than the same type of animal tissue. Human tissue also showed greater variation in the results, due to the "poorer quality" of the human tissues available as postmortem samples.

The mean values of the thermal properties for all the main tissues were also examined. When the relationship between the thermal conductivity and thermal diffusivity was examined, a linear correlation became clear between the thermal conductivity and ρc_p, where ρ is the density and c_p is specific heat capacity. The variation in the thermal conductivity and thermal diffusivity with water content was also analysed using mixture equations, and this showed that the thermal properties of the non-water fraction were slightly different in each tissue type. This was also apparent when the mean thermal conductivity and diffusivity were compared to the mean dielectric constant. The variation in the thermal properties of the non-water fraction of each of tissue types is believed to cause the data to deviate from the fitted mean relationship. Finally, the thermal conductivity was compared to the microwave power attenuation constant. It was found that there was not a distinct relationship between these quantities. This was due to variations in the electrolyte concentration, the amount of water binding to protein molecules, and the thermal properties of the non-water fraction.

Definitions.

This thesis is primarily concerned with the measurement and analysis of the thermal conductivity and thermal diffusivity of biological materials.

The thermal conductivity determines the rate of heat propagation under steady state conditions. The transfer of heat through conduction under time invariant conditions is proportional to the temperature gradient, which is the rate of change of temperature with distance. In the one dimensional case, the heat flow per unit area, q, in the x direction is given by

$$q = -k\frac{dT}{dx}$$

where T is the temperature and k is the thermal conductivity. The units of the thermal conductivity are $Wm^{-1}K^{-1}$.

The thermal diffusivity determines the rate of heat propagation in transient state processes. The non steady state thermal behaviour of a uniform material with no internal sources of heat is given by the following equation

$$\rho c_p \frac{dT}{dt} = k\nabla^2 T$$

where ρ is the density, c_p is the specific heat at constant pressure and t is the time. This can be rewritten

$$\frac{dT}{dt} = \alpha\nabla^2 T \qquad \alpha = \frac{k}{\rho c_p}$$

It was Lord Kelvin here at the University of Glasgow who first called α the thermal diffusivity. This is because the above equation has the form common to all diffusion equations and the units of the thermal diffusivity are m^2s^{-1} which are the units of diffusion coefficients.

Chapter 1: Microwave Radiometry.

1.1 Introduction.

In this chapter, the need for accurate data on the thermal properties of tissues is established with relation to microwave thermography and hyperthermia induction. The basic principles of hyperthermia are discussed and the various methods which have been used to measure the skin and internal temperature of the body are examined. Microwave thermography is then examined in detail, with the relationship between the microwave signal and the temperature and dielectric properties being discussed.

1.2 Microwave Thermography.

Microwave thermography is the technique of measuring tissue temperatures of the human body by detection of the thermally generated microwave radiation which is naturally emitted by body tissues.

At any temperature above absolute zero, objects radiate energy in the form of electromagnetic waves. This is due to the thermally induced agitation of the particles of the object. At microwave frequencies it is found that the spectral intensity of this thermal radiation is a linear function of temperature of the body. Microwave radiation can penetrate distances of several centimetres through biological tissues and hence part of the radiation generated from within the body will reach the surface where it can be detected.

Medical conditions which cause changes in the vascularity of, or the metabolism in, tissue result in a variation of the local temperature of the area affected. Microwave thermography can provide a useful clinical tool for the detection and monitoring of such affected sites. Examples of such temperature rises are seen in the joints affected by arthritis (Ring, 1990, 1995; Kelso, 1995) and in the "hot-spots" associated with many breast cancers (Myers et al, 1980; Brown, 1989; Boquet et al, 1990). The advantage of microwave thermography for the detection of such diseases is that a scan may be taken passively and non-invasively which provides the clinician with novel physiological

information. The technique is also simple to apply and reasonably independent of environmental influence.

Typical equipment for measuring microwave thermal signals, and hence the body's temperature, consists of an antenna linked by a coaxial cable to a radiometer receiver. The antenna, which is often a dielectrically loaded waveguide section, is placed on the surface of the skin. Radiation from the body couples with the antenna and a signal is transmitted to the radiometer which measures its intensity. The radiometer converts the signal to an equivalent Celsius temperature which can be displayed digitally, or recorded by a computer connected to the radiometer and displayed as colour coded temperature pattern at a later time. Apparatus such as this has been used by the Glasgow group as well as other medical application research groups (e.g. Barrett et al, 1980; Abdul-Razzak et al, 1987; Fraser et al, 1987; Kelso, 1995).

The antenna intentionally picks up a broad band of the microwave thermal signals. A Dicke type radiometer (Harvey, 1963) is used to process the signals, amplifying the desired frequency components and discarding all others. The resulting signal displayed is an 'effective microwave temperature' which is a weighted mean of the temperature distribution over all points in the volume viewed by the radiometer.

For microwave thermography to fulfil its potential, and for it to be widely used as a clinical tool, it is important that a full understanding is gained of the factors which affect the microwave signal seen by the antenna. This can only be achieved if theoretical-computational models are produced which predict the behaviour of the signal generation process, with respect to the properties of the volume of tissue of the body under examination. For any such model to be produced, it is essential that both the thermal and the microwave properties of the body tissues are adequately known. It is with the measurement and values of the thermal properties of body tissues for this modelling that this work is primarily concerned.

1.3 Hyperthermia.

The most general definition of hyperthermia is a therapy in which tissue temperature is elevated above normal by external means. In the modern era hyperthermia has come to

mean the treatment of cancer tumours by the process of heating regions of the body containing carcinoma tissue.

It has been shown that cancer cells are more sensitive to heat than normal healthy cells. This has promoted the investigation for use of hyperthermia as a stand alone cancer technique. However hyperthermia has demonstrated most success when it used in conjunction with other cancer treatment techniques. In both radiotherapy and chemotherapy, there is increasing evidence that hyperthermia has an additional effect of making cancer cells more susceptible to these treatments (Storm, 1983).

Clearly for hyperthermia to be used effectively, the thermal properties of biological tissues must be known in order to accurately predict heat diffusion and temperature patterns and allow the target region to be held close to the required temperature for delivery of an appropriate treatment regime.

1.3.1 Local and Systemic Hyperthermia.

In systemic, or total body, hyperthermia, the temperature of the whole body is raised. This can be achieved using Radio Frequency (RF) heating or a water bath. For systemic hyperthermia, the maximum temperature is usually between 41.8°C and 42°C.

Recent research has concentrated more on local hyperthermia. This involves delivery of heat to a specific part of the body. If the volume being treated does not include a sensitive organ, such as the heart or liver, temperatures higher than those associated with systemic hyperthermia can be used. Normally local hyperthermia involves heating a volume of tissue to between 42°C and 45°C. Local hyperthermia is safer than systemic hyperthermia since the risks associated with maintaining the whole body temperature at such high levels for a long period of time are removed in local hyperthermia (Storm, 1983; Hand and James, 1986).

1.3.2 Interstitial Techniques in Local Hyperthermia.

One of the main requirements for local hyperthermia treatment is to produce a non-invasive system which will consistently produce therapeutic temperatures in tumour volumes without overheating normal tissue. Current non-invasive systems have difficulty

achieving this, and there may be tumour sites where this will never be achieved, so invasive or interstitial techniques must be considered along with non-invasive techniques (Strohbehn and Mechling, 1986; Johnson et al, 1995).

Interstitial hyperthermia involves inserting the heat sources into the tumour volume. Coaxial microwave antenna arrays or RF needle electrodes are amongst the invasive techniques used to heat tumour tissue. In RF needle systems, an array of electrodes is inserted into the tumour volume to ohmically heat the tissue, while thin coaxial antennas, of diameter 1-2 mm, have been designed for microwave heating. The temperature rise produced is monitored by invasive thermometers and power is varied to produce an even temperature rise across the tumour. While these invasive methods allow for more accurate heating of the tumour than non-invasive systems, there is always the danger and discomfort associated with placing foreign objects in the human body (Atkinson, 1983; Strohbehn and Mechling, 1986).

1.3.3 Non-invasive Techniques in Local Hyperthermia.

There are three main techniques for non-invasive local hyperthermia: radio frequency, ultrasound and microwave heating.

In radio frequency heating, RF currents pass through well insulated flexible wire arranged in coils. This produces an oscillating magnetic field which produces currents in the tissue volume, heating the tissue. Frequencies in the range 20-30 MHz are used. When attempting to heat deep seated tumours, surface cooling is required to prevent damage to the skin (Hand et al, 1982; Jain, 1983).

Ultrasound has been investigated for use in local hyperthermia because it can be focused to heat very small volumes of tissue. It appears well suited for producing sustainable, uniform hyperthermia in tumours up to 5 cm below the surface in tissue volumes which do not contain bone or air. Ultrasound can not penetrate gas spaces and the high absorption coefficient of bone compared to other biological materials gives rise to high temperatures and pain. Also at high power there is the danger of tissue damage due to cavitation (Atkinson, 1983; Swindell, 1986).

In microwave heating, radiation is applied using a contact microstrip applicator or a dielectrically loaded waveguide. Frequencies between 300-1000 MHz are generally

used. Microwaves are more applicable for the heating of larger volumes of tissues than ultrasound. Attempts have been made to focus the heating by using more than one applicator but, so far, only limited success has been achieved. Microwaves may permit heating of volumes of tissue which are inaccessible to ultrasound (Hand, 1995; Johnson, 1995).

1.4 Biomedical Thermometry.

Measuring the temperature of the human body is an important clinical tool in establishing the status of a patient's response to disease. Regional temperature variations, though known to exist, have not been much exploited as an aid to disease detection and diagnosis. Accurate internal tissue temperature measurement is also required to monitor hyperthermia treatment.

By far the most common temperature value taken in a clinical environment is the general body or core temperature which is estimated from an oral temperature measurement taken with a thermometer. The association with disease and temperature can be traced to the earliest records in Western medicine. But it was not until the middle of the 19th century that Carl Wuderlich realised the advantages of using a thermometer in a clinical environment. He discovered that clinical temperatures taken using a thermometer are precise, objective measurements, and that such measurements are simple to obtain and give information about the human body's response to disease (Ring, 1993).

The body's thermoregulatory system is efficient at keeping the core temperature constant. In a healthy individual there are only small variations due to various biological cycles. However the core temperature will increase in the presence of disease or injury. This rise in temperature is not caused by the disease, but by the body's natural response to the presence of the disease. Certain cells, when fighting disease, release agents into the blood which will, when they reach the brain, cause the core temperature to be raised. This raised value now becomes the norm around which the thermoregulatory system works. Once the illness is defeated the core temperature will fall back to normal. Hence changes in the core temperature give information about the progress of disease. The normal core temperature is roughly 37°C, it being dangerous if the core temperature rises above 41°C or falls below 35°C (Lipton, 1985).

However, measuring the core temperature gives no information about local variations within the human body, and other methods are required to gain information relating to temperature patterns within the body.

1.5 Skin Temperature Measurement Techniques.

The skin temperature is dependant on both environmental and internal factors. The body loses heat through the skin by convection, radiation and evaporation (sweating). Any change in the rate of heat loss will result in a change in the skin temperature. This means that the skin temperature is affected by factors such as air temperature, rate of air flow across the body and the presence of moisture on the skin. Heat loss from the skin will be discussed in greater detail in chapter 2.

Since skin temperature is variable, steps must be taken to ensure reproducibility. The patient must partially disrobe and sit in a controlled environment for a fixed time. Normally the patient has to sit for 10-15 minutes in a room at an air temperature of 20°C (Ring 1995). There are a variety of skin temperature measurement techniques, possessing various advantages and disadvantages.

1.5.1 Contact Probes.

A variety of thermistor and thermocouple probes are available for point measurements of skin temperature (Cetas, 1985). These must be placed in contact with the skin and so may affect the heat flow at the skin surface and hence the skin temperature being measured. The temperature of the probe depends on its thermal resistance to the environment and the thermal resistance of the skin, which may be very variable. This process does not provide a overall picture of the local temperature variations in the area being measured unless a large number of measurements are made, which is extremely time consuming.

1.5.2 Liquid Crystal Thermography.

This technique makes use of liquid crystal compounds which exhibit colour-temperature sensitivity. Initially this procedure was carried out by applying the liquid crystal mixture to skin painted black. This procedure was of little use in most clinical investigations and liquid crystal plate thermography was developed as a more acceptable alternative.

In liquid crystal plate thermography, a thin, blackened sheet, containing liquid crystals encapsulated in a polymer matrix, is applied firmly and uniformly against the surface being examined. The resultant pattern produced can then be photographed to obtain a permanent record of the thermal image.

This system has many of the drawbacks of contact probes since it is also a contact method. The sheet may also fail to make proper contact with the skin or the pressure applied by the sheet may affect the blood circulation just below the skin, either of which would give an incorrect temperature pattern. Also the range of temperatures observed by each plate is limited to about 3°C, so more than one plate may be needed to observe the full temperature pattern. Despite these drawbacks, this is cheap and reasonably effective system and it has been used to investigate thermal patterns in the female breast and spinal root compression (Jones, 1982, 1987; Ring, 1993).

1.5.3 Infra-Red Thermography.

Infra-red thermography is a non-contact method of determining the skin temperature. The infra-red detector is placed in front of the area of interest and the skin surface is imaged by the detector. The resulting thermal image is usual displayed in the form of a colour picture on a monitor and the image can be stored on digital media for future reference. Scanning speeds range from roughly one to fifty frames per second depending on the imaging system. A thermal resolution of 0.2°C is common for limited temperature ranges. This technique is more accurate than liquid crystal plate thermography, but it is also more expensive.

There are two groups of detectors used in infra-red thermography: thermal and photon detectors. Although there are many different types of thermal detector, the only thermal detector still in clinical use is the pyroelectric detector. Electrically the detector behaves

as a capacitor on which an electric charge appears when it is exposed to a change in radiance. The magnitude of this effect depends on the rate of temperature change in the detector, thus the sensor does not respond to a steady flux of radiation. A pyroelectric detector is either used as a single detector, which will give a temperature at a point, or in an array of such detectors to produce a thermograph.

Photon detectors use the photoelectric effect to detect the infra-red signals from the human body. In order for the system to be able to distinguish the external signal from the detector's own thermal noise, it must be cooled to cryogenic temperatures. Photon detectors are more accurate than the pyroelectric devices. Most commercial systems designed for use in clinical environments use photon detectors (Jones, 1982, 1987; Ring 1990).

However the skin temperature tells us little about the internal temperature patterns within the body, such as would be required for the monitoring of hyperthermia. Temperature patterns produced deep within the body are swamped by the temperature patterns produced by the blood vessel network near the skins surface (Land, 1987). Other techniques must be used to detect internal temperatures within the human body.

1.6 Internal Tissue Temperature Measurement Techniques.

For an internal temperature measurement technique to be useful in a clinical situation, it should have a number of desirable characteristics. The system must be accurate with a small temperature resolution, reasonable spatial resolution and be capable of a fast response time. Similar requirements are required for both tumour detection and hyperthermia monitoring. In the case of hyperthermia, trials suggest that a temperature resolution and accuracy of approaching 0.1°C is required, along with a spatial resolution of about 1 cm, and a response time of the order of a second over a temperature range of 35°C to 45°C (Christensen, 1983). Currently there are no non-invasive methods which can fulfil the criteria required for hyperthermia (Struabe and Arthur, 1994).

1.6.1 Invasive Techniques.

The temperature at a point inside the human body can be determined by inserting a thin temperature probe, such as a thermistor or a thermocouple, into the tissue. This is still the most reliable method of determining the internal temperature with quick response times and good temperature resolution. Spatial resolution is limited by the degree of invasion which is acceptable for a patient. A spatial resolution of about 1 cm is common when examining small volumes of tissue (Hand and James, 1986).

Clearly, invasive techniques are limited by the discomfort the temperature probes produce in a patient and the danger of damage to the tissue. A non-invasive technique suffers from none of these drawbacks and would be preferable. There are a number of non-invasive measurement techniques currently under investigation.

1.6.2 Applied Potential Tomography.

Applied potential tomography or electrical impedance tomography identifies temperature changes in tissue by measurement of electrical resistivity variations. An array of electrodes are placed on the skin surface. A alternating current signal, generally between 10-50 KHz, is applied and the subsequent potential distributions are recorded at each electrode site. The image is then reconstructed and compared with previous images to see if there is any variation in electrical resistivity of the tissues. A linear relationship between the resistivity and temperature is assumed so that temperature changes between images can be determined. For the present state of development, this method can measure the temperature change to an accuracy of ~ 1.5°C though errors > 5°C are common. Spatial resolution is determined by the number of electrodes and the circular array diameter. (Conway et al, 1985; Moskowitz et al, 1994).

1.6.3 Microwave Tomography.

Microwave tomography reconstructs the dielectric properties of a body illuminated with microwaves, from measurement of the scattered fields. Radiation is applied to one side of the region under investigation, where it is scattered and attenuated as it propagates

through the tissue. The resulting radial distribution is detected in both amplitude and phase and is used to reconstruct a 2-D model of the volume under consideration. Further scans will show a change in temperature being reflected in a change in the microwave properties of the tissue. The change in the microwave dielectric properties of biological tissues are due to the change in water permittivity present in tissues with temperature. This means the change in the microwave properties are dependant on the water content as well as the temperature change.

Many of the considerations of microwave thermography apply in microwave tomography. Most tomographic systems use frequencies similar to those used in thermographic systems, though some systems may use lower frequencies, sacrificing spatial resolution for deeper penetration into the tissue. At microwave frequencies the spatial resolution is approximately half a wavelength of the radiation in tissue. The temperature resolution will be determined by the accuracy of the measurement of the microwave properties and how well the relationship between the microwave properties and temperature is defined. For example, a prototype system (Broquetas et al, 1991) operating at 2.45 GHz has a useful scan diameter of 20 cm with a spatial resolution of 8 mm. The temperature resolution is 0.5°C in water though this figure will be poorer in biological tissues.

Microwave Tomography still has a number of obstacles to over overcome. The main problem is determining the absolute temperature calibration. Biological tissues can have water contents which are less than 10% of the total mass to greater than 80% of the total mass. This makes it difficult to be sure of the water content and the absolute dielectric properties of the tissues present. Also the most systems are still generating significant spatial artefacts due to the limits of the systems computing algorithms (Pichot et al, 1985; Jofre et al, 1990; Martin et al, 1991).

1.6.4 Ultrasonic Methods.

Many acoustic properties of biological tissue are dependent on the temperature of the tissue and several ultrasonic techniques make use of this when determining the internal temperature. One technique relies on measuring the backscattered signal from an insonified volume of tissue. The temperature dependence of the backscattered signal can

be used to identify the temperature of the volume being sonically illuminated (Straube and Arthur, 1993).

However, the ultrasonic method under most investigation for use as a non-invasive temperature measurement technique is ultrasound tomography. The basic technique is similar to microwave tomography with ultrasound replacing microwaves. The ultrasound scanner can produce images of variations in the attenuation or in the speed of propagation. For temperature mapping, it is reconstruction using speed of propagation that is generally off interest (Christensen, 1983). However ultrasound tomography has some serious drawbacks. It cannot be used where bone or gas filled structures are present. This has meant that the breast region has become a favourite site for tomography (Harris et al, 1991, Hamamoto et al, 1995).

1.6.5 Other Methods.

There are a number of other methods which are currently in clinical use and have been considered for non-invasive internal temperature measurement. X-ray computed tomography has been investigated using the change in attenuation of the x-rays with temperature to produce an map of the internal temperature of the body. But this method is expensive and there is an element of risk to the patient (Hand and James, 1986).

Nuclear Magnetic Resonance (NMR) imaging, which is also known as Magnetic Resonance Imaging (MRI), gives a 3-D display of the distribution of water protons. This method has been considered as a temperature measurement technique because the nuclear magnetic relaxation time is dependant on temperature. However the relation time is also dependant on the water content of the tissues and the state of which the water exists. This is an expensive method with a poor temperature resolution of only about 2°C (Parker, 1984).

1.7 Microwave Radiometry: Thermal Radiation Emission from the Human Body.

A 'black body' is an object which is a perfect absorber of radiation. It is also a perfect emitter of radiation since the power radiated by a black body in thermal equilibrium must

be equal to the power absorbed. The radiation in the range $\nu \rightarrow \nu + d\nu$ depends only on the absolute temperature, T, and is given by Planck's Law:

$$B_V(T)d\nu = \frac{2h\nu^3}{c^2\left(e^{\frac{h\nu}{k_B T}} - 1\right)}d\nu \qquad (1.7.1)$$

where $B_\nu(T)d\nu$ is the power emitted per unit surface area, into unit solid angle in the frequency range $d\nu$. h is Planck's constant, c is the velocity of light and k_B is Boltzmann's constant.

Figure 1.1 shows the intensity spectrum for a Black Body at a temperature of 300K, which is approximately that of a human body. The peak intensity occurs at 3 x 10^{13} Hz (~10 μm) in the infra-red region. While no body is a perfect black body, for the range of frequencies used by infra red thermography, 6 x 10^{12} Hz to 7.5 x 10^{13} Hz, the human skin has a high emissivity of about 0.98 and hence its behaviour is very close to that of a black body (Jones, 1987). But at microwave thermography frequencies of ~3 GHz (~10 cm), the human body no longer behaves as a black body.

1.7.1 The Equation of Transfer.

In the case of a real body, the thermal radiation can be given by the 'Equation of Transfer' (Chandrasekhar, 1939, 1950)

$$\frac{dI_\nu}{dz} = j_\nu \rho - \kappa_\nu \rho I_\nu \qquad (1.7.2)$$

where I_n is the radiation intensity, j_ν is the emission coefficient, κ_ν is the absorption coefficient and ρ is the density.

The Source function, $\Im_\nu$, is defined as the ratio of the emission to absorption coefficients:

$$\Im_\nu = \frac{j_\nu}{\kappa_\nu} \qquad (1.7.3)$$

and thus the equation of transfer can be written

$$-\frac{1}{\kappa_\nu \rho}\frac{dI_\nu}{dz} = I_\nu - \Im_\nu \qquad (1.7.4)$$

In a medium bounded on the z-axis at a point a, the formal solution is given by

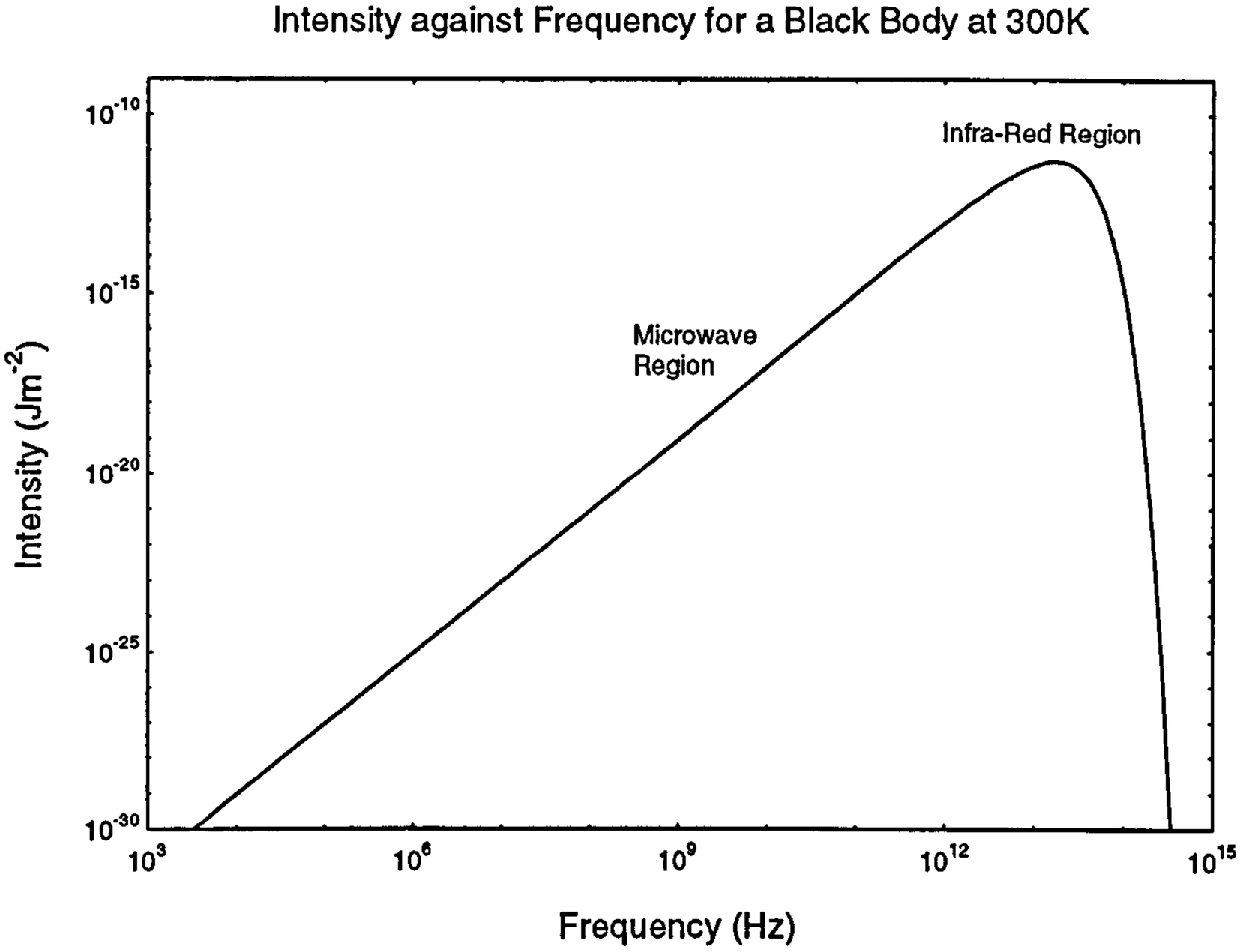

Figure 1.1 Black body spectrum for a material at 300 K.

$$I_\nu(z) = I_\nu(a)e^{-\tau(z,a)} + \int_a^z \Im(z')e^{-\tau(z,z')}\kappa_\nu \rho dz' \tag{1.7.5}$$

were $\tau(z,z') = \int_{z'}^{z} \kappa_\nu \rho dz$ is the optical thickness of the material between z' and z.

The optical thickness is equivalent of the power attenuation constant of electromagnetic radiation.

$$\kappa\rho = 2\alpha \tag{1.7.6}$$

where α is the plane wave electric field attenuation constant, which is related to the complex permittivity $\varepsilon_r = \varepsilon' - j\varepsilon''$ by (Ramo et al, 1965)

$$\alpha = (\omega/c)\,\mathrm{Im}\sqrt{\varepsilon_r} \tag{1.7.7}$$

Kirchoff's Radiation Law states (Chandrasehkar, 1950) that the ratio of the emission to the absorption coefficients, the source function $\Im$, is equal to the specific intensity of the radiation emitted at the same temperature by a black body.

$$\Im = \frac{2h\nu^3}{c^2\left(e^{\frac{h\nu}{k_B T}} - 1\right)} \tag{1.7.8}$$

At microwave frequencies at temperature of 300K, $h\nu/k_B T \ll 1$, so

$$\exp\left(\frac{h\nu}{k_B T}\right) - 1 \approx \frac{h\nu}{k_B T}. \tag{1.7.9}$$

Thus the Planck function may be approximated at microwave frequencies by the Rayleigh-Jeans Function:

$$\Im = B_\nu(T) = \frac{2k_B T\nu^2}{c^2} \tag{1.7.10}$$

This equation shows that at microwave frequencies the thermal signal is linearly dependant on the absolute temperature.

In the simple case of a single semi-infinite medium bounded at $z = 0$, the intensity at the surface is given, from equation 1.7.5, by:

$$I_\nu(0) = \frac{2k_B\nu^2}{c^2}\int_0^\infty 2\alpha T(z)e^{-2\alpha z}dz \tag{1.7.11}$$

This equation means that the emission at a point is dependant on both the temperature at that point and the dielectric properties of the material at that point. The emission from that point is then decreased by a factor $e^{-2\alpha z}$ over the distance to the surface.

1.8 Microwave Radiometry: Considerations in Radiometer Design.

For a microwave radiometer to be useful in a clinical application it should have a number of desirable characteristics. These include a useful lateral spatial resolution, a reasonable penetration depth for the radiation in tissue, a good temperature resolution and a fast response time.

The lateral spatial resolution and penetration depth are dependent on the frequency of the radiation measured, and on the design of the antenna receiving the signal. A good response time is needed if the system is being used in clinical applications, since data collection from a patient must be performed in a restricted time. However, a fast response time causes the radiometer to have a poorer temperature resolution, and compromise must be reached between the response time and the temperature resolution.

1.8.1 The Choice of Measurement Frequency.

For a real antenna, the maximum detectable noise power for a material at temperature T is given by

$$W = k_B TB \tag{1.8.1}$$

where B is the bandwidth. A large bandwidth is desirable, to give a large signal, but in a real radiometer the bandwidth is limited by problems such as antenna impedance mismatch and possible interference from extraneous signals (Brown, 1989).

The lateral spatial resolution for a radiation detecting device is approximately half the wavelength of the radiation in the medium. If the complex permittivity of a medium is given by $\varepsilon_r = \varepsilon' - j\varepsilon''$ then

$$\text{spatial resolution} \approx \lambda_0 / 2\sqrt{\varepsilon'} \tag{1.8.2}$$

where λ_0 is the wavelength in free space.

The penetration depth is determined by the power attenuation constant, 2α. If a plane wave is travelling through a medium, the distance required to attenuate the signal to e^{-1} of its original intensity is given by $1/2\alpha$.

From equation 1.7.7 the field attenuation constant in a dielectric material is

$$\alpha = \frac{2\pi}{\lambda_0}\sqrt{\frac{\varepsilon'}{2}}\left[\left(1+\left(\frac{\varepsilon''}{\varepsilon'}\right)^2\right)^{1/2} - 1\right]^{1/2} \tag{1.8.3}$$

Since for biological tissues, the ratio $\varepsilon''/\varepsilon'$ is generally ~ 0.3 (Gorton, 1996), α may be approximated as

$$\alpha = \frac{\pi\sqrt{\varepsilon'}}{\lambda_0}\tan\delta \tag{1.8.4}$$

where $\tan\delta$ is known as the 'loss tangent' of the tissue. When the permittivity of the medium is given by $|\varepsilon|e^{-j\delta}$, δ, the penetration depth, is defined as

$$\delta = \tan^{-1}\left(\varepsilon''/\varepsilon'\right) \tag{1.8.5}$$

So both equations 1.8.2 and 1.8.4 must be minimised for optimal radiometry performance. This is done by minimising the product of the two expressions, which results in an expression which is dependent only on the loss tangent. Thus the optimal frequency is dependent on the material under investigation.

Most tissue in the human body is mainly composed of water, which accounts for roughly three quarters of the mass of such tissue. However this water is not pure, but is present as an electrolyte, predominately 0.9% by weight NaCl solution. In pure water, at microwave frequencies, the dielectric properties of water are dominated by the orientational polarisation of the water molecules. The permittivity of pure water is given by the Debye dispersion relationship

$$\varepsilon_r = \varepsilon_\infty + \frac{\varepsilon_s - \varepsilon_\infty}{1 + j\omega\tau} \tag{1.8.6}$$

where ω is the angular frequency, τ is the relaxation time, ε_s is the 'static' permittivity and ε_∞ is the 'infinite' permittivity. In the case of a electrolyte, ionic conduction must also be considered. This gives the permittivity of low concentration electrolytic solution as

$$\varepsilon_r = \left[\varepsilon_\infty + \frac{\varepsilon_s - \varepsilon_\infty}{1 + j\omega\tau}\right] + j\frac{\sigma}{\omega\varepsilon_0} \qquad (1.8.7)$$

where σ represents the ionic conduction of the solution (Gorton 1996).

Using equation 1.8.7, it can be found that the loss tangent has a local minimum value at a frequency of about 3 GHz. Thus 3 GHz is commonly chosen as the operating frequency for microwave radiometric measurements on tissues.

1.8.2. Antennas for Microwave Radiometry.

The design of the antenna must also be carefully considered to maximise the signal received. The thermal radiation power per unit bandwidth received by an antenna is

$$W_\nu = \tfrac{1}{2}\int_V I_\nu(\underline{r}) P_n(\underline{r}) d\tau \qquad (1.8.6)$$

where $I_\nu(\underline{r})$ is the intensity of the radiation at frequency ν emitted by the volume element $d\tau$, which is discussed above, and $P_n(\underline{r})$ is the normalised power response pattern of the antenna as a function of position $\underline{r}$ (Mimi, 1990). The factor of ½ occurs since the incident radiation is incoherent and the antenna only picks up one plane of polarisation. The antenna spatial response function is thus fundamental to the process of radiometric signal generation.

The antenna response pattern is dependent on many factors. These include the geometry of the antenna, the operating frequency, the dielectric loading of the antenna, and the geometry and the dielectric properties of the tissue being investigated. To understand the antenna response pattern it must either be modelled theoretically or evaluated experimentally.

Modelling the response mathematically is complex, and has only recently become a viable option as computers become more powerful and inexpensive. However, direct measurement in material simulating body tissue is still popular for its reliability, as well as being used to check the validity of computed models (Mamouni et al, 1991).

The most satisfactory method of measuring the antenna response is the non resonant perturbation technique (Land, 1984, 1988, 1992). In this technique, the antenna which is under examination is supplied with a microwave signal which radiates into a liquid tissue

phantom. The amplitude and phase of the signal reflected from the test antenna are measured. Then field perturbing objects, of known dimensions and permittivity, are introduced to the viewed region and the change in the reflected signal is measured. The field form of the reciprocity relationship is then applied over the stationary boundaries of the system, to yield the change in reflection coefficient at the antenna port produced by the introduction of the perturber. For a non-magnetic dielectric perturber, the change in reflection coefficient, $\Delta\Gamma$, is

$$\Delta\Gamma = \int_V jw(\varepsilon_p - \varepsilon_m)\frac{\mathbf{E_1}.\mathbf{E_2}}{4W_i}dV \qquad (1.8.7)$$

where ε_p and ε_m are the complex permittivities of the perturber and the phantom material respectively, $\mathbf{E_1}$ and $\mathbf{E_2}$ are the electric fields before and after the introduction of the perturber and W_i is the power incident from the antenna. If the $\mathbf{E_1}$ and $\mathbf{E_2}$ fields can be related through the perturber geometry and dielectric properties, the measured $\Delta\Gamma$ gives $\mathbf{E_1}/W_i$. With the conductivity of the medium this is the normalised power dissipation which, by the reciprocity theorem, is the wanted antenna weighting function. Different geometries of perturber can be used to investigate specific characteristics of the field pattern.

1.8.3 The Dicke Radiometer.

A Dicke-type radiometer is used at Glasgow, and elsewhere, to provide accurate microwave temperature measurement in clinical situations.

At temperatures associated with the human body, microwave thermal radiation is of very low intensity, thus the signal has to be amplified. For the case where the total input signal is amplified, the output reading of the radiometer, R, is given by

$$R = G(T_s + T_n) \qquad (1.8.8)$$

where G is the gain of the amplifier, T_s is the source temperature and T_n is the radiometer effective noise temperature. However the gain changes significantly if either the ambient amplifier temperature or the supply voltage changes. Typically, if T_n and T_s are both 300K, a 1% change in G will result in a change of output equivalent to a change of 6K in

T_s. Also this system would be unable to differentiate changes in the source temperature from changes in the amplifier noise temperature.

The Dicke radiometer (figure 1.2) can overcome these problems. This system works by switching its input between the antenna source and a reference load, which is at an accurately known temperature, T_{ref}. The output is now a square-wave signal with the size of the signal representing the difference between the source and the reference temperatures. A synchronous detector is used to measure this signal and give an output, R, which is directly proportional to this difference.

$$R = G(T_s + T_n) - G(T_{ref} + T_n) = G(T_s - T_{ref}) \tag{1.8.9}$$

Hence the signal is now independent of the amplifier noise temperature. Also if T_{ref} is set to be close to the expected T_s then effect of receiver gain fluctuations is greatly reduced. All radiometers have a temperature resolution given by the Gabor relationship

$$\Delta T = \frac{Q(T_s + T_n)}{\sqrt{Bt}} \tag{1.8.10}$$

where Q is the radiometer constant for the receiver, T_n and T_s are the noise and source temperatures respectively, t is the radiometer response time and B is the bandwidth of the radiometer. For Dicke type radiometers, $Q \sim$ 4.6-6.6 typically. Both the noise temperature and the source temperature are roughly 300 K, and the bandwidth at 3 GHz is ~ 500 MHz. Thus a temperature resolution of 0.1 K is obtained for a response time of roughly 2 seconds (Land, 1983).

1.9 Practical Microwave Radiometry.

The use of microwave radiometry in clinical applications was first proposed over 20 years ago. Enander and Larson (1974) first used microwaves to obtain internal temperature information when they used a loop antenna operating at about 1 GHz placed over the abdomen. Since then there have been a number of studies examining the use of microwaves for diagnostic purposes.

Much of the early work failed to take full advantage of the possibilities offered by this technique. Some systems (Gautherie et al, 1980; Abdul-Razzak et al, 1987) used remote "dish" antennas operating at frequencies much higher than 3 GHz. At these frequencies the penetration depth was shallow and the systems gave temperatures similar to those

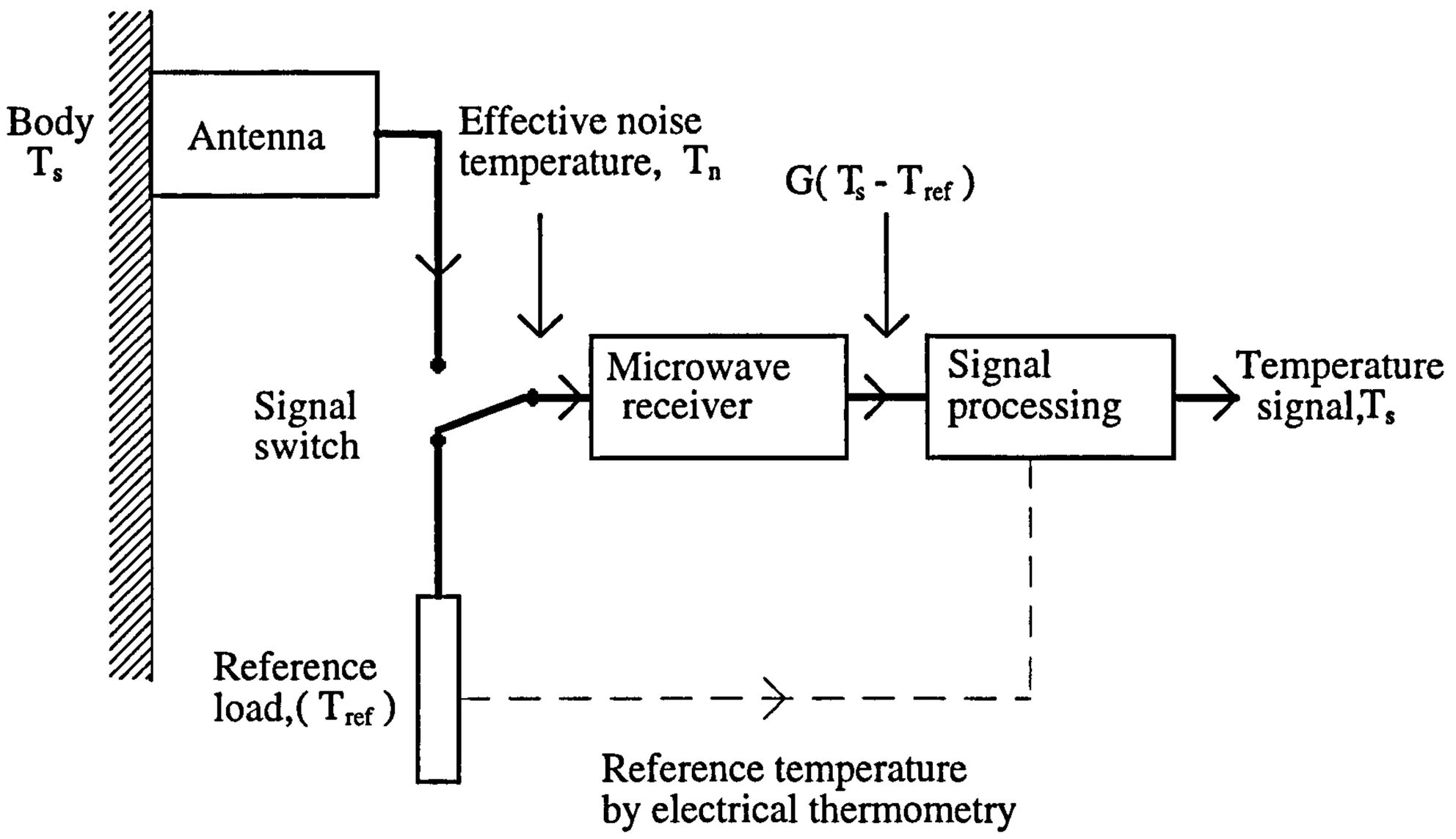

Figure 1.2 Schematic of the Dicke Radiometer.

produced by infra-red systems (Land, 1995). Other systems had failed to realise the importance of coupling the antenna to match the effective impedance at the skin surface. When these early systems were applied to detection of breast cancer, following the poor results obtained by infra-red systems (Moskowitz et al, 1976), it was found that these early microwave detectors faired little better than detectors operating in the infra-red range (Barrett et al, 1980).

However, proper understanding of these considerations has allowed for more productive utilisation of microwave thermography. Radiometers operating at a fixed frequency using a single antenna have been extensively investigated for use as a clinical tool. In the case of inflammatory disease, it has been shown that microwave thermography provides a simple technique for determining the extent of disease in the joint, which compares well with other clinical and laboratory indices of inflammation (Fraser et al, 1987; McDonald et al, 1994). This technique has also been used in the veterinary field to investigate damage in the tendons in horses' legs (Marr, 1992) and in the forensic field for the measurement of post-mortem internal temperatures for help in determining the time of death (al-Alousi et al, 1994).

If measurements are only made with a single antenna at a single frequency, no direct information about the change of temperature with depth can be obtained. However thermal modelling can give us this information indirectly, if the internal tissue geometry is known. For the variation in internal temperature to be measured directly, other techniques such as multi-frequency radiometry must be employed.

1.9.1 Radiometer Refinements.

To gain more information about the dependence of temperature with depth, measurements must be made at more than one frequency or with more than one antenna. Multi-spectral radiometers reduce the need for information obtained by other means about a volume of tissue being examined.

Bocquet et al (1986) looked at the simple case of a water bath at fixed temperature T, containing a cylinder filled with water at $T + \Delta T$. It was found that for a known diameter of cylinder, the distance between the cylinder and the antenna could be determined from the measurement of the microwave temperature at 1.5 GHz and 3 GHz.

A more sophisticated approach is being developed by Bardati and Tognolatti (1993) and Coarsi and Gragnani (1993), where internal temperature distributions are recreated from multi-spectral radiometer data. For this method to work, the prior knowledge of the permittivity of all materials within the viewed volume is needed. However it has been found that, so far, the accuracy and resolution of retrieved temperature data is poor. Bardati and Tognolatti (1993) investigated the possibility of imaging a hot spot, diameter 5 mm, in an homogenous cylindrical liquid phantom of diameter 60 mm. Taking measurements at 4 discrete frequencies at 17 equiangular points, a minimum temperature resolution of only 1.5 - 5 °C (depending on noise propagation estimate) was found. This temperature resolution is not good enough for clinical use.

Another technique to improve spatial resolution is to use multi-probe radiometers. Correlation microwave thermography combines signals from two antennas, which have been placed on the body, using a delay line. Only the volume of material under examination which couples to both of the antennas contributes to the signal. If this volume is small, then thermal structures within the body can be located. Correlation thermography however does not respond to absolute temperatures but only to thermal gradients within the volume under examination. The output becomes zero if a medium of uniform temperature is viewed (Enel et al, 1984; Mamouni et al, 1983, 1991).

However despite all the advances in microwave thermography there has still been reluctance to accept the technique in the medical world. Research which has shown that microwave thermography has possible advantages has not yet been widely taken up in a clinical environment. It "has not yet found a secure niche in the medical community" (Foster and Cheever, 1992) though it is being used in medical research and for hyperthermia control.

Chapter 2: Thermal Modelling.

2.1 Introduction.

In this chapter the modelling of heat transfer in the human body is examined. Firstly, an overview is taken of the body's thermoregulatory system. The conventional bio-heat transfer equation is then introduced, along with more recent bio-heat equations. Next the different methods of heat transfer between the body and the environment are examined. The solution of the time independent form of the conventional bio-heat transfer equation is then studied for simple one dimensional cases, and methods of solving bio-heat equations for more complex geometries, using computers, are also considered. Finally, the combining of thermal and microwave models to produce the effective microwave temperature is examined.

2.2 The Thermoregulatory System.

The human body is continuously exchanging heat with the environment, yet manages to maintain a fairly constant internal temperature, in spite of widely changing environmental factors.

Heat is generated in the human body at a cellular level, mainly as a by-product of the breaking down of proteins, lipids and carbohydrates, which the body has ingested. The major result of this process, which is known as metabolism, is the production of the body's internal energy source, adenosine triphosphate (ATP). The production of ATP is, however, inefficient with nearly two thirds of the energy being "lost" as heat. Further, when energy is required by a part of the body to do work, inefficiencies in the release of energy of ATP mean that only about 25% of the energy taken from foods is used by functional systems. While these energy conversion inefficiencies account for the large majority of the heat produced by the body, they do not account for the total heat production. All internal muscle work will eventually be converted to heat and there are other chemical reactions in the body which purely produce heat.

Once the heat is generated, it is distributed throughout the body by the vascular system, which transfers heat from the sources of heat production, such as the some of the organs,

to areas of the body with low metabolic rates. The body then losses heat to environment, at either the skin surface or the respiratory tract.

For the body to remain at the same temperature, both the heat generated and the heat lost to the environment have to be controlled, and this is achieved by the body's thermoregulatory system. There are number of methods by which the body controls its temperature. When body temperature starts to drop, the thermoregulatory system responds by causing cold-motivated voluntary exercise and shivering. If the body temperature rises and the body can no longer lose heat fast enough to the environment, the body will start to sweat. The body will also increase, or decrease, the flow of blood near the skin surface to increase, or decrease, the rate of heat loss from the skin.

The actual amount of heat produced by the individual body is dependant on many factors, especially the activity level of the individual. For example, under resting conditions, the metabolic rate will be in the region of 30-50 Wm^{-3}. The metabolic rate can increase to greater than 600 Wm^{-3} when doing exercise. This variability is also seen in muscle, which is the major heat source of the body, and which can increase energy usage by 15-20 fold from the base level. The amount of heat being produced is not only dependant on the work being done but the type of work being done. In exercise, energy is required to do external work, while in shivering no external work is done and virtually all the energy is converted into heat.

The heat loss from the body is also highly variable. The body losses heat from the skin and respiratory tract through radiation, convection and evaporation. Thus the heat lost from the body will be dependant on such factors as air temperature, air flow and the humidity as well as internal factors. The type of clothing being worn also dramatically affects the amount of heat lost to the environment.

Despite all the variation in the amount of heat generated and lost by the body, the thermoregulatory system will stop variations in the core temperature of the body being larger than a few tenths of a degree (Shitzer and Eberhart, 1985; Bligh, 1985).

2.3 The Conventional Bio-heat Transfer Equation.

A number of attempts have been made to model the complex heat patterns within the human body. Pennes (1948) introduced what is commonly known as the "conventional

bio-heat transfer equation." Starting from the Fourier Heat Transfer Equation, it is assumed that blood enters the capillaries at arterial blood temperature, T_{art}, thermally equilibrates instantaneously, and leaves the capillaries at the local tissue temperature, T. This gives the heat transfer equation for solids with an extra 'heat sink' term

$$\rho c \frac{dT}{dt} = k\nabla^2 T - w_b c_b (T - T_{art}) + Q \qquad (2.3.1)$$

where ρ, c and k are the density, specific heat and thermal conductivity of the tissue and c_b is the specific heat of the blood. The blood perfusion, the mass of blood entering a unit volume in a unit time, is given by w_b and Q is the metabolic heat production in the tissue. In most body tissues under resting conditions, Q tends to be rather smaller than the other terms. Generally, it is further assumed that all heat transfer takes place in the capillaries so T_{art} can then be taken as equal to the core temperature of the body.

2.4 More Advanced Bio-Heat Equations.

The validity of the conventional bio-heat transfer equation has been critically examined by a number of authors. Wulff (1974) questioned the fact that the equation made no allowance for the directionality of blood flow and pointed out that the assumption of instantaneous thermal equilibration would mean that two temperatures, T and T_{art}, would exist at the same point. Wulff proposed that a vector representing local mean blood velocity , $\mathbf{U}_h$, should be used instead of the non-directional perfusion, w_b

$$\rho c \frac{dT}{dt} = k\nabla^2 T - \rho_b c_b \mathbf{U}_h . \nabla T + Q \qquad (2.4.1)$$

where ρ_b is the density of the blood. This equation is still incomplete. For example, consider a volume element containing parallel artery vein pairs running counter current, that is blood flow in the vein opposite to the flow in the artery. This would give the net blood flow to be zero, and hence the model would maintain that no heat transfer between the blood and the surrounding tissue would take place. This is contrary to what is expected and observed.

Chen and Holmes (1980) and Weinbaum et al (1984) calculated the point at which thermal equilibration between the blood and the surrounding tissue takes place within the body. For each type of vessel, the length of the vessel, l, was compared to the

exponential equilibrium length, X_{eq}, which is the length over which the temperature difference between the tissue and blood will be reduced by a factor e. The conventional bio-heat transfer equation assumes that $X_{eq} = 0$ in the capillaries and is infinite in all other vessels. Table 2.1 shows the values as calculated by Chen and Holmes (1980).

For the largest vessels it can be seen that there is little heat transfer between the tissue and the blood. However, table 2.1 shows that thermal equilibration is reached long before the blood reaches the capillaries. Further, Weinbaum et al found that when counter current heat exchange is considered, the distance required for blood to reach thermal equilibrium could be as much as halved, meaning that equilibration takes place even further away from the capillaries. Thus the behaviour of the medium and smaller side vessels cannot be described by a heatsink term.

Chen and Holmes proposed the following bio-heat equation

$$\rho c \frac{dT}{dt} = \nabla . k \nabla T + w_b^* c_b (T_a^* - T) - \rho_b c_b \mathbf{U_h} . \nabla T + \nabla . k_p \nabla T + Q \qquad (2.4.2)$$

The largest blood vessels are considered separately and modelled individually. The values w_b^* and T_a^* are the blood perfusion and arterial temperature of the blood after it has travelled through the largest vessels which have been considered independently. This equation has a heat sink term allowing for thermal equilibration in the large vessels not considered independently, a flow term to account for directional flow in the smaller vessels and an enhanced conductivity, k_p, to account for the convection of the smallest vessels.

However, Weinbaum and Jiji (1985) demonstrated analytically that the most important heat exchange mechanism was not between the blood and tissue, but incomplete counter current heat exchange, that is heat exchange between arteries and veins. A tensorial effective tissue conductivity, k_{eff}, was introduced to account for the counter current heat exchange, producing the limited k_{eff}, model.

$$\rho c \frac{dT}{dt} = \nabla . k_{eff} \nabla T + Q \qquad (2.4.3)$$

Several investigators have found different expressions for k_{eff}. For example, Weinbaum and Jiji gave k_{eff} for a homogenous medium containing vessels of radius a as

$$(k_{ij})_{eff} = k(\delta_{ij} + \frac{\pi^2 n a^4 \rho_b^2 c_b^2 v^2}{\sigma k^2} l_i l_j) \qquad (2.4.4)$$

Vessel	Radius (mm)	Length l (mm)	X_{eq} (mm)	l/X_{eq}
Aorta	5.0	400	160000	0.0025
Large Arteries	1.5	200	3700	0.054
Arterial Branches	0.5	100	250	0.4
Terminal Branches	0.3	10	68	0.15
Arteriole	0.01	2	0.0038	530
Capillary	0.004	1	0.0001	10000
Venules	0.015	2	0.002	1000
Terminal Veins	0.75	10	92	0.11
Venous Branches	1.2	100	270	0.37
Large Veins	3.0	200	4100	0.049
Vena Cava	6.5	400	180000	0.0022

Table 2.1 The equilibration length compared to the vessel length for the different types of vessels in the human body. Table adapted from the European Society for Hyperthermic Oncology Task Group (1994) using X_{eq} as given by Chen and Holmes (1980).

	h_c ($Wm^{-2}K^{-1}$)	Remarks	Reference
Seated	2.3	Free convection	Seagrave (1971)
	2.1	$0.05 \geq V \geq 0.20$	Gagge et al (1965)
	2.4 - 4.6	$0.15 \geq V \geq 0.20$	Nishi (1973)
	$7.4V^{0.67}$	Forced convection	Seagrave (1971)
Standing	2.7	Free convection	Seagrave (1971)
	2.5 - 4.5	$0.11 \geq V \geq 0.22$	Nishi (1973)
	$8.7V^{0.67}$	Forced convection	Seagrave (1971)
Reclining	5.6	$V = 0.2$	Colin and Houdas (1967)

Table 2.2 The coefficient of convective heat transfer as found by various authors. V is the mean air velocity in ms^{-1}.

where δ_{ij} is the Kronecker Delta function, n is the number density of the vessels, σ is a shape factor, v the mean flow velocity and l_i, l_j are the direction cosines.

The limited k_{eff} model was found to accurately model the behaviour of the small and medium sized blood vessels. Baish et al (1986) found, both theoretically and using model simulations, that in the largest blood vessels, those with diameter > 500μm, the limited k_{eff} model no longer applied. Instead, the behaviour of the large blood vessels was closely approximated by a heat sink term of the form found in the conventional bio-heat transfer equation. This lead Baish et al and other authors (Wissler, 1987) to propose that the limited k_{eff} model should have a heat sink term, to account for the behaviour of the largest, thermally unequilibrated vessel. A task group report of the European Society for Hyperthermic Oncology (1992) proposed that a combined heatsink \ k_{eff} model should be used when no information about the vascular structure is known. That is:

$$\rho c \frac{dT}{dt} = \nabla . k_{eff} \nabla T - f w_b c_b (T - T_{art}) + Q \qquad (2.4.5)$$

where f is a form factor. Where the vascular structure is known the largest vessels should be modelled independently with the limited k_{eff} model used to account for heat transfer in the medium and small radius vessels.

Accurate thermal modelling of tissues is of greatest importance in hyperthermia. Currently there are no systems which can non-invasively monitor heating within the human body during hyperthermia to the degree of accuracy required for a patient's safety. Thus the temperature patterns produced during heating must accurately be modelled prior to a course of hyperthermia treatment. This means the volume being heated must be accurately mapped beforehand, to allow for the planning of the treatment regime to ensure that the temperature is high enough to give therapeutic heating across the whole of the tumour volume without damage being done to healthy tissue. (Creeze, 1994).

However for microwave thermography the same degree of accuracy is not required. As noted by Baish et al (1986), the conventional bio-heat transfer equation is still remarkably successful at predicting thermal responses and although the equation has been criticised theoretically, it has been found to give good representations of the thermal behaviour of the tissue in practical situations. In microwave thermography, the

temperature is averaged over a volume much larger than the microstructure of the vascular system since, at 3 GHz, the spatial resolution in tissue will be roughly 1 cm and the penetration depth will be a few cm. Also there is a degree of uncertainty about the thermal properties and microwave properties of the tissue volume being considered. Given these facts, the use of the conventional bio-heat transfer equation is acceptable.

2.5 Heat Loss to the Environment.

A full model of the body's thermal system is not complete without considering the transfer of heat from the body to the environment. The three main mechanisms for heat transfer to the surroundings are radiation, convection and evaporation (sweating). Gases have a very low thermal conductivity, and thus there is no significant heat transfer by conduction between the skin and air.

The net rate of heat loss per unit surface area by radiation, q_r, for a surface at temperature T_s, surrounded by an environment at temperature T_a, is given by the Stefan-Boltzmann Law

$$q_r = \sigma_s e(T_s^4 - T_a^4) \tag{2.5.1}$$

where σ_s is Stefan's constant and e is the emissivity of the skin surface. For human skin the emissivity is close to 1 (0.98-1.00) since most of the radiation loss occurs in the infra-red region where the behaviour of the skin is close to that of a black body (Jones, 1987).

In a normal environment, the difference between skin and ambient temperature will be small compared to the mean temperature and thus to a good approximation

$$q_r = 4\sigma_s e T_m^3 (T_s - T_a) \tag{2.5.2}$$

where $T_m = \frac{1}{2}(T_s + T_a)$ is the mean temperature (Draper and Boag, 1971). Thus the rate of radiative heat loss can be expressed by

$$q_r = h_r (T_s - T_a) \tag{2.5.3}$$

where the radiative heat transfer coefficient is given by $h_r = 4\sigma_s e T_m^3$. Skin temperature approximately varies between 301-308K and ambient temperature varies between 293-299K thus giving a value of $h_r = 6.1 \pm 0.2$ $Wm^{-2}K^{-1}$

Convection is the loss of heat at the skin surface to moving liquid or gas. In this section only the heat loss in air is considered, though the following is equally applicable to other fluids. The two forms of this mode of heat loss are free convection, where air flows are caused by differences in air densities generated by the warming of air by the skin, and forced convection, were the air movement is generated by external means. The rate of heat loss per unit surface area for both forms of convection, q_c, is given by

$$q_c = h_c(T_s - T_a) \tag{2.5.3}$$

where h_c is the coefficient of convective heat transfer. The coefficient of convective heat transfer is dependant on a number of factors including the geometry of the surface of the skin, the rate of air flow across the skin and the physical properties of the air, such as its density. For free convection, the value of h_c has been calculated for a number of simple geometries. Rice (1926) found that for a vertical plate in air at room temperature h_c was given by

$$h_c = 2.0\left(T_s - T_a\right)^{0.25} \tag{2.5.4}$$

This gives a figure of h_c = 3.6 $Wm^{-2}K^{-1}$ for a temperature difference of 10°C between ambient and surface temperature.

Table 2.2 shows a number of values which have been found for h_c for different body positions and different air speed flows. For air flows of velocity ≤ 0.2 m^2s^{-1}, table 2.2 gives h_c varying from 2.1 $Wm^{-1}K^{-1}$ to 5.6 $Wm^{-1}K^{-1}$. These value agree well with that calculated above.

At room temperature, a normal human body will not produce much sweat, unless it has undergone physical exertion. However, the body will still lose heat through evaporation due to insensible perspiration. This is a diffusion process where water passes through the skin surface. The amount of heat lost through evaporation is given by

$$q_e = h_{fg} m(p_s^* - p_a) \tag{2.5.5}$$

where h_{fg} is the heat of vaporisation, m is the permeation coefficient of skin and $(p_s^* - p_a)$ is difference between the saturated water vapour pressure at skin temperature and the ambient water vapour pressure (Shitzer and Eberhart, 1985). Thus the rate of heat loss is not directly described by

$$q_e = h_e(T_s - T_a) \tag{2.5.6}$$

though Draper and Boag (1971) argued that, given the small contribution by insensible perspiration to the total heat loss, no significant errors would be introduced by assuming it does. If this assumption is made then $h_e \approx 0.8$ $Wm^{-2}K^{-1}$.

Hence the total heat loss per unit surface area is given by

$$q = q_r + q_c + q_e = h(T_s - T_a) \tag{2.5.7}$$

where $h = h_r + h_c + h_e \approx 11$ $Wm^{-2}K^{-1}$ (Brown, 1989).

2.6 Simple Tissue Temperature Profiles.

The steady state temperature profile produced in a semi-infinite homogenous medium is given by the time independent, one dimensional form of the conventional bio-heat transfer equation which is

$$\frac{d^2T}{dz^2} = \frac{w_b c_b}{k}(T(z) - T_{art}) - \frac{Q}{k} \tag{2.6.1}$$

Given the restriction that the temperature must be finite as $z \to \infty$, this equation has the solution

$$T(z) = Ae^{-\beta z} + T'_{art} \tag{2.6.2}$$

where $\beta = \sqrt{w_b c_b / k}$ and $T'_{art} = T_{art} + Q / w_b c_b$ i.e. the body core temperature. In the human body, the temperature will only be slightly lower (~ 0.3°C) than the core temperature at a depth 5 cm into the tissue. Thus any region of the body with a thickness greater than 10 cm can be regarded as semi-infinite.

At the tissue air boundary, the heat loss is given by equation 2.5.7 and thus

$$k\left.\frac{dT}{dz}\right|_{z=0} = h(T_s - T_a) \tag{2.6.3}$$

Applying this boundary condition to equation 2.6.2 gives

$$T(z) = \frac{(T_a - T'_{art})}{(1 + k\beta / h)} e^{-\beta z} + T'_{art} \tag{2.6.4}$$

A more realistic case is to use a plane stratified tissue structure to model the human body. For example, take the case of a layer of fat thickness a, bordered by a semi-infinite layer of muscle, with negligible metabolic heat production. The solution to equation

2.6.1 has boundary conditions given by equation 2.6.3 and

$$T_{fat}(a) = T_{muscle}(a)$$
$$k_1 \left.\frac{dT_{fat}}{dz}\right|_{z=a} = k_2 \left.\frac{dT_{muscle}}{dz}\right|_{z=a} \tag{2.6.6}$$

This gives

$$\begin{aligned} T_{fat} &= X(k_1\beta_1 - k_2\beta_2)e^{\beta_1(z-a)} + X(k_1\beta_1 + k_2\beta_2)e^{\beta_1(a-z)} + T_{art} \quad (0 \le z \le a) \\ T_{muscle} &= 2Xk_1\beta_1 e^{\beta_2(a-z)} + T_{art} \quad (a \le z < \infty) \end{aligned} \tag{2.6.7}$$

where k_1, k_2 are the thermal conductivities of muscle and fat and w_1, w_2 are the blood perfusions in the muscle and fat regions. $\beta_1 = \sqrt{w_1 c_b / k_1}$, $\beta_2 = \sqrt{w_2 c_b / k_2}$ and

$$X = \frac{h(T_a - T_{art})}{(h - w_1 c_b)(k_1\beta_1 - k_2\beta_2)e^{-\beta_1 a} + (h + w_1 c_b)(k_1\beta_1 + k_2\beta_2)e^{\beta_1 a}} \tag{2.6.8}$$

Figure 2.1 shows the temperature variation with depth for an semi-infinite block of muscle with, and without, a 1 cm thick layer of fat in front of it. For muscle tissue k = 0.50 $Wm^{-1}K^{-1}$ and w_b = 0.41 $kgm^{-3}s^{-1}$, while for fat tissue k = 0.20 $Wm^{-1}K^{-1}$ and w_b = 0.145 $kgm^{-3}s^{-1}$. Also h = 11 $Wm^{-2}K^{-1}$, c_b = 3800 $Jkg^{-1}K^{-1}$, T'_{art} = 37°C, T_a = 25°C and the metabolic heat production taken to be negligible (Hand and James, 1982; Brown, 1989; European Society for Hyperthermic Oncology, 1992). It can be seen that the addition of the layer of fat decreases the skin temperature by over 1°C.

Another case to consider is that of a finite slab of material, which can be used to model a limb. For the case of a slab of material, thickness $2d$, centred on $z = 0$, on the boundary conditions are

$$\begin{aligned} k\left.\frac{dT}{dz}\right|_{z=d} &= -h(T(d) - T_a) \\ k\left.\frac{dT}{dz}\right|_{z=-d} &= h(T(-d) - T_a) \end{aligned} \tag{2.6.9}$$

The solution to equation 2.6.1 for these boundary conditions is

$$T(z) = \frac{h(T_a - T'_{art})(e^{\beta z} + e^{-\beta z})}{e^{-\beta d}(h - k\beta) + e^{\beta d}(h + k\beta)} + T'_{art} \tag{2.6.10}$$

Figure 2.2 shows the variation in temperature for an 8 cm thick slab of muscle tissue. The values used in this case are identical to those for the semi-infinite slab of muscle

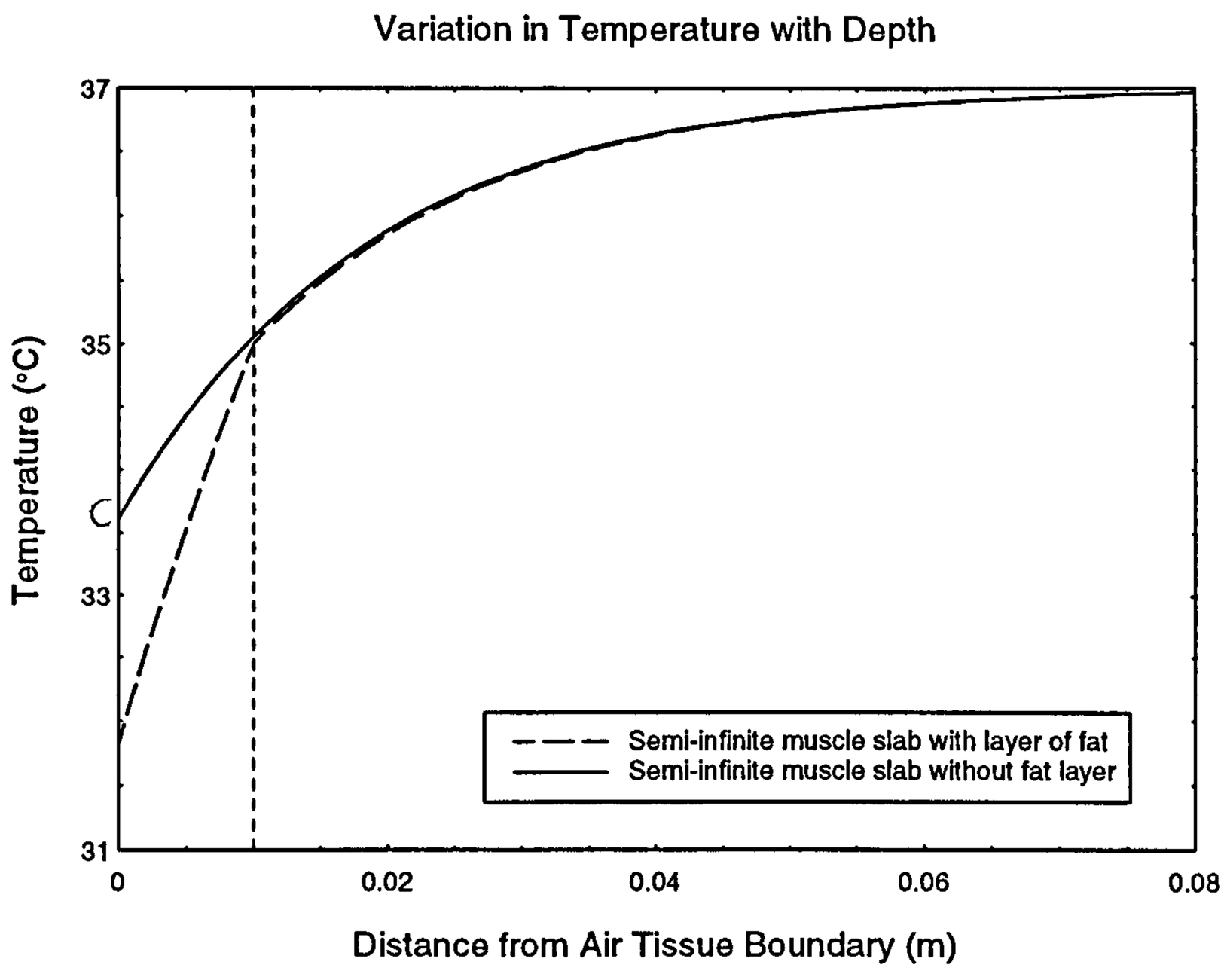

Figure 2.1 The change in temperature with depth for semi-infinite slabs of tissue.

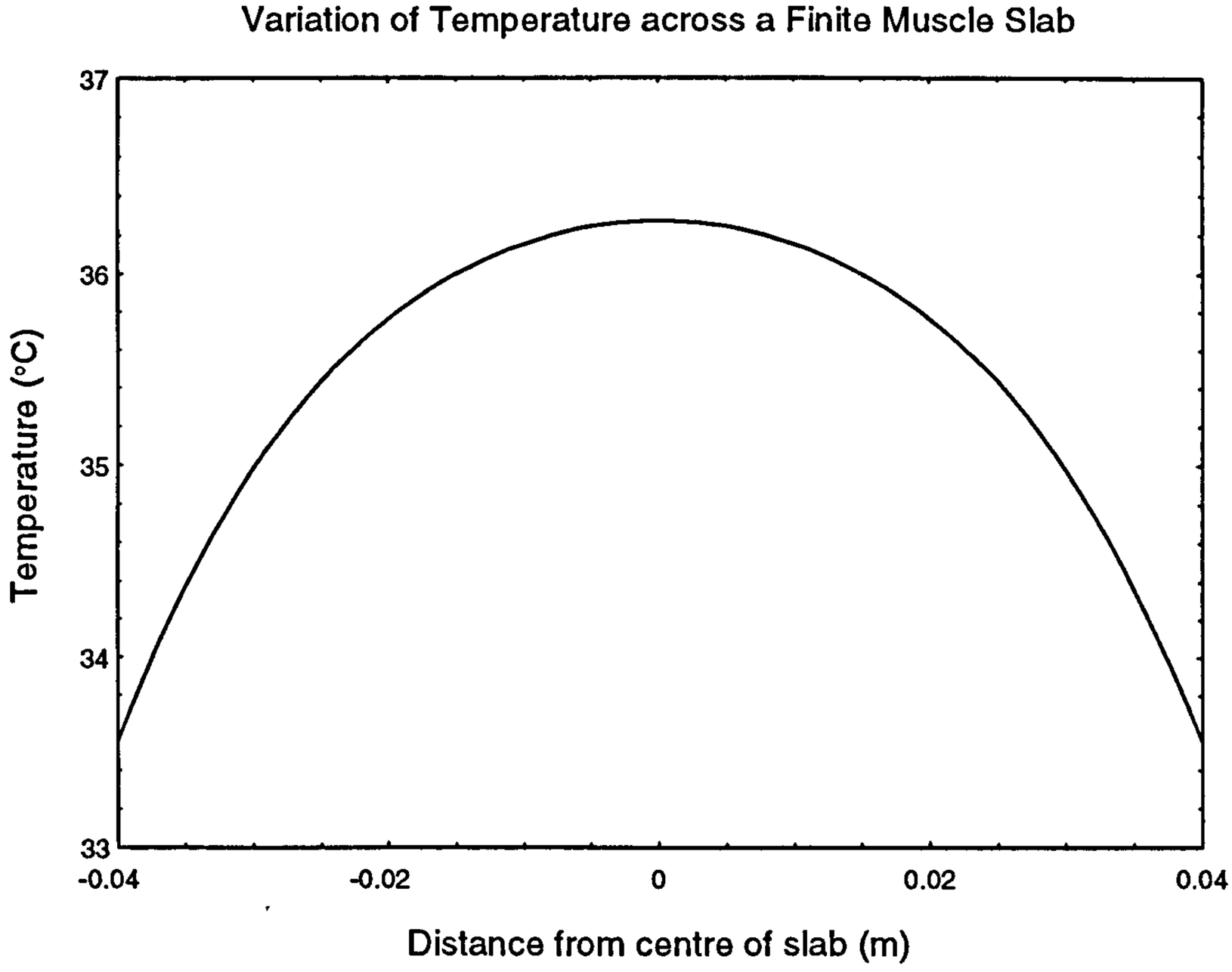

Figure 2.2 The change in temperature with depth for a finite thickness of muscle.

tissue. Modelling of this form has been usefully applied for interpretation of microwave temperature measurements taken across the joints of the arm.

2.7 Computer Aided Thermal Modelling.

For even relatively simple geometries, the solution of the conventional bio-heat transfer equation can soon become unmanageable. Without a computer, this means that the solution of such systems is limited to one dimensional and simple two dimensional models. This also holds for the more complex bio-heat equations, such as those given in section 2.4. A suitable computer program allows for far more complex geometries to be examined. Numerical methods such as the finite difference technique can be used to solve the bio-heat equations for representations of parts of the human body.

The finite difference algorithm is based on the simple definition of the derivative of a function. If a function $f(z)$ is function of z alone then the first derivative is assumed to be of the form

$$\frac{df}{dz} = \frac{f(z+h) - f(z)}{h} \tag{2.7.1}$$

where h is the step size. The second derivative is given by

$$\frac{d^2 f}{dz^2} = \frac{f(z+h) - 2f(z) + f(z-h)}{h^2} \tag{2.7.2}$$

In the case of the one dimensional conventional bio-heat transfer equation, the finite difference algorithm is expressed thus

$$\rho c \frac{T_{i,j+1} - T_{i,j}}{\Delta t} = k \frac{T_{i+1,j} - 2T_{i,j} + T_{i-1,j}}{(\Delta z)^2} - w_b c_b (T_{i,j} - T_{art}) + Q \tag{2.7.3}$$

where Δt is the time step size, Δz is the spatial step size and $T(z_0 + i\Delta z, t_0 + j\Delta t) = T_{i,j}$ (Croft and Lilley, 1977).

To implement the finite difference algorithm, the volume being modelled is divided into a square grid or lattice. Each lattice cell has its thermal characteristics identified and the temperature at each lattice point is calculated. This technique has been used to study the spatial and temporal variations in tissues subjected to local hyperthermia (Hand et al, 1982; Lagendijk, 1982; Kolios et al, 1985; Camart et al, 1996).

Another numerical method used to model the temperature patterns within the human body is the finite element technique. This technique requires greater computing power, but has the advantage that heterogeneous tissue properties and irregular boundary conditions are accounted for as a fundamental part of the mathematical formulation. The finite element technique has the advantage that elements can be of varying shape and size. Harness (1994) used the time independent conventional bio-heat transfer equation to create finite element models of the leg above the quadricep and the index finger to aid in the analysis of clinical microwave thermographic data. This technique has also been used to study the temperature variations in hyperthermia (Moskowitz, 1994).

2.8. Combined Thermal and Microwave Modelling.

Brown (1989) has shown that temperature profiles obtained from thermal models, combined with equations derived for the signal power input into a microwave antenna, give the effective microwave temperature in terms of the ambient, surface and core temperatures and microwave and thermal properties. As discussed in chapter 1, for a perfect antenna in contact with a uniform semi-infinite region, the effective microwave temperature, T_{mw}, is given by

$$T_{mw} = \int_0^\infty 2\alpha T(z) e^{-2\alpha z} dz \qquad (2.8.1)$$

where α is the power attenuation coefficient.

Combining this equation with equation 2.6.4, we find effective microwave temperature is

$$T_{mw} = \frac{(T_a - T'_{art})}{(1+{}^{k\beta}\!/_{h})(1+{}^{\beta}\!/_{2\alpha})} + T'_{art} \qquad (2.8.2)$$

The surface temperature, T_s, is found by setting $z = 0$ in equation. 2.6.4

$$T_s = \frac{(T_a - T'_{art})}{(1+{}^{k\beta}\!/_{h})} + T'_{art} \qquad (2.8.3)$$

And hence the effective microwave temperature can be written as

$$T_{mw} = \frac{(T_s - T'_{art})}{(1+{}^{\beta}\!/_{2\alpha})} + T'_{art} \qquad (2.8.4)$$

All the temperatures T_{mw}, T_s, T_a and T'_{art} can be measured leaving w_b, k and α as the unknown quantities. Both k and α can be estimated for the tissue being examined, allowing the blood perfusion to be found.

A more realistic case is to model the human body as plane stratified layers. In this case

$$T_{mw} = 2\alpha_1 t_{01} \int_0^a T_1(z)\exp(-2\alpha_1 z)dz + 2\alpha_2 t_{12} \int_a^b T_2(z)\exp(-2\alpha_2 z)dz + \ldots\ldots \qquad (2.8.5)$$

where t_{01}, t_{12} are the transmission coefficients after considering reflections of tissue boundaries and α_1, α_2 are the power attenuation coefficients. From section 2.6, $T_i(z)$ is given by

$$T_i(z) = A_i \exp(\beta_i z) + B_i \exp(-\beta_i z) + T'_{art} \qquad (2.8.6)$$

where A_i, B_i are constants dependant on the geometry and the thermal properties of the volume under consideration.

Kelso (1995) used the semi-infinite region model to examine results obtained from clinical measurements of human limbs and breast. Using thermal properties estimated from literature, Kelso estimated blood perfusions which were in reasonable agreement with the values estimated by other techniques. Kelso also found good agreement between the semi-infinite model and a two dimensional finite element solution of the conventional bio-heat transfer equation.

Chapter 3: Properties of Biological Tissues.

3.1 Introduction.

In this chapter the constituents of biological tissue are examined. The composition of the average human body is described and the main biological materials are discussed. Methods of modelling the behaviour of various physical properties in human tissues are examined and the success of these methods is established. The significance of bound water in biological tissue is considered and finally the thermal conductivity, specific heat capacity and density of the body's two main constituents, protein and water, are discussed.

3.2 The Composition of Biological Tissue.

For a full understanding to be gained of the thermal properties of biological tissue, it is essential that the constitution of biological tissues be known and the physical behaviour of these constituents, and the interactions between them, be understood.

All biological tissue is made of cells. These cells vary in size and shape depending on the function they fulfil. Cells are usually made up of a central nucleus, surrounded by a mass of protoplasm and bounded by a membrane. The interior of a cell is approximately 75% water, with the remaining mass being made up of lipids, proteins, salts, sugars and nucleic acids (RNA, DNA) suspended in the water. The membrane is mainly constructed of lipid and is semi-permeable. It functions so as to regulate the exchange of ions and molecules with the water which surrounds the cell (Brooks and Brooks, 1980).

3.2.1 Water.

Water is the major component material of most biological tissue. It constitutes 50% to 70% of total body weight in the human male and 45% to 65% of the female body weight. The actual value is determined by how obese the subject is. Fat tissue has a low water content and hence people with large amounts of fat in their body will have proportionally less water compared to total body weight.

It is convenient to class the body water into to distinct groups. Intracellular water exists within tissue cells and extracellular water exists outside the cell. Extracellular water can itself be subdivided into plasma and interstitial (or intercellular) water. The intracellular water, which is found in protoplasm, makes up two thirds of the total mass of the body water. Interstitial water, which suspends the cells, comprises approximately 25% of the total mass of water with plasma accounting for the remaining 8%. While the proportions of each water type remain fixed by the body, water molecules can transfer from one type to another by osmosis. Different tissues, however, will have different proportions of these types of water. Figure 3.1 shows the relative proportions of each of the different materials for various parts of the body.

Inside a cell water occurs in two forms, free and bound. Free water is able to move as a liquid inside a cell, but bound water is loosely attached to protein molecules by hydrogen bonding caused by dipole attraction. Physiologically, free water is available for metabolic processes whereas bound water is not. Bound water is discussed in greater detail in section 3.9 (Giese, 1979).

3.2.2 Proteins.

Proteins make up the majority of the solid matter found in human body tissues. For example, skeletal muscle is around 75% water by mass, 20% protein and 2% lipid. The remaining few percent is made up of other materials, such as the salts dissolved in water. Proteins are polymer molecules responsible for the structure of the cell. There are many different types of protein molecule within the body which range in molecular weight from several thousand to several million a.m.u.. Proteins molecules are made of chains of different amino acids, of which there are 20 types in the human body. The amino acids in protein are connected by the respective amino and carboxyl group forming peptide links. The angles of these bonds and hydrogen bonding within the protein molecule are responsible for the helical shape of proteins (Giese, 1979).

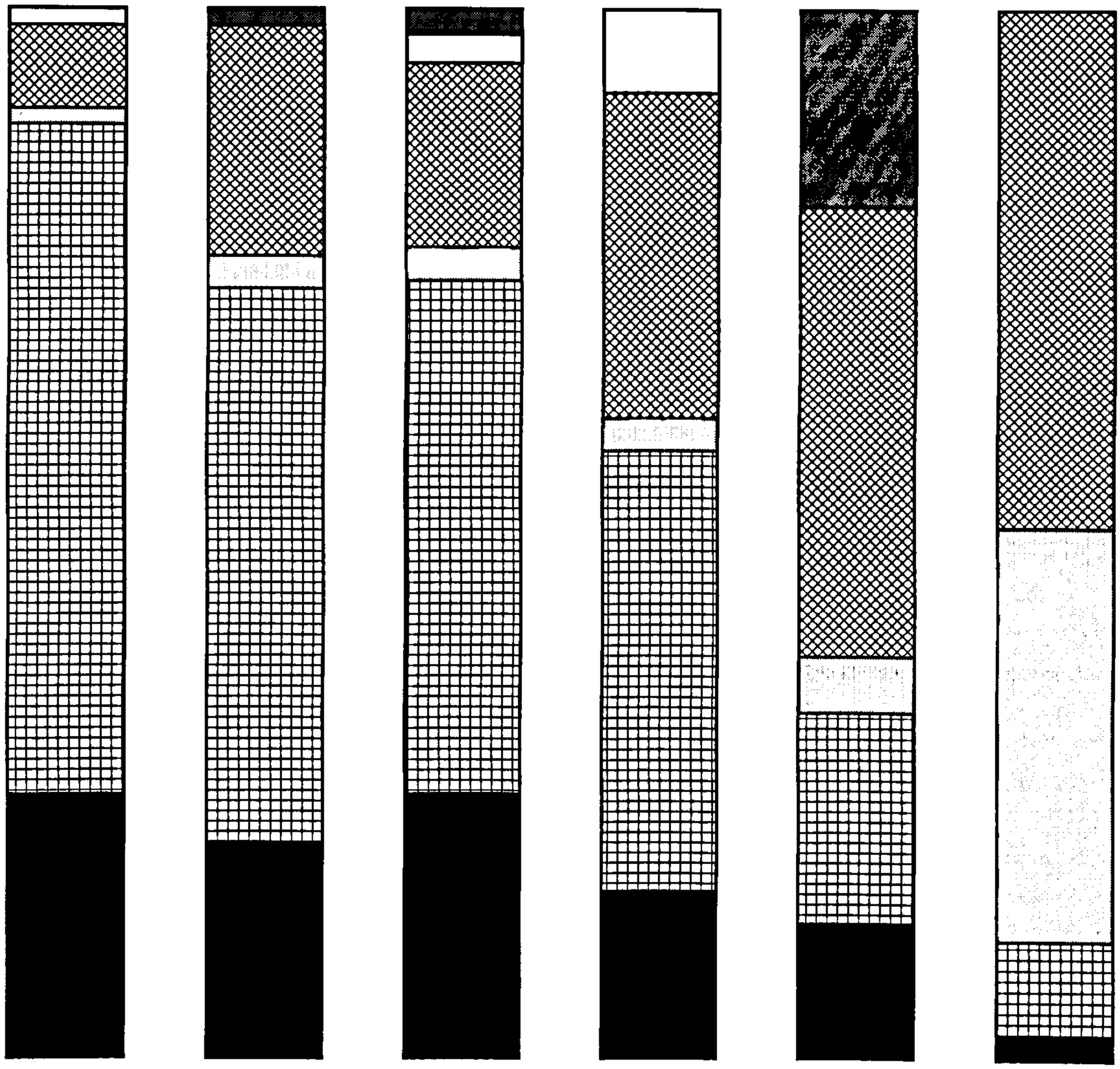

Figure 3.1 The relative proportions of materials in several parts of the body. Adapted from Lowry (1943).

3.2.3 Lipids.

Lipids are fats and fat like substances, found mainly in cells of adipose (fatty) tissues, and in the membranes of cells. Most lipids are esters of fatty acids and have an average molecular weight of 700 a.m.u. (Giese, 1979). Lipids are insoluble in water, but are a vital part of cell membrane, allowing the transfer of ions and molecules between intracellular water and surrounding body fluids.

3.2.4 Salts.

Approximately one percent of total body weight is accounted for by the salts dissolved in water present within the body. Both intracellular and extracellular waters contain many different types of dissolved salts, which are vital for the body to function. The ionic profile of the water present in the body is of importance when discussing the complex dielectric properties.

Tables 3.1 - 3.3 show the typical ionic profiles of the different types of electrolyte in the human body. Ionic concentrations are expressed in terms of the millequivalent weight (mEq), which is given by

$$\text{mEq} = \frac{\text{Gram Molar Weight}}{\text{Valence} \times 1000} \tag{3.2.1}$$

In extracellular plasma and interstitial liquids, the dominant ions are the Na^+ and the Cl^- ions. Thus an aqueous solution of 0.15 molar sodium chloride solution is generally used to model extracellular fluids.

The intracellular fluid contains fewer sodium and chloride ions. Instead there are a large number of K^+ (potassium) and HPO_4^{--} (hydrogen phosphate) ions. Gorton (1996) used an aqueous solution of 0.1 molar K_2HPO_4 as an intracellular fluid phantom to investigate the complex dielectric properties at 3 GHz of intracellular fluid. Gorton found both the dielectric constant and loss factor of the intracellular fluid phantom were very similar to that of an aqueous solution of 0.15 molar sodium chloride solution. Thus the complex dielectric properties at 3 GHz can be modelled by an aqueous solution of 0.15 molar saline.

INTRACELLULAR FLUID			
Cations	**Concentration (mEq/l)**	**Anions**	**Concentration (mEq/l)**
K^{++}	160	Cl^{-}	3
Ca^{++}	2	HPO_4^{--}	100
Na^{+}	10	HCO_3^{-}	10
Mg^{++}	26	SO_4^{-}	20
		Proteins	65
Total = 198 mEq/l		Total = 198 mEq/l	

Tables 3.1 Ionic Profile of Intracellular Fluid. Adapted from Brook and Brook (1980).

EXTRACELLULAR PLASMA			
Cations	**Concentration (mEq/l)**	**Anions**	**Concentration (mEq/l)**
K^{++}	4	Cl^{-}	101
Ca^{++}	5	HPO_4^{--}	2
Na^{+}	142	HCO_3^{-}	27
Mg^{++}	2	SO_4^{-}	1
		Proteins	6
		Organic acids	16
Total = 153 mEq/l		Total = 153 mEq/l	

Tables 3.2 Ionic Profile of Plasma. Adapted from Brook and Brook (1980).

INTERSTITIAL FLUID			
Cations	**Concentration (mEq/l)**	**Anions**	**Concentration (mEq/l)**
K^{++}	4	Cl^{-}	114
Ca^{++}	5	HPO_4^{--}	2
Na^{+}	145	HCO_3^{-}	31
Mg^{++}	2	SO_4^{-}	1
		Proteins	7
		Organic acids	1
Total = 156 mEq/l		Total = 156 mEq/l	

Tables 3.3 Ionic Profile of Interstitial Fluid. Adapted from Brook and Brook (1980).

3.3 Mixture Equations for Modelling Biological Materials.

In the study of biological materials, it is found that in order to comprehend the properties of tissue, the tissue must be modelled as a mixture of its components, rather than trying to predict its behaviour by treating tissue as a single material. Biological tissues must be considered as a combination of two or more individual substances each with its own distinct properties.

A mixture equation is used to predict the physical properties of a two phase material given the properties and relative abundance of each of the individual materials. There are, however, many different mixture equations. In order to predict the macroscopic properties of a composite material, assumptions have to be made about the microscopic structure of the material. Different assumptions of the way the two phases are positioned microscopically will give different macroscopic properties of the composite material.

Different investigators over the years have produced mixture equations for the thermal conductivity, thermal diffusivity, electrical permittivity, and other properties. However it was eventually realised these solutions could be grouped together and that the solution of one case was equally applicable to all the *transport coefficients*. This is "principle of generalised conductivity" (Batchelor, 1974).

In general terms, there is a general conductivity, λ, which is a proportionality constant between the general flux vector, **J**, and the general force, **F**.

$$\mathbf{J} = \lambda \mathbf{F} \tag{3.3.1}$$

If the material contains no source densities then

$$\operatorname{div} \mathbf{J} = 0 \tag{3.3.2}$$

At an interface between two phases, the normalised components of the flux are equal

$$\lambda_1 F_{n1} - \lambda_2 F_{n2} = 0 \tag{3.3.3}$$

The tangential forces are also equal

$$F_{t1} - F_{t2} = 0 \tag{3.3.4}$$

These equations are the general formulation for each of the transport coefficients. What **J, F** and λ are for some of the different transport cases is shown in table 3.4.

Generalised Conduction Case	**Flux Vector J**	**Generalised Force F**	**Generalised Conductivity λ**
Thermal	Heat Flux q	Temperature Gradient grad T	Thermal Conductivity k
Electrostatic	Electric Displacement **D**	Electric Field Intensity **E**	Static permittivity ε_s
Electrodynamic	Conduction Current Density **j**	Electric Field Intensity **E**	Static Conductivity σ_s
Magnetostatic	Magnetic Flux Density **B**	Magnetic Field Intensity **H**	Magnetic Permeability μ
Diffusion	Diffusion Flow M	Concentration Gradient grad C	Diffusion coefficient D

Table 3.4 Cases where a two phase system can be modelled with mixture equations to determine an effective conductivity.

For the remainder of this discussion on mixture equations we will use the terminology of thermal conductivity, but these mixture equations are equally applicable to thermal diffusivity or complex permittivity (Dukhin, 1971; Batchelor, 1974; Hale, 1976).

3.4 Bounds.

Wiener (1912) was first to considered the minimum and maximum limits of transport coefficients. Using a method based on capacitance theory, Wiener considered a mixture to consist of a collection of fibres, lying either parallel or perpendicular to the plates. This gives the upper, k^+, and the lower, k^-, limits of the thermal conductivity of a mixture of materials 1 and 2 as

$$\frac{1}{k^-} = \frac{\phi_1}{k_1} + \frac{(1-\phi_1)}{k_2} \qquad \text{Parallel} \qquad (3.4.1)$$

and

$$k^+ = \phi_1 k_1 + (1-\phi_1)k_2 \qquad \text{Series} \qquad (3.4.2)$$

where ϕ_1 is the *volume* fraction of material 1 and k_1, k_2 are the thermal conductivities of materials 1 and 2 respectively.

Hashin and Shtrikman (1961) obtained more rigorous limits, by maximising and minimising the Gibbs free energy of a mixture in the case of magnetic permeability. This gives the limits of the thermal conductivity, for $k_2 > k_1$, as

$$\frac{k^+ - k_2}{k^+ + 2k_2} = \frac{k_1 - k_2}{k_1 + 2k_2}\phi_1 \qquad (3.4.3)$$

and

$$\frac{k^- - k_1}{k^- + 2k_1} = \frac{k_2 - k_1}{k_2 + 2k_1}(1-\phi_1) \qquad (3.4.4)$$

These bounds make no assumptions about the geometry of the material. The only requirement is that, for the volume considered, the bulk properties of the composite material may be assumed to isotropic and homogeneous. The Hashin and Shtrikman limits always lie within those found by Wiener.

3.5 Maxwell's Mixture Equation.

The first mixture equation was proposed by Maxwell (1881), when he considered the electrical conductivity of a dilute suspension of spherical particles. Corresponding results have been found by Einstein (1906), Wiener (1912), Wagner (1914) and Taylor (1932) for different transport coefficients.

When a small volume of spheres, with thermal conductivity k_1, are suspended in matrix, with thermal conductivity k_2, the thermal conductivity of the composite material, k_{mix}, is given by

$$\frac{k_{mix}-k_2}{k_{mix}+2k_2}=\frac{k_1-k_2}{k_1+2k_2}\phi_1 \qquad (3.5.1)$$

Since this equation has been proposed by many different authors in many different fields, it is referred to by a number of different names. However, it is most commonly called Maxwell's mixture equation.

This equation assumes that the distance between the spheres is great enough that there is no interaction between the spheres. Thus, it is only applicable in mixtures where the concentration of the suspension is low.

Comparing the limits found by Hashin and Shtrikman, given by equations 3.3.3 and 3.3.4, with Maxwell's mixture equation, similarities become apparent. For a mixture where $k_2 > k_1$, the thermal conductivity is bounded above by a suspension of spherical particles of medium 1 in matrix medium 2 and is bounded below by a suspension of spherical particles of medium 2 in matrix medium 1.

3.5.1 Extensions of Maxwell's Mixture Equation.

Fricke (1924) extended Maxwell's mixture equation to allow the suspended particles to be oblate or prolate spheroids. A form factor, x, which is a function of the axial ration, a/b, and the generalised conductivity, is introduced to Maxwell's mixture equation to give the Maxwell-Fricke equation

$$\frac{k_{mix}-k_2}{k_{mix}+xk_2}=\frac{k_1-k_2}{k_1+xk_2}\phi_1 \qquad (3.5.2)$$

The form factor is given by

$$x = \frac{k_1(1-\gamma) - k_2}{k_1 - k_2(1+\gamma)} \tag{3.5.3}$$

where γ is given by

$$\gamma = \frac{(k_1 - k_2)}{3}\left(\frac{2}{k_2 + (k_1 - k_2)M/2} + \frac{1}{k_1 - (k_1 - k_2)M}\right) \tag{3.5.4}$$

For oblate spheroids,

$$M(a<b) = \frac{(\theta - \frac{1}{2}\sin 2\theta)}{\sin^3\theta}\cos\theta \qquad \cos\theta = \frac{a}{b} \tag{3.5.6}$$

and for prolate spheroids

$$M(a>b) = \frac{1}{\sin^2\theta'} - \frac{1}{2}\frac{\cos^2\theta'}{\sin^3\theta'}\log\left(\frac{1+\sin\theta'}{1-\sin\theta'}\right) \qquad \cos\theta' = \frac{b}{a} \tag{3.5.7}$$

If $a = b$ then both equations 3.5.6 and 3.5.7 give $M = 2/3$, setting $x = 2$. Thus the Maxwell-Fricke equation returns to Maxwell's mixture equation for the case of spheres. This theory was extended again by Velick and Gorin (1940) to allow for ellipsoids with all three axes different. The solution is complex and would only be applicable to substances where the geometry of the suspended particle was accurately known.

Chiew and Glandt (1983) proposed a new form of Maxwell's mixture equation. If the original Maxwell equation is expanded in a series of the form

$$\frac{k_{mix}}{k_2} = 1 + K_1\phi_1 + K_2\phi_1^2 + \ldots\ldots \tag{3.5.8}$$

then only the first order term, $K_1 = 3\beta$, is exact, where $\beta = (k_1 - k_2)/(k_1 + 2k_2)$, the reduced thermal polarizability. Chiew and Glandt extended Maxwell's equation so it was exact for terms of the order of ϕ^2

$$k_{mix} = \frac{1 + 2\beta\phi_1 + (K_2 - 3\beta^2)\phi_1^2}{1 - \beta\phi_1} \tag{3.5.9}$$

where $K_2 = K_2^{(0)} + K_2^{(1)}\phi_1$ were $K_2^{(0)}$ and $K_2^{(1)}$ are functions of the thermal conductivity of the medium and the suspended spheres. If $K_2 = 3\beta^2$ then equation 3.5.9 reduces back to Maxwell's mixture equation.

Another application of Maxwell's mixture equation was first considered by Maxwell himself. Maxwell examined the electrical conductance of a shell covered sphere. A suspension of such spheres may prove to be a more realistic simulation of biological tissue.

The equivalent conductivity of a sphere, k_{sphere}, consisting of a inner core, radius r, surrounded by shell of thickness d, is given by

$$\frac{k_{sphere}-k_{shell}}{k_{sphere}+2k_{shell}}=\left(\frac{r}{r+d}\right)^3\frac{k_{core}-k_{shell}}{k_{core}+2k_{shell}} \qquad (3.5.10)$$

where k_{core} and k_{shell} are the thermal conductivities of the inner core and outer shell respectively. The value k_{sphere} can then be used as the conductivity of the suspended spheres in Maxwell's mixture equation. Like all the equations derived from Maxwell's mixture equation, this equation, in theory, only applies to dilute suspensions of non interacting particles.

3.6 Bruggeman's Equation.

All the equations discussed in section 3.5 apply in the case of dilute systems only. At higher concentrations, the interactions between the particles of the suspended material become important. If the spatial distribution of the suspended particles was strictly ordered, the interactions between the suspended particles could be accounted for. However, in real composite materials, the particles are distributed randomly in space.

One solution to this problem is to use *self-consistent theory*, in which it is assumed that each particle is surrounded by composite material, with a thermal conductivity k_{mix}, rather than the matrix, with thermal conductivity k_2 (Hale, 1976).

Bruggeman (1935) examined the case of a high concentration of spherical particles in a matrix. Let a mixture, thermal conductivity k, contain a disperse phase of thermal conductivity k_1 which is suspended in a matrix of thermal conductivity k_2. Then let there be a small increase in the fractional volume concentration of the disperse phase from ϕ_1' to $\phi_1'+\delta\phi_1'$, causing an increase of δk in the mixture conductivity. Maxwell's mixture equation (3.5.1) can then be applied using k as the matrix conductivity, $k+\delta k$ as the mixture conductivity and using the volume fraction $\delta\phi_1'/(1-\phi_1')$. This gives

$$\frac{\delta k(k_1+2k)}{(3k+\delta k)(k_1-k)}=\frac{\delta\phi_1'}{(1-\phi_1')} \tag{3.6.1}$$

which for small δk becomes

$$\frac{\delta k(k_1+2k)}{3k(k_1-k)}=\frac{\delta\phi_1'}{(1-\phi_1')} \tag{3.6.2}$$

Integrating this expression from the matrix conductivity, k_2, to the mixture conductivity, k_{mix}, and from 0 to ϕ_1 gives Bruggeman's equation

$$\left(\frac{k_2}{k_{mix}}\right)^{\frac{1}{3}}\left(\frac{k_1-k_{mix}}{k_1-k_2}\right)=(1-\phi_1) \tag{3.6.3}$$

3.7 Other Mixture Equations.

Rayleigh (1892) derived an equation for cylindrical or spherical particles arranged uniformly at the lattice points of a simple cubic lattice. His equation, as corrected by Runge (1925) is

$$\frac{k_{mix}}{k_2}=1+3\phi_1\left(\frac{k_1+2k_2}{k_1-k_2}-\phi_1-0.525\frac{k_1-k_2}{k_1+\frac{4}{3}k_2}\phi_1^{\frac{10}{3}}\right)^{-1} \tag{3.7.1}$$

This equation is the beginning of a series expansion. At low concentrations, the $\phi_1^{10/3}$ term will become negligible compared to the other terms. In this case, the equation becomes Maxwell's mixture equation leading some authors to refer to Maxwell's mixture equation (3.5.1) as the Rayleigh mixture formula.

Polder and Van Santen (1946) derived a general equation for a random suspension of ellipsoid particles

$$k_{mix}=k_2+\frac{(k_1-k_2)\phi_1}{3}\sum_{i=1}^{3}\frac{k_m}{k_m+A_i(k_1-k_m)} \tag{3.7.2}$$

where k_m is the effective mean thermal conductivity of the medium around each particle and A_i is the depolarisation factor given by

$$A_i=\frac{a_1a_2a_3}{2}\int_0^{\infty}\frac{d\lambda}{(\lambda+a_i^2)\sqrt{(\lambda+a_1^2)(\lambda+a_2^2)(\lambda+a_3^2)}} \tag{3.7.3}$$

where a_1, a_2, a_3 are the semi-axes of the ellipsoids. While equation 3.7.2 is too complex to be of use in modelling biological tissues, the limiting cases of this equation for spherical particles are of interest.

When the suspended particles are spheres, $A_i = \frac{1}{3}$ and when the suspension is concentrated $k_m = k_{mix}$. Putting these values into equation 3.7.2 gives Böttcher's Equation.

$$\frac{k_{mix} - k_2}{3k_{mix}} = \frac{(k_1 - k_2)}{k_1 + 2k_{mix}}\phi_1 \tag{3.7.4}$$

In fact, Böttcher (1945) had derived this equation using a self consistent scheme approach before Polder and Van Santen showed it to be a particular case of their equation.

The low concentration limit of equation 3.7.2 is given by setting $k_m = k_2$, giving an equation which was later derived directly by Landau and Lifshitz (1959).

$$\frac{k_{mix} - k_2}{3k_1} = \frac{(k_1 - k_2)}{k_1 + 2k_2}\phi_1 \tag{3.7.5}$$

Boned and Peyrelasse (1983) took this low concentration limit and, using an argument similar to that used to derive Bruggeman's Equation, derived the following expression for high concentration ellipsoidal suspensions

$$(1-\phi_1) = \left(\frac{k_2}{k_{mix}}\right)^{3d}\left(\frac{k_1 - k_{mix}}{k_1 - k_2}\right)\left(\frac{k_2 - rk_1}{k_{mix} - rk_1}\right)^{R}\left(\frac{k_2 - qk_{mix}}{k_{mix} - qk_2}\right)^{Q} \tag{3.7.6}$$

where d, r, R, q and Q are all functions of the semi-major axes of the ellipsoids. In the case of spheres, equation 3.7.6 reduces to Bruggeman's Equation.

Lichteneker (1929) and Looyenga (1965) have both proposed simple mixture equations which are considered to be fundamentally flawed despite being supported by some experimental evidence. Lichteneker proposed a logarithmic form of mixture equation

$$\log k_{mix} = \phi_1 \log k_1 + (1-\phi_1)\log k_2 \tag{3.7.7}$$

Looyenga's mixture equation states

$$k_{mix}^{\frac{1}{3}} = \phi_1 k_1^{\frac{1}{3}} + (1-\phi_1)k_2^{\frac{1}{3}} \tag{3.7.8}$$

However, Dukhin (1971) pointed out that both Lichteneker's and Looyenga's equations were flawed, since both equations require the disperse phase of the composite material to be both random and ordered at the same time. In addition, Dukhin noted Looyenga's

equation had been derived more rigorously by Landau and Lifshitz (1959), who had found that the equation only applied when the conductivities of the two materials were similar i.e. $|k_2 - k_1| << k_{mix}$.

3.8 Experimental Verification of Mixture Equations.

The success of Maxwell's mixture equation in predicting the behaviour of the a two phase system has been shown by many researchers, for many different transport coefficients (Chiew and Glandt, 1983).

Fricke and Morse (1925) measured the electrical conductivity of spherical cream particles in skimmed milk, over a frequency range of 1600 Hz to 200 KHz. The measured values were found to agree to within 0.5% with those given by the Maxwell equation up to a concentration of 62%.

Fricke (1925) also examined the electrical conductivity of red corpuscles in blood, comparing the results with his own version of Maxwell's equation. Fricke assumed the axial ratio of the red corpuscles was $1/4.25$ and found that the measured values agreed to within 0.5% of those theorised up to a concentration of 80%. Velick and Gorin (1940) also verified their equation at volume fractions up to 50% for suspensions of duck's blood in saline.

These results are surprising, since correlations between the measured and the theoretical values are shown at concentrations far greater than the dilute suspensions for which Maxwell's mixture equation is strictly valid. Lewin (1947) examined electrical conductivity and suggested, in the case of non conducting suspensions, the term dilute applied up to the stage where neighbouring spheres where touching each other.

Other researchers have found that how well Maxwell's equation predicts the generalised conductivity at higher volume fractions is dependant on $\alpha = k_1/k_2$. Turner (1975) found that Maxwell's equation holds adequately provided α and the volume fraction of the dispersed phase are "not both high". Chiew and Glandt (1983) examined the thermal conductivity of mixtures and estimated the highest volume fraction of the disperse phase for which the Maxwell equation could still be said to be applicable. Figure 3.2 shows

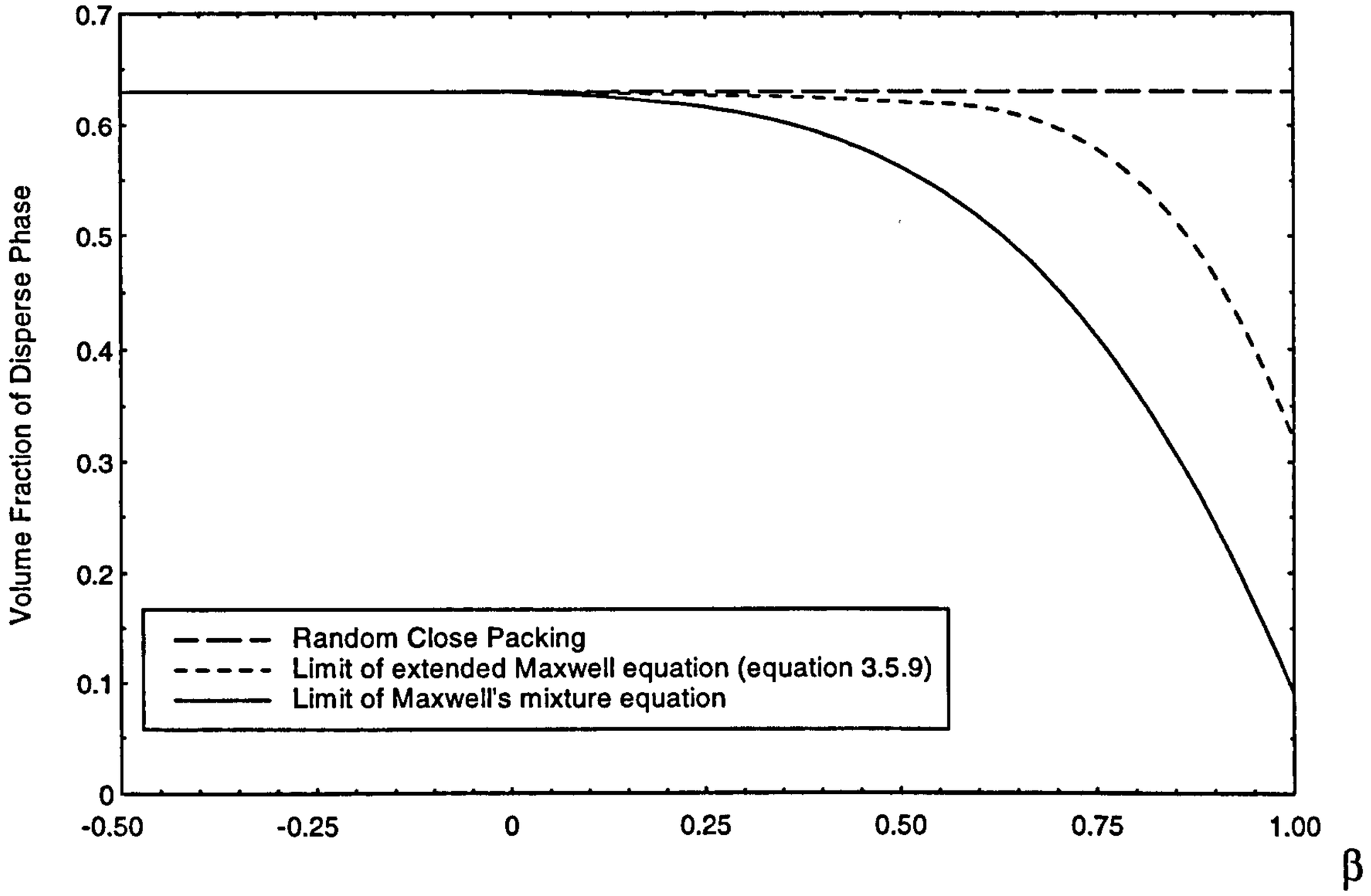

Figure 3.2 The estimated limit of applicability of Maxwell's mixture equation and the extended Maxwell equation (equation 3.5.9) as a function of β, the reduced thermal polarizability, where $\beta = {(k_1 - k_2)}/{(k_1 + 2k_2)}$.

Adapted from Chiew and Glandt (1983).

this upper limit for Maxwell's mixture equation and the extended Maxwell mixture equation 3.5.9 which was proposed by Chiew and Glandt. The upper limit is bounded by ϕ_c, which corresponds to close packing.

Bruggeman (1935) examined the static permittivity of mixtures of water, alcohol and paraffin oil to demonstrate the validity of his equation. Hania and Koizumi (1975) examined the complex permittivity of water/oil emulsions over a range of 20 Hz to 3 GHz. They reported that Bruggeman's equation predicted the permittivity more reliably than Maxwell's mixture equation and they also reported good agreement at disperse volume fractions up to 80%.

Dukhin (1971) examined the data of several authors who had measured the dielectric constant of systems of spherical particles in a continuum and concluded that for $\phi_1 < 0.1$ Maxwell's mixture equation applies with "excellent accuracy". Also, as the volume concentration increased, the dielectric constant will lie somewhere between the values given by Maxwell's Equation and Bruggeman's equation with Bruggeman's equation generally giving the better estimation. Further, Dukhin also notes that both Böttcher's equation and Polder and Van Santen's equation (3.7.2) only give good agreement with measured values when the conductivities of the two materials were similar.

Since the success of Maxwell's mixture equation and Bruggeman's equation have been widely verified, it is these two equations which will be used to analyse the behaviour of biological systems. The other mixture equations are less suitable for use in this study. There is no information on the microscopic structure of the samples being examined. This means that equations which require this knowledge, such as the Fricke-Maxwell equation, are of limited use. Lichteneker's equation is considered flawed while Looyenga's equation, Böttcher's equation and Polder and Van Santen's equation have been found, theoretically or experimentally, only to apply when the conductivities of the two materials are similar.

3.9 Applicability of Mixture Equations to Biological Tissue.

Mixture equations are only truly applicable to predicting the behaviour of mixtures of two non-interacting substances. One of the basic assumptions of mixture equations is that there is no interaction between the two phases of the mixture, and the success of

mixture equations in predicting the required property is no longer guaranteed if the two phases of the mixture interact.

However the two main constituents in biological tissues do have a degree of interaction. Water is a polar molecule capable of forming dipole bonds with other molecular species. In biological tissues, a fraction of the water molecules hydrogen bond to the protein molecules. This bound water has physical and biological properties which often differ from that of free water. Approximately 0.4 grams of water is bound per gram of protein (Cornillon et al, 1995; Gorton, 1996).

3.9.1 Dielectric Behaviour of Water / Protein Mixtures.

To illustrate the problems that hydrogen bonding can cause in mixture equations, figure 3.3 shows the complex permittivity, at a frequency of 3 GHz, of an aqueous solution of ethylene glycol. As can be seen, the dielectric constant (ε') is still modelled extremely well, by both Maxwell's and Bruggeman's equations. However, the loss factor (ε'') shows behaviour which markedly deviates from that predicted by the mixture equations. In biological tissue, the effect of the hydrogen bonding of water on the complex permittivity is different. In the aqueous solution considered above, the dielectric behaviour of both the ethylene glycol and the water were altered by hydrogen bonding. In biological tissue, only the dielectric behaviour of the water molecules are changed and the behaviour of the protein itself is unchanged. When hydrogen bonds are formed between protein and water, the huge size of the protein macromolecules compared to the water molecules means that the protein molecules are not affected by the bonding. Thus biological tissue can be thought of as containing three distinct materials, which are free water, bound water and protein, and there is no need to consider new cross species states with unknown behaviour. For a full discussion of the effect of bound water on the permittivity of biological tissues see Gorton (1996).

The variation of the complex permittivity of free water, ice and bound water with frequency is shown in figure 3.4, which shows that the behaviour of the complex permittivity is far closer to that of free water than that of ice. While the frequency at which bound water has maximum loss is a factor of 10 less than that of free water, it is a factor of a hundred thousand greater than that of ice, which can be considered as water

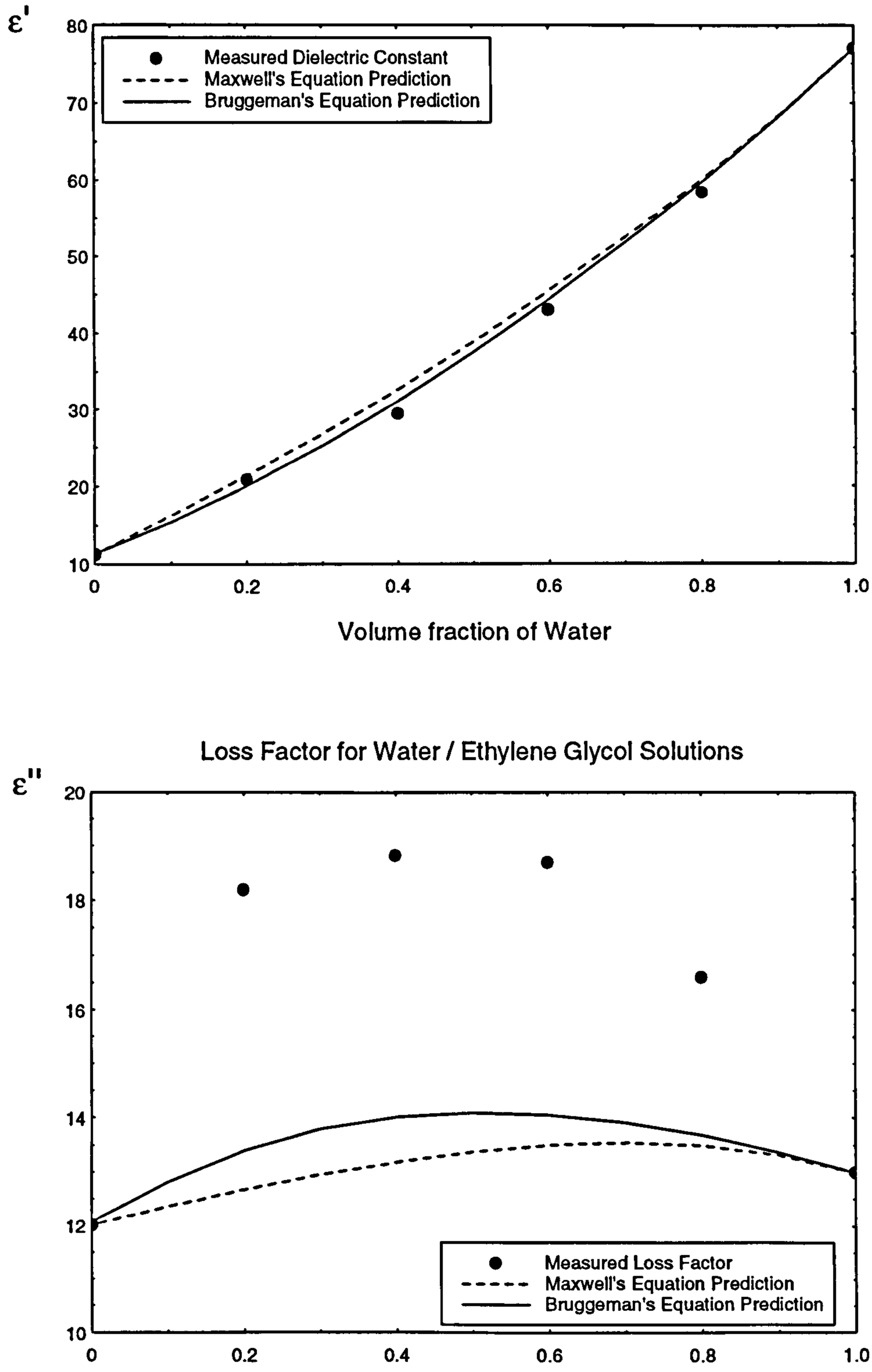

Figure 3.3 Comparison between Maxwell and Bruggeman predictions and the measured complex permittivity for an aqueous solution of ethylene glycol. Adapted from Gorton (1996).

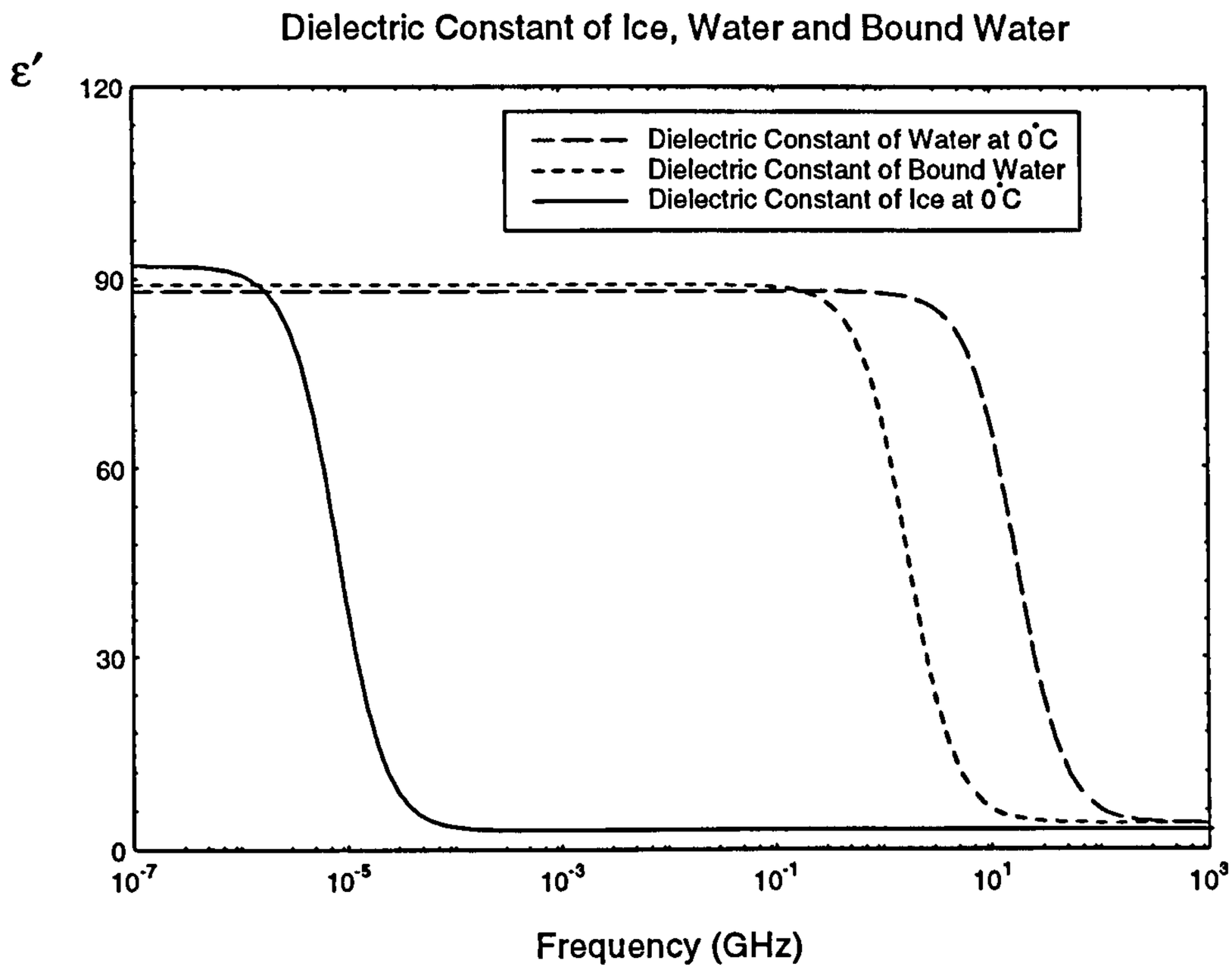

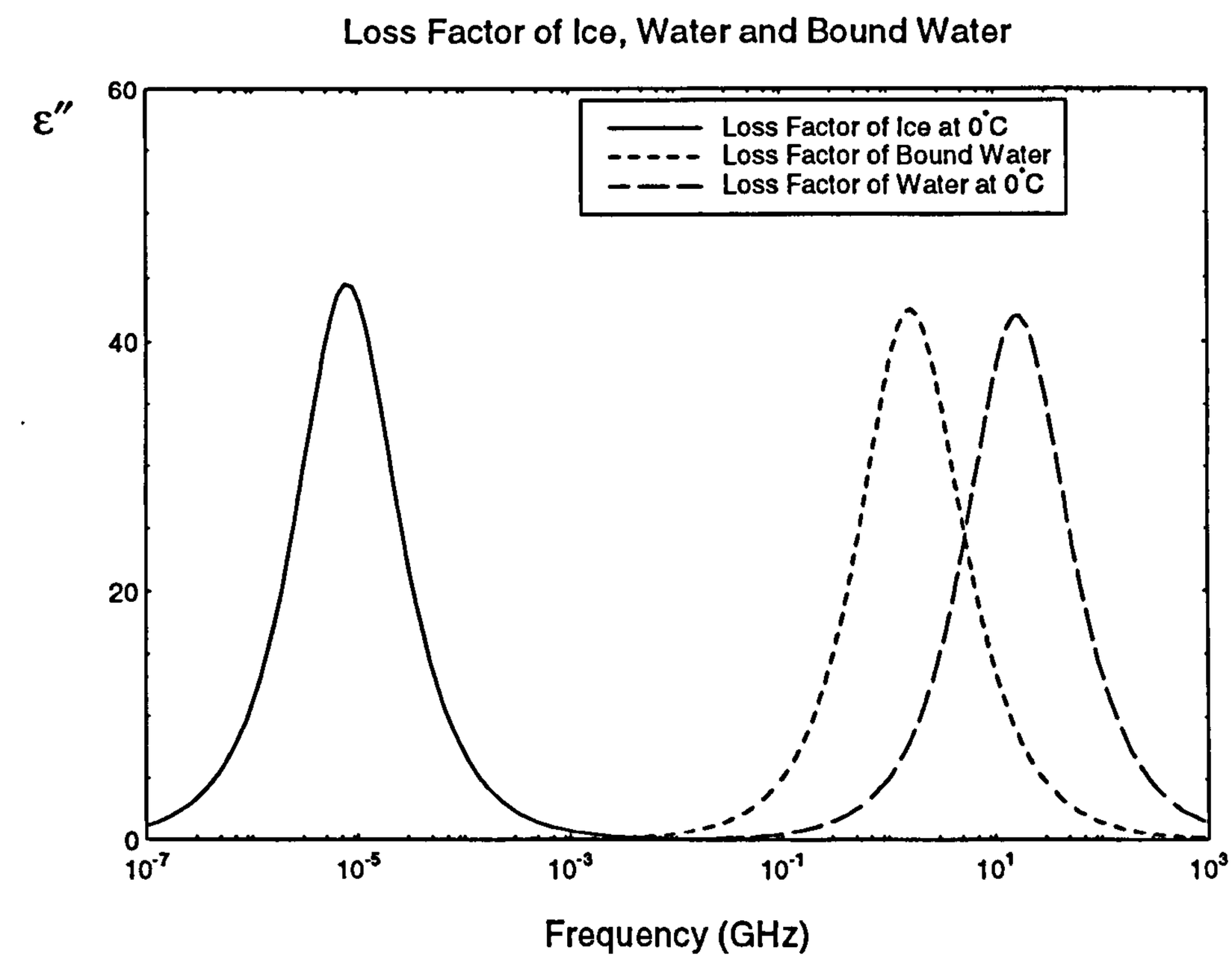

Figure 3.4 Schematic variation with frequency of the dielectric constant and loss factor for ice, bound water typical of that found in biological tissues and free water. Adapted from Schawn (1965).

which is hydrogen bonded to the maximum possible extent. This indicates that the bonding between water and protein in biological tissues is far weaker than the strong bonding found in ice.

3.9.2 The Thermal Behaviour of Bound Water.

Given the bonding in water-protein mixtures is far weaker than that found in ice, it would be expected that the thermal behaviour of the bound water found in biological tissues should be similar to that of free water and this is what is found. Foster et al (1984) examined the thermal and electrical conductivity of an aqueous polyethylene oxide solution in a comparative approach to understand the behaviour of bound water in tissue. Foster et al found that there was no significant deviation in the thermal conductivity of the mixture from that estimated by Maxwell's mixture equation for free water and polyethylene oxide. However the bound water present in the mixture caused the measured electrical conductivity to be significantly lower than that predicted by Maxwell's mixture equation.

Miles et al (1983) examined the thermal conductivity, specific heat and density of meats and other foodstuffs. By examining results produced by other researchers, it was found that, for unfrozen foodstuffs, there was no need to consider bound water and free water separately when modelling these properties.

For frozen protein and water mixtures, the thermophysical behaviour is slightly more complex. Figure 3.5 shows the behaviour of a 10% gelatin in water gel. The thermal conductivity was measured and used to estimate the mass fractions of each of the constituents. This shows that above freezing, there is no distinction between bound and free water. But below freezing there remains a fraction of the total water content which has the thermal conductivity of unfrozen water. This corresponds to the amount of bound water in the gel. Even below freezing bound water has the thermal characteristics of unbound water. This has lead to the bound water present in water protein mixtures to be called "unfreezable water" (Cornillon et al, 1995; Renaud, 1992).

Since this thesis deals only with biological tissues at temperatures well above the freezing point of water, the thermal conductivity, specific heat and density of bound water will be assumed as that of free water and there will no distinction made between the two forms

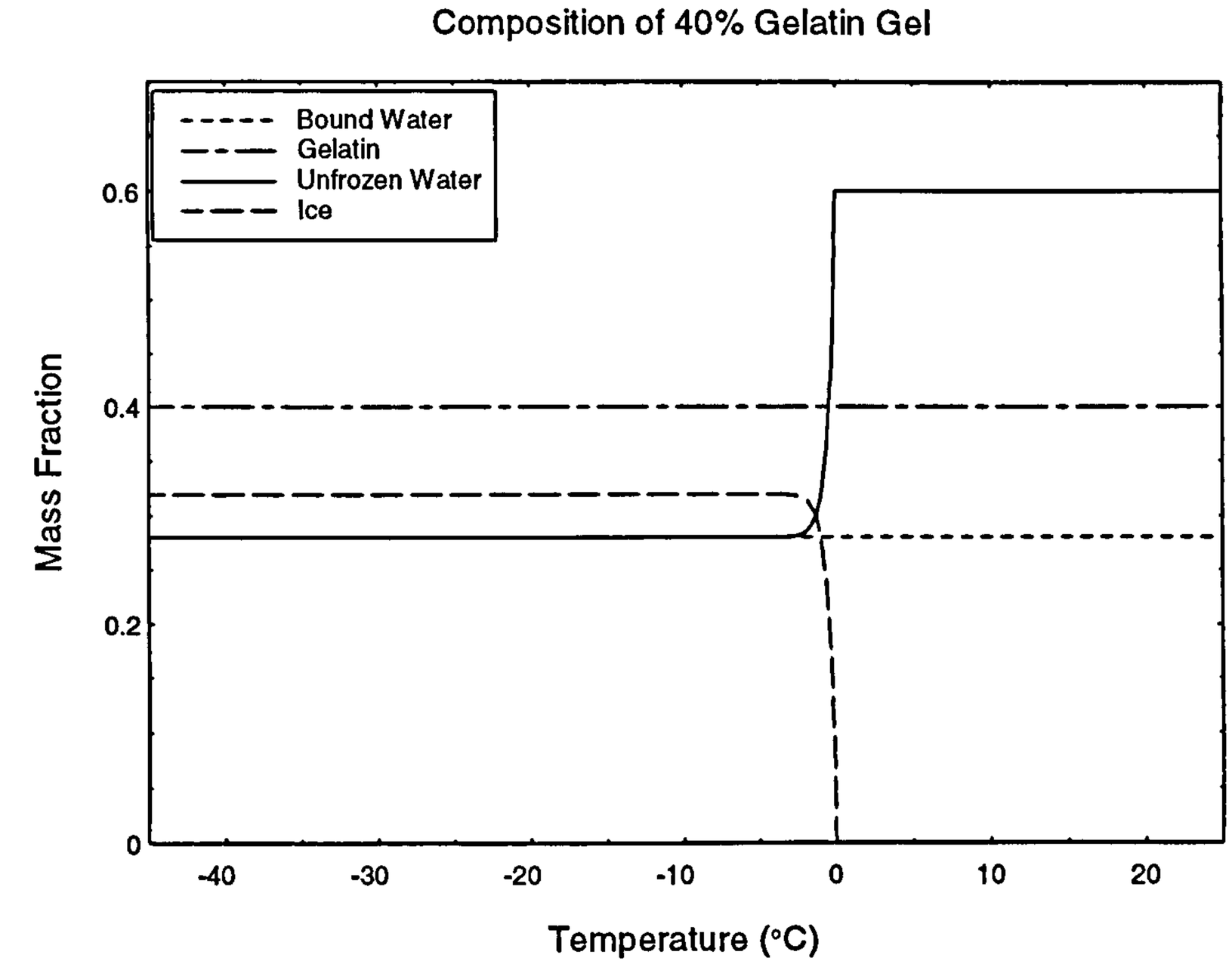

Figure 3.5 The fractional mass content of a gelatin and water gel estimated from the measured thermal conductivity. Adapted from Renaud et al (1992).

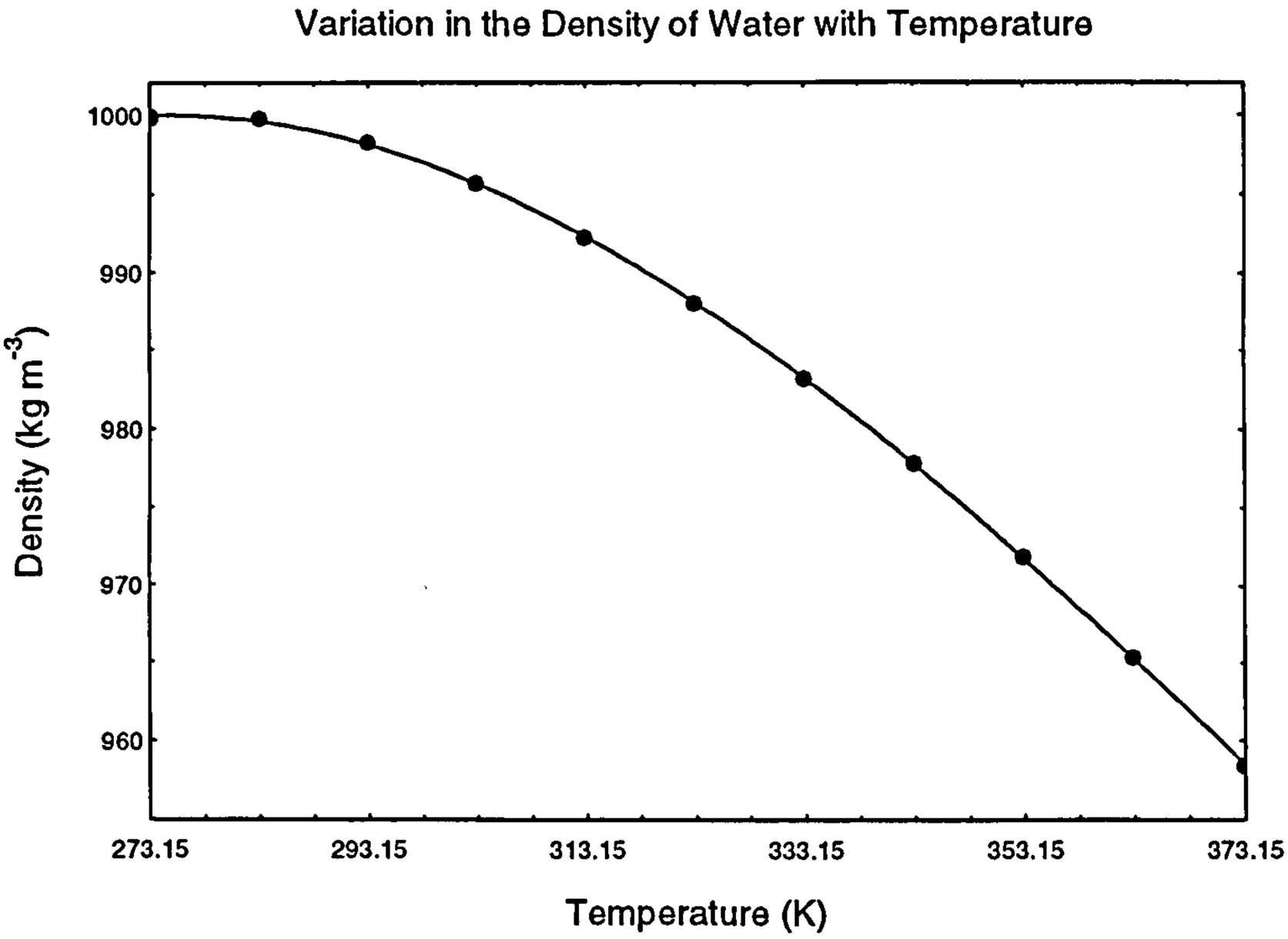

Figure 3.6 The CRC Handbook of Chemistry and Physics (1993) data and the cubic fit of the variation of the density of water with temperature.

of water found in the body. Also, from the definition of the thermal diffusivity $\alpha = {}^{k}/_{\rho c_p}$, where ρ is the density and c_p the specific heat, the thermal diffusivity of bound water will also be equal to that of free water.

3.10 The Thermal Properties of Water.

The thermophysical properties of water have been widely measured and the thermal conductivity, density and specific heat are all accurately known.

3.10.1 The Thermal Conductivity of Water.

The thermal conductivity of water has been measured by many different researchers. The cubic fit of the data given in The CRC Handbook of Chemistry of Physics (1993) gives the thermal conductivity of water, k_w, as

$$k_w = -0.498411 + 0.00517006T - 2.91489\times10^{-6}T^2 - 6.66278\times10^{-9}T^3 \quad (3.10.1)$$

where T is the temperature in Kelvin. The values given by this equation agree to within $< 0.5\%$ of the values given by Touloukian et al (1970a), who examined the experimental values in over 60 works and derived the following equation for the thermal conductivity of water

$$k_w = -0.58179 + 6.35704\times10^{-3}T - 7.96625\times10^{-6}T^2 \quad (3.10.2)$$

Equation 3.10.1 was eventually chosen to give thermal conductivity of water since it gave the best fit to experimental thermal diffusivity data (see below).

3.10.2 The Specific Heat of Water.

Touloukian and Makita (1970) give the specific heat at constant pressure, c_{pw} as

$$c_{pw} = 8952.67 - 40.5069T + 0.112355T^2 - 1.01311\times10^{-4}T^3 \quad (3.10.3)$$

Touloukin and Makita note that since water is the material most studied as a reference material in the measurement of heat capacity, c_{pw} is known extremely accurately. This is

supported by the fact that The CRC Handbook for Chemistry and Physics agrees to within $< 0.1\%$ of the values given by the equation 3.10.3.

3.10.3 The Density of Water.

The density of water is also extremely well known. Figure 3.6 shows the variation of the density of water with temperature. The cubic fit of this data is

$$\rho_w = 233.172 + 6.76474T - 0.0187743T^2 + 1.56896\times10^{-5}T^3 \qquad (3.10.3)$$

The maximum deviation between the CRC Handbook for Chemistry and Physics data and the cubic fit of the data is $< 0.014\%$.

3.10.4 The Thermal Diffusivity of Water.

Since there exists little data produced by the measurement of the thermal diffusivity of water directly, the thermal diffusivity of water is calculated directly from the definition of thermal diffusivity, $\alpha_w = {k_w}/{\rho_w c_{pw}}$.

The data that does exist was used to check which of the expressions would be used to give the thermal conductivity of water. Figure 3.7 compares the experimental data given by Touloukian et al (1970b) with the thermal diffusivities given using the conductivities given by equations 3.10.1 and 3.10.2. This shows that equation 3.10.1 gives the better estimation of the thermal diffusivity and hence is used as the expression to give the thermal conductivity of water.

3.11 The Thermal Properties of Protein.

The accuracy to which the thermophysical properties of water are known, is in stark contrast to the information known about the properties of protein. As indicated previously, the protein present in the human body contains many different types of molecule of widely ranging weights. Thus there is not one fixed value of thermal conductivity, as found in water, but a range of values dependant on the make up of the protein being examined. Since there is no fixed value for the thermal conductivity or

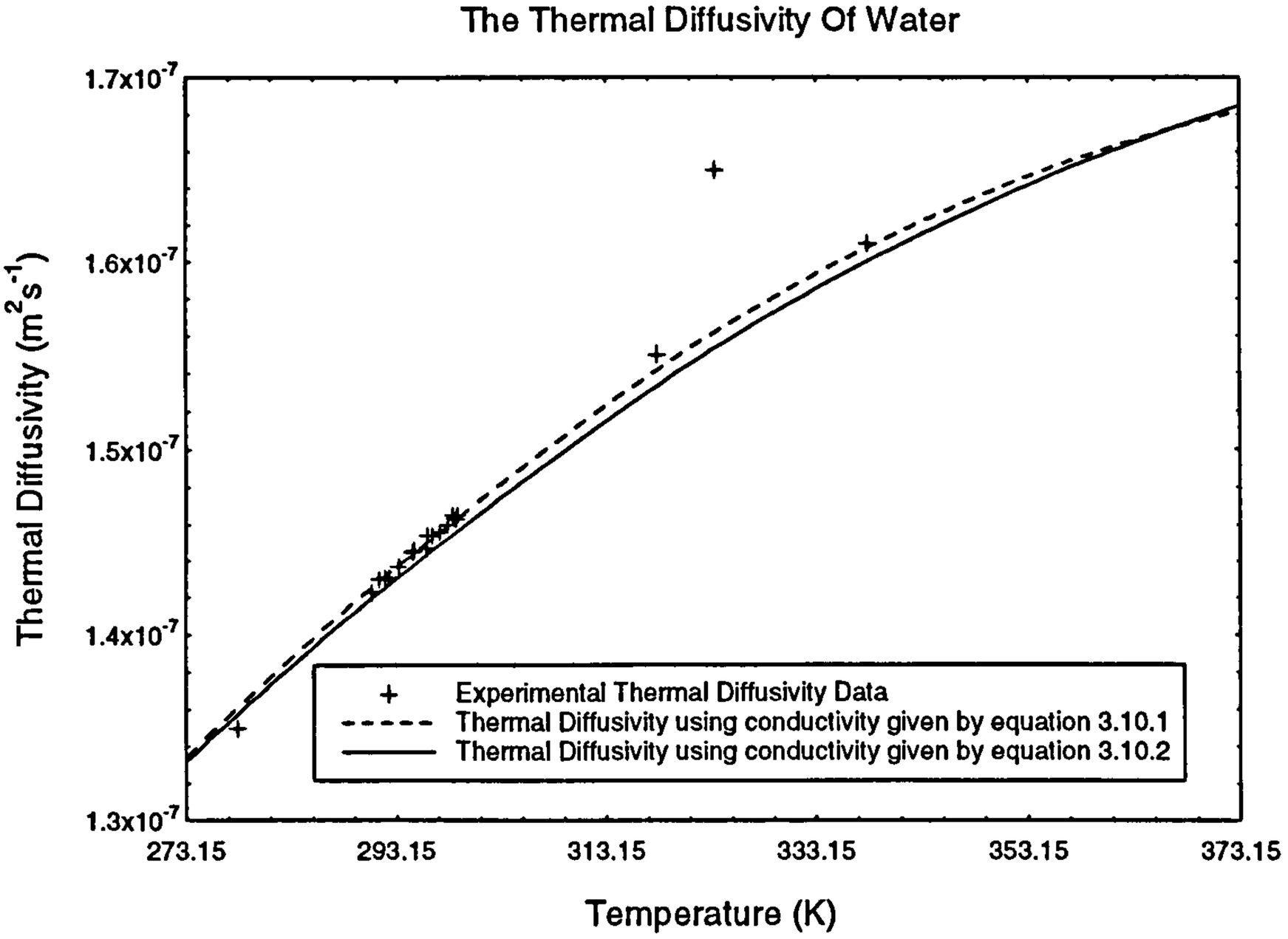

Figure 3.7 Comparison between the thermal diffusivity estimated using the thermal conductivity data given by Touloukian et al (1970a) and The CRC Handbook of Chemistry and Physics (1993) and measured values given by Touloukian et al (1970b).

thermal diffusivity of protein, this section will examine the range of values rather than trying to find a single value.

3.11.1 The Thermal Conductivity of Protein.

The "intrinsic" thermal conductivity of proteins can not be measured directly. This is due to the porous structure of protein, which means that a protein specimen is filled with air or water. If the thermal conductivity of a dry protein is measured directly, what is in reality being measured is the thermal conductivity of a protein-air mixture. Thus the thermal conductivity of protein must be measured indirectly (Kong et al, 1982a).

The most common method is to measure the thermal conductivity of protein-water gels at various concentrations of the protein and then use a mixture equation and work backwards to find the "intrinsic" thermal conductivity. This introduces an extra source of uncertainty to the thermal conductivity of protein, since different mixture equations will give different estimates of the thermal conductivity. Kong et al (1982b) found that, for various proteins, the series model (equation 3.4.2) produced the best estimate of the thermal conductivity since it best described the behaviour seen in the protein-water gels.

Another technique for measuring the thermal conductivity of proteins is discussed in Sakiyama et al (1991). This method does not involve mixture equations, thus removing a source of uncertainty. This technique is based on the principle that when a mixture has the thermal conductivity of the liquid phase, the solid phase must also have that thermal conductivity. Sakiyama et al used gelatin in an solution of aqueous 2-propanol, varying the relative amounts of 2-propanol and water, while keeping the relative amount of gelatin fixed. The thermal conductivity of aqueous 2-propanol solution is well known and thus the thermal conductivity of the gelatin can be found.

Table 3.5 shows the thermal conductivities of various proteins. Gelatin is an animal protein product derived from the hides of cattle and albumin is a protein found in eggs. This table shows a wide spread in values of the thermal conductivity.

Even in a single material such as gelatin, there is a wide range of values given for thermal conductivity. The parallel fit clearly does not give a good representation of the behaviour of the aqueous gelatin solution. The other data tends to suggest a thermal

Protein	Thermal Conductivity ($Wm^{-1}K^{-1}$)	Reference
Gelatin	0.281 (Series) 0.088 (Parallel) 0.179 (Maxwell)	Kong et al (1982a)
Gelatin	0.31-0.33 (Series)	Andrieu et al (1986)
Gelatin	$0.303 + 0.0012T - 2.27 \times 10^{-6} T^2$ (Series)	Renaud et al (1992)
Gelatin	0.340 (Series) 0.237 (Parallel) 0.280 (Maxwell)	Pongsawatmanit et al (1993)
Gelatin	0.28-0.30 (Varying Liquid Phase)	Sakiyama et al (1991)
Albumin	0.238 (Series) 0.168 (Maxwell)	Kong et al (1982b)
Albumin	0.268 - 0.0025T (Series)	Renaud et al (1992)
Albumin	0.377 (Series) 0.237 (Parallel) 0.280 (Maxwell)	Pongsawatmanit et al (1993)
Wheat Gluten	0.219 (Series) 0.148 (Maxwell)	Kong et al (1982b)
Milk Casein	0.200 (Series) 0.131 (Maxwell)	Kong et al (1982b)
Soy Protein	0.300 (Series)	Kong et al (1982b)
Unspecified	0.180	Poppendiek et al (1966)
Unspecified	$0.1788 + 1.196 \times 10^{-3} T - 2.718 \times 10^{-6} T^2$	Choi and Okos (1986)
Unspecified	0.200	Miles et al (1993)

Table 3.5 The thermal conductivity of various proteins. T is the temperature in Celsius. Series, Parallel and Maxwell refer to the type of fit used to produce the data. Varying Liquid Phases refers to technique of varying the thermal conductivity of the liquid phase.

conductivity of gelatin in the region of 0.3 $Wm^{-1}K^{-1}$ which agrees with Sakiyama (1991) whose data was independent of a mixture equation model.

3.11.2 The Specific Heat, Density and Thermal Diffusivity of Protein.

Firstly, the specific heat and density of protein are considered. Table 3.6 shows the specific heat of various proteins. As with the thermal conductivity, the specific heat is calculated indirectly by measuring the specific heat of protein-water gels . Generally the specific heat is then calculated by assuming that the specific heat of the gel is linearly dependant on the mass fractions of the constituents.

Again the spread in values is noticeable. The value for gelatin was extrapolated by Duck (1990) from data produced by Hampton and Mennie (1934). The Hampton and Mennie data shows significant variation in the measured heat capacity as the proportion of gelatin increases. Kong et al (1982a) also examined the Hampton and Mennie data and argued that taking just the high water content data (which has least deviation) would give a specific heat, for gelatin, of approximately 2250 $Jkg^{-1}K^{-1}$ compared to the 1190 $Jkg^{-1}K^{-1}$ given by Duck.

Table 3.7 shows the density of protein. The density of protein does not require indirect measurement. There is less variation in the density than there is in the thermal conductivity or specific heat.

The thermal diffusivity of protein has not been established by many researchers and the large variations in the properties of protein mean that it is impossible to obtain a meaningful range of values of the thermal diffusivity of protein using the minimum and maximum values shown in tables 3.5, 3.6 and 3.7. For example, using the values in these tables, the minimum value of the thermal diffusivity of gelatin is 0.290×10^{-7} m^2s^{-1} and the maximum value is 2.070×10^{-7} m^2s^{-1}.

However if the values stated for the thermal conductivity, specific heat and density by each individual researcher are used to find the thermal diffusivity, a better indication of the range of values for the thermal diffusivity of protein is obtained.

Table 3.8 shows the thermal diffusivity of various proteins. Choi and Okos (1986) were the only authors to give the thermal diffusivity of protein directly. Kong et al (1982a, b), Andrieu et al (1986) and Miyawaka et al (1988) all measured the thermal diffusivity of

Protein	Specific Heat ($Jkg^{-1}K^{-1}$)	Reference
Gelatin	2250	Kong et al (1982a)
Gelatin	1940	Andrieu et al (1986)
Gelatin	1190	Duck (1990)
Albumen	1660	Bull and Breeze (1968)
Wheat Gluten	1300	Kong et al (1982b)
Milk Casein	1300	Kong et al (1982b)
Unspecified	1900	Miles et al (1983)
Unspecified	$2008 + 1.209T - 1.313\times10^{-3}T^2$	Choi and Okos (1986)
Unspecified	1260	Miyawaki et al (1988)
Unspecified	2000	Cornillon et al (1995)

Table 3.6 The specific heat of various proteins. T is the temperature in °C.

Material	Density (kgm^{-3})	Reference
Gelatin	1380	Andrieu et al (1986)
Albumin	1280	Bull and Breeze (1968)
Unspecified	1300	Schepps and Foster (1980)
Unspecified	1380	Miles et al (1983)
Unspecified	$1330-0.5184T$	Choi and Okos (1986)
Unspecified	1300	Miyawaki et al (1988)
Unspecified	1330	Miyawaki and Pongsawatmanit (1994)

Table 3.7 The density of various proteins. T is the temperature in °C.

protein-water gels but they then used estimates of the specific heat and density of protein to give the thermal conductivity of the gels. Mixture equations were then used to estimate the thermal conductivity of protein. The values stated in table 3.8 are calculated from the author's estimates of the thermal conductivity, specific heat and density of protein rather than values calculated directly from the thermal diffusivity data.

As with the thermal conductivity, there is a large spread of values. The value given by Miyawaka et al (1988) gives a thermal diffusivity well above that of water. This does not agree with the other data and is ignored. The other data suggests that the thermal diffusivity of protein lies in the region $0.6\text{-}1.2\times10^{-7}$ m^2s^{-1}.

As stated at the beginning of this section, the variation in the thermal properties of protein, as given by other authors, make it impossible to give definite values for the thermal conductivity and thermal diffusivity of protein. However, the data does serve to indicate a range of possible values for the thermal properties of protein. It can be assumed that the thermal conductivity of protein lies in the range 0.15 - 0.35 $Wm^{-1}K^{-1}$ while the thermal diffusivity of protein lies in the range 0.6×10^{-7} - 1.2×10^{-7} m^2s^{-1}. The density of protein is better known and in this study it is assumed that the density of protein is 1300 kgm^{-3} unless otherwise stated.

Protein	Thermal Diffusivity ($\times 10^{-7} m^2 s^{-1}$)	Reference
Gelatin	0.961 (Series) 0.612 (Maxwell)	Kong et al (1982a)
Gelatin	1.158 (Series)	Andrieu et al (1986)
Albumin	1.144 (Series) 0.808 (Maxwell)	Kong et al (1982b)
Wheat Gluten	1.296 (Series) 0.876 (Maxwell)	Kong et al (1982b)
Milk Casein	1.183 (Series) 0.775 (Maxwell)	Kong et al (1982b)
Soy Protein	1.813 (Series)	Miyawaka et al (1988)
Unspecified	$0.68714 + 4.7578\times10^{-3}T - 1.4646\times10^{-5}T^2$	Choi and Okos (1986)
Unspecified	0.763	Miles et al (1993)

Table 3.8 The thermal diffusivity of various proteins. T is temperature in Celsius. Series and Maxwell refer to the type of fit used to find the thermal conductivity of the protein.

Chapter 4: Measuring the Thermal Properties of Biological Tissue.

4.1 Introduction.

In this chapter, the self heated thermistor probe method of measuring thermal properties is examined. First, the criteria required for the measurement of the thermal conductivity of biomaterials are stated and a number of different measurement methods are examined. Then the theory behind the thermistor probe is examined and expressions are determined for the thermal conductivity and the thermal diffusivity of materials as measured by the probe. The use of the technique to measure the thermal properties of biomaterials is then discussed. Next the calibration of the probe is examined and the thermal conductivity and thermal diffusivity of mixtures of the calibration materials, agar gelled water and glycerol, are determined. Finally the accuracy of the probe technique is examined.

4.2 Required Characteristics for a Thermal Conductivity Measurement Technique.

When choosing a technique to measure the thermal conductivity of human and animal tissues, a number of factors must be considered.

Firstly, the geometry of the samples must be considered. Human tissue samples are often small and the anatomy of the organ being examined can also put restrictions on the sample size. Also biological tissues tend to be inhomogeneous, so the technique used should be able to examine a volume of tissue as small as reasonably possible to limit the variation in the thermophysical properties.

Further, since a large number of samples were being examined, the technique used to measure the thermal conductivity of the biological samples must be reasonably simple and not require excessively long measurement periods which may also degrade the sample.

Also, as part of a program of combined thermal and dielectric tissue modelling, a colleague measured the complex permittivity at 3 GHz of all the samples. Thus the measurement of the thermal conductivity should not render the sample useless for measurement of the complex permittivity, and should enable the complex permittivity to be measured in approximately the same volume as the thermal conductivity.

Finally, as the water content of every sample investigated was measured after the thermal and microwave properties were examined, the measurement procedure should not damage or degrade the tissue prior to establishing the water content.

Each of these requirements must be fulfilled for a technique to be able to be used in this study to measure the thermal conductivity of tissues.

4.3 Steady State Methods.

Steady state methods are, historically, the most commonly used techniques of measuring the thermal conductivity of biomaterials. These techniques subject a sample to a temperature gradient which is time invariant. The measured sample geometry is of a simple planar or cylindrical design.

In the planar design, which is also known as the *guarded hot plate technique*, the sample is placed in between two parallel plates, one which heats the sample and the other which is at a fixed temperature. The planar sample is thin enough, compared to the area of the plates, that all the heat flow can be considered normal to the plates and radial heat flow can be ignored. To ensure that there no heat flow in the radial direction, the sample is surrounded by a ring of thermal insulator. When steady state conditions are achieved, the thermal conductivity, k, is simply given by

$$k = \frac{qd}{A\Delta T} \tag{4.3.1}$$

where A is the area of the plates, q the heat supplied, d the thickness of the sample and ΔT being the temperature difference of the two plates. Poppendiek et al (1966) used the guarded hot plate method to measure the thermal conductivity of a wide range of biological tissues and fluids, while Kvadsheim et al (1996) used a similar technique to measure the conductivity of whale blubber.

The cylindrical form is based on the same principle with an inner heating cylinder and outer cylinder at fixed temperature. The sample is thin enough that all the heat can be considered to flow in a radial direction. In steady state conditions, the conductivity is given by

$$k = \frac{q \ln(r_2/r_1)}{2\pi L \Delta T} \qquad (4.3.2)$$

where L is the length of the cylinder and r_2 and r_1 are the outer and inner radii of the cylinders. Such a method was used by Pongsawatmanit et al (1993) to measure the thermal conductivity of various aqueous protein gels.

Steady state methods have the advantage of being accurate and simple. However, steady state methods give no information about the transient behaviour of a sample and hence give no information about the thermal diffusivity. Also these techniques require samples which correspond to the required geometry, i.e. thin planar or cylindrical samples. Hence this technique is difficult to apply when measuring the thermal conductivity of biological tissues.

4.4 Semi-invasive and Non-invasive Techniques.

There have been a number of non-steady state techniques used to measure the thermal conductivity of biological samples which do not involve inserting a heat source into the tissue. These techniques have the advantage of giving information about the transient behaviour of the sample. This information is given by the *thermal inertia*, $k\rho c$, or the *thermal diffusivity*, $\alpha = k/\rho c_p$, where ρ is the density and c_p is the specific heat.

Some of these techniques can be used for measuring the thermal conductivity of biological tissues *in-vivo*, as well as *in-vitro*. It must be remembered that when the in-vivo thermal conductivity is measured it is an *effective* conductivity, dependant not only on the type of tissue but other factors, such as the rate of blood flow in the volume being sampled. Thus the in-vivo conductivity is dependant on external factors, unlike the in-vitro conductivity.

Further, the in-vivo thermal conductivity can be affected by the act of measuring the thermal conductivity. The thermoregulatory system will respond to the changes in skin temperature caused by measuring the in-vivo thermal properties of tissue. The in-vivo thermal conductivity measured is not the normal effective conductivity, but the effective conductivity when the body is responding to the temperature change in the skin produced by the measurement procedure.

In semi-invasive techniques, thermocouples are inserted into the tissue and the tissue surface is heated, either with a contact heater or electromagnetic radiation. In non-invasive techniques, electromagnetic radiation is used to heat the tissue, with the subsequent variation in the tissue surface temperature with time being measured using a infra-red detector or thermocouples. Both methods give information about the thermal inertia.

Non-invasive techniques have been more widely investigated than semi-invasive techniques. Derksen et al (1957) examined the in-vivo thermal inertia of human skin using various radiation sources, measuring the skin's surface temperature with thermocouples. Lipkin and Hardy (1954) used a non-invasive technique to find the in-vitro thermal inertia of muscle, skin and fat and the in-vivo thermal inertia of skin. Renaud et al (1992) used a variation of the non-invasive technique when investigating the thermal inertia of various gels, by measuring the variation in temperature on the opposite surface of disk shaped sample to that surface which was heated.

Clearly the methods which allow for in-vivo measurement can only be used close to the skins surface. Semi-invasive techniques may give information about the variation of temperature with depth, if many thermocouples are used, but there is the added difficulty of accurately determining the position of the thermocouples. Non-invasive techniques can give no information about the variation of temperature with depth and will just give an average thermal inertia. This is important for in-vivo measurement, where the thermal properties of the tissues close to the surface of the skin can vary widely (Cui and Barbenel, 1991).

Another technique which has be used to measure both the in-vivo and in-vitro thermal inertia of biological materials was explored by Vendrik and Vos (1957). This technique used the principle that if two semi-infinite, homogenous bodies, each at uniform but different temperatures, are brought in contact with each other, the interface temperature takes a value solely dependent on the thermal inertia of the two bodies. However this method is considered flawed since biological tissues are not homogenous, neither of the bodies is semi-infinite, and the tissue will not be a uniform temperature in the case of in-vivo measurement.

All the techniques in this section suffer from one major drawback. These techniques only give the thermal inertia, and assumptions about the density and specific heat must be

made to allow the thermal conductivity to be indirectly estimated. Also, all these techniques require relatively large tissue samples / regions.

Non-invasive methods may have advantages for measuring the in-vivo thermal inertia, but semi-invasive and non-invasive techniques are of limited use in the measurement of the in-vitro thermal conductivity compared to the probe techniques described below.

4.5 Probe Techniques.

In recent years invasive probe techniques have overtaken the guarded hot plate method as the most common technique of measuring the thermal conductivity of biological tissues. In invasive probe techniques, a heat source is inserted into tissue and the temperature is monitored by an invasive sensor. There have been a few methods where the heater and temperature sensor are housed in different probes. However these methods suffer a number of difficulties, the greatest of which is accurately determining the position of the temperature sensor with respect to the heater. Thus most systems now used have the temperature sensor and heater forming one probe.

There are several different types of invasive probe used to measure the thermal conductivity and thermal diffusivity of biological tissue. In the heated thermocouple and hot wire probes, a separate heater and temperature sensor are housed in the same probe. In the thermistor probe, the thermistor serves as both heat supply source and temperature sensor.

The heated thermocouple and hot wire probes are both based on the same idea but have different assumed geometry. In the heated thermocouple probe, a heater and thermocouple are housed in a small cylindrical probe. Generally the probe will be a several millimetres long and about a millimetre in diameter. Despite the cylindrical geometry of the probe, it is assumed to be spherical when finding the thermal conductivity. Gibbs (1933), Levy et al (1967) and Grayson et al (1971) have all used this system to monitor the blood flow in various animal organs by measuring the effective thermal conductivity.

The hot wire technique has been far more widely used than the heated thermocouple technique. In the hot wire technique, the heater and thermocouple are contained in a long thin metal cylinder, usually a hypodermic needle. Generally the probe will be

several centimetres long and about a millimetre in diameter. Thus the probe is long enough that all heat flow is considered to be in the radial direction.

This method has been widely used in the measurement of the thermal conductivity and thermal diffusivity of biological tissue, both in-vitro and in-vivo. Cooper and Trezek (1971, 1972) measured the in-vitro thermal conductivity and diffusivity of various human organs. Liang et al (1991) measured the in-vitro conductivity of various porcine organs and the in-vivo conductivity of live snake head and Renaud et al (1992) measured the thermal conductivity of various protein / water solutions.

This technique provides a reasonably accurate method of determining the thermal properties of biological tissues. However this technique requires large tissue samples compared to the samples required for the self-heated thermistor technique used in this study (see below).

4.6 The Thermistor Probe.

The technique finally chosen to measure the thermal properties of biological tissues was the self heated thermistor probe method. This is now a widely used technique for measuring the thermal conductivity and thermal diffusivity of biomaterials and fulfils all the required criteria. The probe can measure the thermal properties of small tissue samples and it is a reasonably simple method which does not require unduly long measurement times. This technique will also not degrade the tissue sample, allowing the sample to have its microwave properties and water content measured.

There are two different techniques of heating the thermistor which can be used to measure the thermal properties of samples. The first is "thermal pulse decay" method. In this technique, power is applied to the thermistor for a few seconds. After the power pulse, the thermistor acts solely as a temperature sensor with the rate of temperature decrease being measured and compared to the theoretically calculated temperature decay. Arkin et al (1986a, b) used this technique to find the in-vivo thermal conductivity and blood perfusion in order to check the accuracy of thermal models such as those described in chapter 2.

In the other method, which was the one used in this study, the power to the thermistor is varied so that the temperature observed in the thermistor is constant, and the probe

temperature remains at a temperature ΔT above the initial equilibrium temperature. This method is discussed in detail in the rest of the chapter.

4.7 Spherical Heat Source Model.

The thermistor probe technique was first proposed by Chato (1968). Chato assumed that the thermistor could be modelled by a spherical heat source in an infinite medium. For an in-vitro tissue sample, there are no internal heat sources and thus, assuming the tissue is uniform and isotropic, the temperature in the medium is governed by the diffusion equation

$$\frac{\partial v_m}{\partial t} = \alpha \nabla^2 (v_m) = \alpha \left(\frac{\partial^2 v_m}{\partial r^2} + \frac{2}{r} \frac{\partial v_m}{\partial r} \right) \tag{4.7.1}$$

where $v_m = T - T_0$ where T is the temperature of the medium at time t and T_0 is temperature of the medium before heating commences.

Assuming that heating commences at a $t = 0$ and that the probe is held at a temperature T_R after heating commences then the boundary conditions are given by

$$\left.\begin{array}{llll} T = T_0 & \text{at} \quad t = 0 & r > a \\ T = T_a & \text{at} \quad t > 0 & r = a \\ T = T_0 & \text{at} \quad t > 0 & r \to \infty \end{array}\right\} \tag{4.7.2}$$

where a is the radius of the probe. This has a solution given by

$$\frac{T - T_0}{T_R - T_0} = \frac{R}{r} \text{erfc}\left(\frac{\text{r - R}}{2\sqrt{\alpha t}} \right) \tag{4.7.3}$$

where efrc(x) is defined by

$$\text{erfc}(x) = \frac{2}{\sqrt{\pi}} \int_x^{\infty} \exp(-u^2) du \tag{4.7.4}$$

The heat flow passing through the surface of the thermistor is given by

$$q = -4\pi R^2 k \left. \frac{\partial T}{\partial r} \right|_{r=R} \tag{4.7.5}$$

and thus

$$q = 4\pi R k \Delta T + \frac{4R^2 \sqrt{\pi k \rho c} \Delta T}{\sqrt{t}} \tag{4.7.6}$$

where $\Delta T = T_R - T_0$. Hence a graph of q against $t^{-1/2}$ should be a straight line with the intercept proportional to the thermal conductivity and the gradient proportional to $\sqrt{k\rho c}$ or $k/\sqrt{\alpha}$. Thus such a graph should yield the thermal conductivity and thermal inertia or thermal diffusivity (Carslaw and Jaeger, 1947; Chato, 1968).

However this method ran in difficulties when used in experimental situations. Chato found it impossible to calibrate the probe for the measurement of the thermal diffusivity. Further, it was found that the relative thermal properties of the probe and the biological material are such that this analysis does not apply. The solution only applies when the thermal conductivity of the sample is very much smaller than that of the bead and this is not the case for biological samples (Balasubramaniam and Bowman, 1974; Bowman et al, 1975).

4.8 A More Complete Model of the Thermistor Probe.

Given the failure of the spherical heat source model, Balasubramaniam and Bowman (1974) proposed a new model. This approach involved treating the thermistor bead as a distinct thermal mass and solving for the coupled thermal response of both the thermistor and the medium.

It was assumed that if thermistor was held as constant temperature ΔT above the initial equilibrium temperature, the heat generation term is dependant on $t^{-1/2}$, where t is the time form the start of heating, as Chato (1968) found. That is

$$q = \Gamma + \beta t^{-1/2} \tag{4.8.1}$$

And thus the expressions for the thermal behaviour of the thermistor bead and the medium are given, for $t > 0$, by

$$\frac{1}{r^2}\frac{\partial}{\partial r}\left(r^2 \frac{\partial v_b}{\partial r}\right) + \frac{\Gamma + \beta t^{-1/2}}{k_b} = \frac{1}{\alpha_b}\frac{\partial v_b}{\partial t} \qquad 0 \le r \le a \tag{4.8.2}$$

$$\frac{1}{r^2}\frac{\partial}{\partial r}\left(r^2 \frac{\partial v_m}{\partial r}\right) = \frac{1}{\alpha}\frac{\partial v_m}{\partial t} \qquad r \ge a \tag{4.8.3}$$

where a is the radius of the thermistor, v_b is the temperature rise in the thermistor, and v_m is the temperature rise in the medium. The thermal diffusivity of the thermistor and the

medium are given by α_b and α respectively, and k_b is the thermal conductivity of the thermistor bead.

The boundary conditions are given by

$$\left.\begin{array}{lll} v_b = v_m = 0 & \text{at} & t = 0 \\ v_b \text{ is finite} & \text{as } r \to 0 & t > 0 \\ v_m \text{ is finite} & \text{as } r \to \infty & t > 0 \\ v_b = v_m & \text{at } r = a & t > 0 \end{array}\right\} \qquad (4.8.4)$$

$$k_b \frac{\partial v_b}{\partial r} = k \frac{\partial v_m}{\partial r} \qquad \text{at } r = a \qquad t > 0$$

The solution to equations 4.8.2 and 4.8.3 given the boundary conditions given by equations 4.8.4 is

$$v_b(r,t) = \frac{a^2\Gamma}{k_b}\left\{\frac{1}{3}\frac{k_b}{k} + \frac{1}{6}\left(1 - \frac{r^2}{a^2}\right) - \frac{2ab}{\pi r}\int_0^\infty \frac{\exp\left(-\alpha y^2 t/a^2\right)(\sin y - y\cos y)\sin(ry/a)}{y^2[(c\sin y - y\cos y)^2 + b^2 y^2 \sin^2 y]}dy\right\} \qquad (4.8.5)$$

$$+ \frac{2\beta a}{k_b}\sqrt{\frac{\alpha_b}{\pi}}\int_0^\infty \frac{\exp\left(-\alpha y^2 t/a^2\right)}{y^2}\left\{-1 + \frac{ak}{rk_b}\frac{(y\cos y - c\sin y + by^2\sqrt{\alpha_b/\alpha}\sin y)\sin(ry/a)}{(c\sin y - y\cos y)^2 + b^2 y^2 \sin^2 y}\right\}dy$$

$$v_m(r,t) = \frac{a^3\Gamma}{rk_b}\left\{\frac{1}{3}\frac{k_b}{k}\right\}$$

$$- \frac{a^3\Gamma}{rk_b}\frac{2}{\pi r}\int_0^\infty \frac{\exp\left(-\alpha y^2 t/a^2\right)(\sin y - y\cos y)[by\sin y\cos\sigma y - (c\sin y - y\cos y)\sin\sigma y]}{y^3[(c\sin y - y\cos y)^2 + b^2 y^2 \sin^2 y]}dy \qquad (4.8.6)$$

$$- \frac{2\beta a^2}{k_b}\sqrt{\frac{\alpha_b}{\pi}}\int_0^\infty \frac{\exp\left(-\alpha y^2 t/a^2\right)(\sin y - y\cos y)[by\sin y\sin\sigma y + (c\sin y - y\cos y)\cos\sigma y]}{y^2[(c\sin y - y\cos y)^2 + b^2 y^2 \sin^2 y]}dy$$

where $b = \left(k_b/k\right)\sqrt{\alpha_b/\alpha}$, $c = 1 - k/k_b$, and $\sigma = \left(-1 + r/a\right)\sqrt{\alpha_b/\alpha}$ (Balasubramaniam and Bowman, 1974).

Examining equation 4.8.5, it can be seen that this equation can be written in the form

$$v_b(r,t) = v_{bss}(r) + v_{b\Gamma}(r,t) + v_{b\beta}(r,t) \qquad (4.8.7)$$

where $v_{bss}(r)$ is the steady state temperature distribution, and $v_{b\Gamma}(r,t)$ and $v_{b\beta}(r,t)$ are the non steady state temperature distributions dependant on Γ and β respectively.

Thus the volume averaged temperature in the thermistor bead at any time t can be expressed as

$$\overline{v_b}(t) = \Delta T + \overline{v_{b\Gamma}}(t) + \overline{v_{b\beta}}(t) \qquad (4.8.8)$$

where ΔT is the average steady state temperature rise. Since the thermistor is maintained at a constant temperature for all values of t, the average temperature rise must be equal to the average steady state temperature rise i.e.

$$\overline{v_b}(t) = \Delta T \tag{4.8.9}$$

This means that

$$\overline{v_{b\Gamma}}(t) = \overline{v_{b\beta}}(t) \tag{4.8.10}$$

The steady state temperature distribution of the thermistor bead is, from equation 4.8.5,

$$v_{bss}(r) = \frac{a\Gamma}{k_b}\left\{\frac{1}{3}\frac{k_b}{k} + \frac{1}{6}\left(1 - \frac{r^2}{a^2}\right)\right\} \tag{4.8.11}$$

The volume averaged steady state bead temperature rise is given by

$$\Delta T = \frac{1}{\frac{4}{3}\pi a^3}\int_0^a V_{bss}(r)4\pi r^2 dr \tag{4.8.12}$$

And from equation 4.8.9, the average temperature in the thermistor bead is

$$\Delta T = \frac{a^2\Gamma}{3k_b}\left(\frac{k_b}{k} + 0.2\right) \tag{4.8.13}$$

Hence the thermal conductivity of the medium can be written as

$$k = \frac{1}{\left(A\,{}^{\Delta T}\!/_{\Gamma} + B\right)} \tag{4.8.14}$$

where A and B are constants dependant solely on the probe (Balasubramabiam and Bowman, 1977).

To calculate an expression for the thermal diffusivity, equation 4.8.10 must be solved. The solving of this equation is complex and thus the method of solution is not explored in this thesis; just the expressions derived for the thermal diffusivity are given.

Valvano et al (1984) gave the solution to equation 4.8.10 as

$$\alpha = \left(\frac{G}{(1+Hk)\,{}^{\beta}\!/_{\Gamma}}\right)^2 \tag{4.8.15}$$

Where G and H are constants. This was later modified by Patel et al (1987) to

$$\alpha = \frac{1}{\left(C\,{}^{\beta}\!/_{\Gamma} + D\right)^2} \tag{4.8.16}$$

Where C and D are constants dependant solely on the thermistor. Equation 4.8.16 will be used to find the thermal diffusivity in this study and equation 4.8.14 will be used to find the thermal conductivity.

4.9 Experimental Apparatus and Procedure.

The apparatus used to measure the thermal conductivity and thermal diffusivity of the biological samples examined in this study is shown in figure 4.1.

The digital to analogue converter channels, *DAC 0* and *DAC 1*, in the PC-30 interface card were used to produce a voltage across the thermistor and series resistor. Two analogue to digital converters, *ADC 0* and *ADC 1*, were used to measure the voltages produced by *DAC 0* and *DAC 1*, V_0 and V_1 respectively. A third analogue to digital converter, *ADC 2*, was used to measure the voltage, V_2 dependant on the relative resistances of thermistor and the resistor.

Thus the resistance of the thermistor, R_T, is simply given by

$$R_T = R_f \frac{(V_0 - V_2)}{(V_2 - V_1)} \tag{4.9.1}$$

where R_f, is the fixed resistance of the resistor. The temperature dependence of the resistance of the thermistor is such that its temperature in Kelvin, T, is then given by

$$T = \frac{E}{\ln R_T + F} \tag{4.9.2}$$

where E and F are constants dependant on the thermistor.

Finite Element studies have shown that the effective volume of measurement in biological tissue for a thermistor probe is 5-10 thermistor radii (Hayes and Valvano, 1984). All three probes used in this study had diameters of approximately 1.6 mm and thus the minimum sample diameter was always greater than 16 mm.

To ensure accurate measurement, the sample must be in thermal equilibrium. The sample and the visible part of the probe were wrapped in a plastic film to ensure that no water could enter the sample and affect its thermal properties. This was then placed in a water bath where the water temperature was constant. The water bath temperature was set at 25°C, stabilised to ±0.05°C.

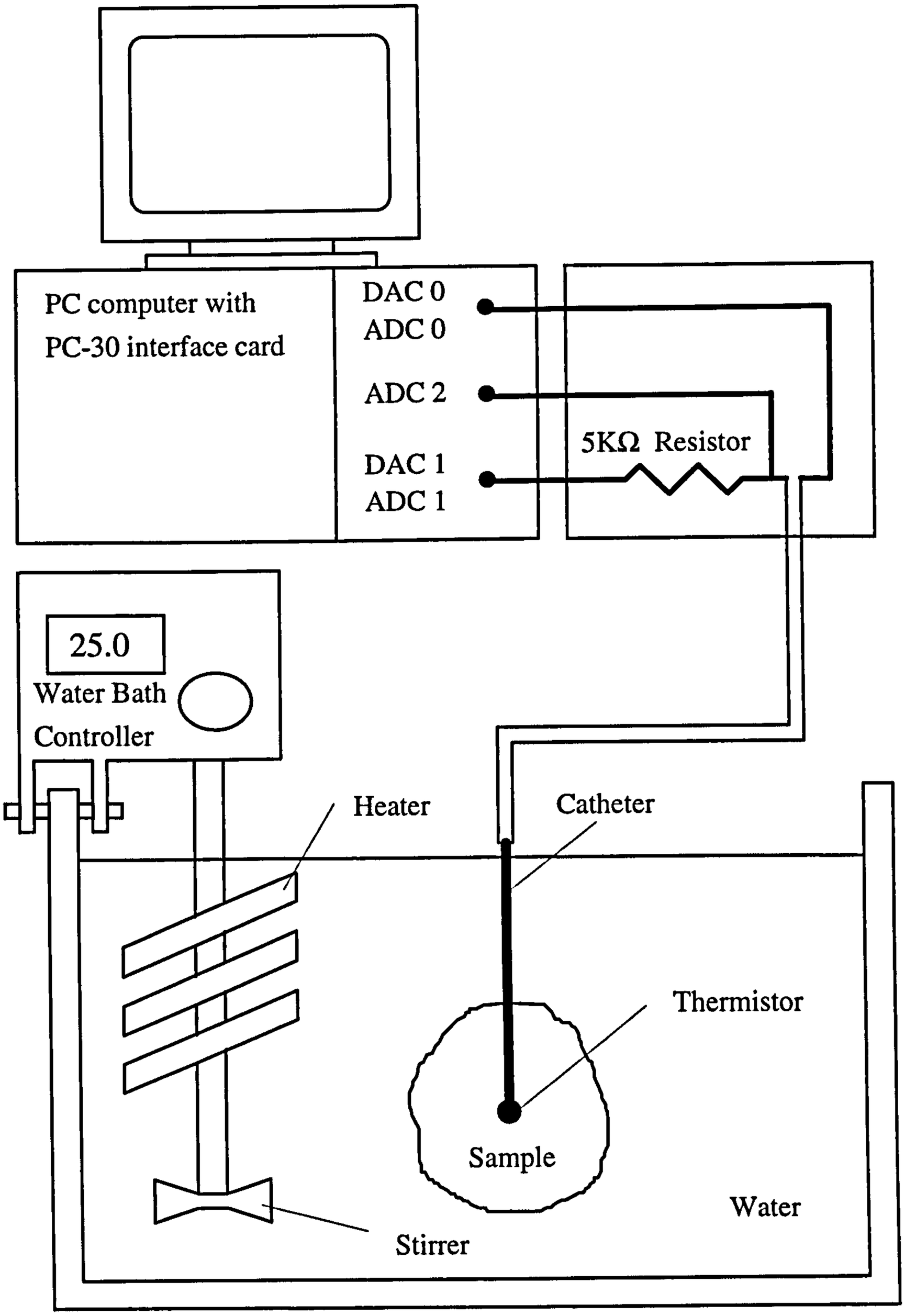

Figure 4.1 Schematic of the apparatus used.

The sample was allowed five minutes in the water bath to ensure it was thermally equilibrated before measurement began. The variation with temperature against time for a typical measurement run is shown in figure 4.2 and the variation in the power supplied to the thermistor with time is shown in figure 4.3.

For five seconds before the start of heating, the thermistor is used solely as a temperature sensor in order to establish the equilibrium temperature. For this, the voltage is set low enough not to cause any significant heating. At time, $t = 0$, the voltage is increased. The voltage is kept at a maximum level (~20V) for three seconds. The temperature rise at 3 seconds is then set as the temperature difference, ΔT. The temperature is then monitored and the voltage is varied in order to maintain this temperature difference ΔT. After twenty seconds the power is reduced and the thermistor starts to return to the equilibrium temperature. At forty seconds the experiment finishes and the voltage across the resistor and thermistor drops to zero. This process is repeated another 4 times for each sample, with five minutes between each measurement period to ensure the sample has time to return to equilibrium.

The heating curve of each experimental run is then analysed. A least squares fit of the power against $t^{-1/2}$, for the time period 5 to 19 seconds after the start of heating, is used in order to find β and Γ. Although in the theoretical argument in section 4.8, β and Γ are expressed in terms of heat generated per unit volume, it is easier just to use the heat generated in the probe in practice. The calibration constants adjust to allow this change. The thermal conductivity can then be found using $k = \left(A\,\Delta T/\Gamma + B\right)^{-1}$, and the thermal diffusivity can be found using $\alpha = \left(C\,\beta/\Gamma + D\right)^{-2}$.

4.10 Equipment Specifications and Accuracy.

In the PC-30 interface card, the analogue to digital channels and digital to analogue channels were set to the -10V to 10V range. The PC-30 card has 12 bit resolution, that is 1 in 4096. Thus the voltage resolution for both ADCs and DACs is approximately 5 mV.

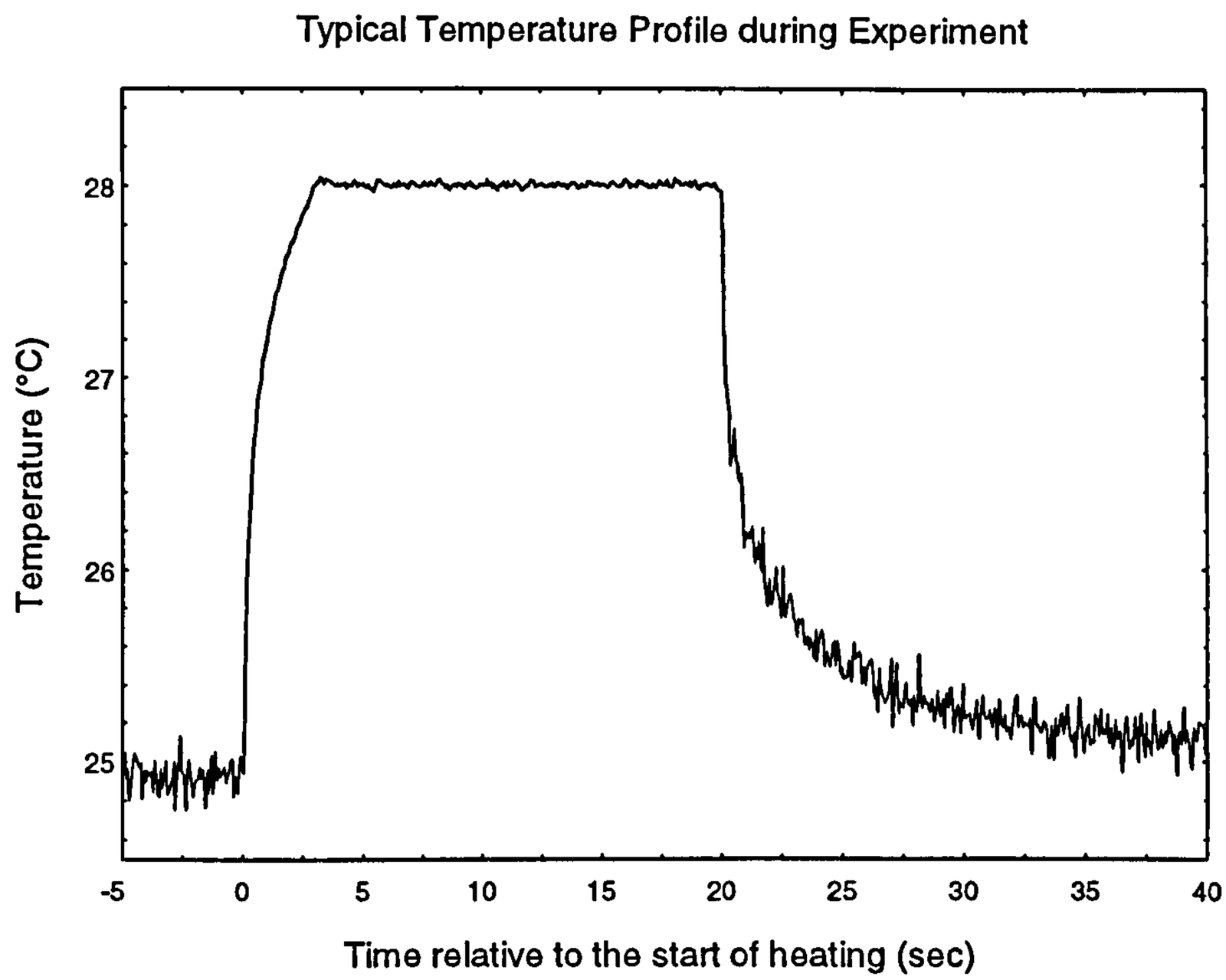

Figure 4.2 Typical variation in temperature with time during an experimental run.

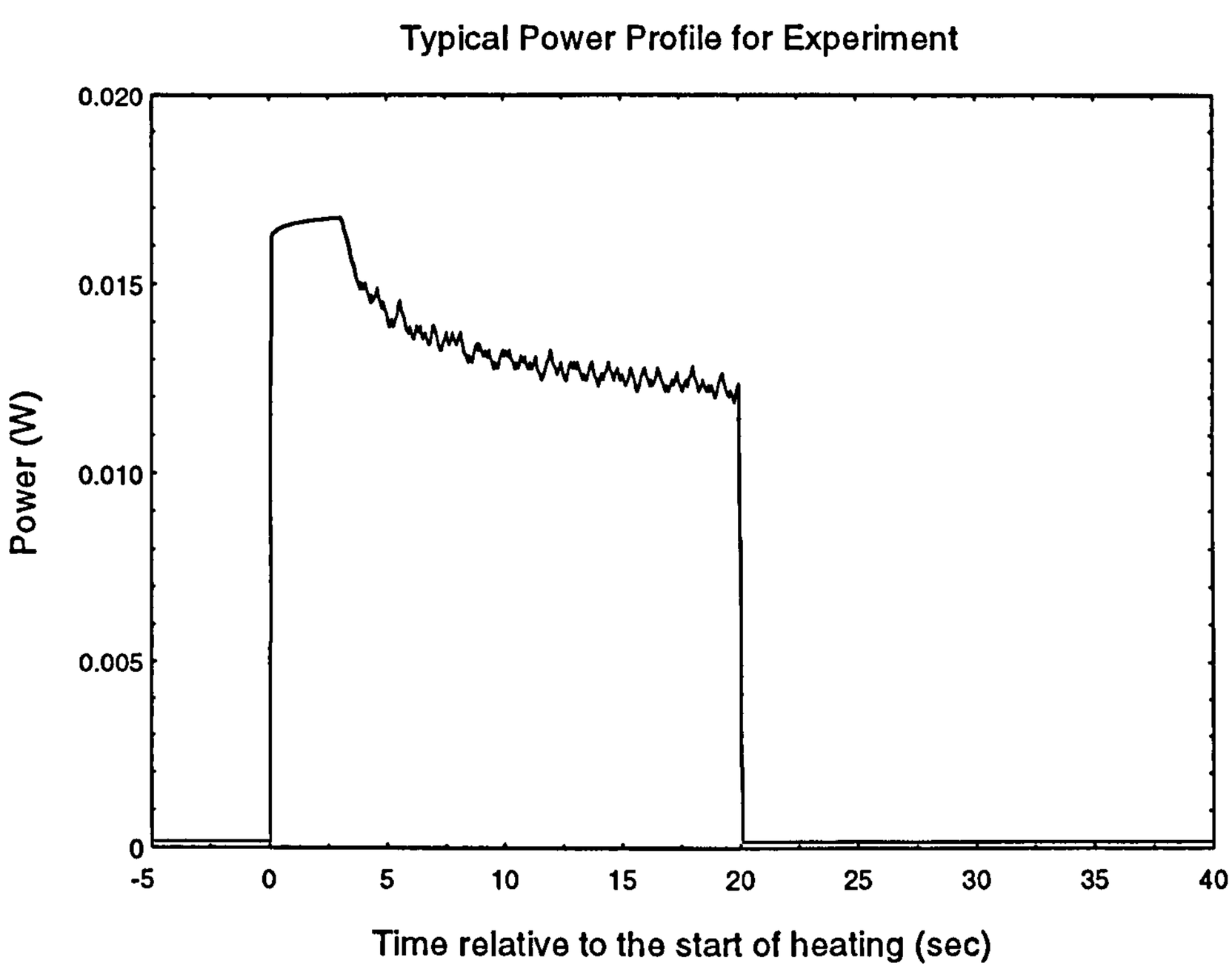

Figure 4.3 Power produced in thermistor during a typical experimental run.

The resistor used in this experiment was a 5 KΩ precision wire bound resistor. This resistor had a given tolerance of ± 0.1% and a very good temperature stability of ± 3 ppm/°C.

However the resolution of the PC-30 card presents problems, especially at the low voltages required to measure the temperature of a sample without heating. For example, let ΔV = 2V, ΔV being defined by $\Delta V = |V_0 - V_1|$, where V_0 and V_1 are the voltages produced by *DAC 0* and *DAC 1* respectively. The 5 mV resolution of the ADCs means, for a thermistor with a resistance of 5 KΩ, the resistance resolution is only in the region of 50Ω. To overcome this problem, all the resistances measured in this study, regardless of the value of ΔV, had their voltage measured 10 times by the ADC channels. These average voltages found were then used in equation 4.9.1 to find the resistance of the thermistor.

In order to ascertain how well the resistance of the thermistor probe could be measured using this system, the thermistor probe was replace with test precision wirebound resistors with resistances of 1KΩ, 5KΩ and 10KΩ. The resistances were measured for a range of voltages.

Figure 4.4 shows the distribution of the measured resistances of a 5KΩ test resistor, for voltages of ΔV = 1V, ΔV = 2V and ΔV = 10V. A total of 1000 measurements were made of the resistance at each voltage. As can be seen, the spread in values for ΔV = 1V is far greater than that seen in ΔV = 2V. Also, the mean voltage for ΔV = 2V approximately agrees with that for ΔV = 10V, while the average resistance for ΔV = 1V is higher than the average resistances found by the higher voltages. Similar results are found if the 5KΩ test resistor is replaced with a 1KΩ or 10KΩ resistor. To measure the resistance, and hence the temperature, of a material without heating, as low as possible a voltage should be used. Thus, a value of ΔV = 2V was used since it was the lowest voltage which gave reasonable resistance (temperature) resolution.

The water bath, used to keep the samples at constant temperature, produced a uniform temperature throughout the water. The water temperature was also very stable with time. At 25°C, there was no measurable difference in the water temperature taken at various points in the water bath. This agrees with the manufacturer's specification of a variation of < 0.05°C throughout the bath. The variation of temperature with time was

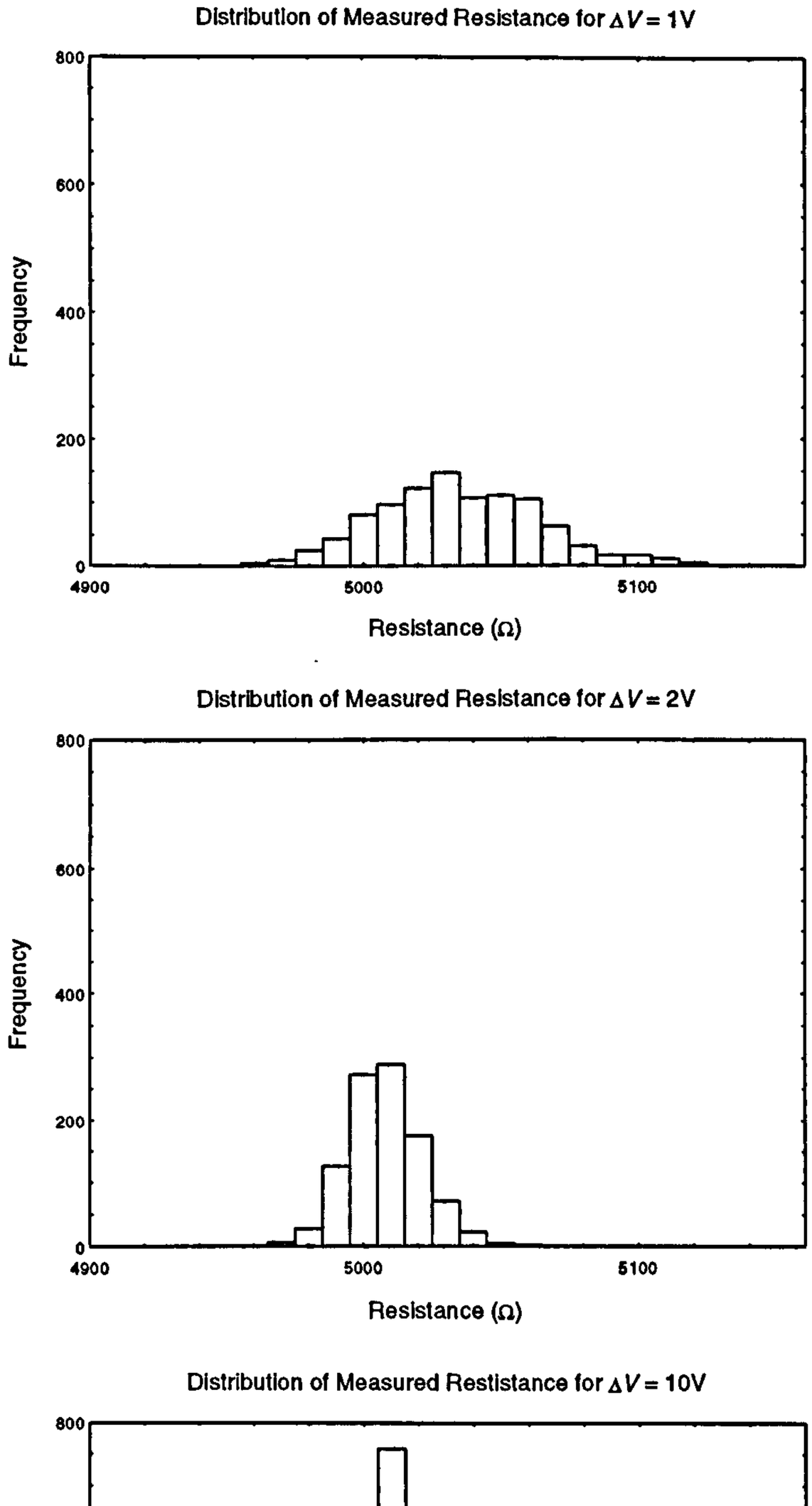

Figure 4.4 Variation in distribution of measured resistance for different ΔV.

dependant on environmental factors. Generally the temperature of the bath would slowly rise with time, but this temperature rise was never significant and the temperature drift was always less than 0.4°C in an hour.

The design of the thermistor probe is shown in figure 4.5. There were three different probes used during the period of this study to measure the thermal conductivity but there was little variation in their design or measured behaviour. For all probes, the thermistor resistance was 10 KΩ at 25°C. The probe shown in figure 4.5 was the probe which was used to make the majority (>75%) of the measurements, including all the measurements on human tissues. The ceramic tube and plastic tube are both good enough thermal insulators not to alter the heat entering the tissue sample. The plastic tube was added to give the probe extra structural stability.

4.11 Probe Temperature Calibration.

Before the thermistor probe could be used in the measurement of the thermal properties of biological tissues, the variation in resistance of the thermistor with temperature must be known. To calibrate the thermistor, the probe was placed in the water bath and the temperature varied. The temperature of the water was measured with a thermometer accurate to ± 0.05°C. The resistance of the thermistor was measured over a water temperature range of 15°C to 45°C.

Equation 4.9.2 can be re-written

$$\ln R_T = \frac{E}{T} - F \qquad (4.11.1)$$

and thus a graph of ln R_T against $1/T$ will have gradient E and intercept -F, where T is the temperature in Kelvin.

A voltage difference of 5V across the thermistor and resistor was used to give a better calibration. Although there is a small amount of heating at this voltage, the water bath is efficient at removing excess heat and there is no measurable rise in temperature. The resistance of the thermistor was measured approximately 100 times and a mean resistance was found at each temperature. Figure 4.6 shows the variation in ln R_T against $1/T$ for the thermistor probe shown in figure 4.5. As can be seen, the relationship

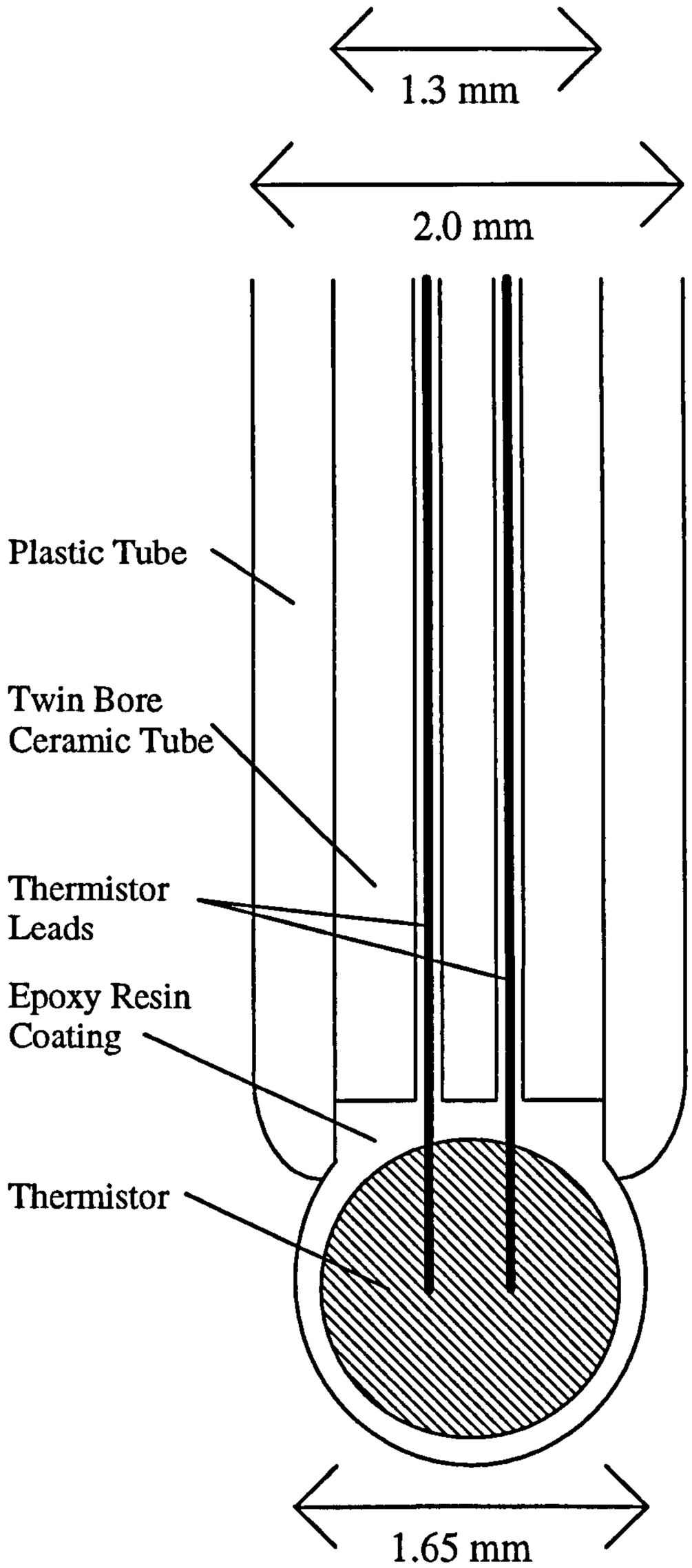

Figure 4.5 The Thermistor Probe.

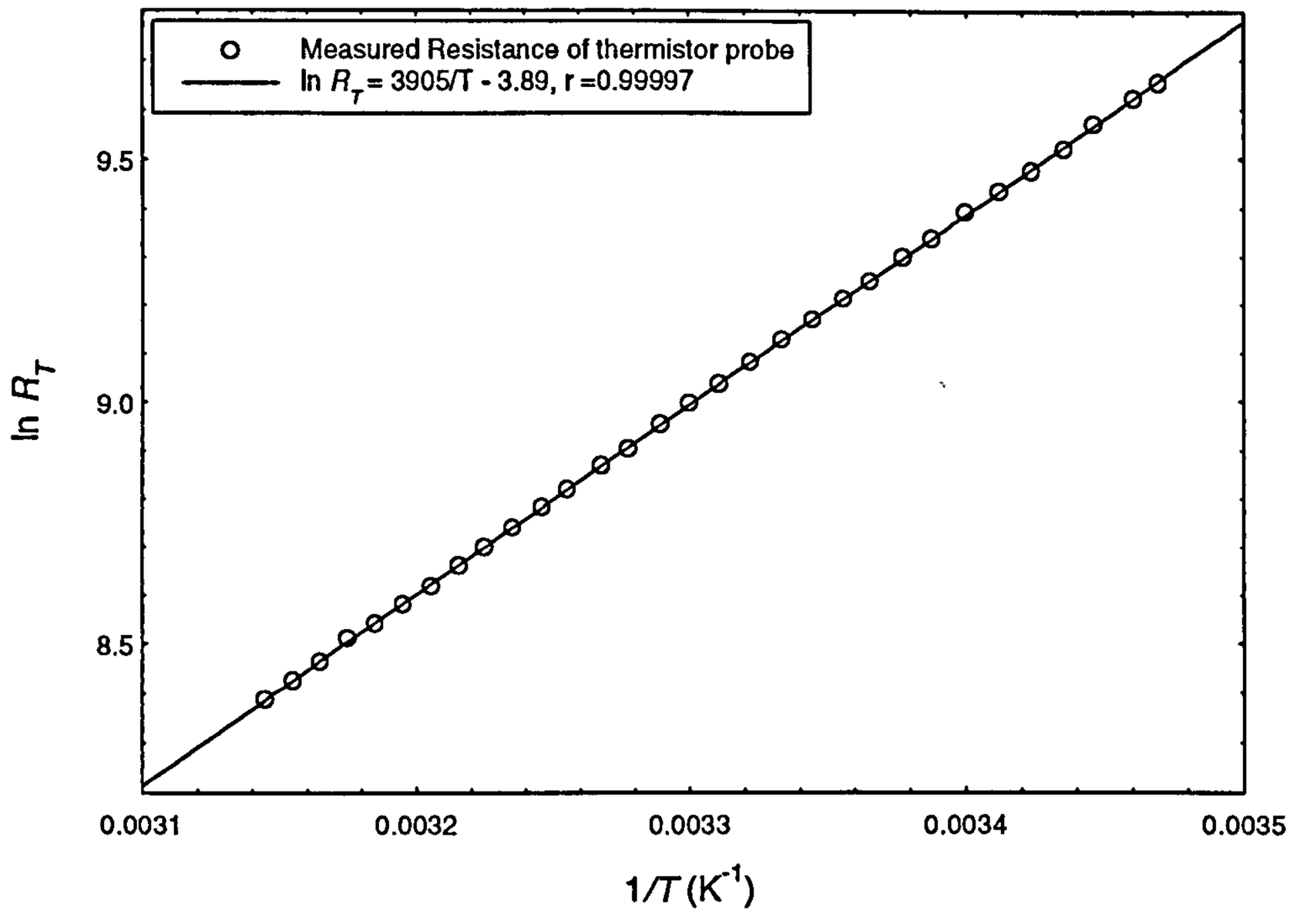

Figure 4.6 The variation of the resistance of the thermistor probe with temperature over the temperature range 15°C - 45°C.

Gel	Temp. (°C)	k ($Wm^{-1}K^{-1}$)	α (10^{-7} m^2s^{-1})	Reference
Agar 1%	-	0.607	-	Cooper and Trezek (1972)
Agar 1.5%	-	0.607	-	Hansen et al (1974)
Agar 1.5%	21	0.609±0.005	1.42±0.05	Balasubramanian and Bowman (1977)
Gelatin 2%	20	0.619	-	Morley (1966)
Carrageenan 2%	25	0.609	1.32-1.73	Kent et al (1984)

Table 4.1 The thermal conductivity and diffusivity of various gels.

between temperature and resistance is accurately known. The linear least squares fit of data shown in figure 4.5 has a correlation given by $r = 0.9997$. This calibration was found to give ΔT to an accuracy of $\pm 0.05°C$.

4.12 Probe Calibration Materials.

Once the probe has been accurately calibrated for temperature, the probe's response to a material's thermal conductivity and thermal diffusivity must be investigated.
Glycerol and agar gelled water were chosen as the two substances to calibrate the probe. Glycerol and water were chosen because the thermal properties of mixtures of these two substances are well known and correspond to the thermal properties of biological tissues. Glycerol and agar gelled water mixtures also had the right consistency to allow the probe to be inserted and achieve good thermal contact.

4.12.1 The Thermal Properties of the Agar Gelled Water.

The thermal properties of water are given in section 3.10. The water was gelled with agar so that there was no convection present. It is assumed that, for the purposes of calibration, the thermal conductivity and diffusivity of the agar gelled water are the same as water for the levels of agar used, which was approximately 1% agar by mass.
Table 4.1 shows the thermal conductivity and diffusivity of various low concentration gels. The thermal conductivity of water at 25°C is 0.607 $Wm^{-1}K^{-1}$ and all the thermal conductivities of the gels are very close to this figure so it safe to assume that the thermal conductivity of the agar is the same as that of water. There is less data about the thermal diffusivity of gels but the assumption will be made that it is the same of that as water.

4.12.2 The Thermal Conductivity of Glycerol.

The thermal conductivity of glycerol, as stated by different authors, is shown in figure 4.7. All the curves show a gradual increase with temperature, except for the thermal conductivity stated in Miner and Dalton (1953), which has the thermal conductivity of glycerol independent of temperature. Touloukian et al (1970a) examined 24

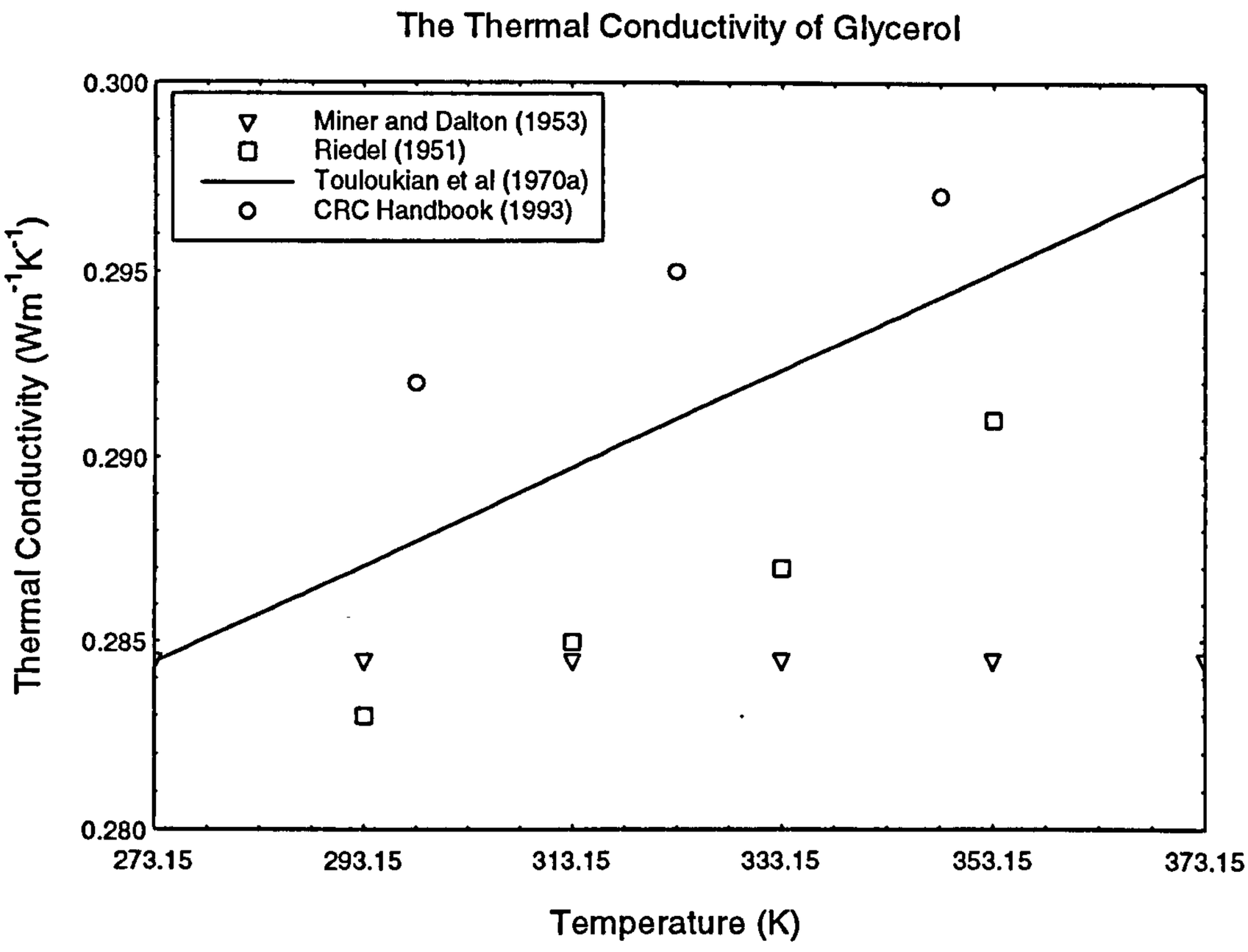

Figure 4.7 The thermal conductivity of glycerol as stated by various authors.

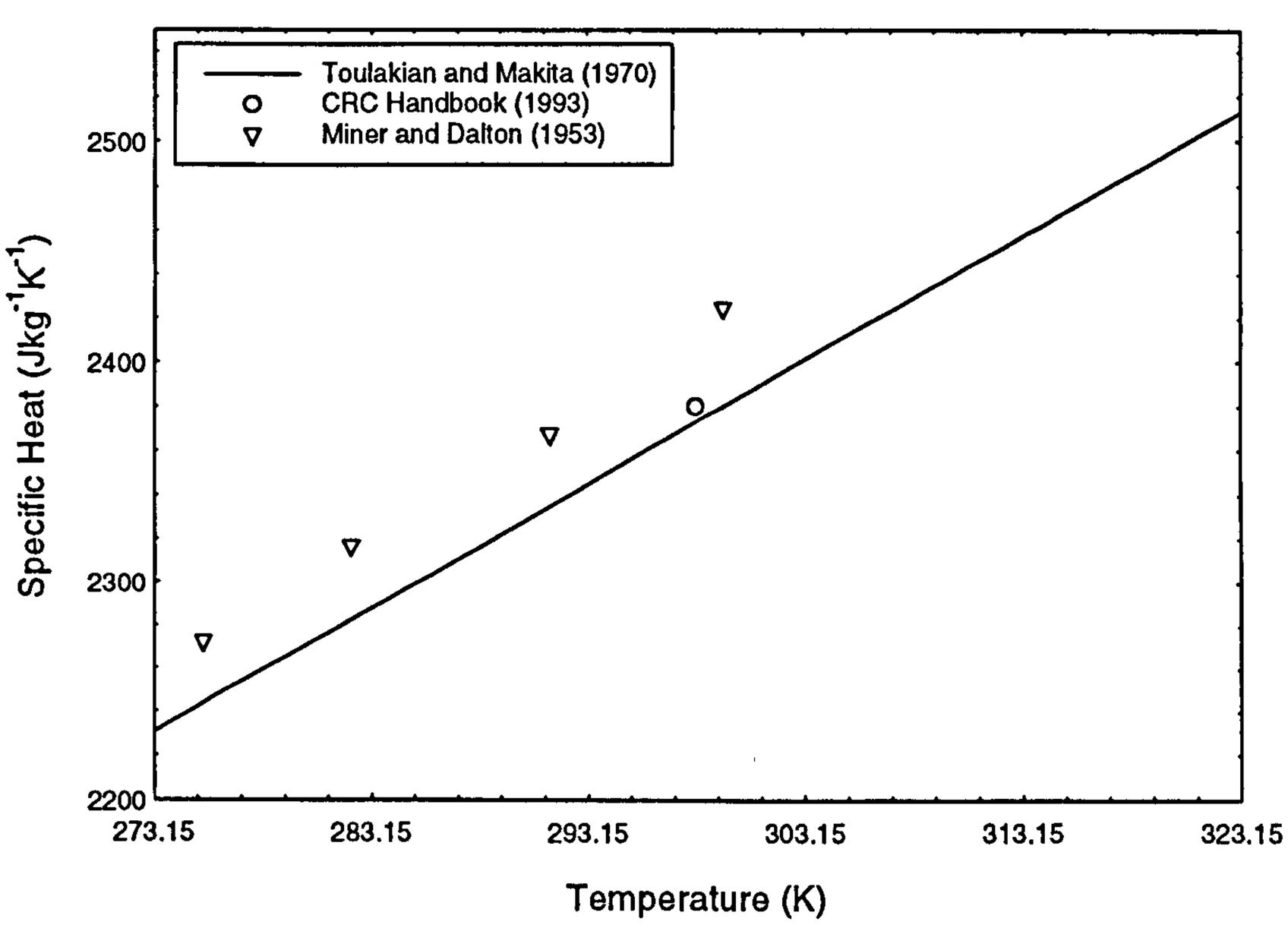

Figure 4.8 The specific heat capacity of glycerol as stated by various authors.

experimental works on the thermal conductivity of glycerol and derived the following equation, which is shown in figure 4.7

$$k_g = 0.248434 + 1.31839 \times 10^{-4} T \qquad (4.12.1)$$

where T is the temperature in Kelvin. The Riedel (1951) and the CRC Handbook for Chemistry and Physics (1993) data does not agree with that of Touloukian et al (1970a) but a linear curve fit of these data points gives a curve close to it. Thus equation 4.12.1 is assumed to give the thermal conductivity of glycerol.

4.12.3 The Thermal Diffusivity of Glycerol.

There exists little direct data on the thermal diffusivity of glycerol and thus it will be found by using the definition of thermal diffusivity, $\alpha_g = {}^{k_g}\!/\!_{\rho_g c_{pg}}$.

The specific heat of glycerol, as given by different authors is shown in figure 4.8. Touloukian and Makita (1970) examined the data produced by seven different works and produced the following equation

$$c_{pg} = 412.731 + 7.89333T - 5.70815 \times 10^{-3} T^2 + 4.31647 \times 10^{-6} T^3 \qquad (4.12.2)$$

where, again, T is temperature in Kelvin. The CRC Handbook for Chemistry and Physics (1993) gives only one point at 25°C, but this point agrees well with the Touloukian and Makita curve. The older Miner and Dalton (1953) data is slightly higher than the other curves. Since the CRC Handbook for Chemistry and Physics and Touloukian and Makita are in such good agreement, equation 4.12.2 will be taken as the specific heat capacity of glycerol.

The CRC Handbook for Chemistry and Physics (1993) gives the density of glycerol as 1256.7 kgm^{-3} at 25°C. This is in agreement to within 0.1% of the value given in Miner and Dalton and thus the density of glycerol will be taken as ρ_g = 1256.7 kgm^{-3}.

4.12.4 The Thermal Conductivity of Water / Glycerol Mixtures.

A number of researchers have measured the thermal conductivity of mixtures of water and Glycerol. Figure 4.9 shows the thermal conductivity of aqueous glycerol mixtures at

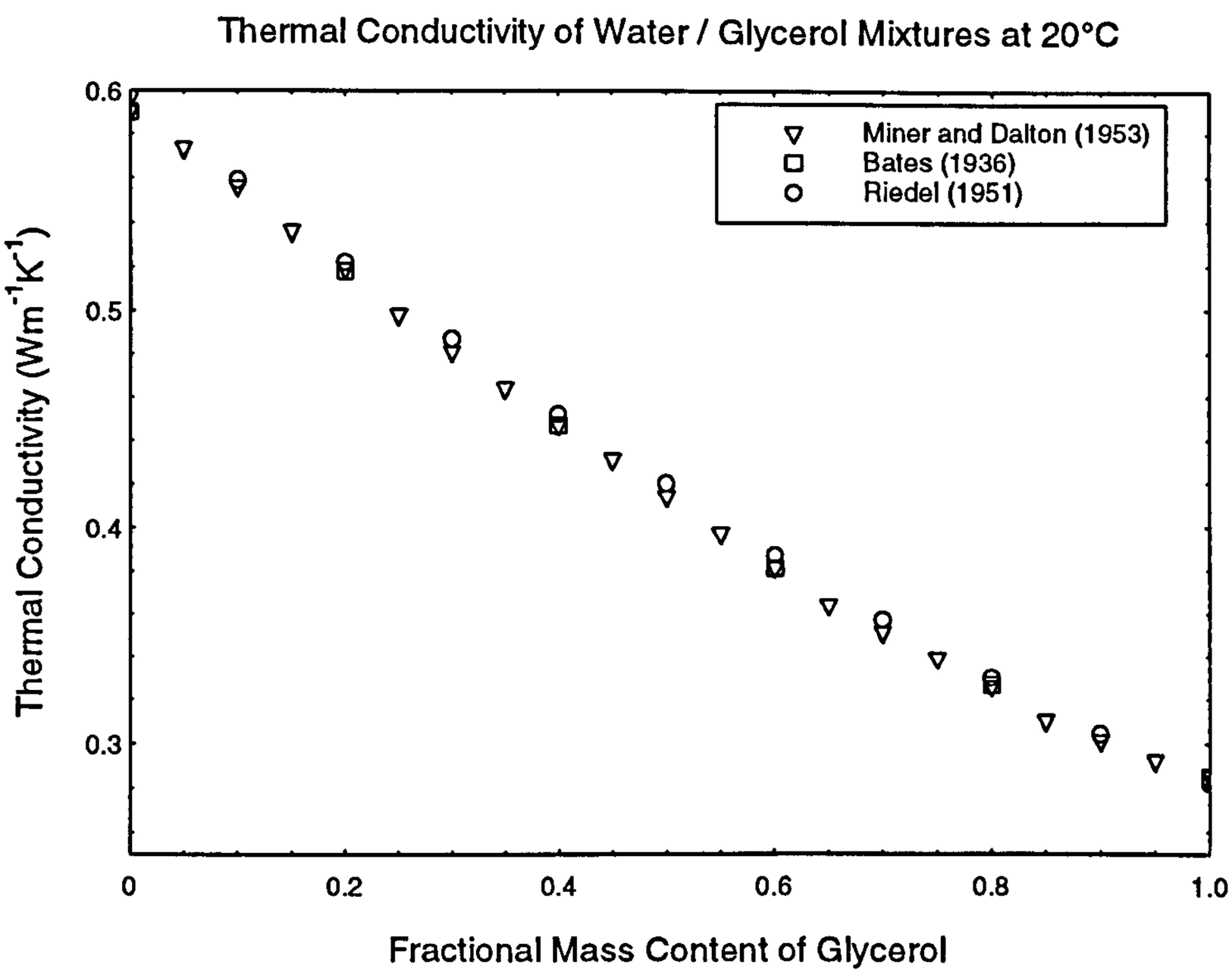

Figure 4.9 The thermal conductivity of glycerol / water mixtures at 20°C.

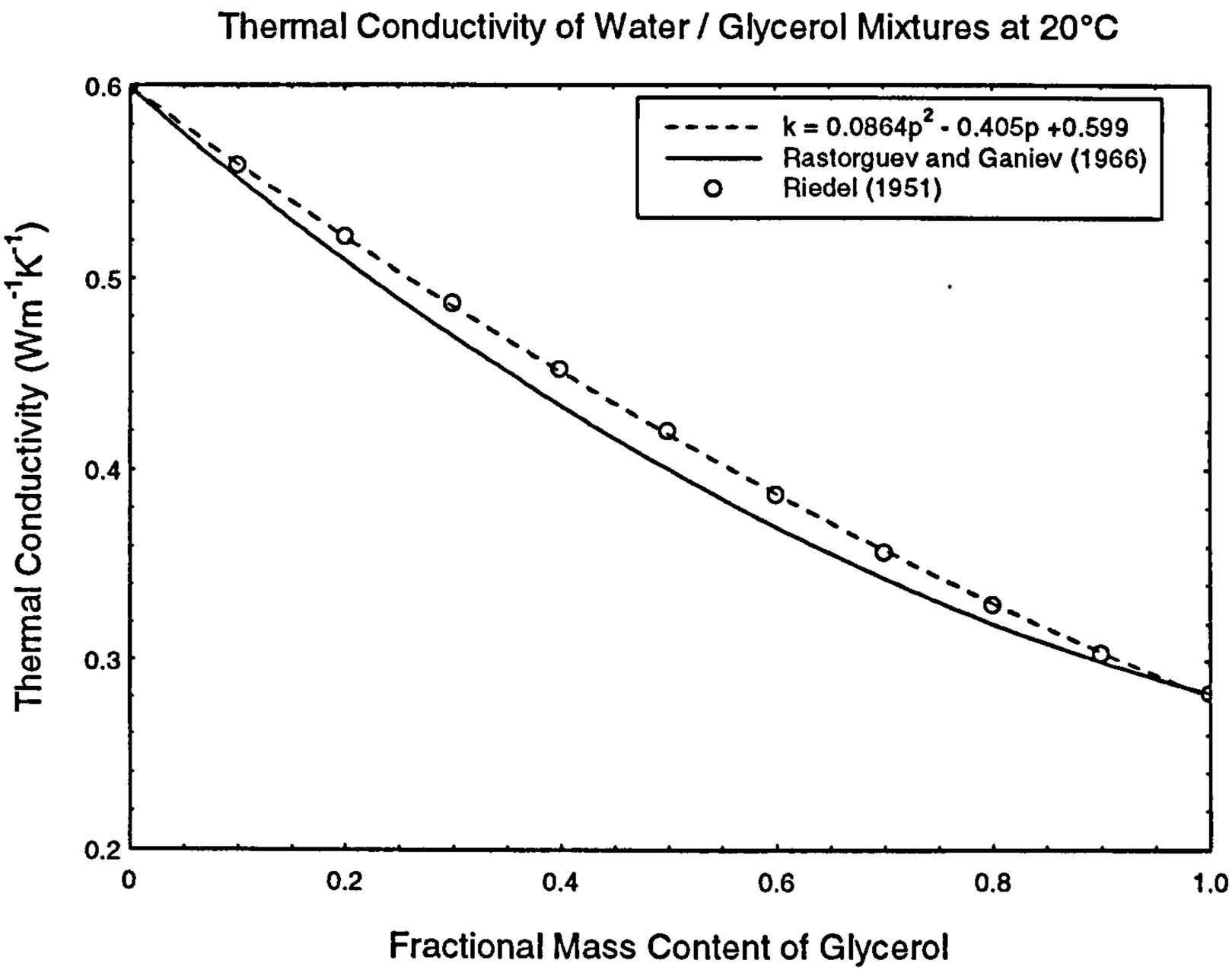

Figure 4.10 Comparison between measured data and equation 4.12.3.

20°C as measured by various authors. As can be seen the thermal conductivity measured by Bates (1936), Riedel (1951) and Miner and Dalton (1953) all agree well.

Rastorguev and Ganiev (1966) examined the data produced by Riedel for the thermal conductivity of aqueous solutions of organic liquids, including glycerol, and proposed the following equation

$$k = pk_g + (1-p)k_w - 1.4p(1-p)(k_w - k_g - 0.2) + 0.0014p(1-p)(T_c - 20) \qquad (4.12.3)$$

where k_g is the thermal conductivity of the organic liquid (such as glycerol), k_w is the thermal conductivity of water, p is the mass fraction of the organic liquid, and T_c is the mixture temperature (°C). This equation has been widely used to predict the thermal conductivity of aqueous solutions of glycerol in papers such as Valvano et al (1985) and Patel et al (1987).

Figure 4.10 shows a comparison between Riedel's data at 20°C, a cubic fit of Riedel's data and Rastorguev and Ganiev's equation 4.12.3, with k_w and k_g as found by Riedel. This shows that equation 4.12.3 actually provides a rather poor fit of the data. The maximum deviation between the data measured by Riedel and the values produced by equation 4.12.3 is 5%. Therefore Rastorguev and Ganiev's equation 4.12.3 is rejected as a method of determining the thermal conductivity of glycerol and water mixtures.

The fit of the Riedel data at 20°C, as shown in figure 4.10, is given by

$$k_{20} = 0.0864p^2 - 0.405p + 0.599 \qquad (4.12.4)$$

where p is the mass fraction of glycerol. Of course, this equation is only true at a temperature of 20°C. At different temperatures, the thermal conductivity of the water and the glycerol will be different from that at 20°C. Thus, a temperature correlation factor was introduced. The thermal conductivity of a water glycerol mixture was assumed to be given by

$$k = \left\{ \left(\frac{k_g - k_{g20}}{k_{g20}} \right) p + \left(\frac{k_w - k_{w20}}{k_{w20}} \right) (1-p) + 1 \right\} k_{20} \qquad (4.12.5)$$

where k_{g20} and k_{w20} are the thermal conductivities of glycerol and water at 20°C as given by equation 4.12.4, and k_g and k_w are the new thermal conductivities of glycerol and water at the different temperature.

To check the validity of this expression, the values produced by equation 4.12.3 and equation 4.12.5 were compared with Riedel experimental data at 40°C and 80°C. Figure

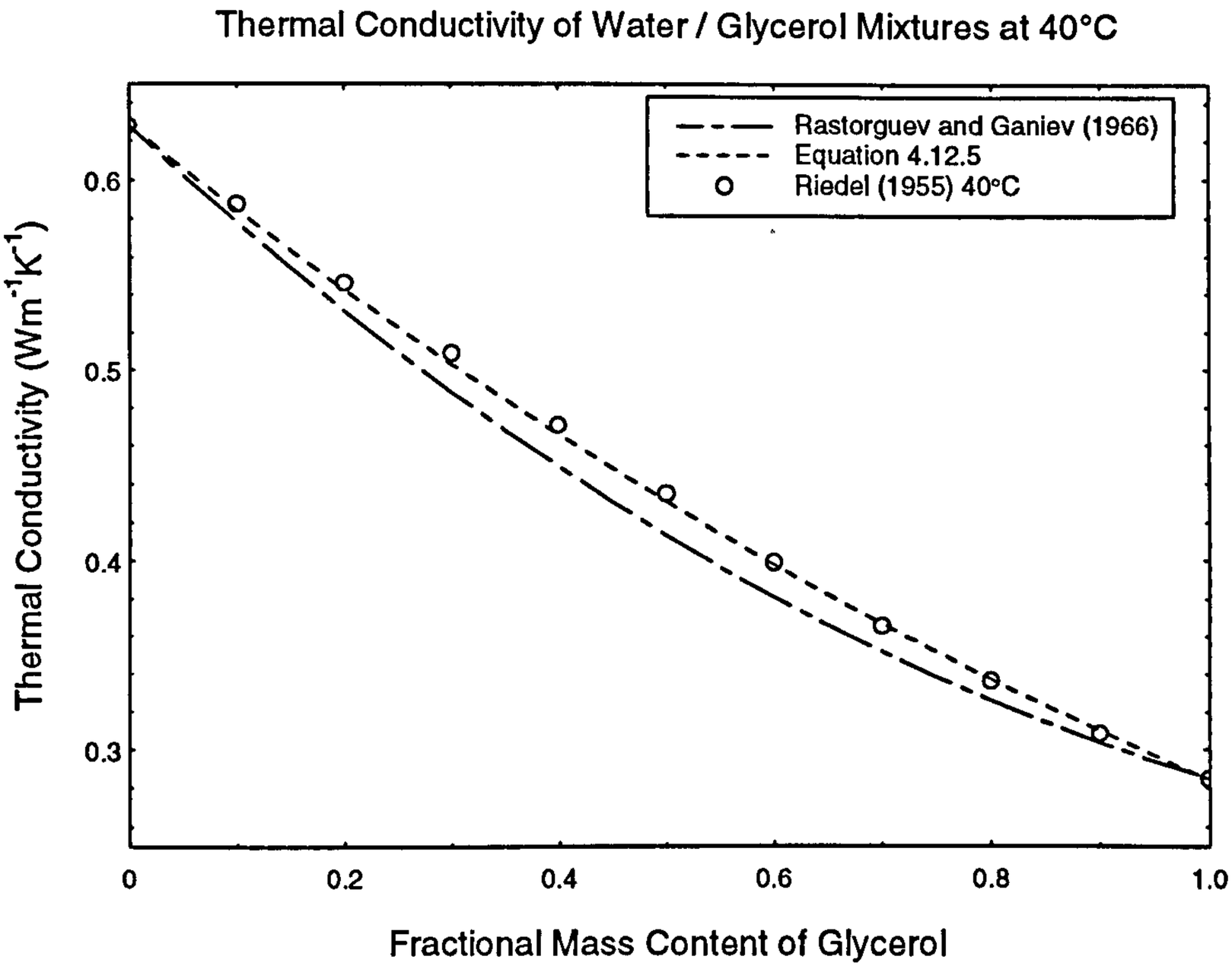

Figure 4.11 The thermal conductivity of water / glycerol mixtures at 40°C.

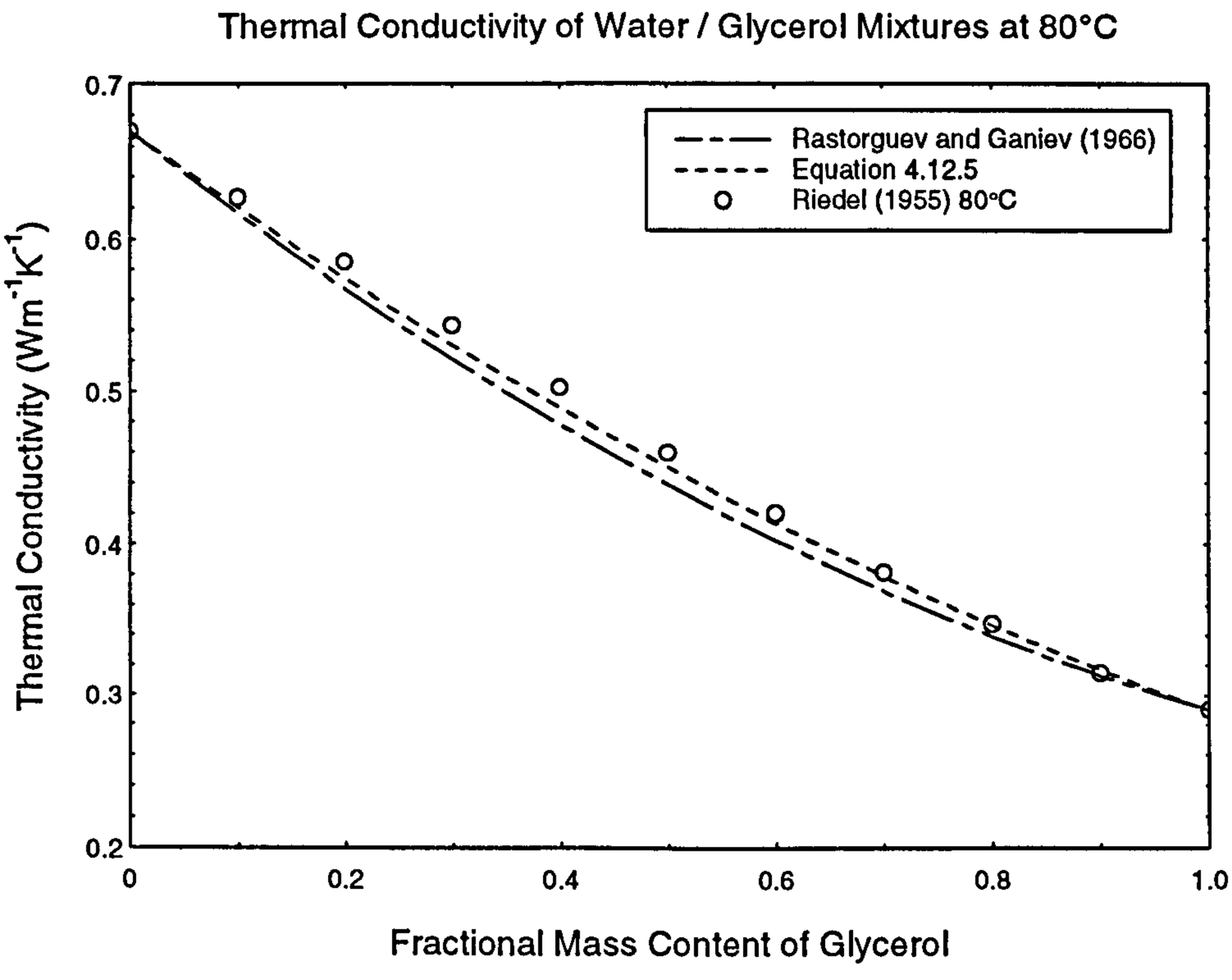

Figure 4.12 The thermal conductivity of water / glycerol mixtures at 80°C.

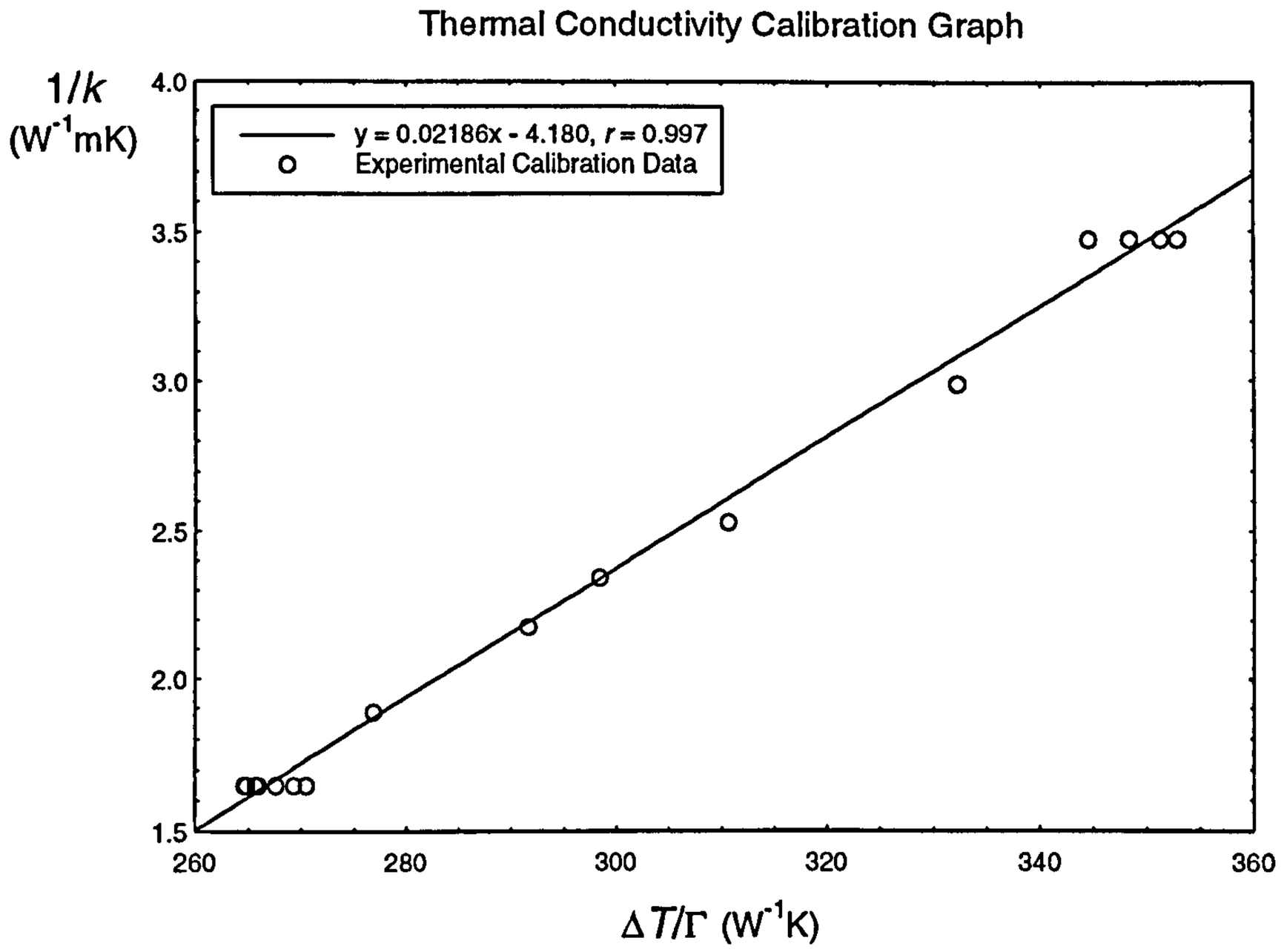

Figure 4.13 The thermal conductivity calibration curve.

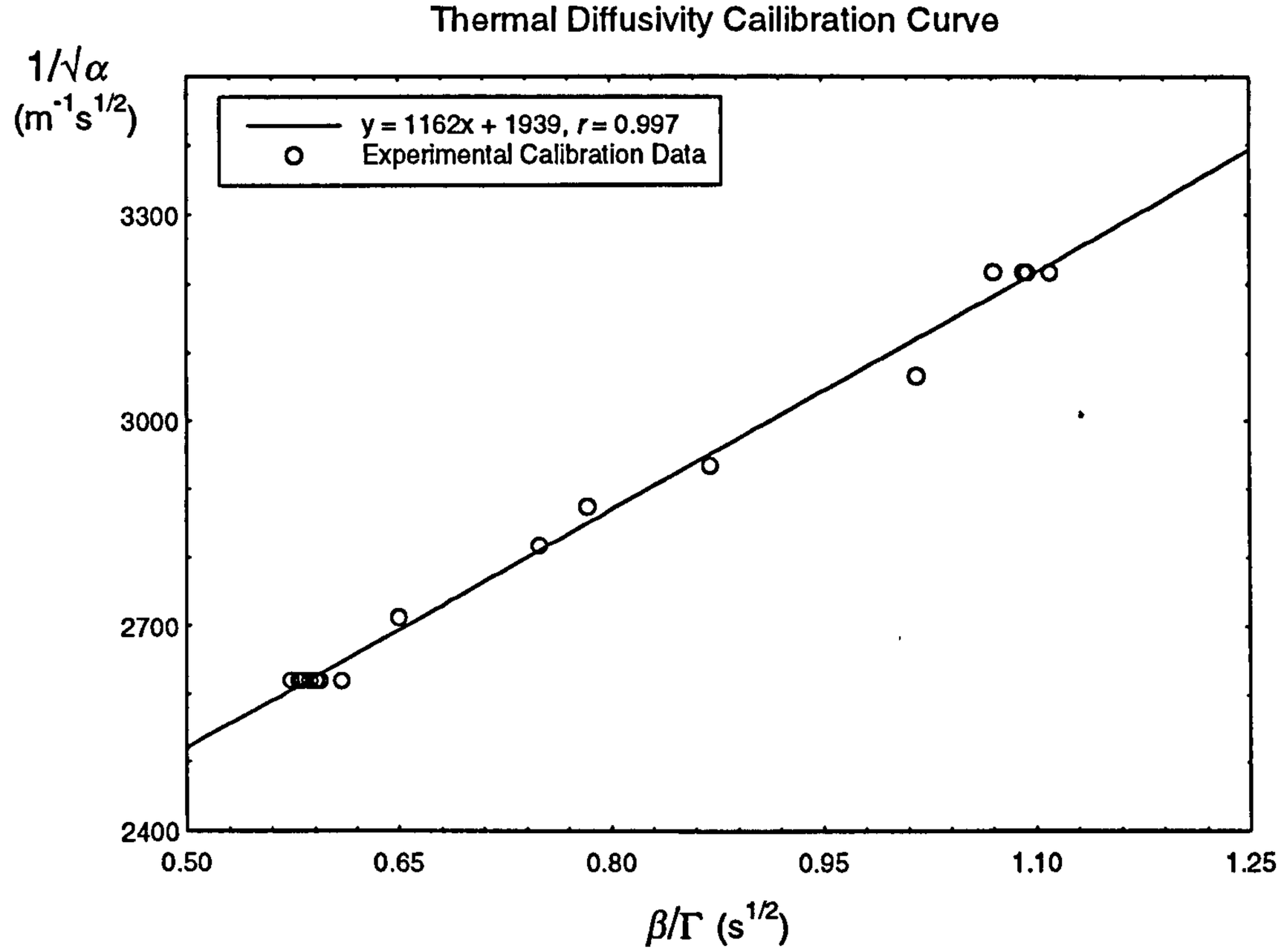

Figure 4.14 The thermal diffusivity calibration curve.

4.11 shows this comparison at 40°C and figure 4.12 shows the comparison at 80°C. As can be clearly seen in both cases, equation 4.12.5 gives a better fit of the data than that Rastorguev and Ganiev's equation 4.12.3. Thus equation 4.12.5 was used to give the thermal conductivity of aqueous solutions of glycerol.

4.12.5 The Thermal Diffusivity of Water / Glycerol Mixtures.

Valvano et al (1985) and Patel (1987) stated that the thermal diffusivity of the mixture was a linearly dependant on the mass fraction of the constituents. That is

$$\alpha = p\alpha_g + (1-p)\alpha_w \qquad (4.12.6)$$

where p is the mass fraction of glycerol. As shown below, this equation gives the expected straight line in the thermal diffusivity calibration graph. There is little data on the thermal diffusivity of water / glycerol mixtures which would support or reject this equation, and thus equation 4.12.6 will be used to give the thermal conductivity of aqueous solutions of glycerol.

4.13 Thermal Conductivity and Diffusivity Calibration.

The procedure for calibrating the probe was the same as that used to measure the thermal properties of biological substances. To ensure an accurate calibration, many (> 50) measurements were made for each calibration sample prepared. An average value was then found for each sample. As previously stated, the thermal conductivity is given by $k = \left(A\,{}^{\Delta T}\!/_{\Gamma} + B\right)^{-1}$, and the thermal diffusivity is given by $\alpha = \left(C\,{}^{\beta}\!/_{\Gamma} + D\right)^{-2}$. Thus a graph of ${}^{1}\!/_{k}$ against ${}^{\Delta T}\!/_{\Gamma}$ will have gradient A and intercept B, while a graph of ${}^{1}\!/_{\sqrt{\alpha}}$ against ${}^{\beta}\!/_{\Gamma}$ will have gradient C and intercept D.

Figure 4.13 shows the thermal conductivity calibration curve for the probe shown in figure 4.5, while figure 4.14 shows the thermal diffusivity calibration curve. This gave the calibration constants as A = 0.02186 m, B = -4.180 $W^{-1}mK$, C = 1162 m^{-1} and D = 1939 $m^{-1}s^{1/2}$.

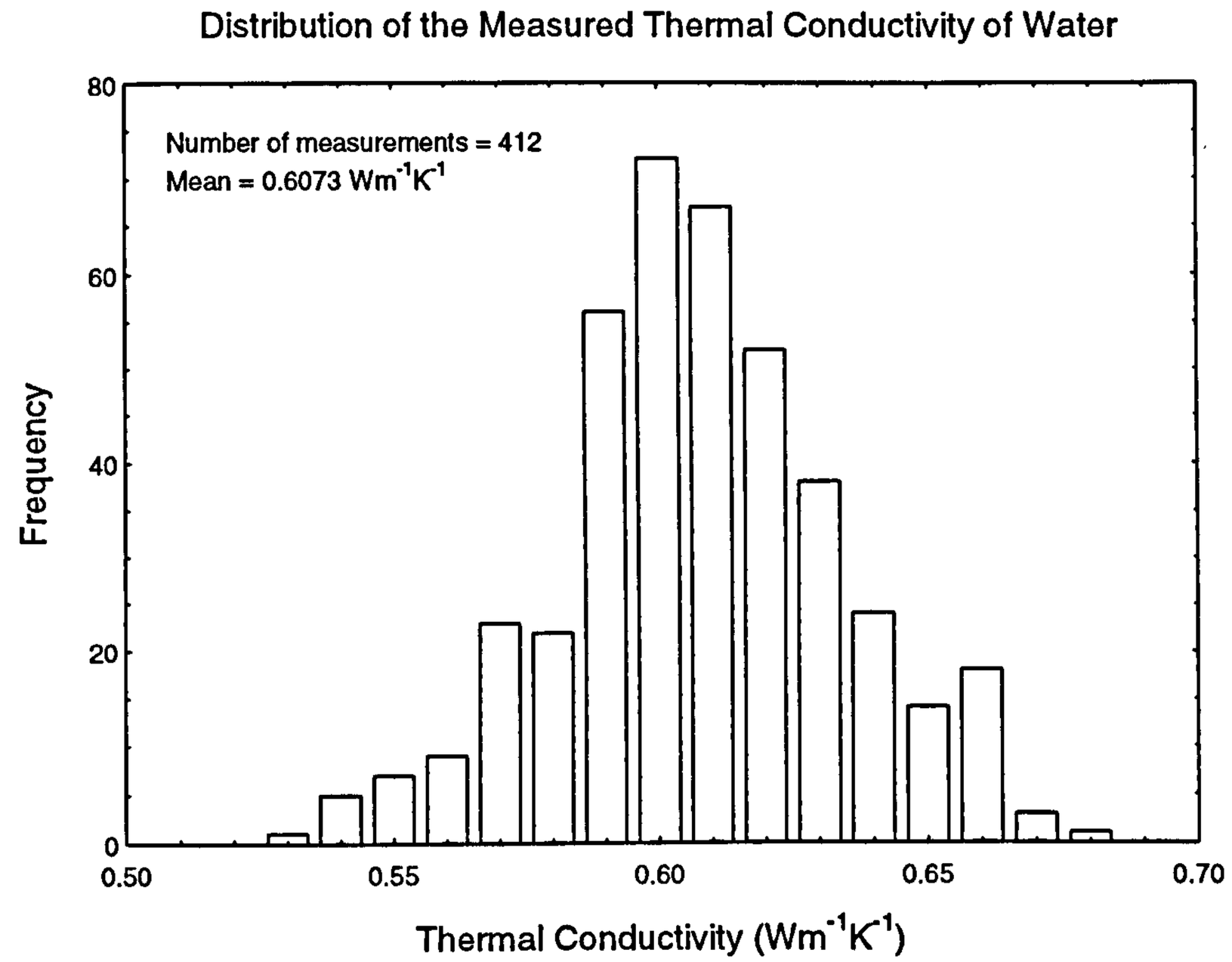

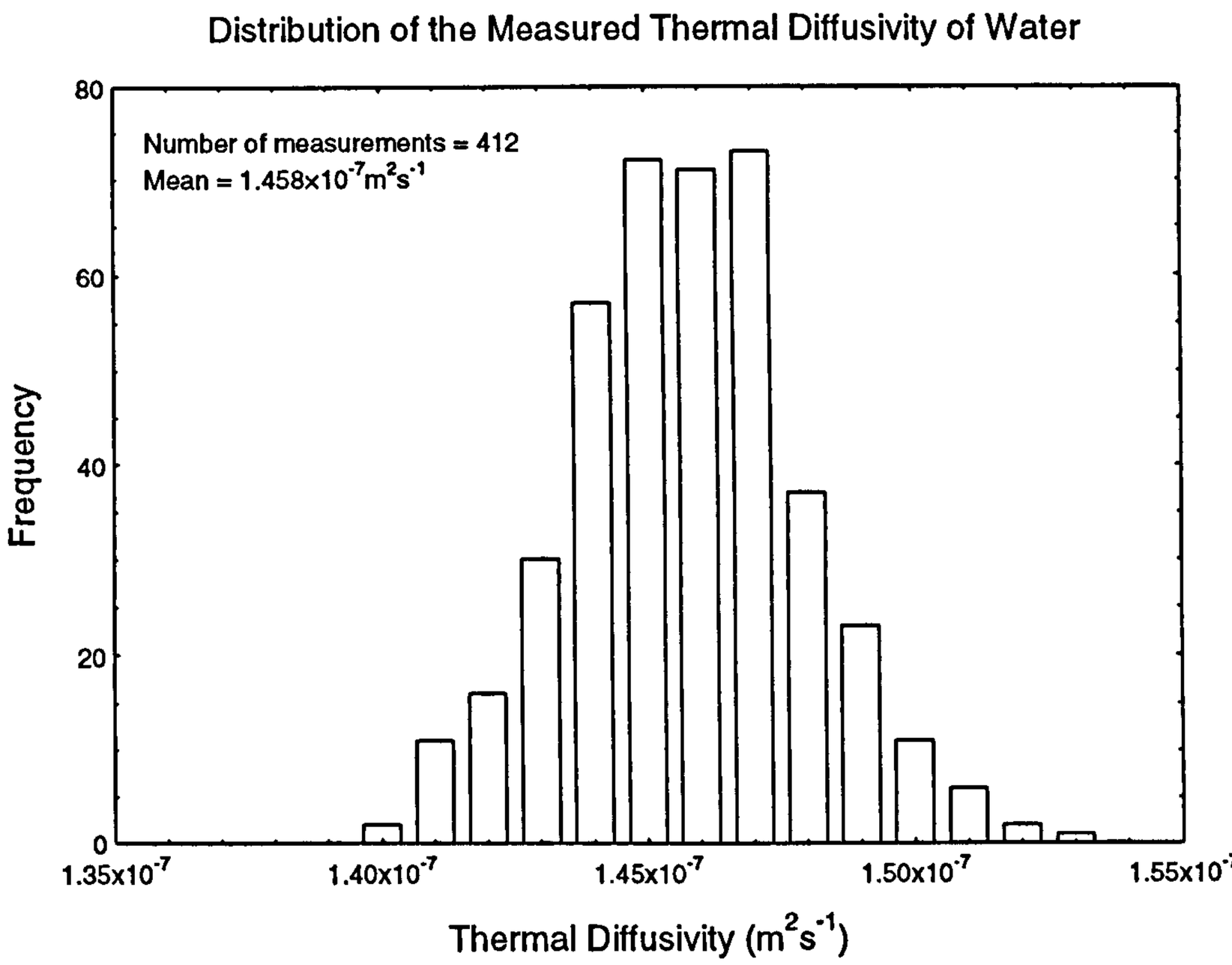

Figure 4.15 The distribution of the measured conductivity and thermal diffusivity of water as measured by the probe shown in figure 4.5.

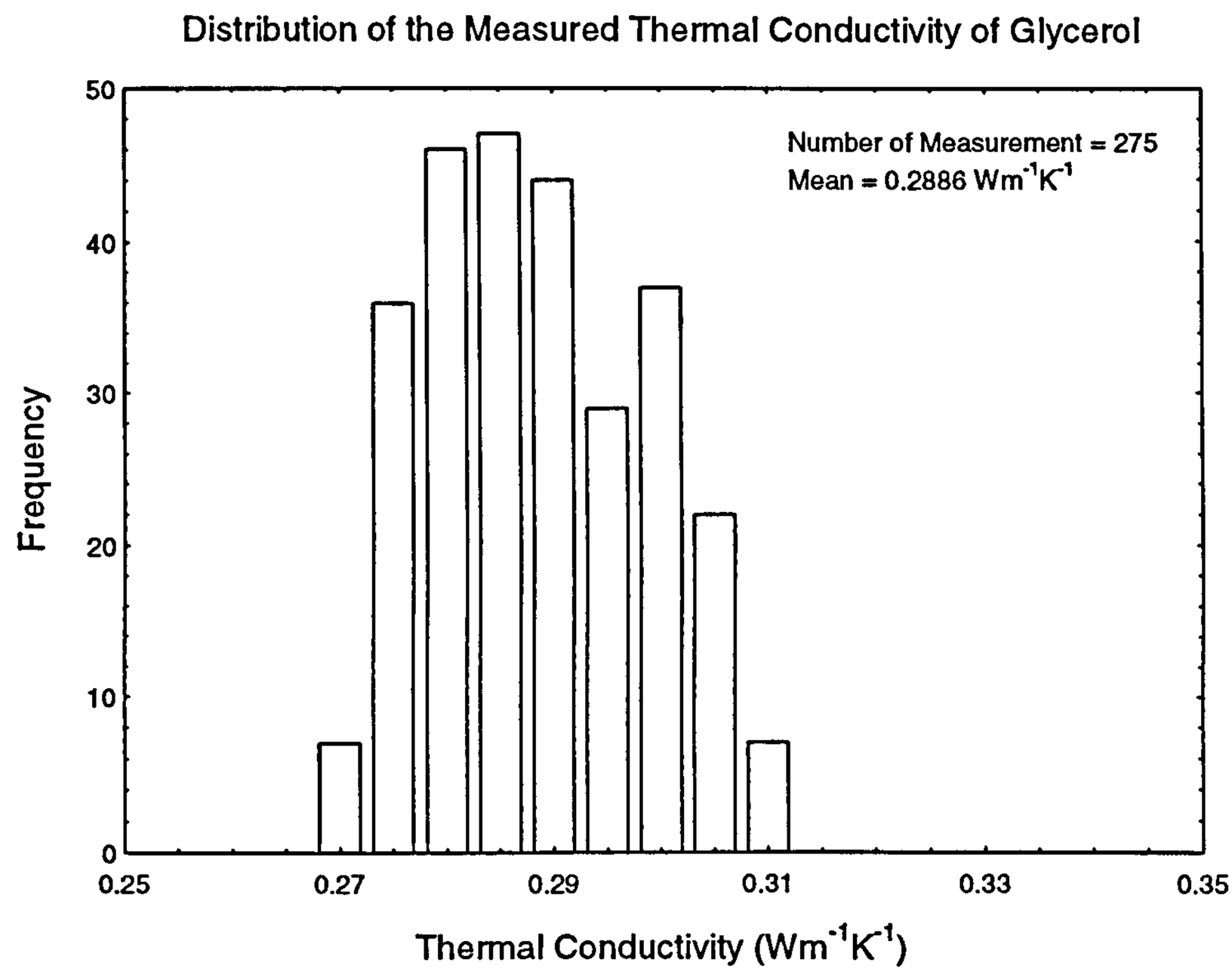

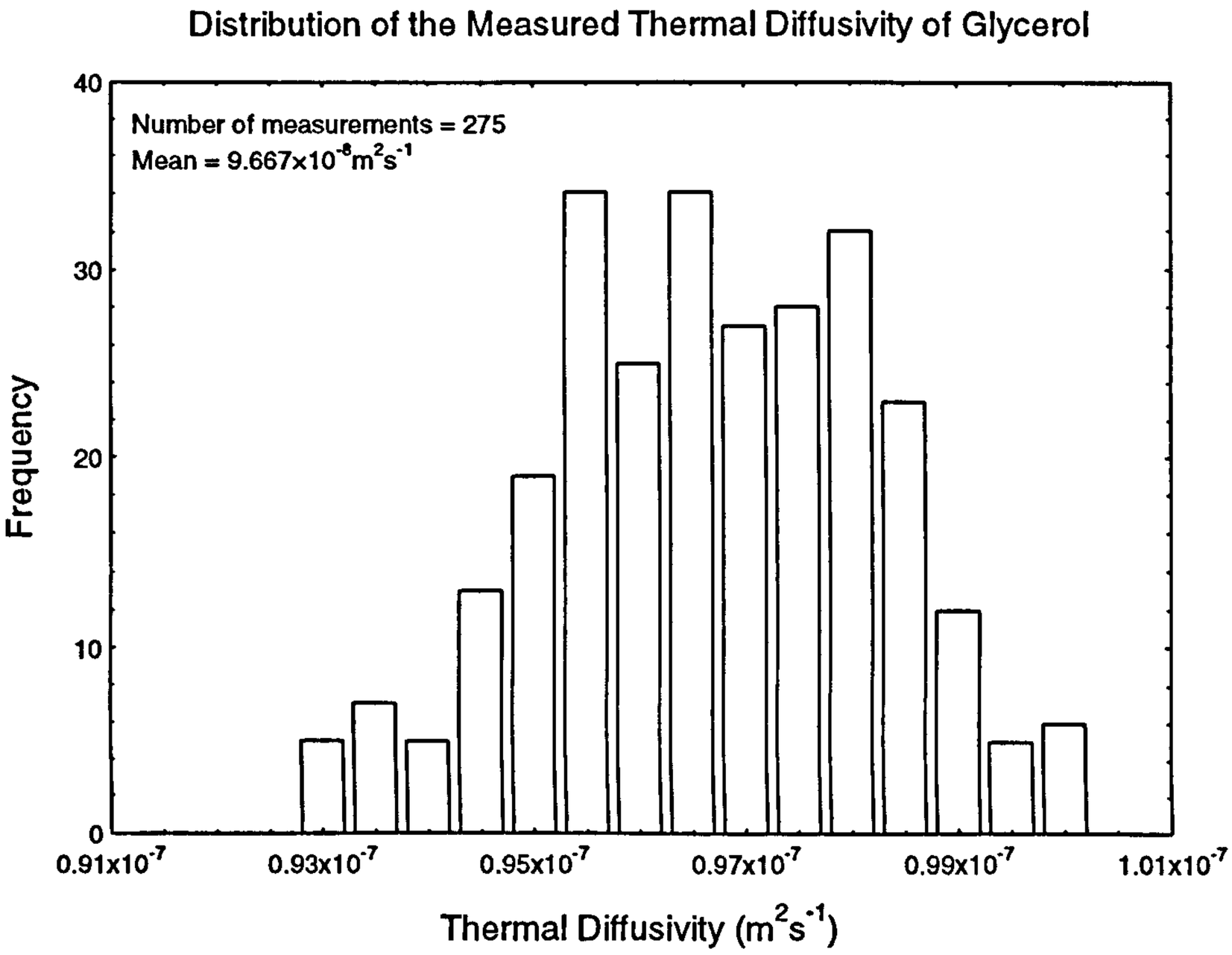

Figure 4.16 The distribution of the measured conductivity and thermal diffusivity of glycerol as measured by the probe shown in figure 4.5.

4.14 The Accuracy of the Probe Calibration.

Once the calibration constants were determined, the values measured for the agar gel and glycerol were re-examined. The distribution of measured thermal conductivities and thermal diffusivities of water are shown in figure 4.15 and that of glycerol are shown in figure 4.16.

The mean of the measured values of the thermal conductivity and thermal diffusivity of water and glycerol match extremely well with the values predicted by theory. This is not surprising given that this data was used to calibrate the probe. Of interest is the spread in the values measured. In order to examine this further, the standard deviation in the measured thermal conductivity and thermal diffusivity for each of the calibration samples is examined.

Table 4.2 compares the theoretical values of the thermal conductivity with the experimental mean value and gives the standard deviation in the measured thermal conductivities. Table 4.3 gives similar values for the thermal diffusivity.

Both tables show small differences between the measured and the expected values of the thermal conductivity and diffusivity of the water / glycerol mixtures. This is to be expected, since there is a possibility that, for mixtures of water and glycerol, the mass fractions of the two materials may not be exactly that stated. This appears to be the case for the 80% glycerol 20% agar gel mixture, where both the thermal conductivity and thermal diffusivity indicate that the sample had a greater fraction of glycerol than expected.

The percentage deviation of the thermal conductivity, σ/k_m, where k_m is the experimental mean thermal conductivity, is approximately 3-4%. There is an indication that the technique becomes slightly more accurate as the conductivity drops.

The probe technique is more accurate in determining the thermal diffusivity. The percentage deviation in this case lies in the range 1.2% - 1.7% and appears to be independent of the thermal diffusivity being measured.

The measurements made on each individual calibration sample were made over a twelve hour period. However different samples did not have the calibration measurements made

Calibration Material	Theoretical Value $Wm^{-1}K^{-1}$	Number of Measurements (Samples)	Experimental Mean Value $Wm^{-1}K^{-1}$	Standard Deviation $Wm^{-1}K^{-1}$	Percentage Deviation
Agar Gel	0.6073	412 (6)	0.6073	0.0261	4.3%
80 % Agar Gel 20% Glycerol	0.5300	68 (1)	0.5325	0.0210	3.9%
60 % Agar Gel 40% Glycerol	0.4593	69 (1)	0.4552	0.0166	3.6%
50 % Agar Gel 50% Glycerol	0.4264	68 (1)	0.4280	0.0114	2.7%
40 % Agar Gel 60% Glycerol	0.3953	69 (1)	0.3831	0.0098	2.6%
20 % Agar Gel 80% Glycerol	0.3381	68 (1)	0.3203	0.0082	2.6%
Glycerol	0.2877	275 (4)	0.2886	0.0100	3.4%

Table 4.2 Comparison between the theoretical and measured thermal conductivity for each of the calibration materials and the standard deviation found.

Calibration Material	Theoretical Value m^2s^{-1}	Number of Measurements (Samples)	Experimental Mean Value m^2s^{-1}	Standard Deviation m^2s^{-1}	Percentage Deviation
Agar Gel	1.458×10^{-7}	412 (6)	1.458×10^{-7}	0.022×10^{-7}	1.50%
80 % Agar Gel 20% Glycerol	1.359×10^{-7}	68 (1)	1.375×10^{-7}	0.020×10^{-7}	1.45%
60 % Agar Gel 40% Glycerol	1.261×10^{-7}	69 (1)	1.264×10^{-7}	0.018×10^{-7}	1.42%
50 % Agar Gel 50% Glycerol	1.211×10^{-7}	68 (1)	1.234×10^{-7}	0.021×10^{-7}	1.70%
40 % Agar Gel 60% Glycerol	1.162×10^{-7}	69 (1)	1.147×10^{-7}	0.016×10^{-7}	1.39%
20 % Agar Gel 80% Glycerol	1.064×10^{-7}	68 (1)	1.026×10^{-7}	0.013×10^{-7}	1.26%
Glycerol	0.965×10^{-7}	275 (4)	0.967×10^{-7}	0.016×10^{-7}	1.65%

Table 4.3 Comparison between the theoretical and measured thermal diffusivity for each of the calibration materials and the standard deviation found.

during the same period of time. Instead the calibration measurements were made at various times during the period when the thermal properties of tissue were being measured. Thus for the agar gelled water and glycerol samples, any change in the calibration with time will show as a change in the mean values of the thermal properties for each sample. These mean values show variations which were far smaller than measurement to measurement variation.

4.15 Probe Behaviour.

The probe is measuring two quantities at the same time, the thermal conductivity and the thermal diffusivity. When examining the measurements made on biological tissues, the measured thermal conductivity and thermal diffusivity will be examined to determine whether there is a relationship between these two properties in biological materials. However, the possibility that the relationship between the thermal conductivity and thermal diffusivity is being generated by the probe must first be examined.

Figure 4.17 shows the variation of the measured thermal diffusivity with the thermal conductivity for all the measurements made on agar gelled water. Since there is no variation in the thermal properties of agar gelled water, any pattern seen in the variation must be due to the measurement system. It is clear that there little evidence of any relationship between the thermal diffusivity and the thermal conductivity.

Examining the definition of the thermal diffusivity, $\alpha = k/\rho c_p$, it can be seen that another quantity can be found, ρc_p. This quantity has been referred to as the volumetric heat capacity, since it is amount of energy required to raise the temperature of a unit volume of material by one Kelvin.

Figure 4.18 shows the relationship between ρc_p and the thermal conductivity for all the measurements made on agar gelled water. In this case the relationship is clear. There is a linear relationship between ρc_p and the thermal conductivity.

These two graphs, shown in figures 4.17 and 4.18, appear at first to contradict one another. A linear behaviour in the ρc_p against k graph should give a relationship between thermal diffusivity and the thermal conductivity of the form $\alpha = k/(ak+b)$.

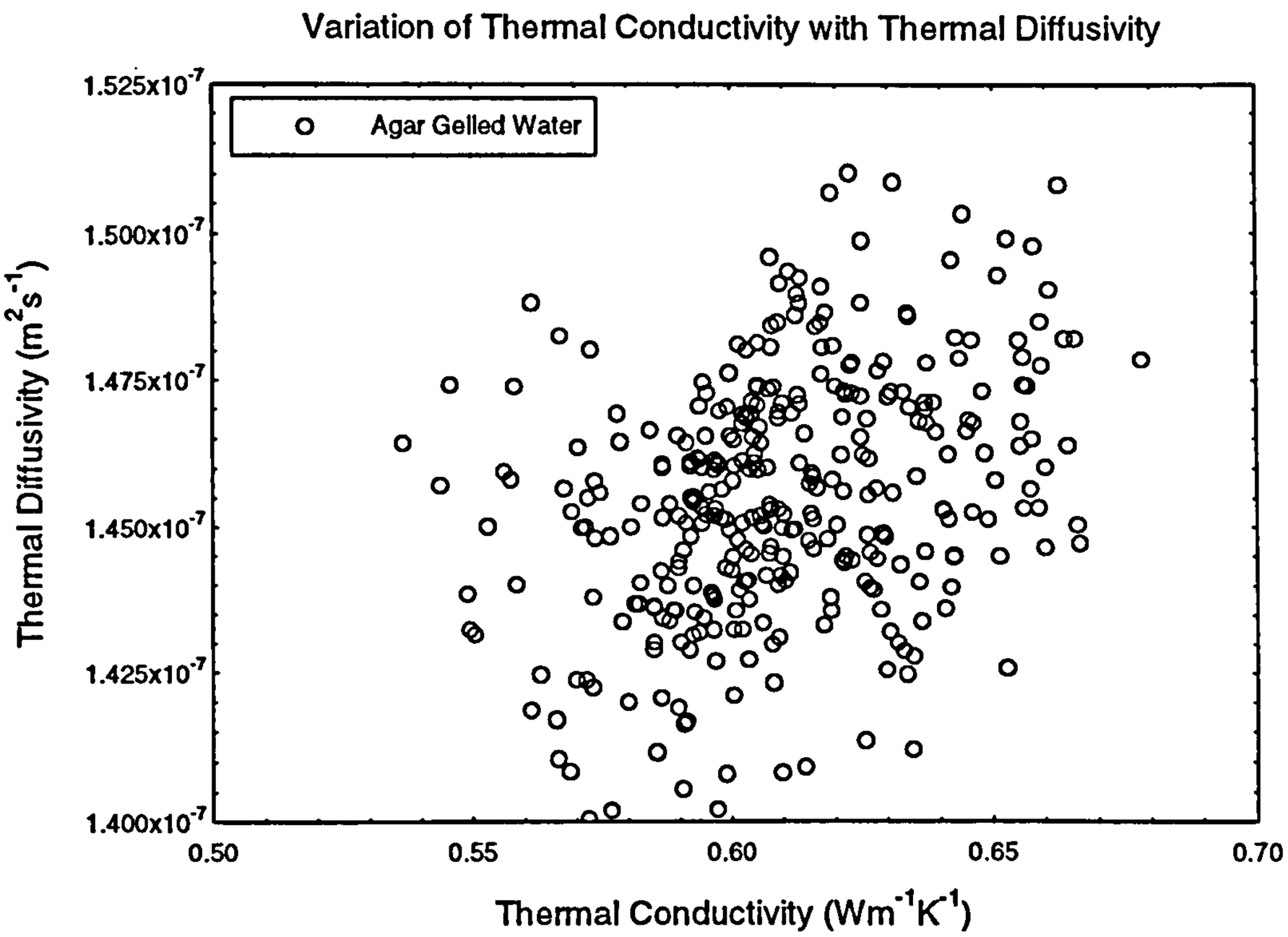

Figure 4.17 The relationship between α and k for agar gelled water.

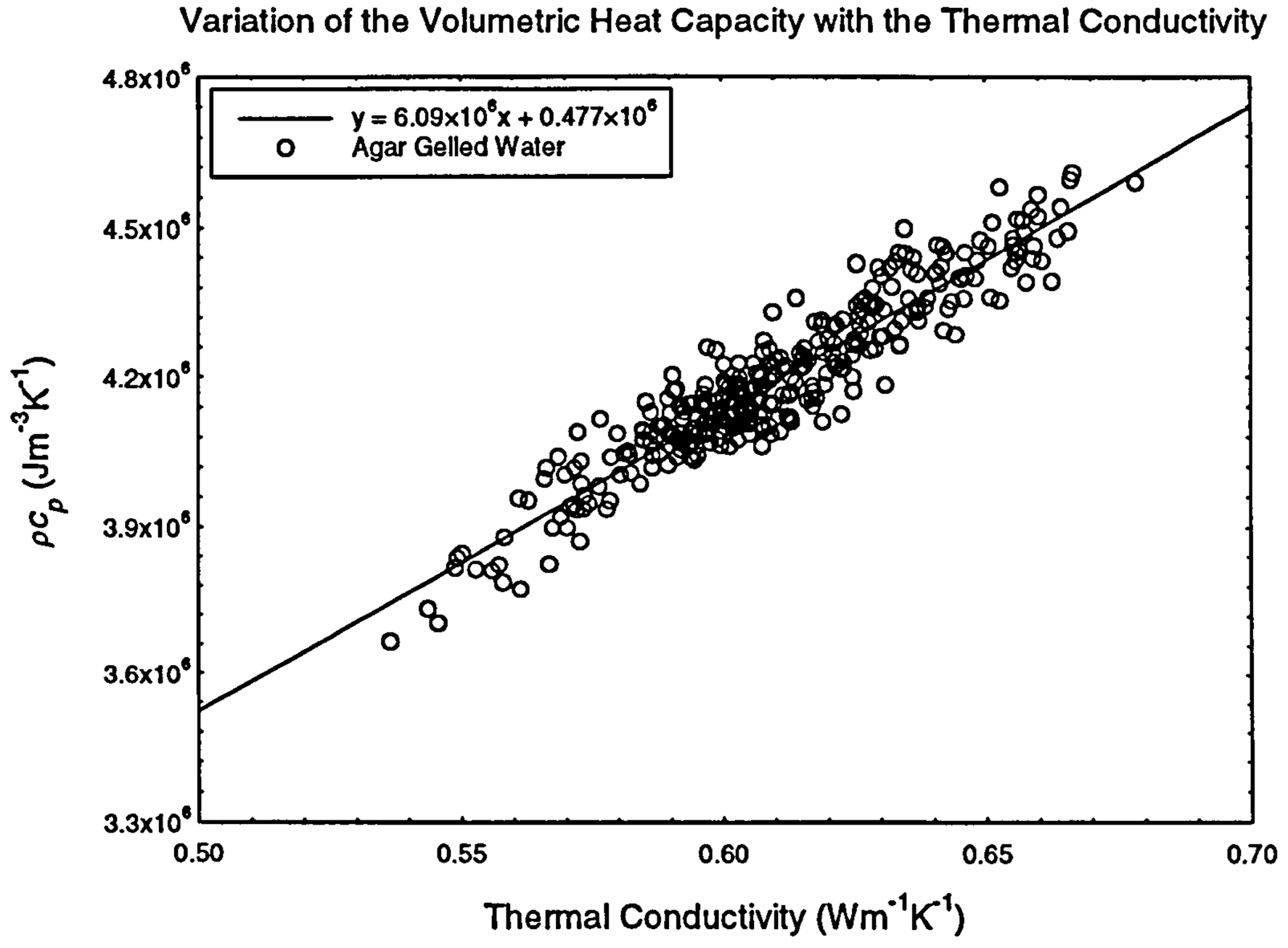

Figure 4.18 The relationship between ρc_p and k for agar gelled water.

However it can be seen that in figure 4.18, that although there is a linear relationship, there is an significant amount of spread in the data on either side of the linear fit. It is this deviation from the fitted straight line which causes the relationship between the thermal diffusivity and thermal conductivity due to the probe to become less clear.

Figure 4.19 shows the relationship between ρc_p and the thermal conductivity for all the calibration data. It can be seen that the expected relationship between ρc_p and the thermal conductivity is also linear. However the behaviour of the individual calibration materials is different from the overall behaviour. Also the gradient of the individual calibration materials tends to decrease as the conductivity increases. Thus when examining the relationship in individual tissue types, only the relationship between the thermal diffusivity and the thermal conductivity can be examined. If there is any definite trend shown, it will most probably be due to the tissue rather than the probe. However over the longer range, when examining all tissue types, the behaviour of the tissue will dominate over probe behaviour and hence the relationship between ρc_p and k can be examined.

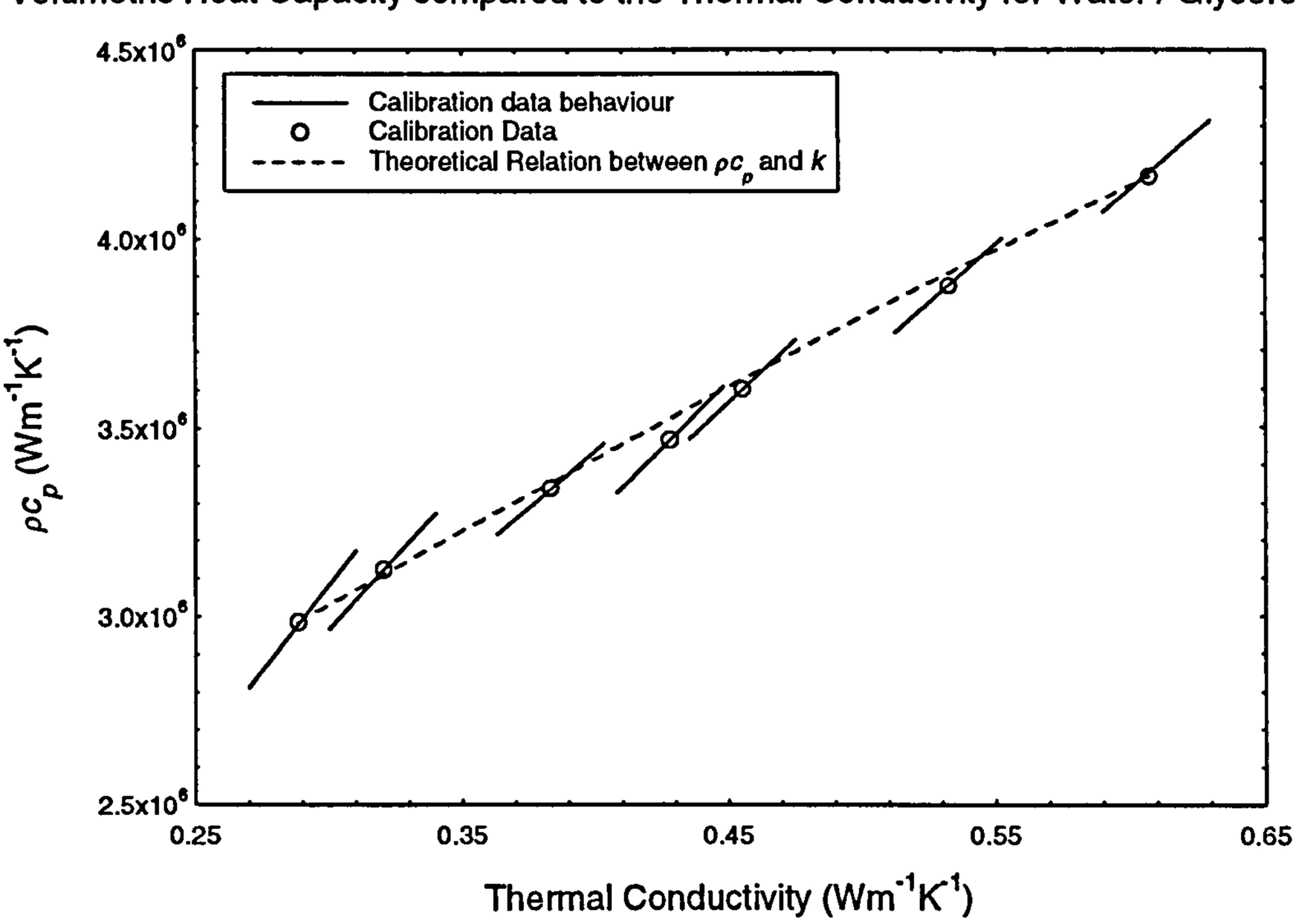

Figure 4.19 Comparison between the variation of ρc_p against k for the individual calibration materials and the variation of ρc_p against k over the range of all the calibration materials.

Chapter 5: Results of the Thermal Property Measurements on Biological Tissue.

5.1 Introduction.

In this chapter, new thermal conductivity and thermal diffusivity data for human and animal tissues, measured *in-vitro*, are presented and discussed. The data is presented by tissue type, with the animal data being compared to the results found for human tissue. The measured data is also compared to the thermal conductivity and thermal diffusivity found for similar tissues by other authors.

For the purposes of clarity, the number of *specimens* refers to the number of donors from which human tissue was obtained. The number of *samples* refers to the number of separate pieces of tissue that were examined. The number of samples is equal to the number of water content measurements made. Finally, the number of *measurements* refers to the number of times the thermal properties of a tissue were taken. During this chapter, the sample thermal conductivity or the sample thermal diffusivity is referred to. This value is just the average of the measurements of the thermal conductivity or diffusivity made on the particular sample.

5.2 Sample Sources.

The animal tissues used in this study were obtained from local tradesmen in a state fit for human consumption. After purchase, the animal tissues were kept refrigerated in a sealed container and used within 48 hours.

The human tissues examined were obtained from postmortem and surgery subjects from the mortuary and pathology departments of the Western Infirmary and Royal Infirmary Hospitals, Glasgow. The majority of tissue was supplied from postmortem subjects.

For hygiene reasons, only otherwise healthy tissue was taken from postmortem subjects who had deceased no more than 24 hours prior to tissue excision. Once obtained, the samples were stored in a similar fashion to the animal tissue samples. Samples were kept stored until measurements were made, which was usually within 48 hours of excision. Unless stated otherwise, it should be assumed that the human tissue being examined came from postmortem subjects.

5.3 Measurement of Sample Water Content.

After the thermal conductivity and diffusivity had been measured, the water content of each of the samples was established. The sample was placed in a glass petri dish lined with aluminium foil, and weighed on an electronic balance, the mass of the petri dish and foil having being measured beforehand. The sample was then dehydrated in an oven until it reached a stable mass. Finally the sample was removed from the oven and the mass of the petri dish, aluminium foil and sample were again measured.

After preliminary investigations into the oven drying procedure, made with computer monitored thermocouples, it was decided that a temperature of 85°C should be used to dehydrate the samples. At this temperature, most tissue samples showed a balance between the energy absorbed through conduction and the energy lost through evaporation. An average sized sample took approximately 12-16 hours to dry out and reach stable mass. The measurements of the mass were made with an electronic balance with a resolution of 0.001g. This resolution was sufficient to allow the accurate measurement of the water content.

When the thermal properties of a tissue are being compared to the measured water content, it is important to remember that the volume of tissue that was significant in the measurement of the thermal conductivity and diffusivity will be smaller than the total sample volume. As discussed in chapter 4, the effective measurement volume is a sphere of radius 5-10 times that of the thermistor. This gives a measurement volume no greater than 2.2 cm^3 compared to a typical sample volume of 8 cm^3. Thus the measured water content may not accurately reflect the water content associated with the measured thermal properties. To reduce any inconsistencies, the specimens used were, as far as possible, cut to give as uniform as possible a sample so that the water content of the whole sample reflected the water content in the measurement volume. However, given that the judgement about uniformity was made on the subjective basis, it is inevitable that the measured water content will often not reflect the water content of the measurement volume.

5.4 Variation Between Animal and Human Tissue.

Along with human tissue, porcine, agnine and bovine tissue were examined in this study. Physiologically, human, porcine, agnine and bovine tissue are all very similar. Since all animal tissues undergo similar processes before sale, it would be expected that there would be no significant differences between the thermal conductivity, thermal diffusivity and water content measured in the samples from animal species. However, there may be differences between the values measured in human tissue compared to animal tissue. The tissue of young animals used for commercial meats has a higher water content than that of the adults (Biology Data Book, 1972). For the animal tissues to be in a state fit for human consumption, the residual blood present in animal tissue had been drained. This may cause a drop of several percent in the water content of the sample. Finally human tissue was generally less uniform under visual inspection than animal tissue. The difference between animal and human tissues will be discussed in detail later, where appropriate.

5.5 Fat Tissues.

Fat tissue is a low water content connective adipose tissue, mainly composed of lipid. Lipids are fat and fat like substances. Lipids can be classed in to simple lipids, compound lipids and sterols. A simple lipid is an ester of a fatty acid and an alcohol, while a compound lipid contains other products beside the fatty acid and alcohol. Sterols are high molecular weight monohydroxy alcohols derived from the cyclic hydrocarbon cyclopentanoperhydrophenanthrene.

Fat tissue is found subcutaneously and around internal organs and it serves to support, protect, insulate and store energy. Fat tissue consists of a fine network of delicate fibres and has a very low blood supply, as blood is not usually required for fat tissue to perform it functions.

Fat Tissue	No. of Samples	No. of Meas.	Mean Thermal Conductivity ($Wm^{-1}K^{-1}$)	Mean Thermal Diffusivity (m^2s^{-1})	Mean % Water Content by Mass
Agnine	11	55	0.213	0.788×10^{-7}	12.8
Bovine	18	90	0.202	0.715×10^{-7}	12.9
Porcine	29	145	0.253	0.861×10^{-7}	14.0
Overall	58	290	0.229	0.802×10^{-7}	13.4

Table 5.1 The mean thermal conductivity, thermal diffusivity and water content of the animal fat tissues measured in this study.

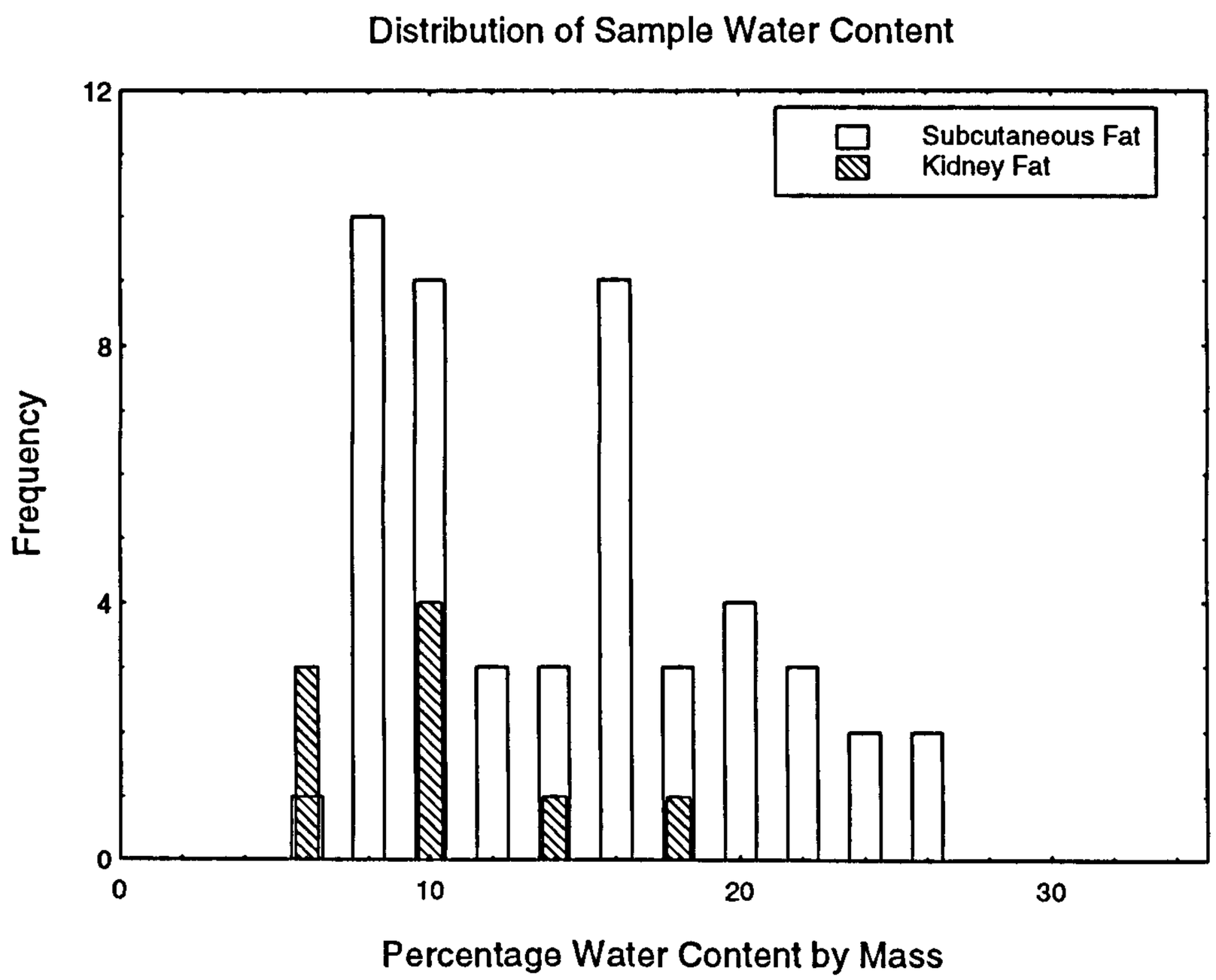

Figure 5.1 The distribution of measured water content for all animal fat samples.

5.6 Animal Fat Tissue.

In total, 290 measurements were made on 58 animal fat samples. A total of 145 measurements were made on 29 samples of porcine fat, all of which was subcutaneous fat. Fifty-five measurements were made on 11 samples of agnine fat. Twenty of these measurements were made on 4 samples of internal fat from the region around the kidney and the rest of the measurements were made on subcutaneous fat. Ninety measurements were made on 18 samples of bovine fat. Twenty-five of these measurements were made on 5 samples of internal fat from the region around the kidney and the rest were made on subcutaneous fat.

Table 5.1 shows the mean thermal conductivity, thermal diffusivity, and water content of all the animal fats measured in this study.

The distribution of sample water content for animal fat is shown in figure 5.1, while the distribution of measurements of the thermal conductivity and thermal diffusivity of animal fat are shown in figures 5.2 and 5.3 respectively. The range of values of water content, thermal conductivity and thermal diffusivity are

Water Content (%)	Minimum	5.0	Maximum	26.7	Mean	13.4
Thermal Conductivity ($Wm^{-1}K^{-1}$)	Minimum	0.097	Maximum	0.338	Mean	0.229
Thermal Diffusivity ($\times 10^{-7}\ m^2s^{-1}$)	Minimum	0.361	Maximum	1.070	Mean	0.802

As can be seen in the figures 5.2 and 5.3, the maximum values of the thermal conductivity and thermal diffusivity were not exceptional. The maximum values are associated with the upper range of values seen in the subcutaneous fat tissue. The histogram also shows that the lowest values of both the thermal conductivity and thermal diffusivity are associated with fat which was taken from a region around the kidney. The lowest water content is also measured in a kidney fat sample.

5.6.1 Subcutaneous and Kidney Fat.

The difference between the characteristics of subcutaneous and kidney fat is shown in table 5.2. This shows that the kidney fat has far lower thermal conductivity and thermal diffusivity than subcutaneous fat. When the minimum and maximum values are

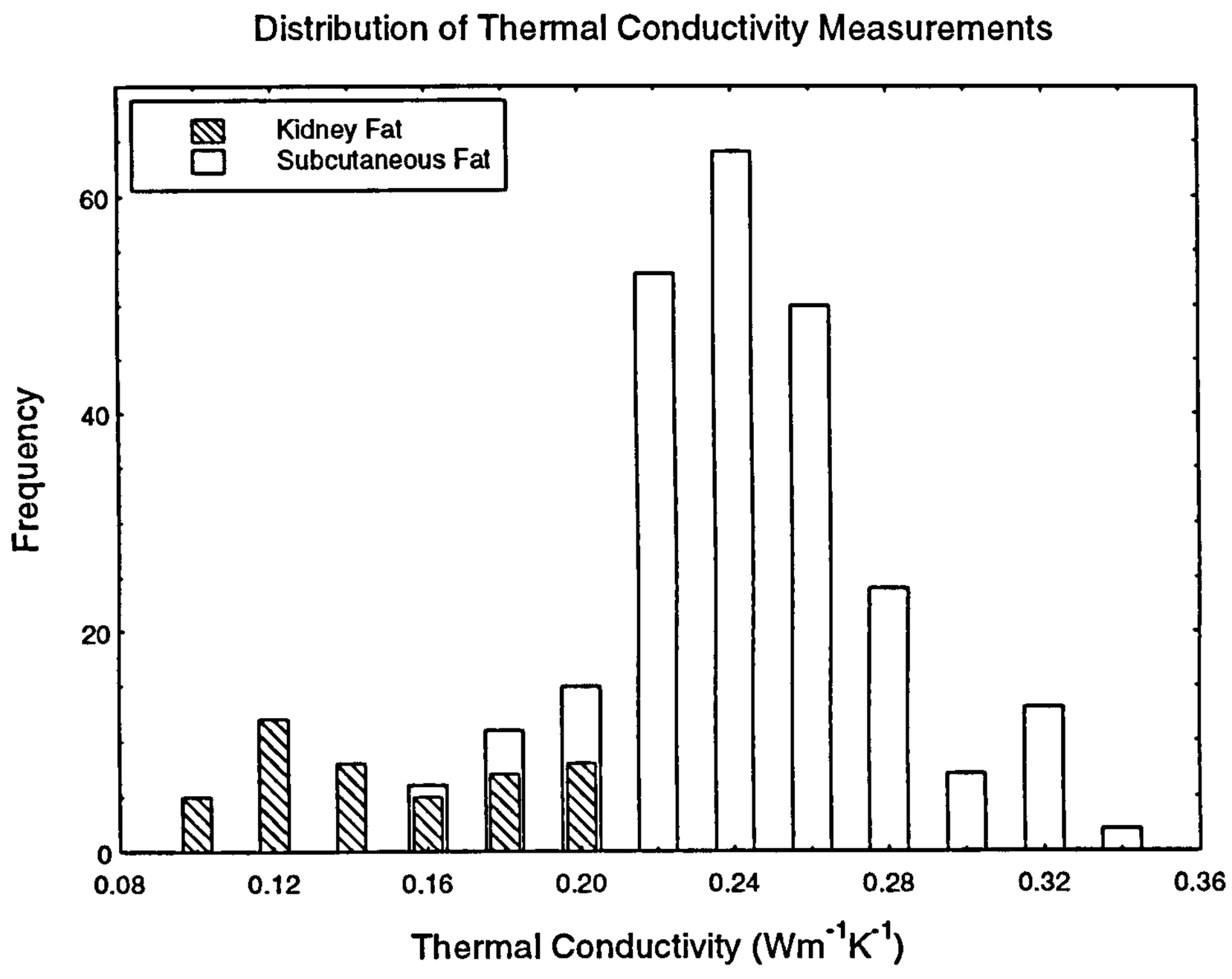

Figure 5.2 The distribution of thermal conductivity for all animal fat measurements.

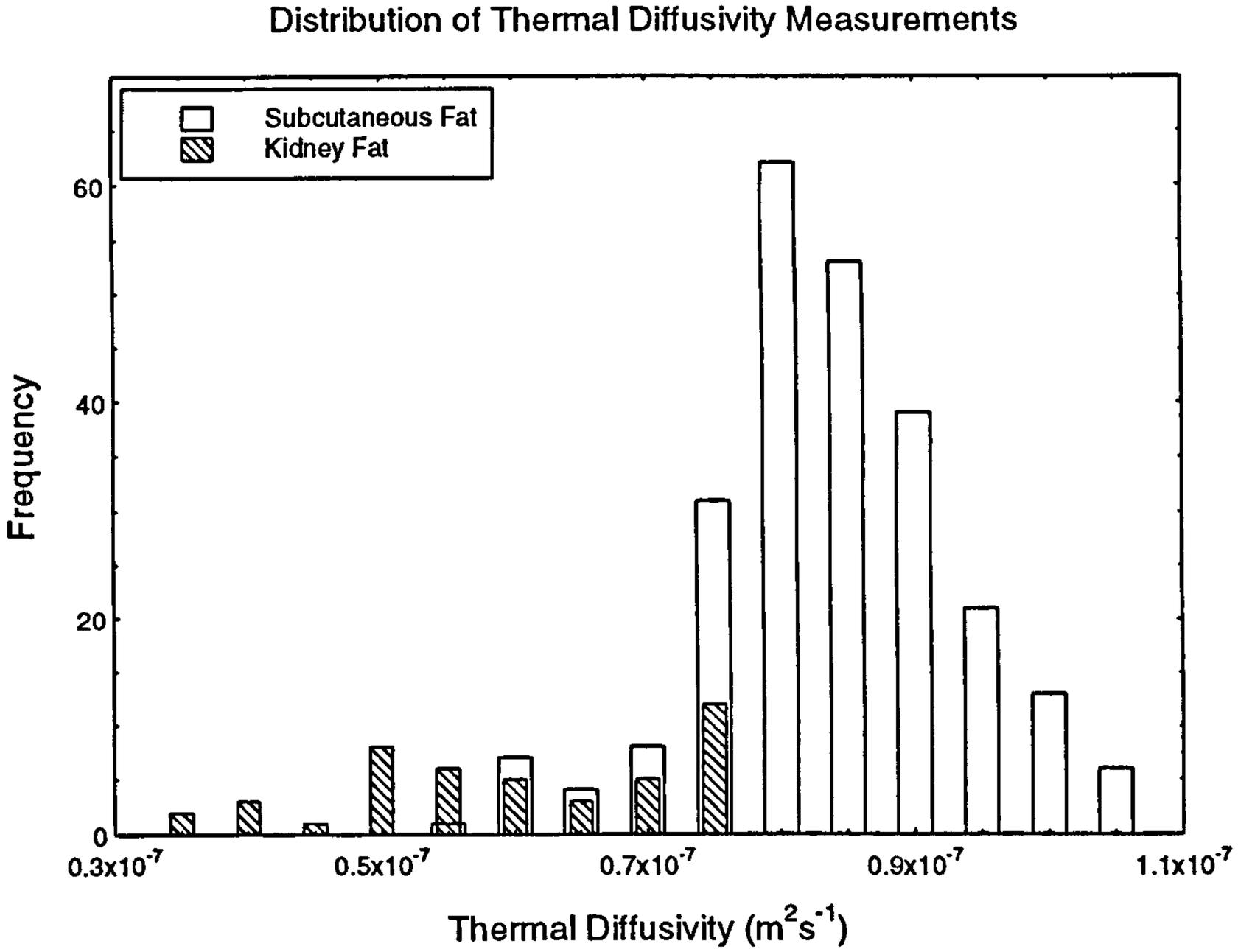

Figure 5.3 The distribution of thermal diffusivity for all animal fat measurements.

Fat Tissue Type	No. of Samples	Number of Measurements	Thermal Conductivity ($Wm^{-1}K^{-1}$)			Thermal Diffusivity (m^2s^{-1})			Mean % Water Content by Mass
			Mean	Maximum	Minimum	Mean	Maximum	Minimum	
Porcine									
Subcutaneous	29	145	0.253	0.338	0.152	0.861×10^{-7}	1.027×10^{-7}	0.572×10^{-7}	14.0%
Agnine									
Subcutaneous	7	35	0.229	0.261	0.212	0.827×10^{-7}	0.963×10^{-7}	0.768×10^{-7}	16.7%
Kidney	4	20	0.185	0.201	0.156	0.719×10^{-7}	0.761×10^{-7}	0.667×10^{-7}	6.1%
Bovine									
Subcutaneous	13	65	0.232	0.314	0.166	0.796×10^{-7}	1.070×10^{-7}	0.584×10^{-7}	13.0%
Kidney	5	25	0.122	0.144	0.097	0.503×10^{-7}	0.592×10^{-7}	0.361×10^{-7}	12.6%
Overall									
Subcutaneous	49	245	0.244	0.338	0.152	0.839×10^{-7}	1.070×10^{-7}	0.572×10^{-7}	14.1%
Kidney	9	45	0.150	0.201	0.097	0.599×10^{-7}	0.761×10^{-7}	0.361×10^{-7}	9.71%

Table 5.2 Comparison between the mean, maximum and minimum values of the thermal conductivity, diffusivity and water content of subcutaneous and internal kidney fat tissues.

examined, it can be seen that, for each species, the maximum values of the thermal conductivity and thermal diffusivity of kidney fat are equivalent to the minimum values measured for subcutaneous fat. This is explained by the low water content seen in the internal kidney fats compared to the subcutaneous fats. The mean water content values seen in kidney fats are lower than the mean water content values seen in the any of the subcutaneous fats. In fact, the water content of bovine kidney fat is actually lower than stated. The four samples of bovine kidney fat came from one specimen. This specimen contained an interior artery, which raised the water content of some of the samples and hence the mean water content. The true water content of the internal bovine fat is likely to be close to that measured in the agnine samples.

Table 5.3 shows the thermal conductivity of various animal fats as measured by other researchers. The source of the tissue, or the tissue water content, is given where the information is known. The range of values shown is consistent with the values measured in this study. Of particular interest are the results of Lapshin (1954) and Morley (1966). Lapshin's measured range of fat thermal conductivities agrees well with the range of values measured in this study. Lapshin also shows that a higher water content in fat gives the expected higher thermal conductivity. Morley (1966) quotes values for subcutaneous and kidney fat which agree well with those found in this study.

Table 5.4 shows the thermal diffusivity of various animal fats, as quoted by other authors. Fewer measurements have been made on the thermal diffusivity than the thermal conductivity, but those measurements that do exist fall within the range of values measured in this study. Lapshin again shows that increasing the water content of the bovine fat increases the measured thermal diffusivity.

5.6.2 Analysis of Measured Animal Fat Tissue Values

Figure 5.4 shows the variation of thermal diffusivity with thermal conductivity for all the animal fat samples examined in this study, while figures 5.5 and 5.6 show the variation of thermal diffusivity with conductivity for all the measurements made on bovine and porcine fat respectively. Not enough measurements were made on agnine fat to provide a meaningful graph. These graphs show a linear correlation between the thermal conductivity and thermal diffusivity.

Fat Tissue Type	Thermal Conductivity ($Wm^{-1}K^{-1}$)	Reference
Bovine	0.204	Hardy and Soderstrom (1938)
Bovine	0.161-0.197	Hatfield and Pugh (1951)
Bovine	0.220	Hatfield (1953)
Bovine 2.0% water Bovine 15.2% water Bovine 29.5% water	0.093 0.180 0.345	Lapshin (1954)
Bovine 7% water	0.237	Cherneeva (1956)
Bovine 20% water	0.230	Poppendiek et al (1966)
Bovine (Sirloin) Bovine (Kidney)	0.209 0.188	Morley (1966)
Porcine (Subcutaneous)	0.160	Henriques and Moritz (1947)
Porcine (Loin)	0.195	Morley (1966)
Porcine	0.206	Liang et al (1991)
Whale Blubber	0.21-0.31	Kvadsheim et al (1996)
General	0.132-0.156	Bruer (1924)

Table 5.3 Published thermal conductivity of various animal tissue fats.

Fat Tissue Type	Thermal Diffusivity (m^2s^{-1})	Reference
Bovine 2.0% water Bovine 15.2% water Bovine 29.5% water	0.552×10^{-7} 0.633×10^{-7} 0.706×10^{-7}	Lapshin (1954)
Bovine 7% water	0.78×10^{-7}	Cherneeva (1956)

Table 5.4 Published thermal diffusivity of various animal tissues fats.

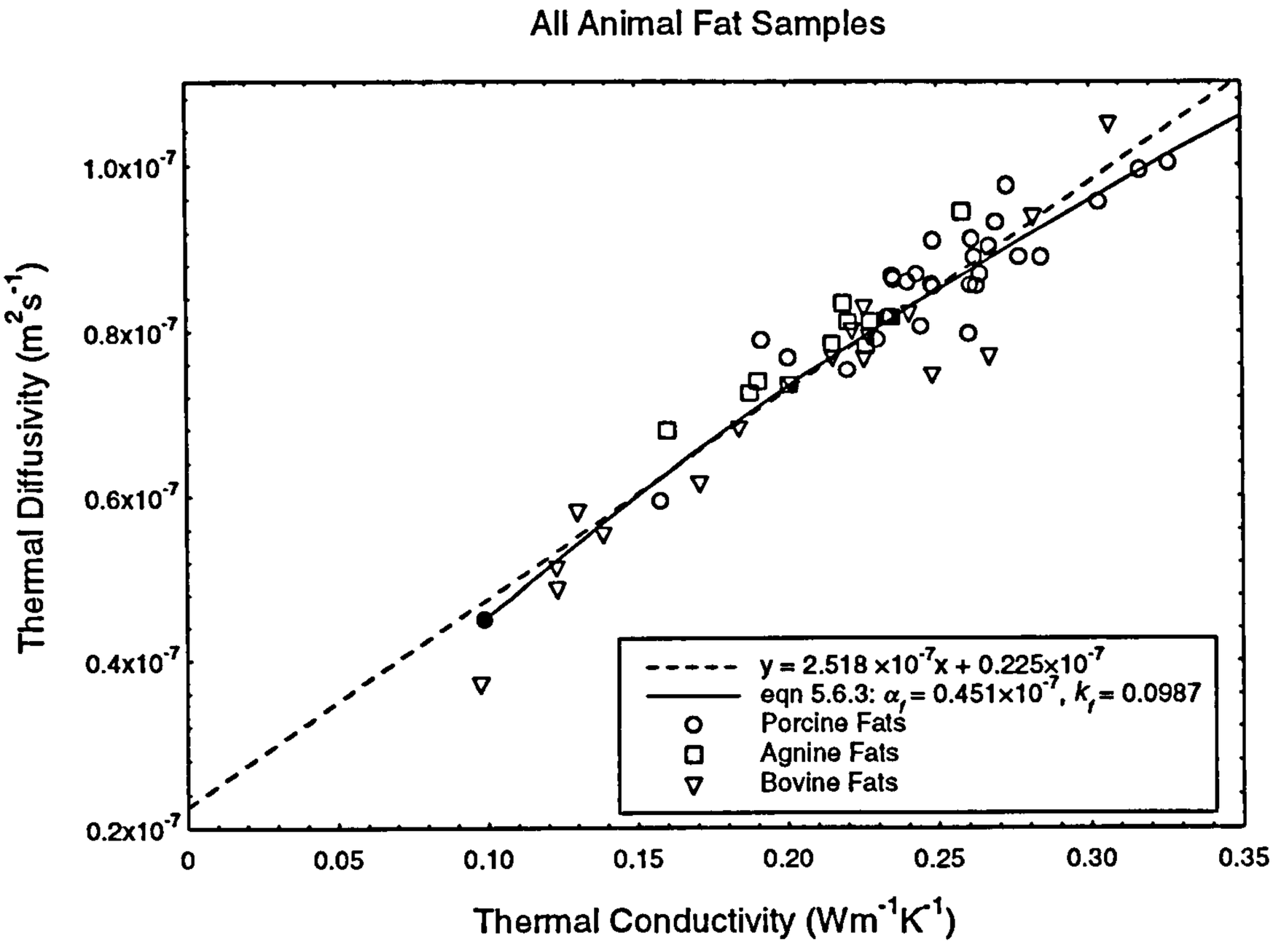

Figure 5.4 Thermal diffusivity and conductivity for all the animal fat samples.

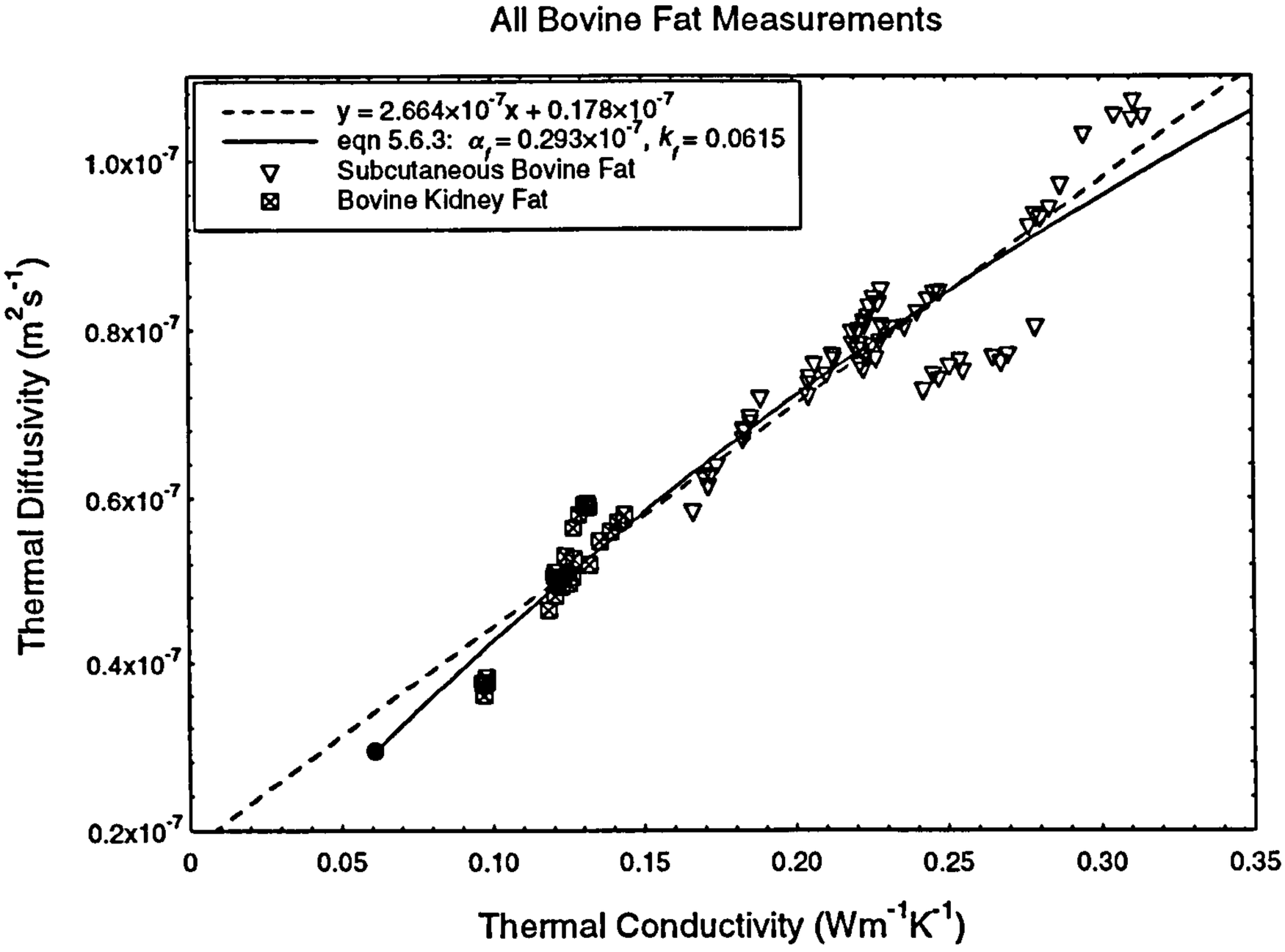

Figure 5.5 Thermal conductivity and diffusivity for all bovine fat measurements.

There are two fits of the data. The first fit assumes there is a linear fit between the thermal conductivity and diffusivity. The linear fits of the data give the following values

All animal fat samples: $\alpha = (2.518k + 0.225) \times 10^{-7}\ m^2s^{-1}$

All bovine fat measurements: $\alpha = (2.664k + 0.200) \times 10^{-7}\ m^2s^{-1}$

All porcine fat measurements: $\alpha = (2.108k + 0.328) \times 10^{-7}\ m^2s^{-1}$

The other fit assumes that both the thermal conductivity and thermal diffusivity can be modelled by Maxwell's mixture equation.

Maxwell's mixture equation gives that thermal conductivity and thermal diffusivity of a mixture of water and pure dry fat as

$$\frac{k-k_f}{k+2k_f} = \frac{k_w-k_f}{k_w+2k_f}\phi_w \tag{5.6.1}$$

$$\frac{\alpha-\alpha_f}{\alpha+2\alpha_f} = \frac{\alpha_w-\alpha_f}{\alpha_w+2\alpha_f}\phi_w \tag{5.6.2}$$

where k_f , k_w, and k are the thermal conductivities of fat, water, and the mixture respectively, while α_f , α_w, and α are thermal diffusivities of fat, water, and the mixture respectively. The water content by volume is given by ϕ_w. Combining equations 5.6.1 and 5.6.2 gives

$$\alpha = \alpha_f \frac{(2k_f\alpha_f - k_f\alpha_w - k_w\alpha_w)k + 2(k_f\alpha_w - k_w\alpha_f)k_f}{(k_f\alpha_w - k_w\alpha_f)k + (2k_f\alpha_f - k_w\alpha_f - k_w\alpha_w)k_f} \tag{5.6.3}$$

This equation is not directly dependant on the water content of the mixture.

There are little accurate data on the thermal conductivity and thermal diffusivity of dehydrated fat. What data do exist appear to contradict the results in this study, and other researchers results, with a value which is higher than many of the measured values of fat. The thermal conductivity of dry fat is given as 0.19 $Wm^{-1}K^{-1}$ by Poppendiek et al (1966), while Miles et al (1983) and Choi and Okos (1986) both give a value of 0.18 $Wm^{-1}K^{-1}$. Nearly all the measured thermal conductivities of kidney fat lie below these values. As noted previously, the water content in the measurement volume will often be different from the water content in the whole sample. This appears to be particularly true of fat tissues, with there being no clear correlation between the measured thermal properties and the measured water content.

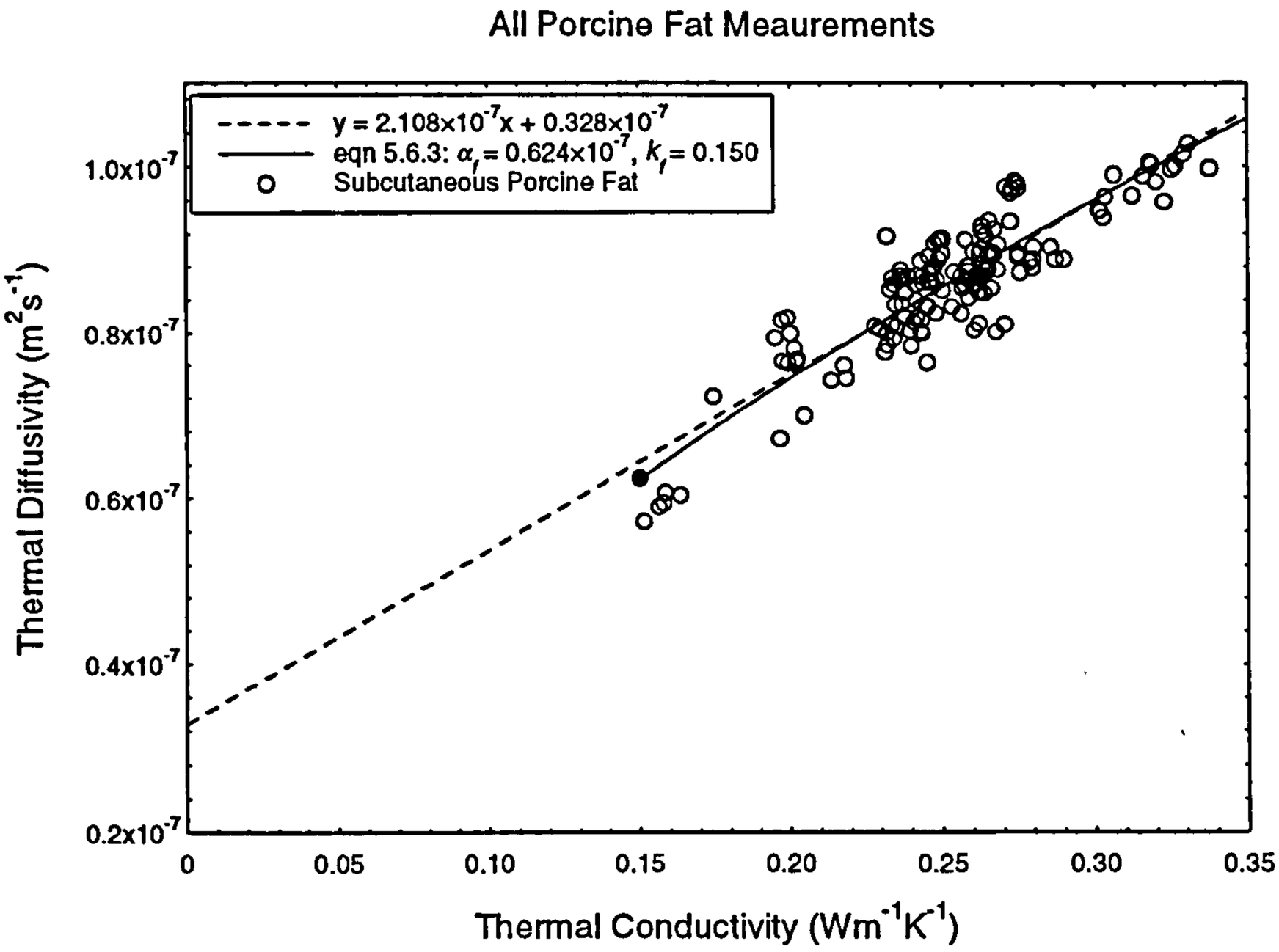

Figure 5.6 Thermal conductivity and diffusivity for all porcine fat measurements.

Fat Tissue	No. of Samples	No. of Meas.	Mean Thermal Conductivity ($Wm^{-1}K^{-1}$)	Mean Thermal Diffusivity (m^2s^{-1})	Mean % Water Content by Mass
Breast:					
Surgery	2	10	0.202	0.711×10^{-7}	12.7
Postmortem	20	100	0.210	0.728×10^{-7}	15.0
Heart	4	20	0.252	0.822×10^{-7}	28.6
Overall	26	130	0.216	0.741×10^{-7}	17.3

Table 5.5 The mean thermal conductivity, thermal diffusivity and water content of the human fat tissues measured in this study.

The thermal conductivity and thermal diffusivity were measured at the same time with the same probe, so the same volume of tissue is probed. Thus the measured thermal conductivity and diffusivity will always be dependant on the same water content. Given that the thermal conductivity and thermal diffusivity of water are accurately known, equation 5.6.3 can be used to determine the thermal conductivity and thermal diffusivity of dehydrated fat.

Equations similar to equation 5.6.3 can be produced for other mixture equations. However, when the thermal conductivity and thermal diffusivity are modelled by the series limit, no solution can be gained, and when modelled by the parallel limit or Hashin and Shtrikman upper limit, unrealistic values of thermal conductivity and thermal diffusivity of fat are gained.

The fit using equation 5.6.3 gives the dehydrated thermal conductivity and thermal diffusivity of fat as

All animal fat samples: $k_f = 0.099\ \mathrm{Wm^{-1}K^{-1}}$, $\alpha_f = 0.451\times10^{-7}\ \mathrm{m^2s^{-1}}$

All bovine fat measurements: $k_f = 0.062\ \mathrm{Wm^{-1}K^{-1}}$, $\alpha_f = 0.293\times10^{-7}\ \mathrm{m^2s^{-1}}$

All porcine fat measurements: $k_f = 0.150\ \mathrm{Wm^{-1}K^{-1}}$, $\alpha_f = 0.624\times10^{-7}\ \mathrm{m^2s^{-1}}$

These values will be explored in detail later on in the chapter.

5.7 Human Fat Tissue.

In total, 130 measurements were made on 26 human fat samples. The vast majority of these measurements were made on fat tissue which came from the female human breast. A total of 100 measurements were made on 20 samples of breast fat which had been removed postmortem from one subject. Another 10 measurements were made on two samples of breast fat which had been removed during surgery from two different subjects.

The other fat tissue studied was taken from around the region of the human heart. Twenty measurements were made on 4 samples of fat which were removed postmortem from one subject. It should be noted that the human heart fat was not stored in ideal conditions. Before probing, the heart fat was stored in water for a period of time. This will have an effect on the water content and hence the thermal conductivity and thermal diffusivity of the tissue.

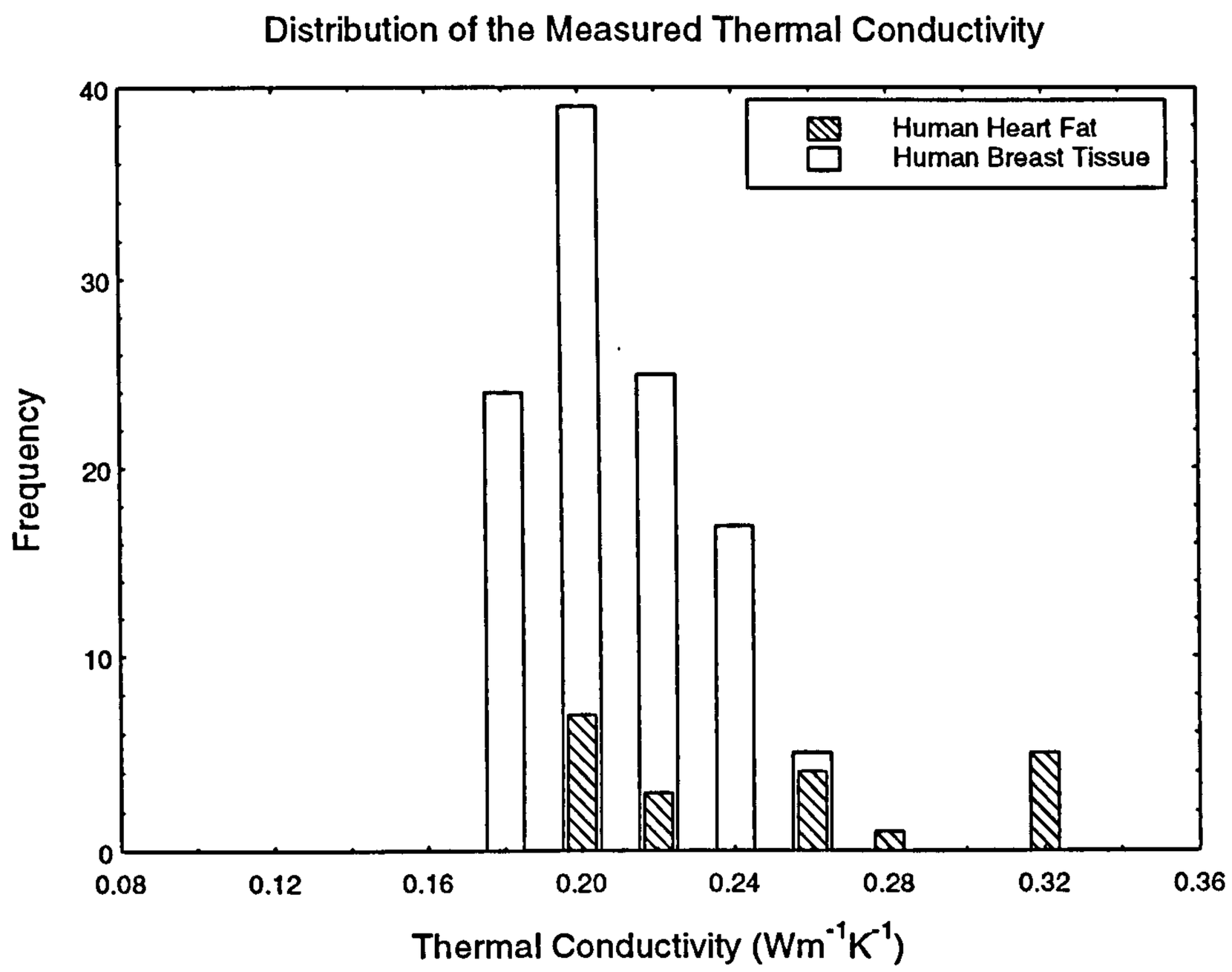

Figure 5.7 Distribution of thermal conductivity for all measurements on human fat.

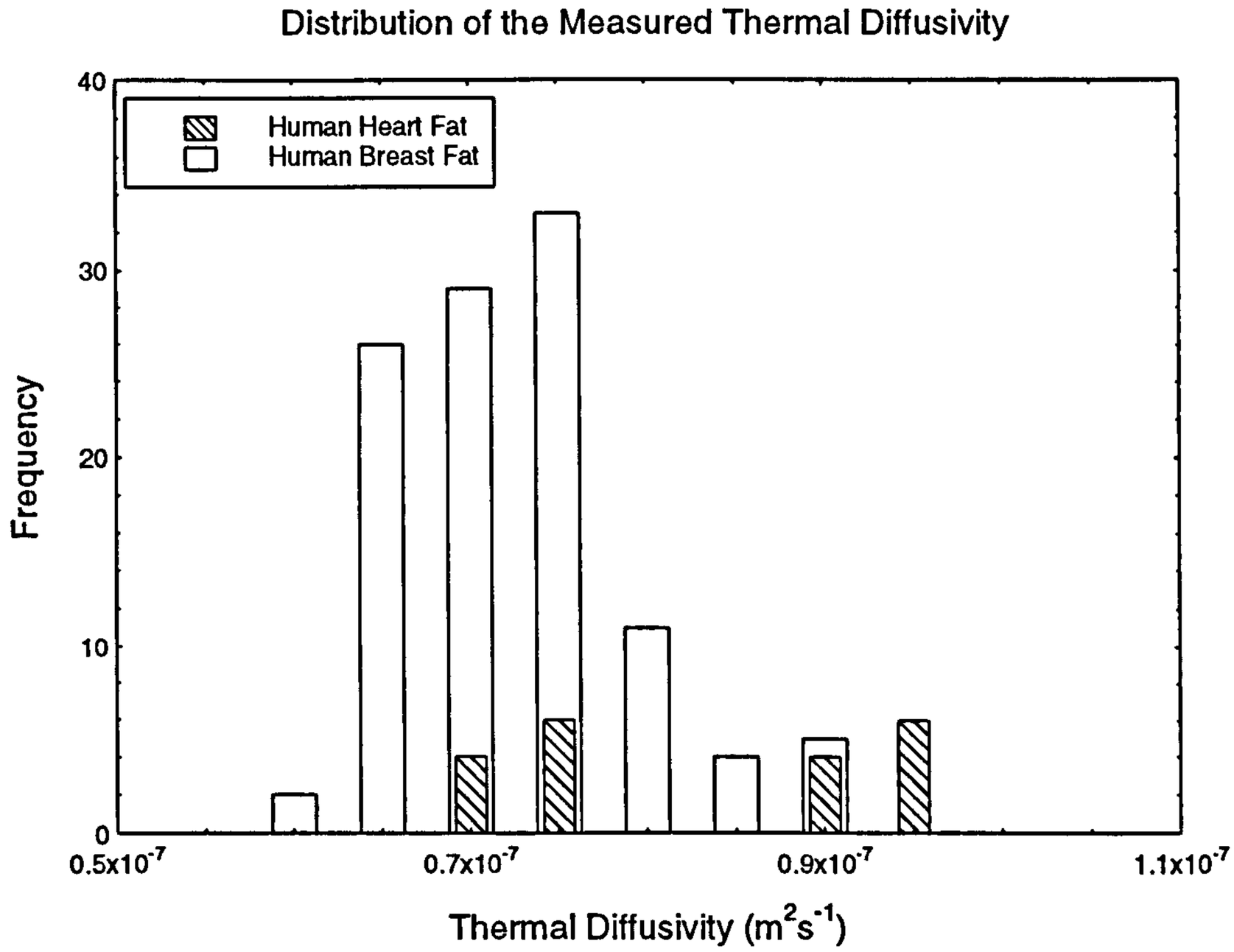

Figure 5.8 Distribution of thermal diffusivity for all measurements on human fat.

Table 5.5 shows the average thermal conductivity, thermal diffusivity, and water content for the human fat tissues examined in this study.

The distribution of the measurements of the thermal conductivity and thermal diffusivity of human fat are shown in figure 5.7 and figure 5.8, while the distribution of the measured sample water content of human fat samples is shown in figure 5.9. The range of measured water content, thermal conductivity, and thermal diffusivity are as follows:

Water Content (%)	Minimum 10.8	Maximum 33.8	Mean 16.9
Thermal Conductivity ($Wm^{-1}K^{-1}$)	Minimum 0.171	Maximum 0.321	Mean 0.216
Thermal Diffusivity ($\times 10^{-7}\ m^2s^{-1}$)	Minimum 0.601	Maximum 0.940	Mean 0.741

For figures 5.7, 5.8, and 5.9, it is clear that the highest values for the water content, thermal conductivity and thermal diffusivity are all associated with human heart fat. This is due to the immersion in water of the heart fat. This gave all the heart fat samples very high water contents, resulting in an average water content almost twice as high as that seen in any other fat tissue. However, when the thermal conductivity and the thermal diffusivity of the heart fat samples are examined, we see that there is an indication of the true thermal properties of heart fat.

There are two behaviours seen in the thermal conductivity and thermal diffusivity of heart fat. Measurements made on two of the samples gave thermal properties similar to that of breast fat, while the other two samples gave thermal properties which lay at the upper range of values found. The lower values were most probably taken in measurement volumes which had been relatively unaffected by the immersion in water and give a truer indication of the thermal properties of human heart fat.

The range of values measured for the breast fat alone is;

Water Content (%)	Minimum 10.8	Maximum 25.4	Mean 14.8
Thermal Conductivity ($Wm^{-1}K^{-1}$)	Minimum 0.171	Maximum 0.253	Mean 0.209
Thermal Diffusivity ($\times 10^{-7}\ m^2s^{-1}$)	Minimum 0.601	Maximum 0.923	Mean 0.728

We also see from table 5.5, that the properties of the breast fat removed during surgery is similar to properties of the breast fat that was removed postmortem. The difference between the properties of the surgery and postmortem fat tissues is small compared to the range of values measured in the human breast.

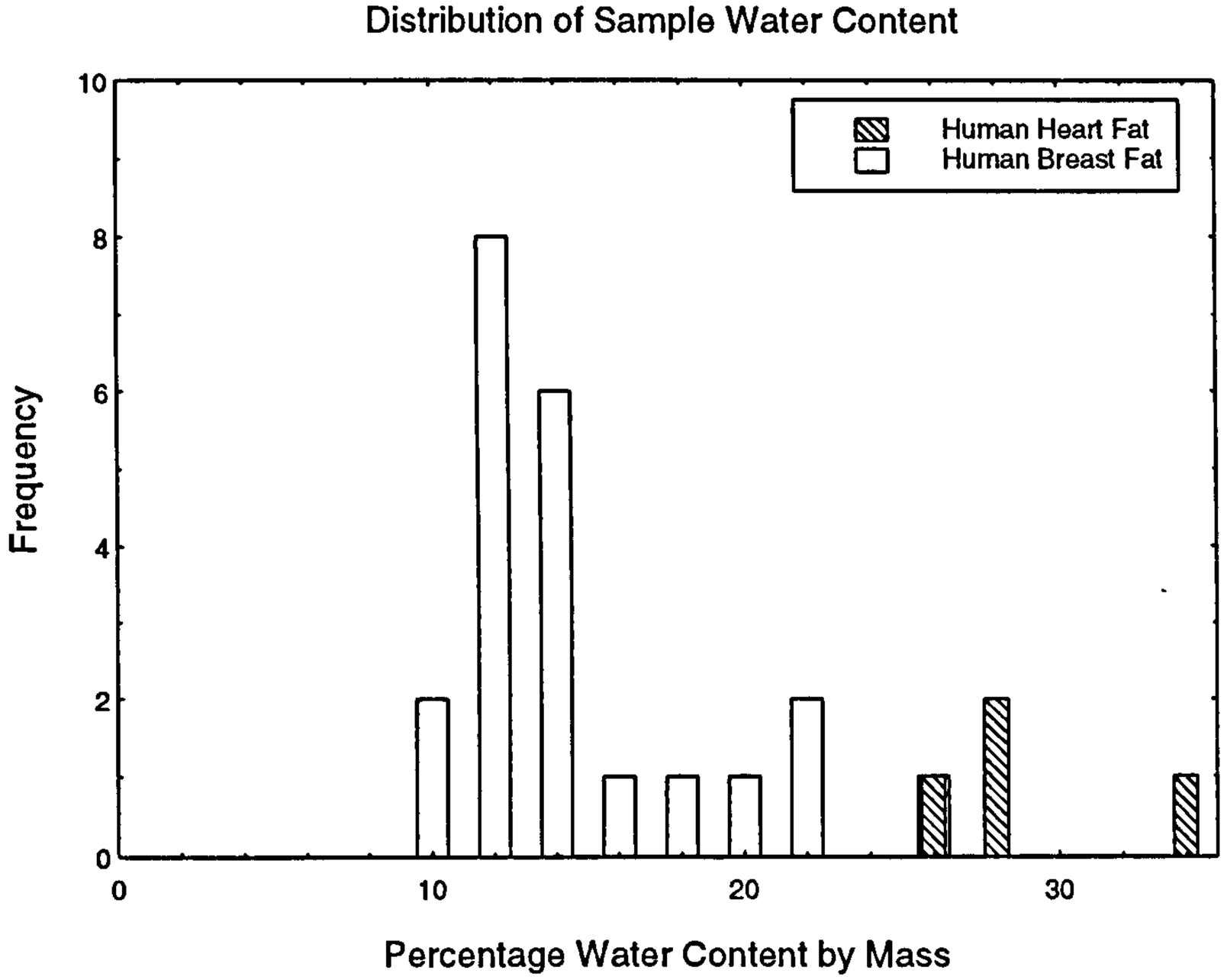

Figure 5.9 Distribution of water content for all human fat samples.

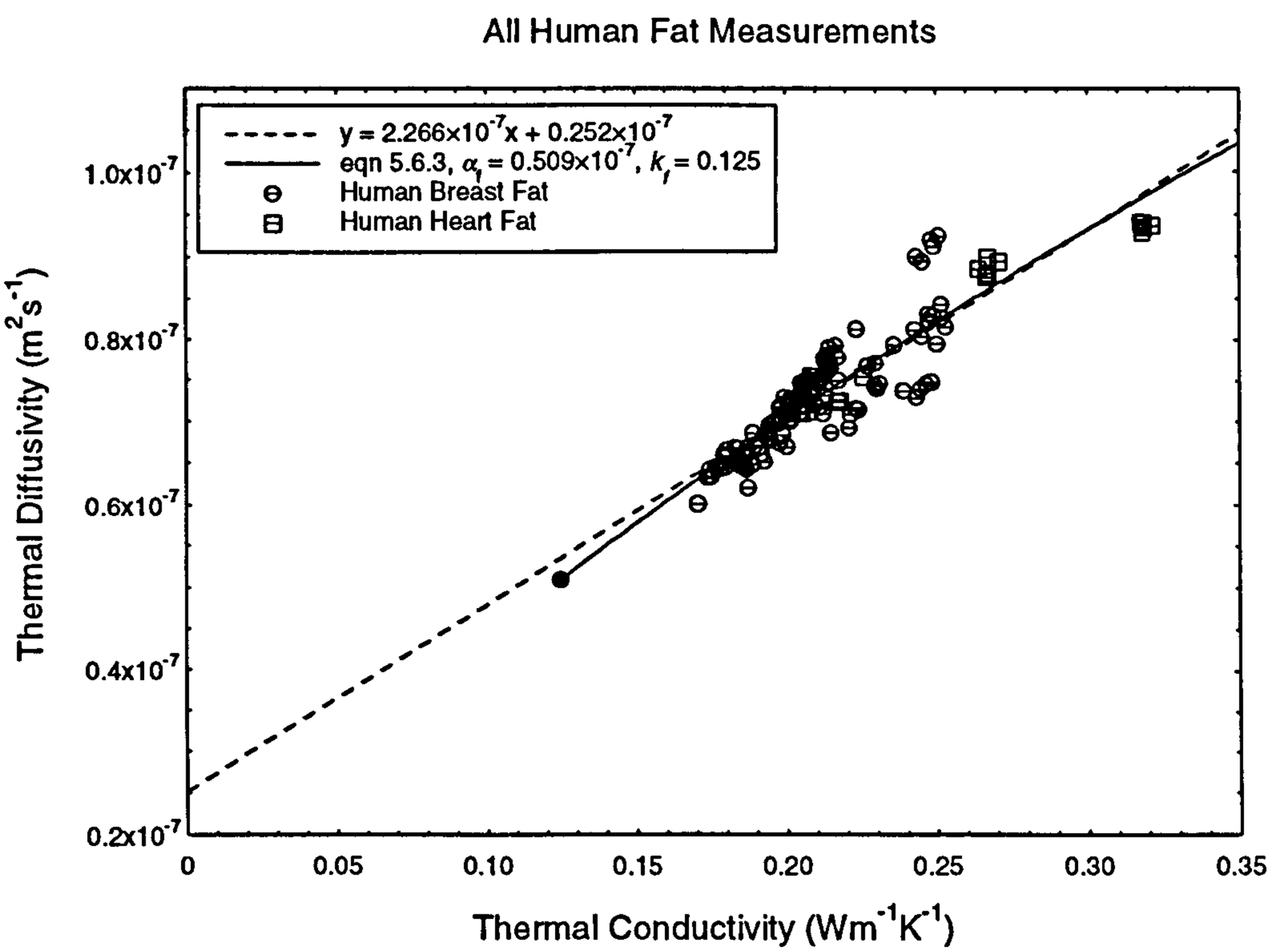

Figure 5.10 Thermal conductivity and diffusivity of all measurements on human fat.

Fat Tissue Area	Thermal Conductivity ($Wm^{-1}K^{-1}$)	Reference
General	0.204	Hatfield and Pugh (1951)
General	0.199	Hatfield (1953)
General	0.160	Gordon et al (1976)
Subcutaneous	0.200-0.246	Bowman (1981)
Surface of fat (4.8 mm)	0.268	
Intermediate fat (6.4 mm)	0.248	
Deep fat (9.8 mm)	0.219	
General	0.200	Hand et al (1982)
Spleen	0.343	Valvano et al (1985)
General	0.22	Schwab (1988)

Table 5.6 The published thermal conductivity of human fat.

Fat Tissue Area	Thermal Diffusivity (m^2s^{-1})	Reference
General	0.749×10^{-7}	Gordon et al (1976)
General	0.925×10^{-7}	Hand et al (1982)
Spleen	1.270×10^{-7}	Valvano et al (1985)
General	0.815×10^{-7}	Schwab (1988)

Table 5.7 The published thermal diffusivity of human fat.

Table 5.6 shows the thermal conductivity of various human fats as measured by other researchers. The spread in the values mirrors the spread in values of the thermal conductivity of breast fat. Of particular interest are the results of Bowman (1981). Bowman measured the thermal conductivity of fat at 4.8 mm, 6.4 mm and 9.8 mm below the surface of the skin and found that the thermal conductivity of fat is lower deep inside the body than it is at the surface. Table 5.7 shows the thermal diffusivity of various human fats as stated by other authors. There is less data about the thermal diffusivity of fats than the thermal conductivity, and the little data which does exist does not give one clear value.

Figure 5.10 shows the variation in thermal diffusivity with thermal conductivity for all the measurements made on human fat. As with the animal fat samples, we see a correlation between the thermal diffusivity and conductivity. The fits used to examine the human fat data were identical to those used to examine the variation of thermal diffusivity with thermal conductivity for animal fat tissues.

The linear fit gives that $\alpha = (2.266k + 0.252) \times 10^{-7}\ m^2s^{-1}$

The fit using equation 5.6.3 gives $k_f = 0.125\ Wm^{-1}K^{-1}$, $\alpha_f = 0.509 \times 10^{-7}\ m^2s^{-1}$

5.8 Comparison Between Human and Animal Fat.

When the average values for each of the fat tissues are examined, it is seen that human breast fat has a water content which is very similar to the water content of the subcutaneous animal fats. However, the thermal conductivity and thermal diffusivity of human breast fat is lower than that seen in the subcutaneous animal fats. The thermal behaviour of human breast fat appears to lie somewhere between the behaviour seen in the subcutaneous animal fats and the internal fats.

Given that Bowman (1981) found that the thermal conductivity of internal fat is lower than that of subcutaneous fat, it might also have been expected that the human heart fat would be similar in behaviour to the animal fat which came from around another organ, the kidney. The data however appears to suggest that the heart fat has similar properties to the animal subcutaneous fat. However, this is most probably due to the extended storage of the heart fat in water and, as stated earlier, the actually thermal conductivity and diffusivity of heart fat is lower than actually stated in this study.

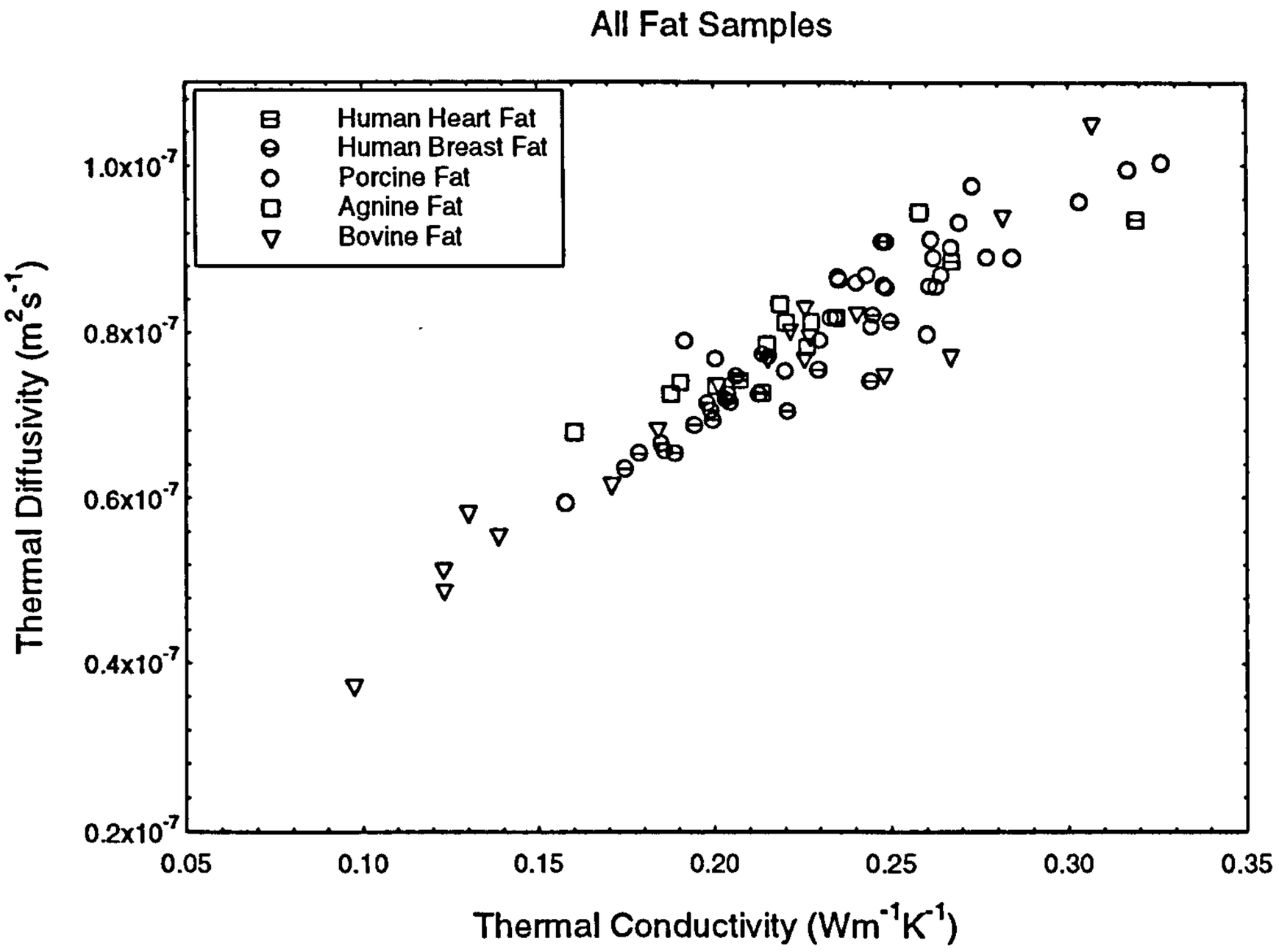

Figure 5.11 Thermal conductivity and diffusivity for all human and animal samples.

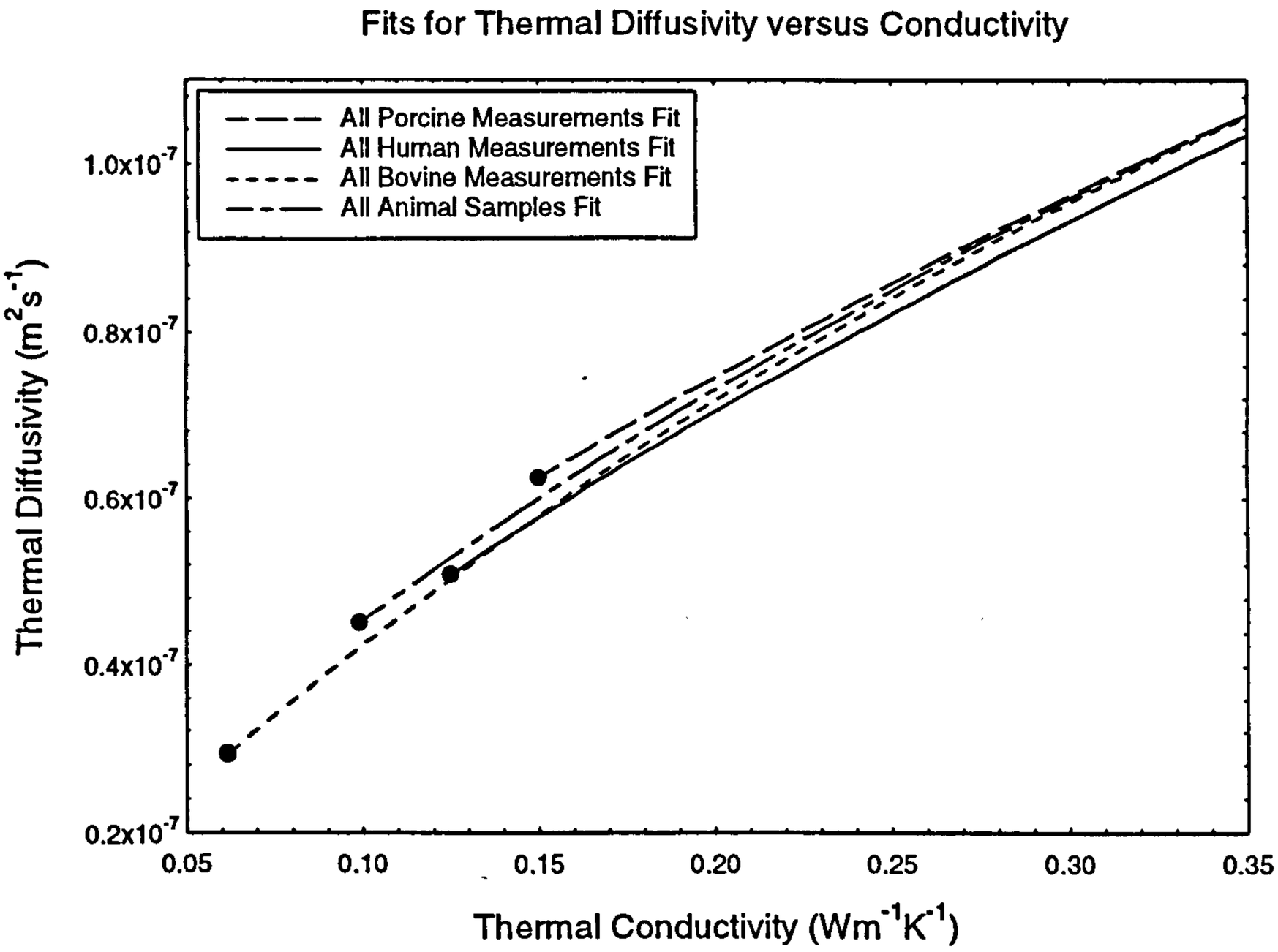

Figure 5.12 Curve fits of animal and human fat data.

Figure 5.11 shows the measured thermal conductivity for all the fat samples examined in this study. It can be seen that the relationship between the thermal diffusivity and conductivity differs little for animal and human fat tissues. However, there is a significant variation in the results which the curve fits produce. The difference between the maximum and minimum values of the thermal diffusivity predicted for a particular value of the thermal conductivity is always greater than 6% for the linear curve fits.

Figure 5.12 shows the curve fits produced using equation 5.6.3. This gives closer agreement between the four curves than the curves produced using the linear fit. However, this presents a fresh problem. The predicted values of the thermal conductivity and thermal diffusivity of dehydrated fat varied by greater than a factor of 2, but the actual curves are in very close agreement to each other. Thus it is clear that the estimated values of the thermal conductivity and thermal diffusivity of dehydrated fat are only approximate.

Figure 5.13 shows the variation of the measured thermal conductivity with the measured water content of all the fat samples examined in this study, while figure 5.14 shows the variation of the measured thermal diffusivity with the measured water content for all the fat samples. It is clear that there is no correlation between the water content as measured and the measured thermal property.

This is partly due to the probe error and partly due to the water content in the measurement volume not being reflected in the sample as a whole. A colleague found that the short range inhomogenity of breast fat samples examined in this study was such that the minimum and maximum values of the measured permittivity was virtually independent of the measured water content of the sample (Gorton, 1996). It is possible that this short range variation would be seen in the thermal properties of human tissue, giving the poor relationship between water content and thermal property.

5.9 Muscle Tissue.

Muscle tissue is by far the most common tissue in the human body, and it is characterised by its ability to contract. There are three types of muscle tissue; skeletal, smooth and cardiac. Skeletal muscle is uniform looking muscle which is under voluntary control. As the name of this tissue suggests, skeletal muscle is connected to the bone. As skeletal

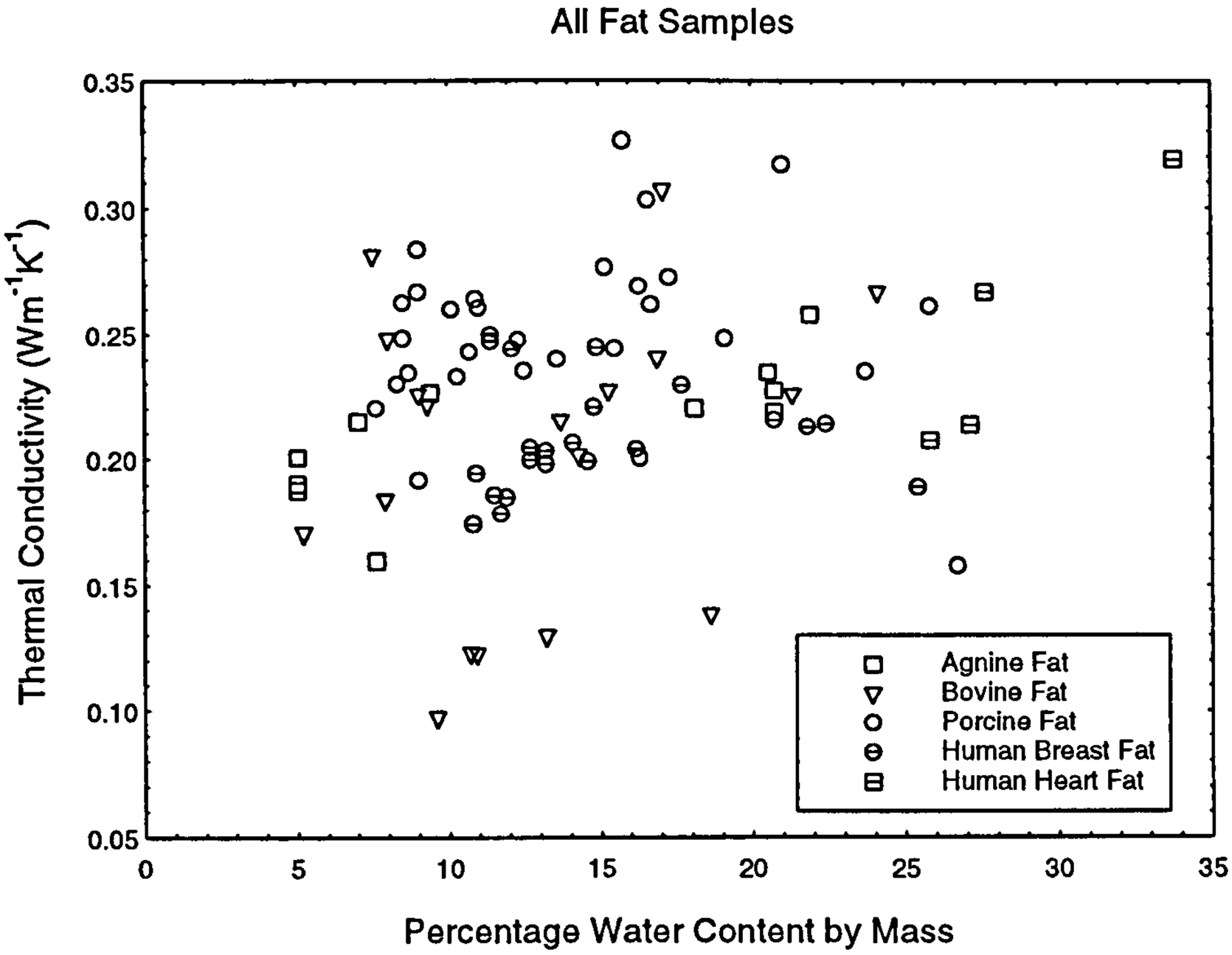

Figure 5.13 The measured thermal conductivity compared to sample water content.

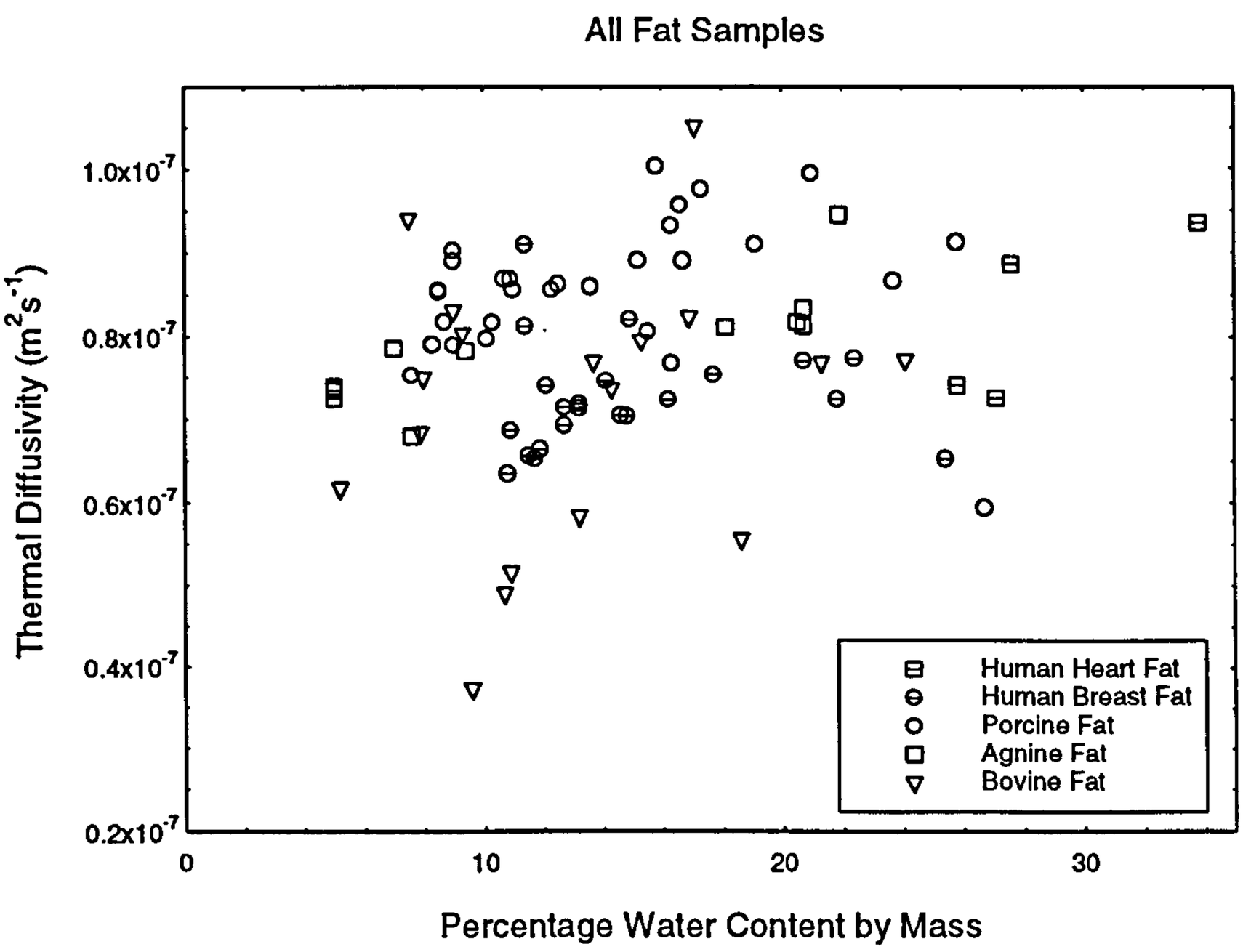

Figure 5.14 The measured thermal diffusivity compared to sample water content.

Skeletal Muscle Tissue	No. of Samples	No. of Meas.	Mean Thermal Conductivity ($Wm^{-1}K^{-1}$)	Mean Thermal Diffusivity (m^2s^{-1})	Mean % Water Content by Mass
Agnine	19	93	0.498	1.314×10^{-7}	75.4
Bovine	30	148	0.492	1.290×10^{-7}	73.9
Porcine	21	105	0.504	1.322×10^{-7}	73.7
Overall	70	346	0.497	1.306×10^{-7}	74.2

Table 5.8 The mean thermal conductivity, thermal diffusivity and water content of all the animal muscle tissues measured in this study.

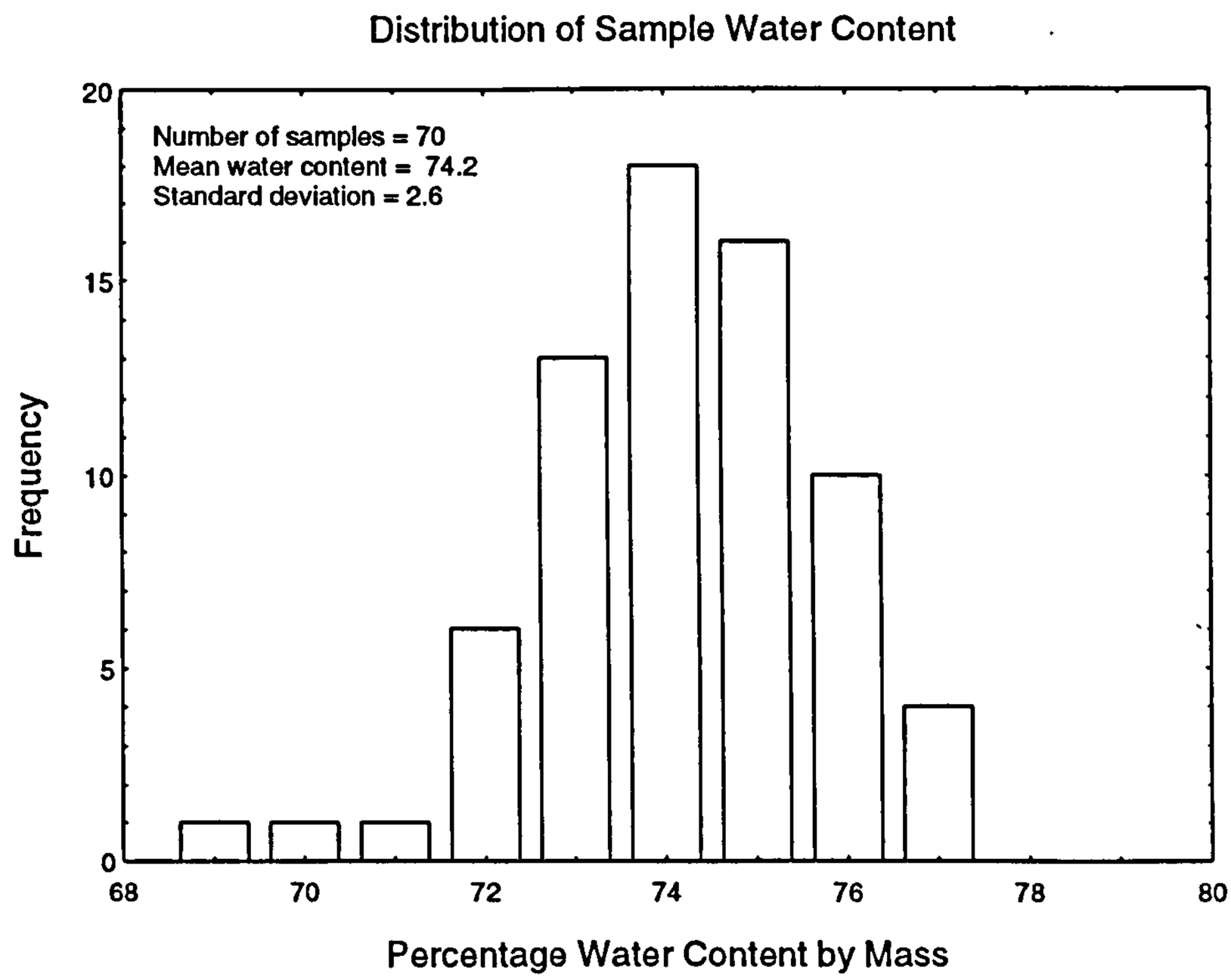

Figure 5.15 The distribution of the water content measured in all animal muscle samples.

makes up two thirds of total body weight, it is clear that it particularly important to determine the thermal properties of this type of muscle. This section will examine this type of muscle tissue.

Smooth muscle is the muscle of the digestive system, which is largely under involuntary control. Smooth muscle takes its name from its cellular structure and not its appearance, which is extremely variable. Cardiac muscle is the muscle of the heart. Cardiac muscle is characterised by its rhythm and its automatism (Brooks and Brooks, 1980). These two types of muscle will be examined later in this chapter.

5.10 Animal Skeletal Muscle.

In total, 346 measurements were made on 70 animal skeletal muscle samples. A total of 148 measurements were made on 30 samples of bovine skeletal muscle, with a further 105 measurements being made on 21 samples of porcine skeletal muscle, and 93 measurements being made on 19 samples of agnine skeletal muscle.

Table 5.8 shows the average thermal conductivity, thermal diffusivity, and water content for all the animal skeletal muscle tissues examined in this study. The distribution of the measured sample water content of animal skeletal muscle tissue is shown in figure 5.15. The distributions of measurements of the thermal conductivity and thermal diffusivity of agnine tissue are shown in figures 5.16 and 5.17, while those for bovine tissue are shown in figures 5.18 and 5.19, and those for porcine tissue are shown in figures 5.20 and 5.21. The range of measured water content, thermal conductivity and thermal diffusivity for agnine skeletal muscle tissue are

Water Content (%)	Minimum	74.0	Maximum	77.0	Mean	75.4
Thermal Conductivity ($Wm^{-1}K^{-1}$)	Minimum	0.440	Maximum	0.557	Mean	0.498
Thermal Diffusivity ($\times 10^{-7}$ m^2s^{-1})	Minimum	1.245	Maximum	1.398	Mean	1.314

For Bovine tissue, the mean maximum and minimum values are

Water Content (%)	Minimum	68.6	Maximum	76.5	Mean	73.9
Thermal Conductivity ($Wm^{-1}K^{-1}$)	Minimum	0.411	Maximum	0.575	Mean	0.492
Thermal Diffusivity ($\times 10^{-7}$ m^2s^{-1})	Minimum	1.201	Maximum	1.418	Mean	1.290

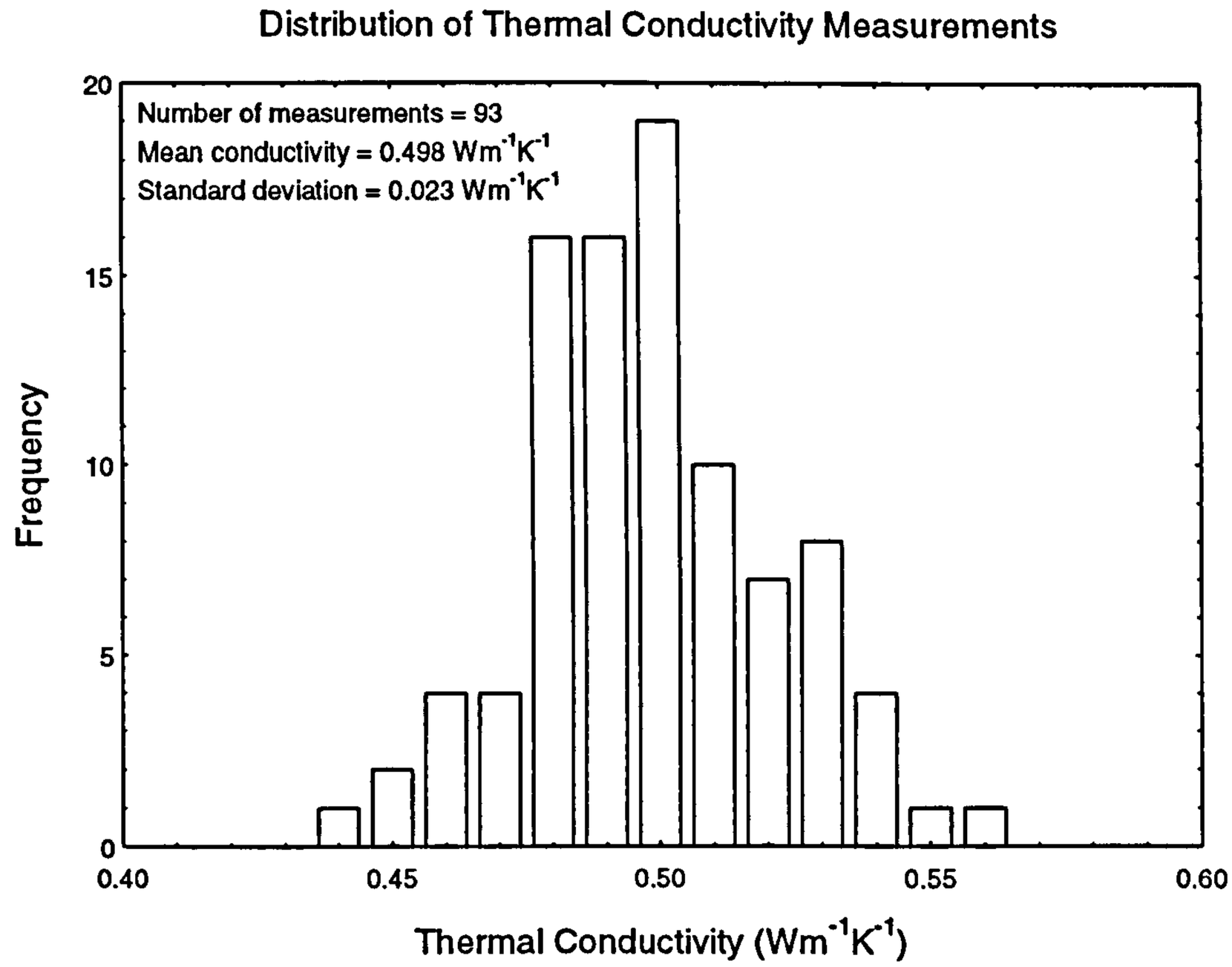

Figure 5.16 Distribution of thermal conductivity for agnine skeletal muscle tissue.

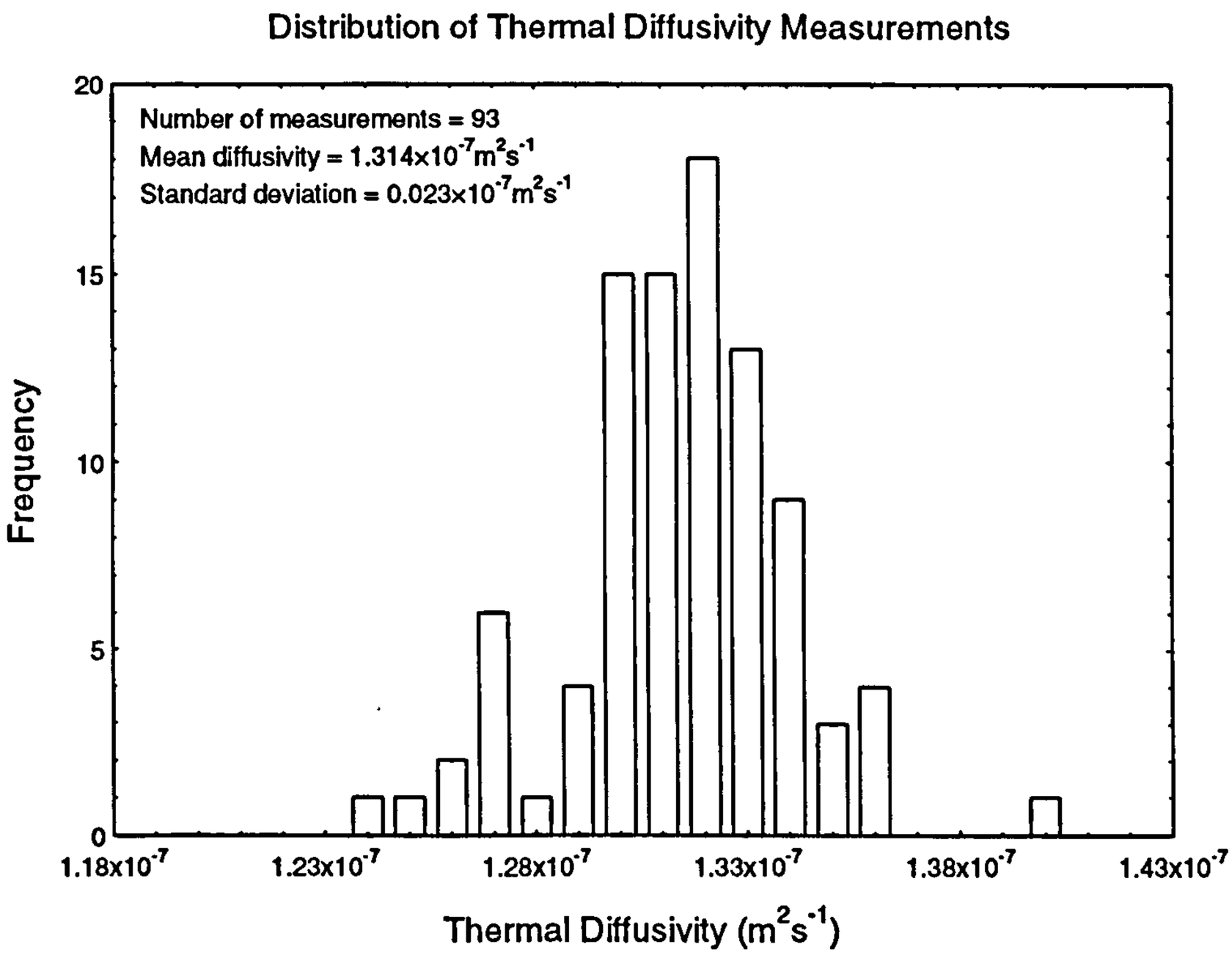

Figure 5.17 Distribution of thermal diffusivity for agnine skeletal muscle tissue..

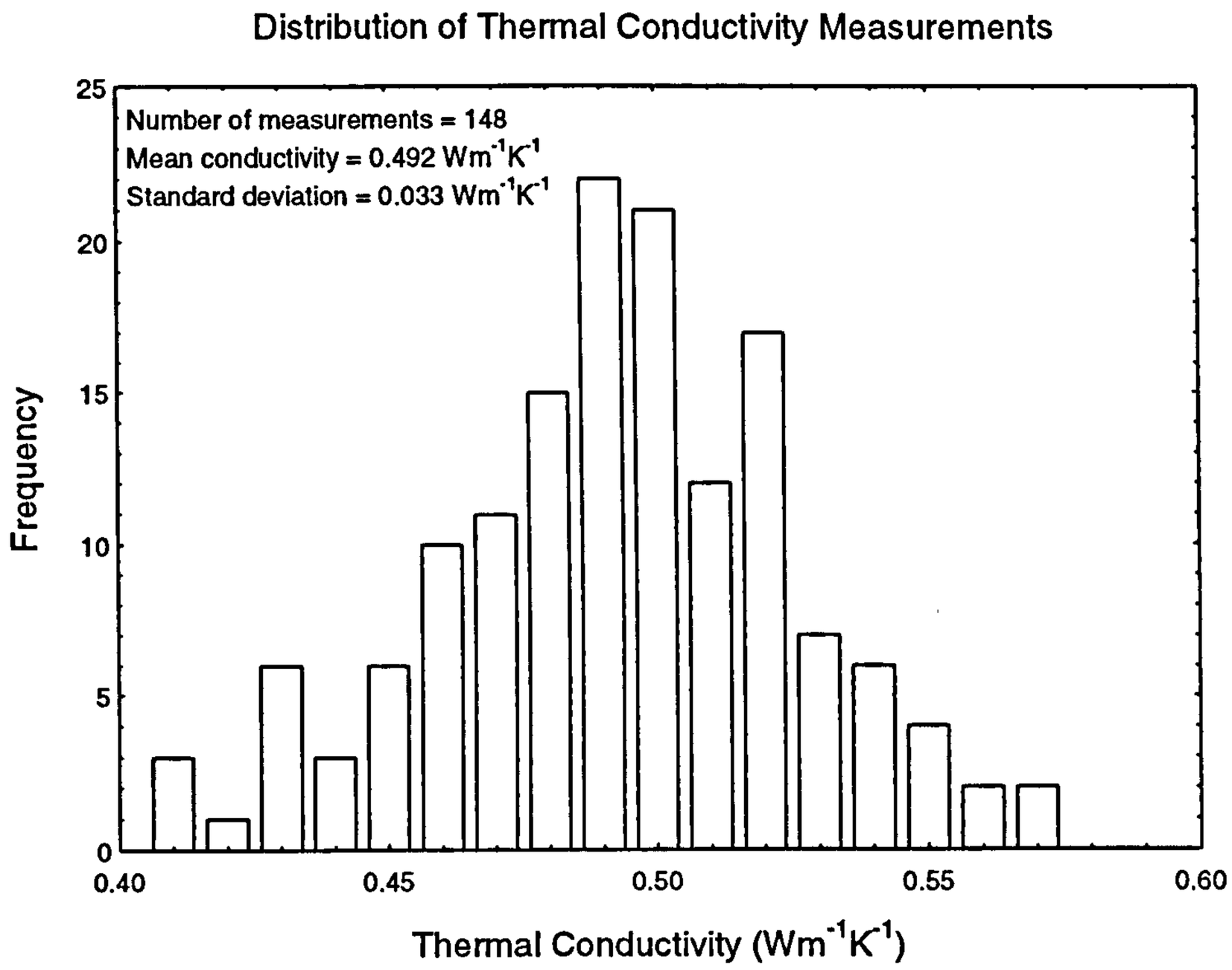

Figure 5.18 Distribution of thermal conductivity for bovine skeletal muscle tissue.

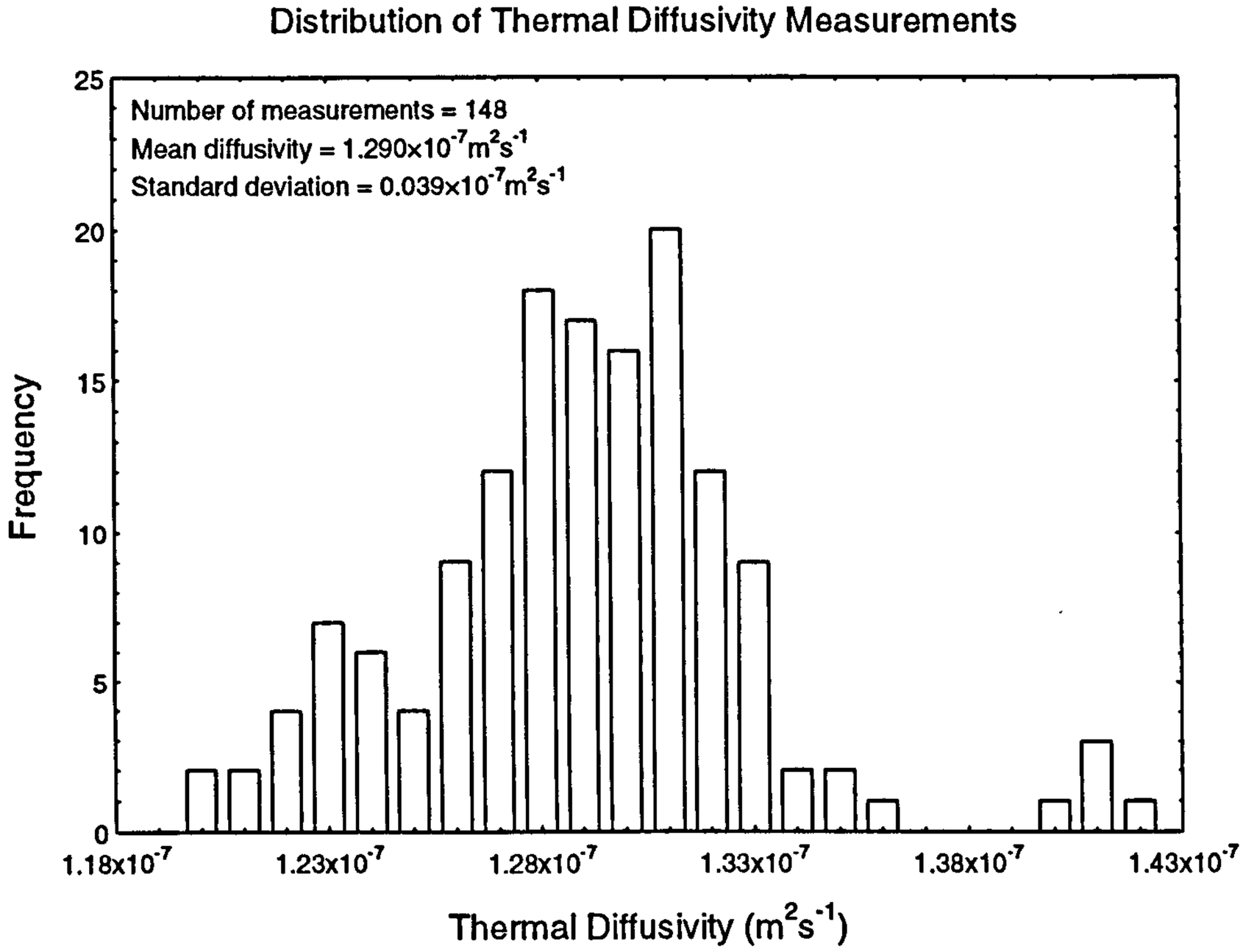

Figure 5.19 Distribution of thermal diffusivity for bovine skeletal muscle tissue.

The mean, maximum and minimum values for porcine tissue are

Water Content (%)	Minimum	71.6	Maximum	77.4	Mean	73.7
Thermal Conductivity ($Wm^{-1}K^{-1}$)	Minimum	0.451	Maximum	0.565	Mean	0.504
Thermal Diffusivity ($\times 10^{-7}\ m^2s^{-1}$)	Minimum	1.225	Maximum	1.406	Mean	1.322

As can be seen, the average thermal conductivity, thermal diffusivity, and water content of the different types of animal skeletal muscle tissue are very similar. Skeletal muscle has less variation than that seen in fat, with the range of the measured thermal conductivity, thermal diffusivity, and water content being significantly less than that seen in the fat tissues. The lowest measured values of the thermal conductivity and thermal diffusivity are associated with bovine skeletal muscle. If the distribution of the measured thermal conductivity and thermal diffusivity for each type of tissue is examined, it can be seen that porcine and agnine distributions are roughly symmetrical. However, the bovine distribution is asymmetrical, with a number of lower than expected values. These values are associated with samples which came from a bovine skeletal muscle specimen which was of lower quality than the majority of the bovine samples. These lower quality samples were less uniform than higher quality samples, with layers of fat and connective tissue running through the muscle tissue.

As can be seen in the histograms, the highest measured values of the thermal diffusivity were exceptional. The highest measurement of the diffusivity in the agnine and porcine distributions were in samples where the other diffusivity measurements were nearer the expected average. In bovine tissue, the five highest measurements of the diffusivity are significantly higher than any other. These five measurements were made on one sample which also had higher than average thermal conductivity. The highest measured values of the thermal conductivity were less exceptional.

Table 5.9 shows the thermal conductivity of various animal skeletal muscle tissues as stated by different authors. There is a large spread in the range of measured thermal conductivities. Examining all the data tends to suggest that the thermal conductivity of animal skeletal muscle lies close to 0.5 $Wm^{-1}K^{-1}$, as was found in this study. Hill et al (1967) found the thermal conductivity of skeletal muscle varied depending on the direction of heat flow with respect to the muscle fibres present in the tissue. Since the

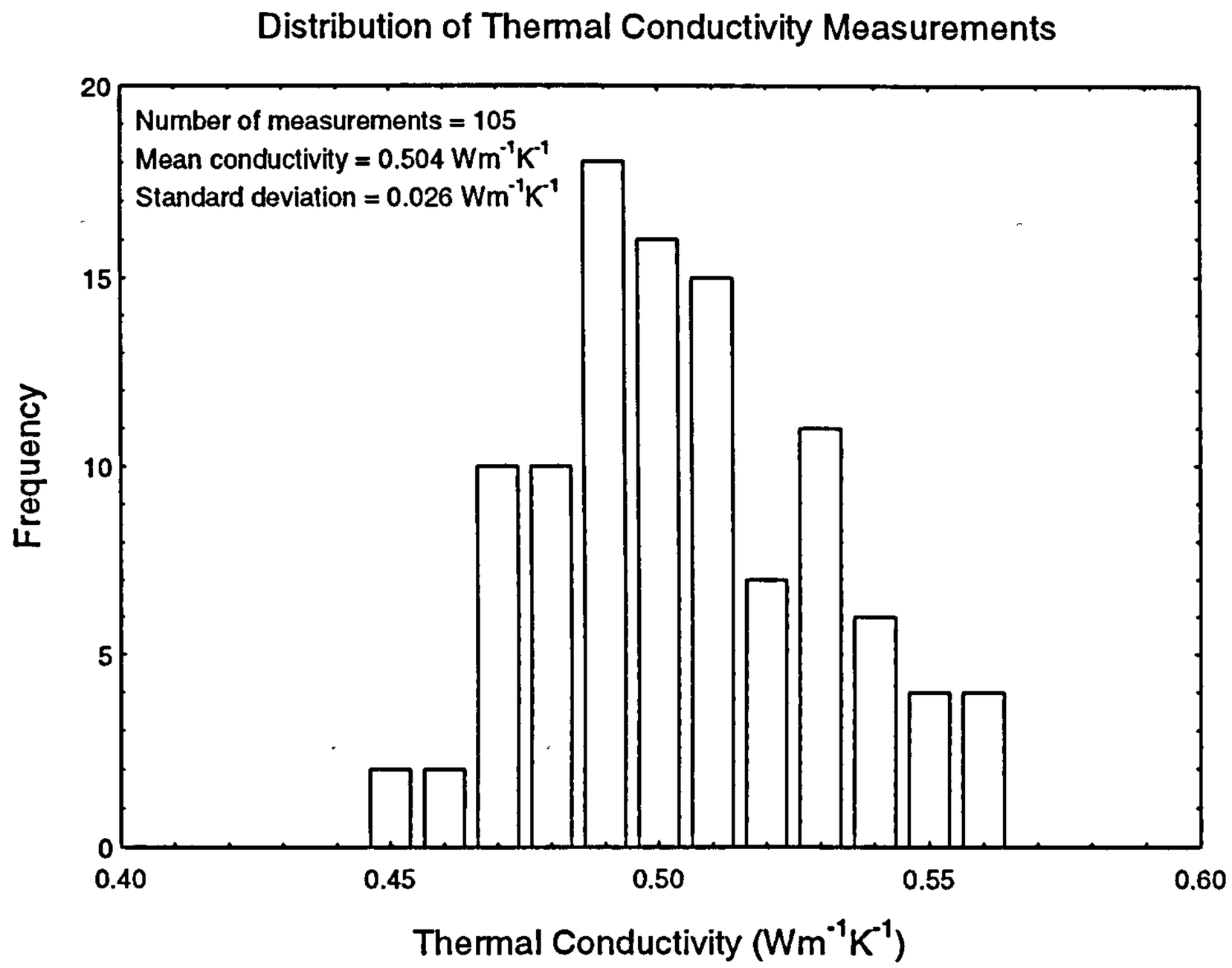

Figure 5.20 Distribution of thermal conductivity for porcine skeletal muscle tissue.

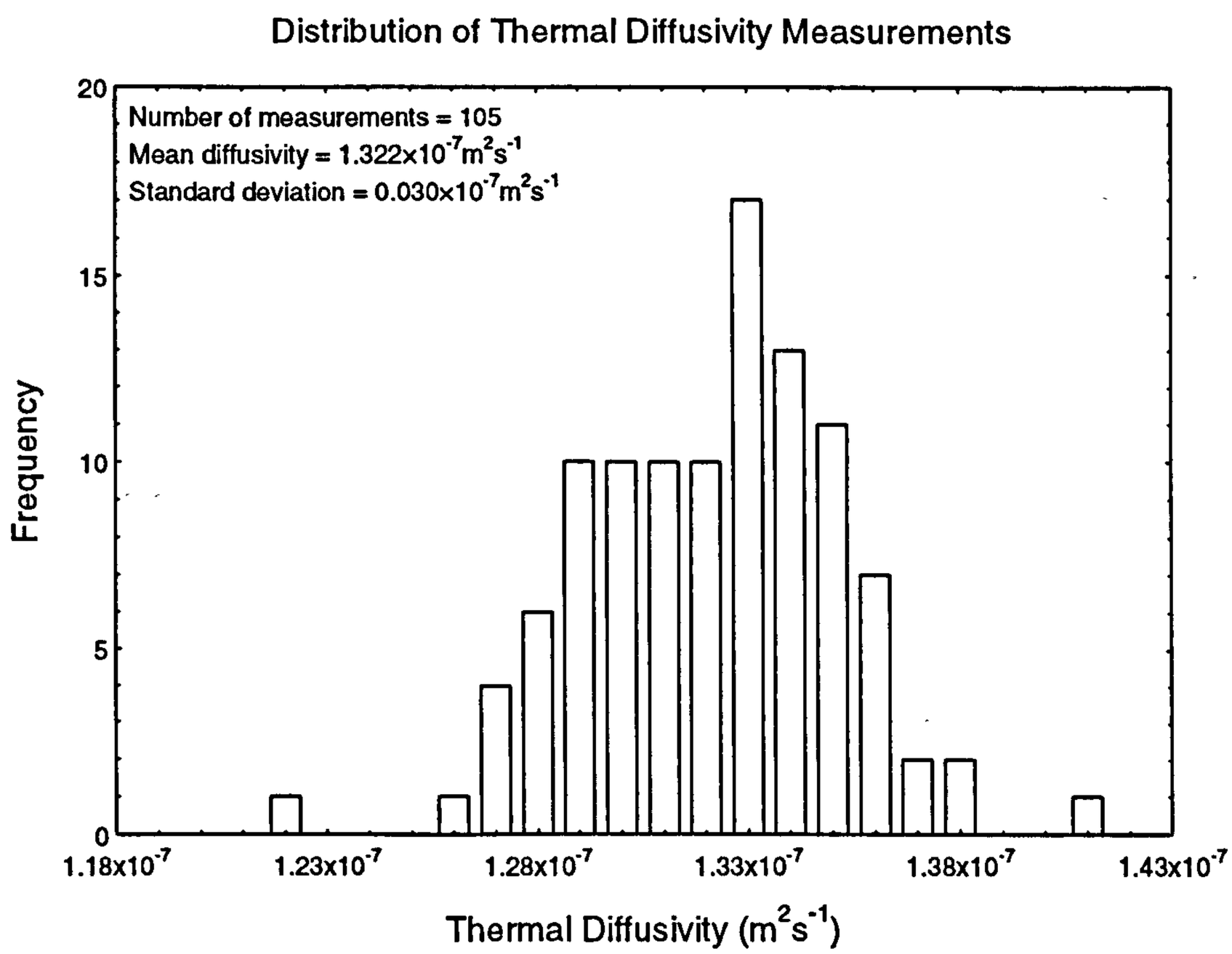

Figure 5.21 Distribution of thermal diffusivity for porcine skeletal muscle tissue.

Skeletal Muscle Tissue Type	Thermal Conductivity ($Wm^{-1}K^{-1}$)	Reference
Agnine	0.478	Balasubramaniam and Bowman (1977)
Bovine	0.280	Hatfield and Pugh (1951)
Bovine	0.532	Hatfield (1953)
Bovine (lumbar region) Bovine (pectoralis)	0.515 0.498	Morley (1966)
Bovine (76.2% water) Bovine calf (80% water)	0.527 0.545	Poppendiek et al (1966)
Bovine (along fibres) Bovine (across fibres)	0.434 0.467	Hill et al (1967)
Porcine	0.460	Henrique and Moritz (1947)
Porcine (lumbar region)	0.515	Morley (1966)
Porcine (along fibres) Porcine (across fibres)	0.485 0.530	Hill et al (1967)
Porcine	0.383	Tanasawa and Katsuda (1972)
Porcine	0.464	Liang et al (1991)
General	0.406-0.418	Bruer (1924)

Table 5.9 Published thermal conductivity of various animal skeletal muscle tissues.

Skeletal Muscle Tissue Type	Thermal Diffusivity (m^2s^{-1})	Reference
Agnine	1.59×10^{-7}	Balasubramaniam and Bowman (1977)
Bovine	1.25×10^{-7}	Cheerneva (1956)
Porcine	1.25×10^{-7}	Cheerneva (1956)
Porcine	1.43×10^{-7}	Tanasawa and Katsuda (1972)

Table 5.10 Published thermal diffusivity of various animal skeletal muscle tissues.

probe used in this study to measure the thermal conductivity was based on spherical geometry, this statement could not be checked.

Table 5.10 shows the thermal diffusivity of various animal skeletal muscle tissues as stated by different authors. As usual, there is far less data on the thermal diffusivity than there is on the thermal conductivity. This limited data does not agree on a single value, though the thermal diffusivity measured by Cheerneva (1956) lies close to the mean thermal diffusivity of the animal tissues examined in this study.

5.10.1 Analysis of Measured Animal Skeletal Muscle Tissue Values.

Figure 5.22 shows the variation of the thermal diffusivity with the thermal conductivity for all agnine skeletal muscle measurements. It can be seen there is a large spread in the data. This makes it impossible to use a method similar to that used to calculate the thermal conductivity and diffusivity of dehydrated fat. The thermal conductivity and thermal diffusivity of water and protein mixtures, as given by Maxwell's equation, are

$$\frac{k-k_w}{k+2k_w}=\frac{k_p-k_w}{k_p+2k_w}(1-\phi_w) \tag{5.10.1}$$

$$\frac{\alpha-\alpha_w}{\alpha+2\alpha_w}=\frac{\alpha_p-\alpha_w}{\alpha_p+2\alpha_w}(1-\phi_w) \tag{5.10.2}$$

where k_p, k_w, and k are the thermal conductivities of protein, water, and the mixture respectively, while α_p, α_w, and α are thermal diffusivities of protein, water, and the mixture. The water content by volume is given by ϕ_w. Combining equations 5.10.1 and 5.10.2 gives

$$\alpha=\alpha_w\frac{(2k_w\alpha_w-k_w\alpha_p-k_p\alpha_p)k+2(k_w\alpha_p-k_p\alpha_w)k_w}{(k_w\alpha_p-k_p\alpha_w)k+(2k_w\alpha_w-k_p\alpha_w-k_p\alpha_p)k_w} \tag{5.10.3}$$

Figure 5.12 showed how very different values of the thermal conductivity and diffusivity of dehydrated fat gave very similar curves. However, the measured fat data followed a defined curve allowing for a unique estimate of the thermal conductivity and diffusivity of dehydrated fat to be produced for each tissue type. This is not true of the muscle tissues. When equation 5.10.3. is used to curve fit the data shown in figure 5.22, it was found that a unique value for k_p and α_p could not be found.

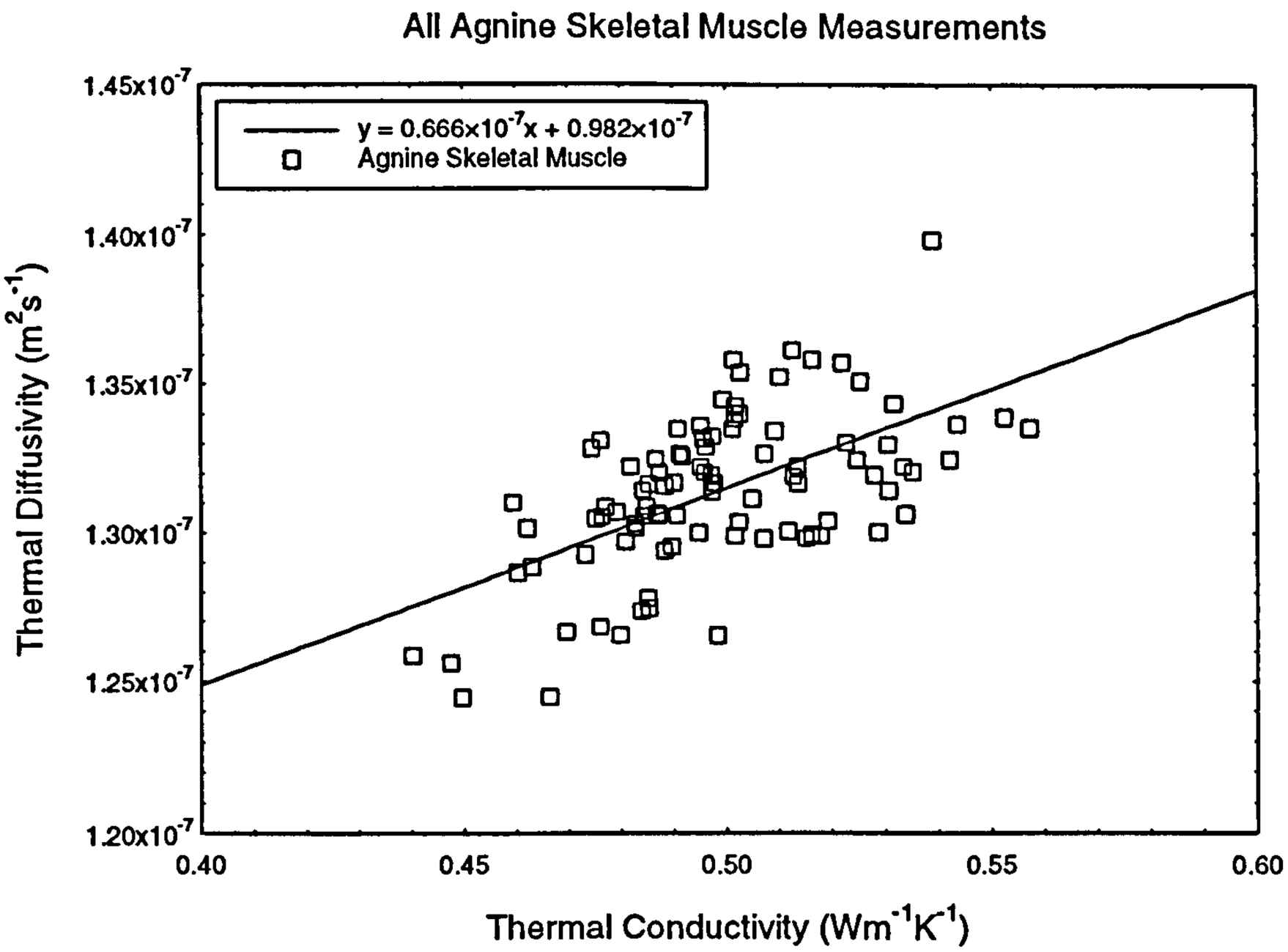

Figure 5.22 The variation of α with k for all agnine skeletal muscle measurements.

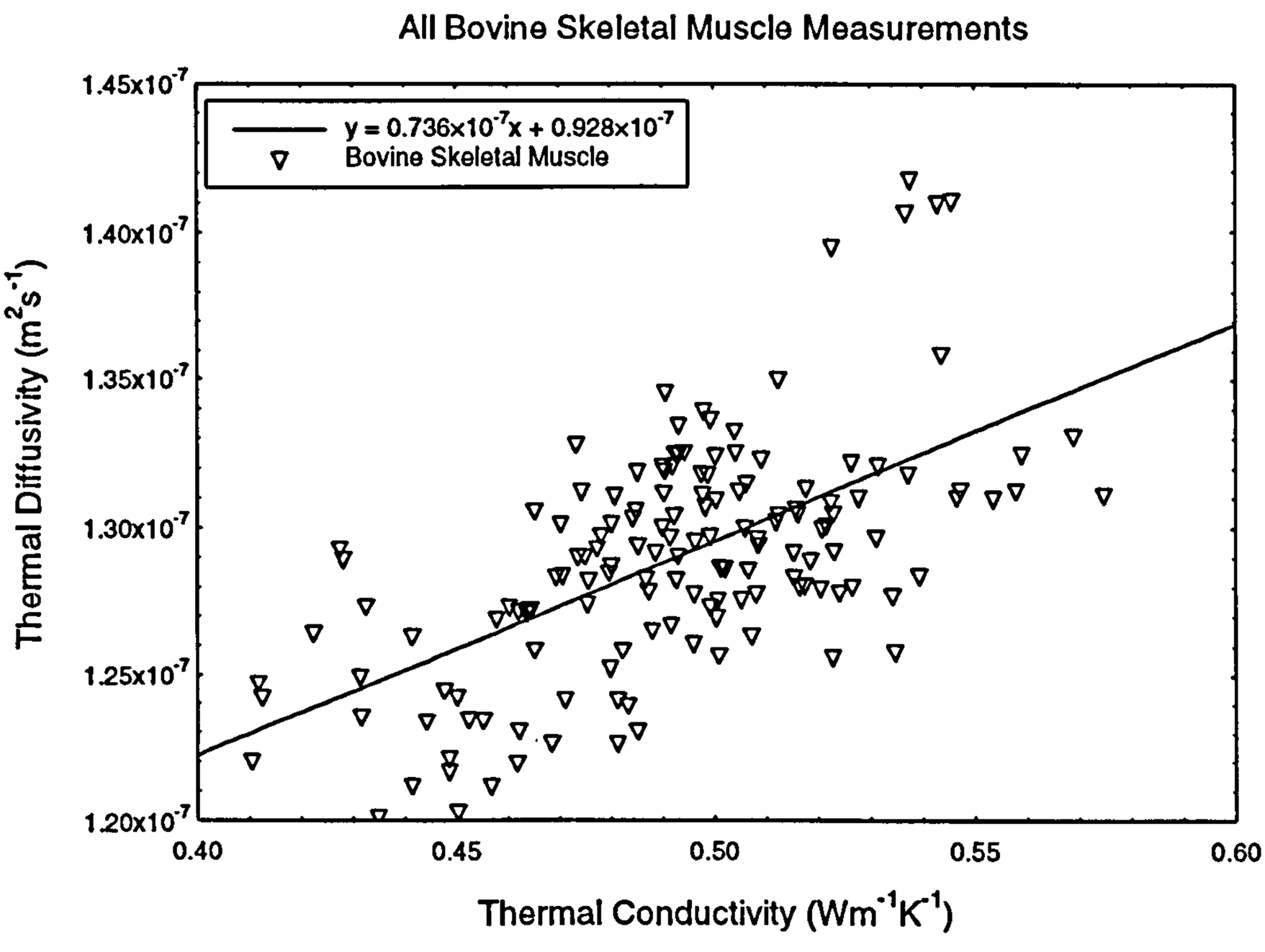

Figure 5.23 The variation of α with k for all bovine skeletal muscle measurements.

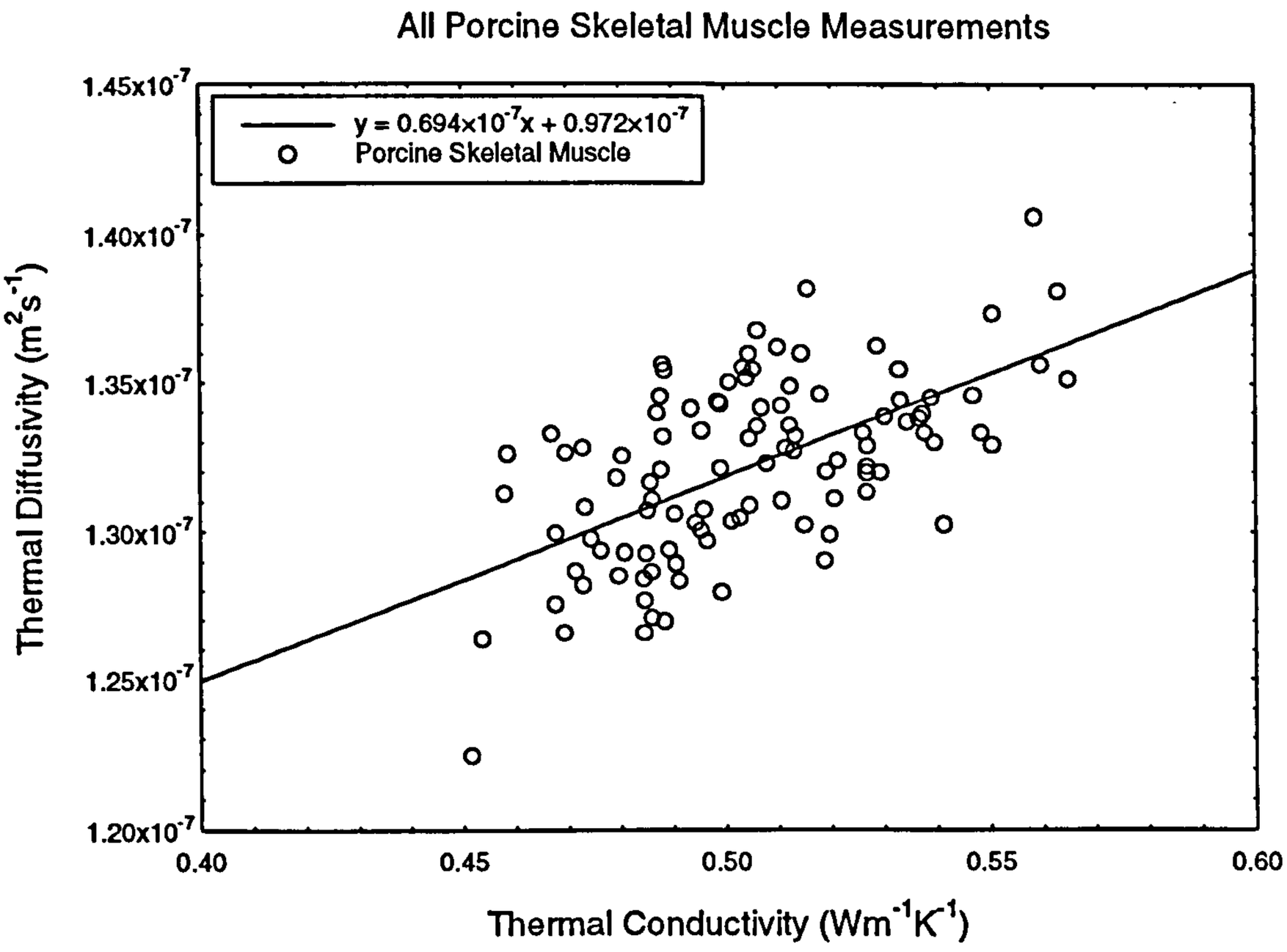

Figure 5.24 The variation of the thermal diffusivity with the thermal conductivity for all the measurements made on porcine skeletal muscle.

Skeletal Muscle Tissue	No. of Samples	No. of Meas.	Mean Thermal Conductivity ($Wm^{-1}K^{-1}$)	Mean Thermal Diffusivity (m^2s^{-1})	Mean % Water Content by Mass
Abdominal	9	45	0.472	1.293×10^{-7}	74.8
Calf	4	19	0.545	1.333×10^{-7}	79
Quadricep	19	88	0.540	1.289×10^{-7}	78.4
Soleus	7	32	0.477	1.303×10^{-7}	76.8
Overall	39	184	0.513	1.297×10^{-7}	77.3

Table 5.11 The mean thermal conductivity, thermal diffusivity and water content of the human skeletal muscle tissues measured in this study.

Figures 5.23 and 5.24 show the variation of the thermal diffusivity with the thermal conductivity for all bovine and porcine skeletal muscle measurements respectively. The linear least square fits of the thermal diffusivity against thermal conductivity data, with the correlation given by r, are

Agnine skeletal muscle measurements: $\alpha = (0.666k + 0.982) \times 10^{-7}\ m^2s^{-1}$: $r = 0.586$

Bovine skeletal muscle measurements: $\alpha = (0.736k + 0.928) \times 10^{-7}\ m^2s^{-1}$: $r = 0.614$

Porcine skeletal muscle measurements: $\alpha = (0.694k + 0.972) \times 10^{-7}\ m^2s^{-1}$: $r = 0.591$

As the figures show, there is a some variation in the data. However the curve fits of the data are reasonably similar.

5.11 Human Skeletal Muscle.

In total, 184 measurements were made on 39 human skeletal muscle samples. There were four different specimens of tissue examined, each from a different skeletal muscle tissue. Forty-five measurements were made on nine samples of unknown skeletal muscle from the abdominal area. A further 19 measurements were made on 4 samples of gastrocnemius muscle, which is located in the lower leg, while 32 measurements were made on 7 samples of soleus muscle which is also found in the lower leg. Finally, 88 measurements were made on 19 samples of quadricep muscle, which comes from the thigh region. Gastrocnemius muscle will hence be referred to as calf muscle.

Table 5.11 shows the mean thermal conductivity, thermal diffusivity, and water content for each of the human skeletal muscle types. The distribution of measurements of the thermal conductivity and thermal diffusivity are shown in figure 5.25 and figure 5.26 respectively, while the distribution of the sample water content of human skeletal muscle is shown in figure 5.27. The minimum, maximum, and mean values of water content, thermal conductivity, and thermal diffusivity are

Water Content (%)	Minimum	69.6	Maximum	81.4	Mean	77.3
Thermal Conductivity ($Wm^{-1}K^{-1}$)	Minimum	0.408	Maximum	0.590	Mean	0.513
Thermal Diffusivity ($\times 10^{-7}\ m^2s^{-1}$)	Minimum	1.189	Maximum	1.390	Mean	1.297

The average thermal conductivity of human skeletal muscle is slightly higher than that of animal skeletal muscle, as would be expected given that human muscle has a higher

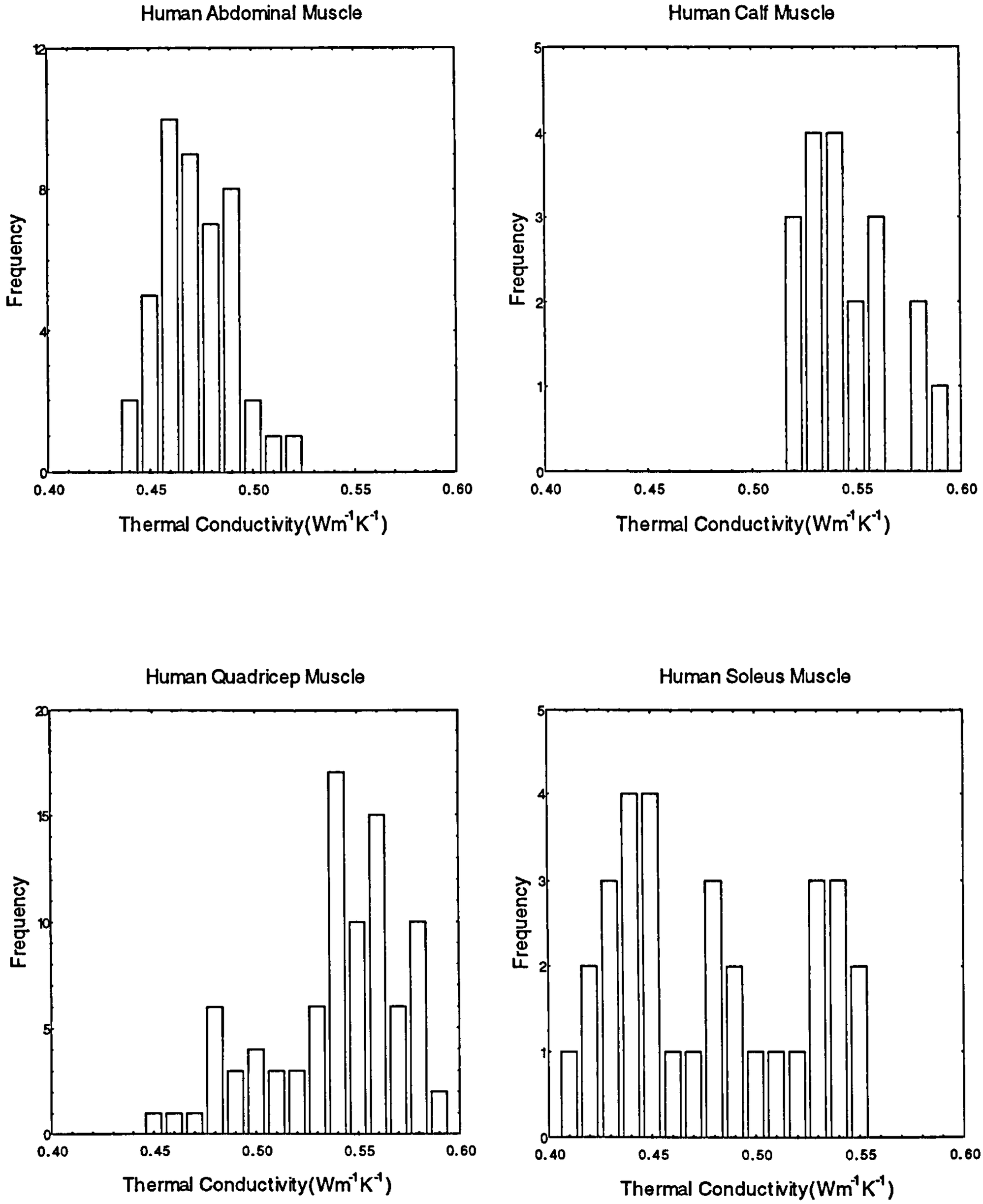

Figure 5.25 Distribution of thermal conductivity measurements for each of the human skeletal muscle tissues examined.

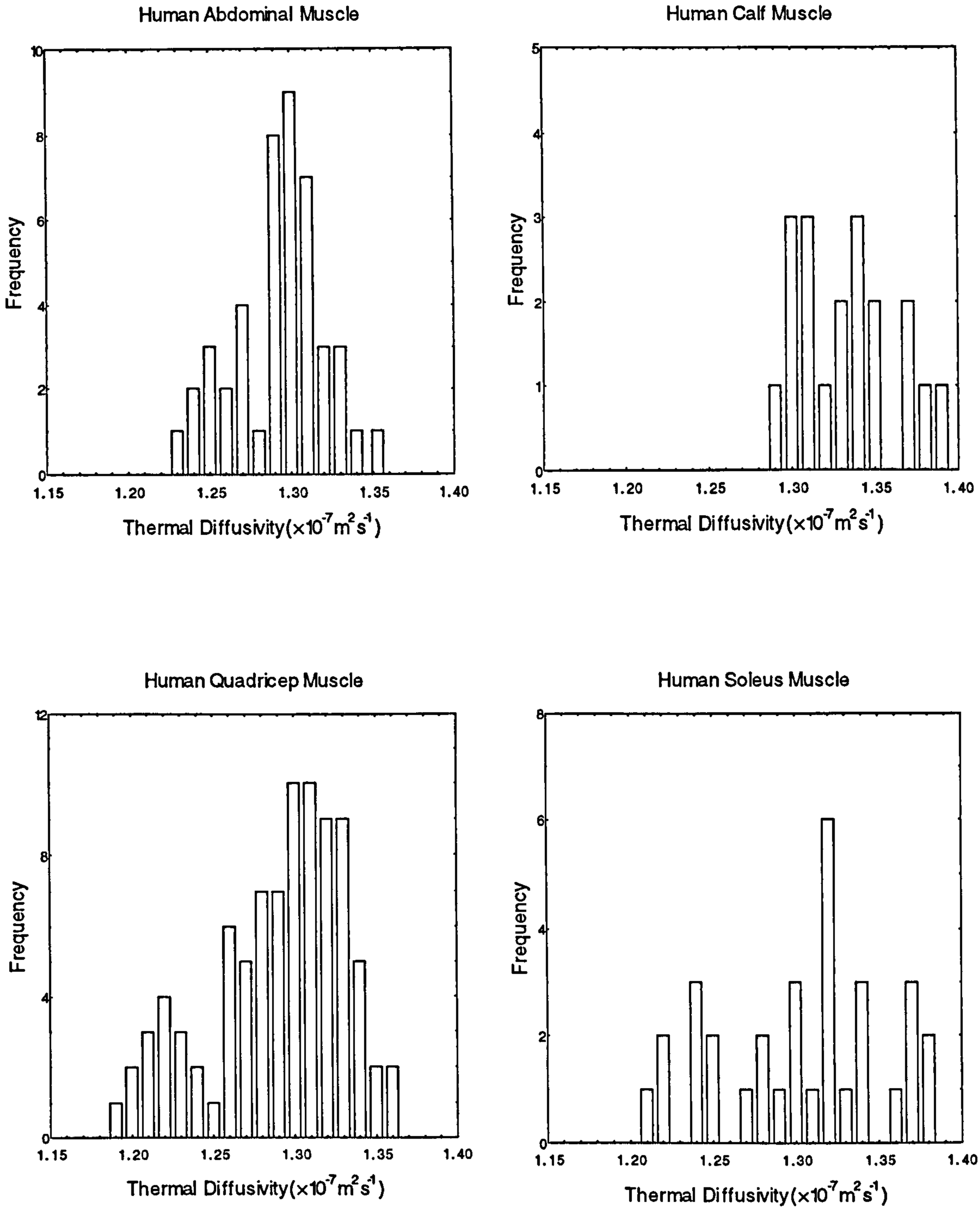

Figure 5.26 Distribution of thermal diffusivity measurements for each of the human skeletal muscle tissues examined.

water content. However, the average thermal diffusivity of human skeletal muscle is similar to that which we find in animal skeletal muscle. When the individual types of tissue are examined, a large variation in the thermal properties of each of the types of tissue becomes apparent. This variability is also shown in the histograms.

Abdominal skeletal muscle tissue has a peak which lies close to 0.45 $Wm^{-1}K^{-1}$. However, the peak values for the calf and quadricep tissue lie close to 0.55 $Wm^{-1}K^{-1}$. Soleus muscle tissue also has a peak close to 0.45 $Wm^{-1}K^{-1}$, though there is evidence of a second peak close to 0.55 $Wm^{-1}K^{-1}$, though no firm conclusion can be drawn on the behaviour due to the small number of measurements made on soleus muscle.

This pattern is not repeated when the distribution of the thermal diffusivity is examined. Abdominal, soleus, and quadricep muscles all have average thermal diffusivities similar to the average values seen in animal tissues. Only calf muscle has an average thermal diffusivity which is much higher than that seen in the rest of the tissues, though this is the tissue which fewest measurements were made.

Table 5.12 shows the thermal conductivity and thermal diffusivity of human skeletal muscle as stated by various authors. There is a wide range of stated values for both the conductivity and diffusivity.

Figure 5.28 shows the variation of thermal diffusivity with thermal conductivity for all the measurements made on human skeletal muscle. As the figure shows, there are two different behaviours apparent in human skeletal muscle tissue. The first fit is for the quadricep and calf muscle; that is the tissues which had thermal conductivity peaks near 0.55 $Wm^{-1}K^{-1}$. The linear least square fit of the data, with correlation r, is given by

$$\alpha = (1.204k + 0.645) \times 10^{-7}\ m^2s^{-1}: r = 0.812$$

The linear least square fit of the tissues which had peaks at 0.45 $Wm^{-1}K^{-1}$, that is the soleus and abdominal muscle tissues, is

$$\alpha = (0.980k + 0.832) \times 10^{-7}\ m^2s^{-1}: r = 0.803$$

5.12 Comparison Between Human and Animal Skeletal Muscle.

There are a number of significant differences between the human and animal skeletal muscle examined in this study. Firstly, the water content observed in the human tissue is significantly higher than that seen in animal tissues. Human tissue does not naturally

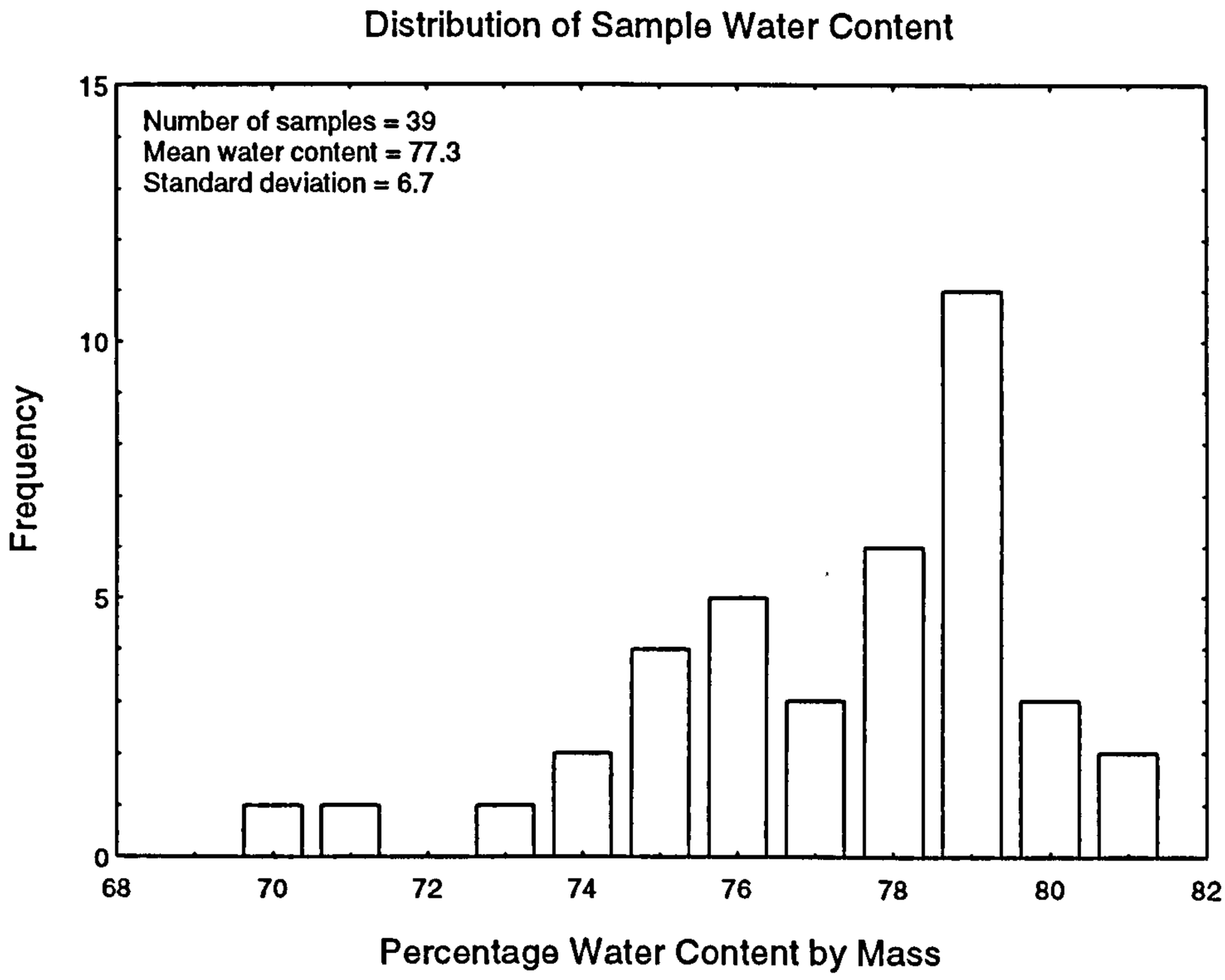

Figure 5.27 The distribution of measured water content for all the human skeletal muscle samples.

Thermal Conductivity ($Wm^{-1}K^{-1}$)	Thermal Diffusivity (m^2s^{-1})	Reference
0.385	-	Hatfield and Pugh (1951)
0.440	-	Hatfield (1953)
0.420	1.061×10^{-7}	Gordon et al (1977)
0.508	-	Bowman (1981)
0.590	1.575×10^{-7}	Hand et al (1982)
0.600	1.429×10^{-7}	Schwab (1988)

Table 5.12 Thermal conductivity and diffusivity of human skeletal muscle as stated by various authors.

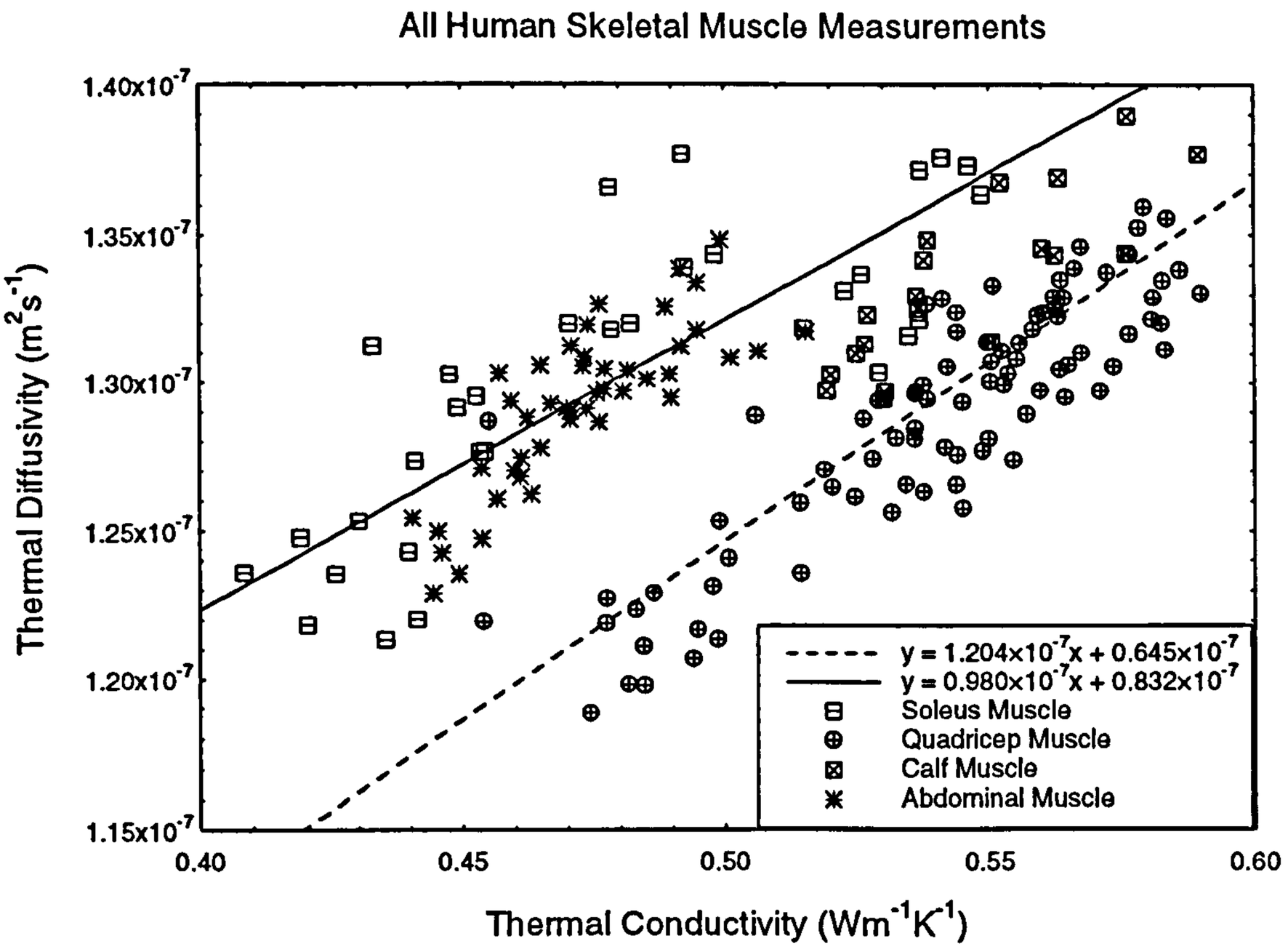

Figure 5.28 Variation of α with k for measurements made on human skeletal muscle.

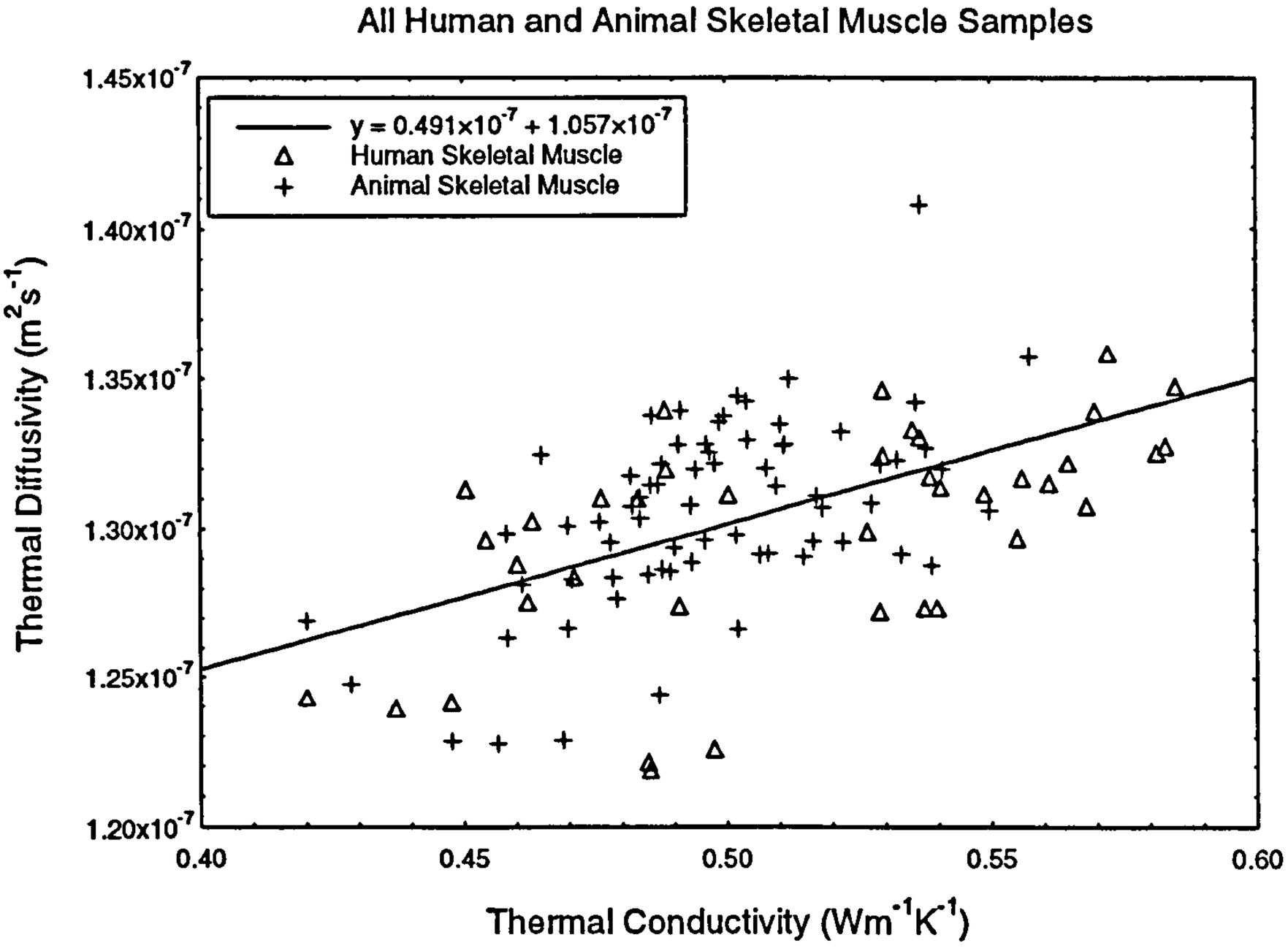

Figure 5.29 Variation of α with k for all human and animal skeletal muscle samples.

have a higher water content than the other tissues examined in this study. This variation is caused by the way animal tissue is prepared. All the animal specimens examined in this study were fit for human consumption and hence the residual blood of the animal samples had been drained, lowering the average water content.

The other major difference between the human and animal tissues was the quality of the tissue. Animal tissue generally looked uniform to the naked eye. However the human skeletal muscle was variable with layers of fat running through the muscle. Often it was difficult to ensure that the measurement volume would solely contain muscle tissue. This causes the measured value of the thermal conductivity and thermal diffusivity to be more variable in human skeletal muscle than in animal.

Figure 5.29 shows the variation of the thermal diffusivity with thermal conductivity for all the human and animal skeletal muscle sample. The linear fit of the sample thermal diffusivity against the sample thermal conductivity for all skeletal muscle samples is

$$\alpha = (0.491k + 1.057) \times 10^{-7}\ \mathrm{m^2 s^{-1}}: r = 0.527$$

Figure 5.30 shows the variation of the thermal conductivity with sample water content, and figure 5.31 shows the variation of the thermal diffusivity with sample water content. As can be seen, no relationship between the thermal property and the water content can be discerned. As with the fat tissues, this is partly due to the water content in the measurement volume not matching the water content of the sample, and partly due to the probe error associated with measuring the thermal properties of the sample.

It must also be remembered that for a single type of tissue, such as skeletal muscle, there is only a limited range of water content associated with that tissue type. This limited range of water content will produce a restricted range of thermal property values compared to the total range of values seen in biological tissues. The restricted range of values allow the errors discussed above to mask any relationship present between the thermal properties and the water content.

5.13 The Liver.

The liver is a key part of the digestive system and is the largest organ of the body. It is located below the diaphragm and it weighs several kilograms in the average adult. The liver's chemical functions includes helping metabolise carbohydrates, proteins, and fats;

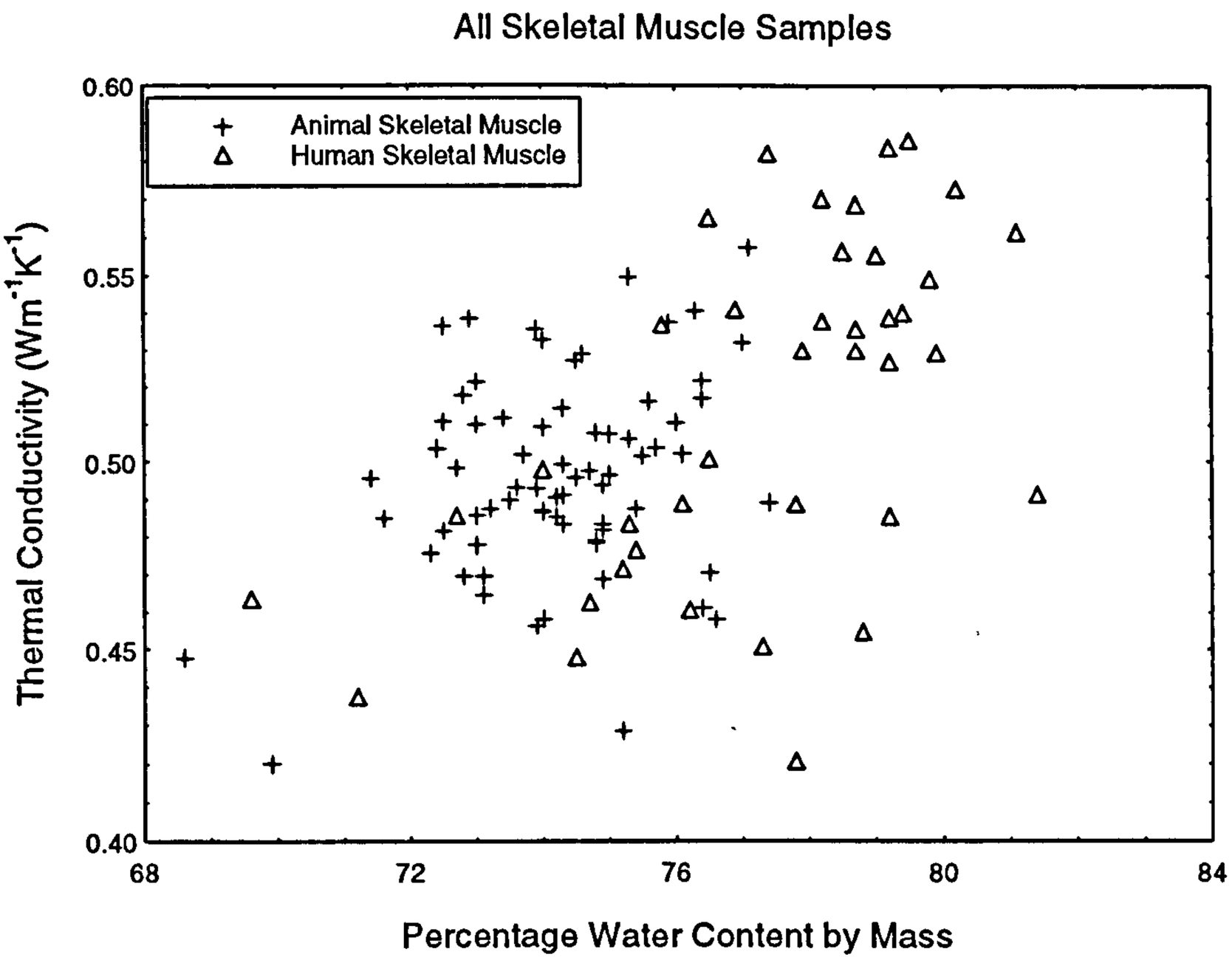

Figure 5.30 Variation in thermal conductivity with sample water content.

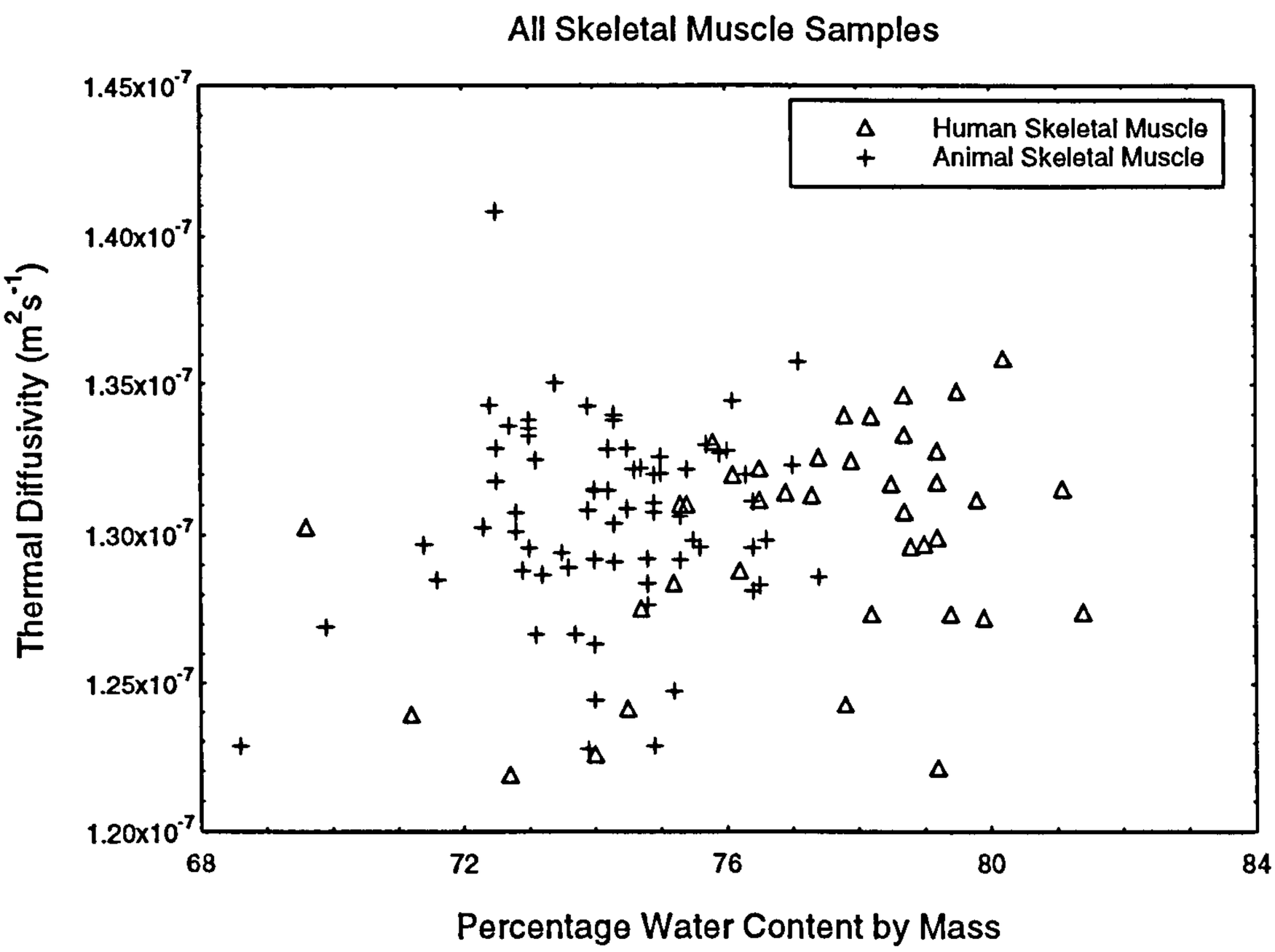

Figure 5.31 Variation in thermal diffusivity with sample water content.

Liver Tissue	No. of Samples	No. of Meas.	Mean Thermal Conductivity ($Wm^{-1}K^{-1}$)	Mean Thermal Diffusivity (m^2s^{-1})	Mean % Water Content by Mass
Agnine	21	100	0.475	1.269×10^{-7}	66.9
Bovine	6	30	0.501	1.257×10^{-7}	67.7
Porcine	19	94	0.490	1.301×10^{-7}	67.5
Overall	46	224	0.485	1.281×10^{-7}	67.3

Table 5.13 The mean thermal conductivity, thermal diffusivity and water content of the animal liver tissues measured in this study.

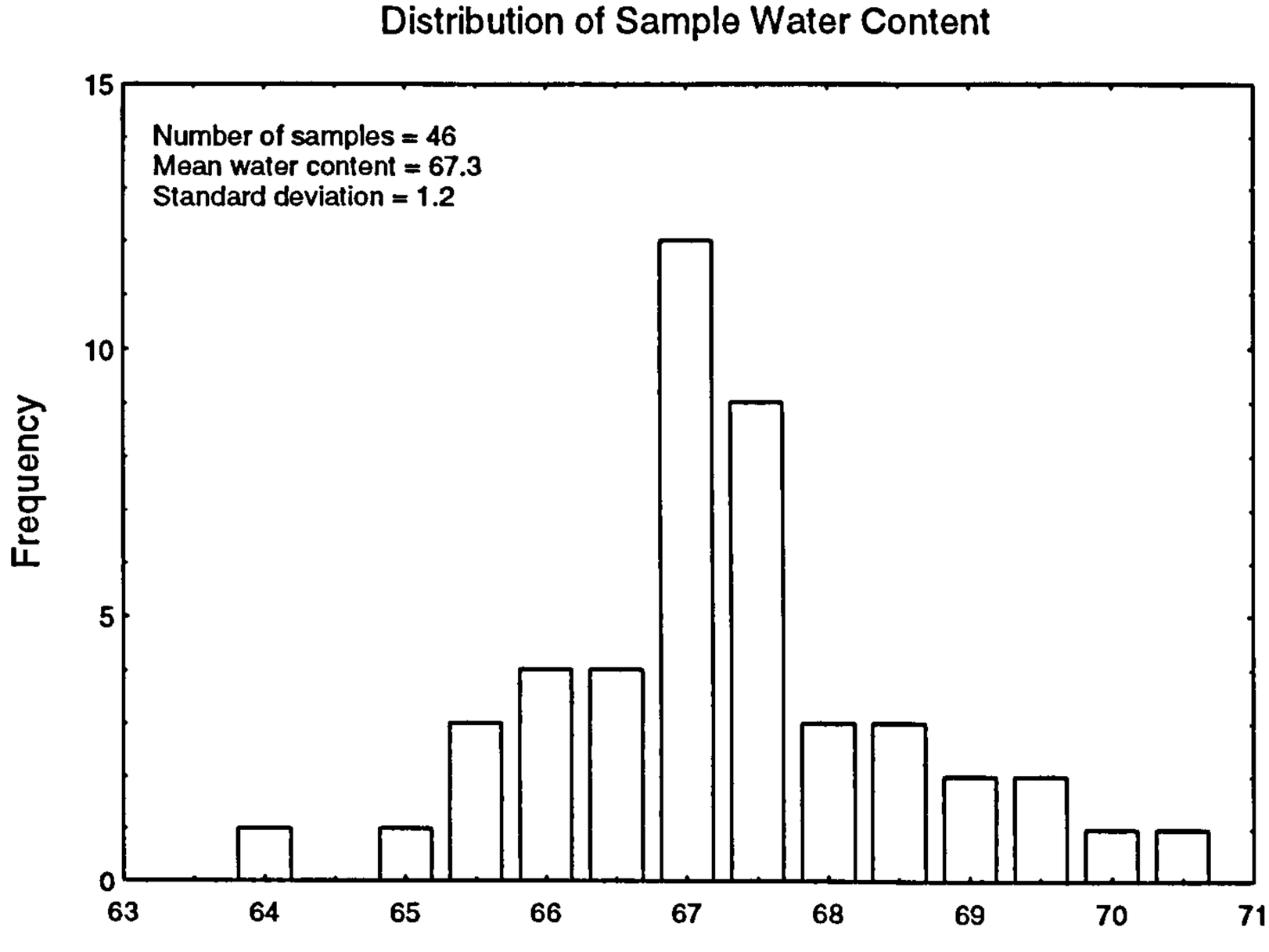

Figure 5.32 The distribution of measured sample water content for all animal liver samples.

storing vitamins and minerals; detoxifying harmful substances; and manufacturing various body chemicals. Along with these chemical functions, the liver produces large amount of heat. On average, the liver is second only to skeletal muscle as biggest source of heat in the body.

5.13.1 Animal Liver Tissue.

A total of 224 measurements were made on 46 samples of animal liver tissue. One hundred measurements were made on 21 samples of agnine liver, while a further 30 measurements were made on 6 samples of bovine liver, and 94 measurements were made on 19 samples of porcine liver. Table 5.13 gives the average thermal conductivity, thermal diffusivity, and water content for the animal liver tissues examined in this study.

The distribution of the water content of all the animal liver samples examined in this study is shown in figure 5.32, while the distribution of thermal conductivity and thermal diffusivity of all the measurements on animal liver are shown in figure 5.33 and figure 5.34 respectively.

The range of measurements made on animal liver of the thermal conductivity, thermal diffusivity, and water content are as follows

Water Content (%)	Minimum	64.1	Maximum	70.3	Mean	67.3
Thermal Conductivity ($Wm^{-1}K^{-1}$)	Minimum	0.419	Maximum	0.534	Mean	0.485
Thermal Diffusivity ($\times 10^{-7}\ m^2s^{-1}$)	Minimum	1.199	Maximum	1.383	Mean	1.281

Animal liver tissue has a lower average water content than animal skeletal muscle tissue. This is reflected in the fact that the average thermal conductivity and thermal diffusivity of liver are lower than the values seen in muscle.

The lowest measurements of the thermal conductivity, thermal diffusivity, and water content were all made on samples which had come from one particular specimen of agnine liver. This specimen had lower water content than the other agnine liver tissues examined and hence it is no surprise that the lowest thermal conductivity and thermal diffusivity were also found in that specimen.

Whereas all the lowest values are associated with agnine tissue, no one species of tissue had the highest thermal conductivity, thermal diffusivity and water content.

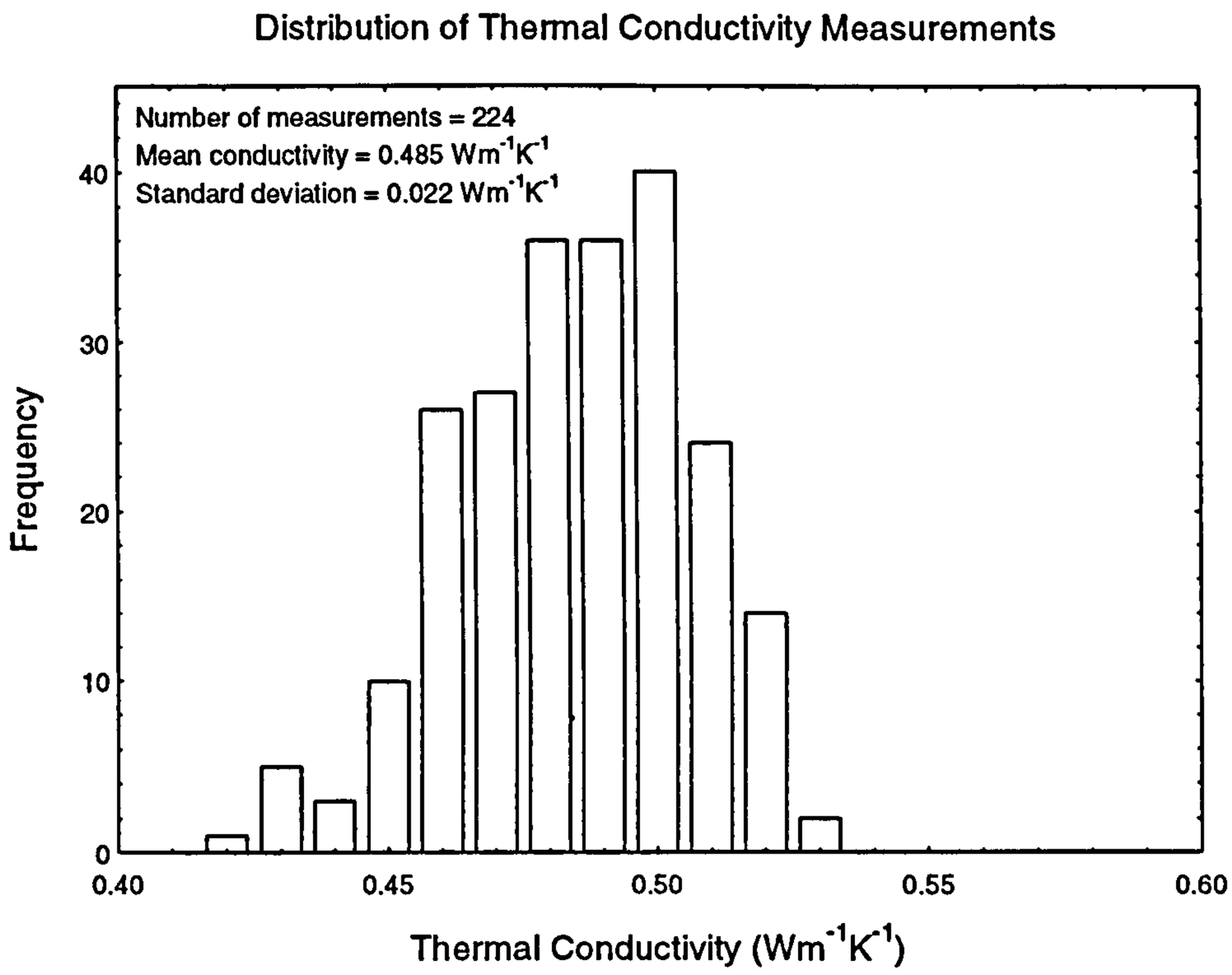

Figure 5.33 Distribution of thermal conductivity for all measurements on animal liver.

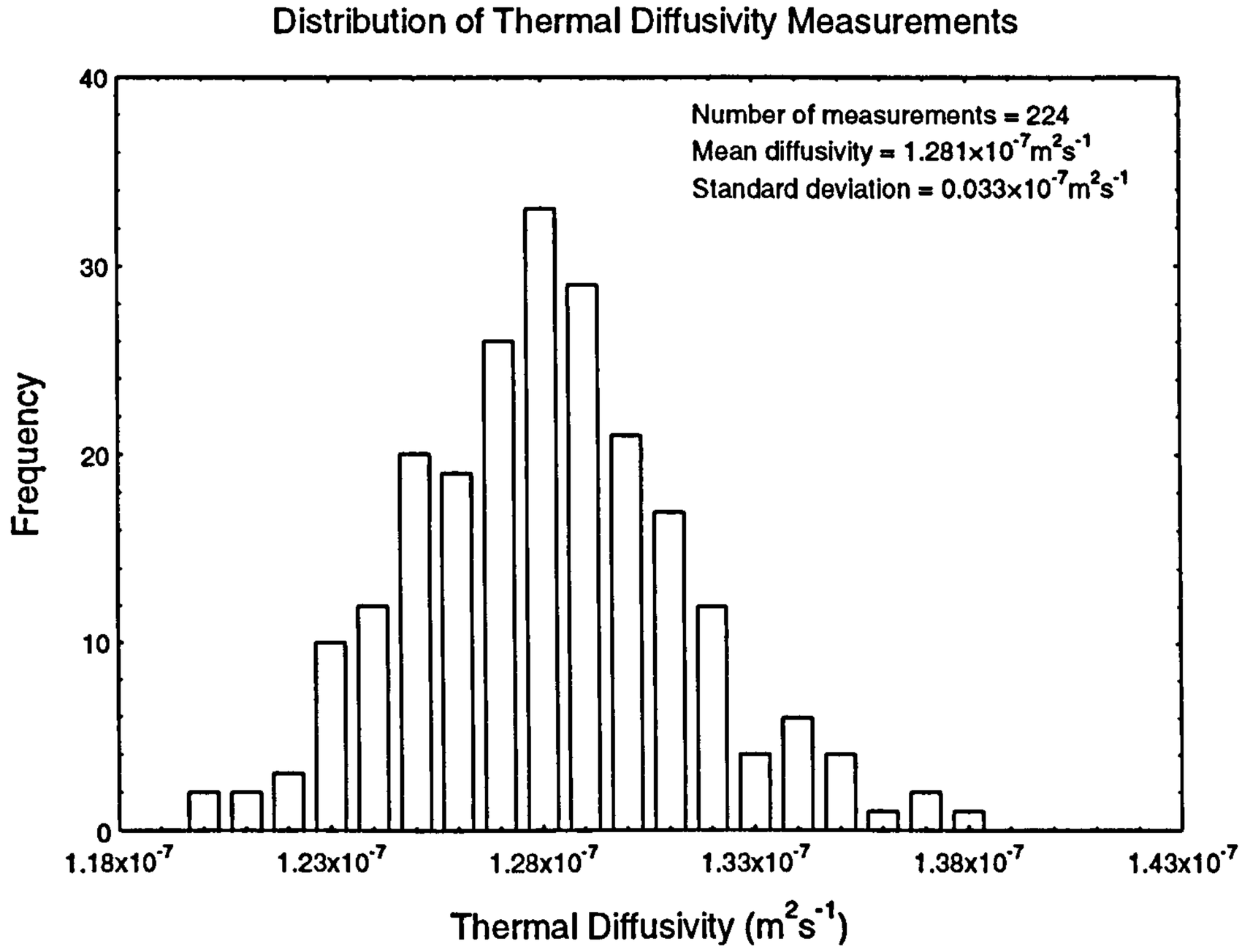

Figure 5.34 Distribution of thermal diffusivity for all measurements on animal liver.

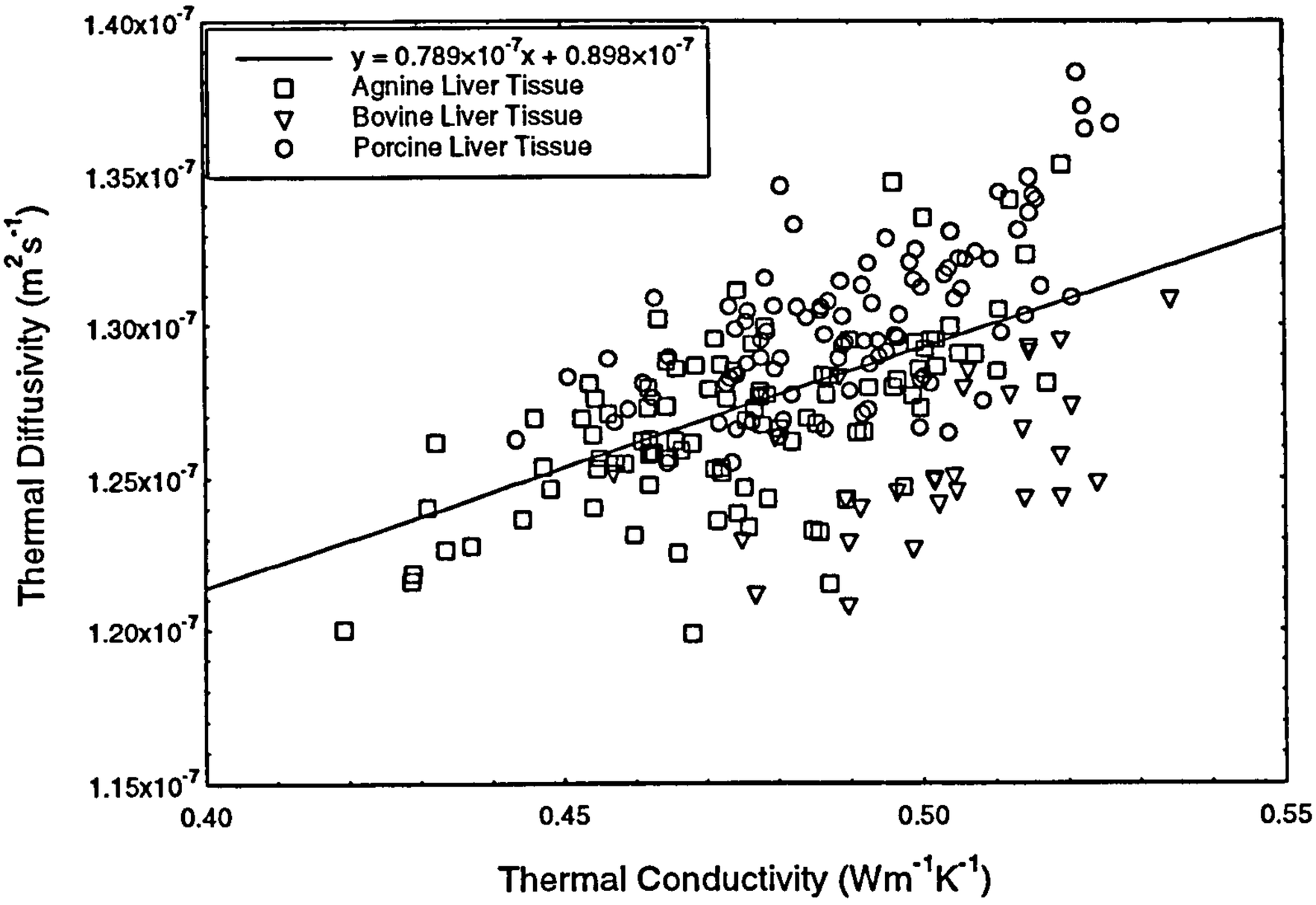

Figure 5.35 The variation of α with k for all measurements on animal liver.

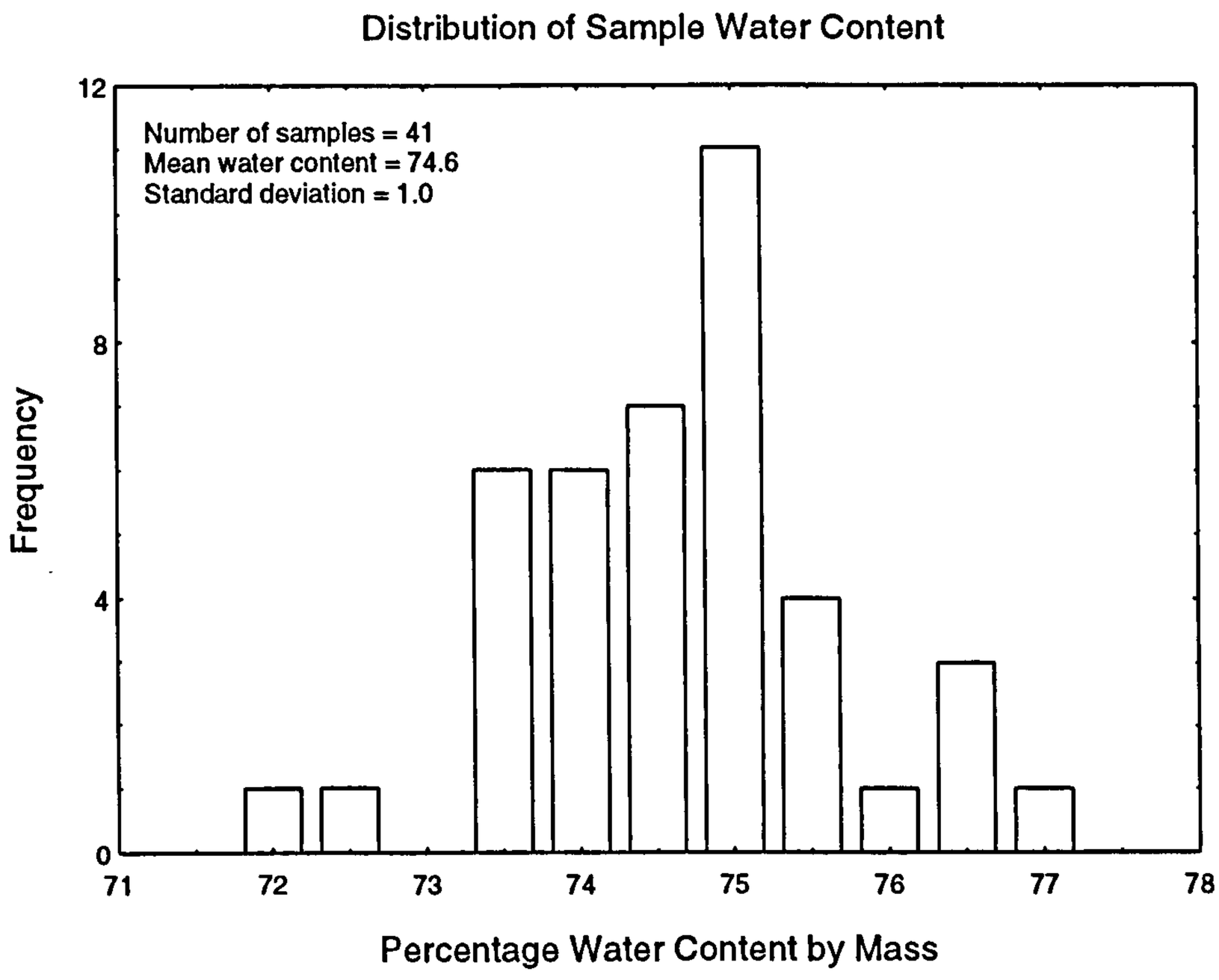

Figure 5.36 The distribution of measured water content for all human liver samples.

Figure 5.35 shows the variation of the thermal diffusivity with the thermal conductivity for all the measurements made on animal liver. The linear least square fit of the thermal diffusivity against thermal conductivity data, with the correlation given by r, is

$$\alpha = (0.789k + 0.898) \times 10^{-7}\ \mathrm{m^2 s^{-1}}: r = 0.526$$

5.13.2 Human Liver Tissue.

In total, 201 measurements were made on 41 samples of human liver tissue. The human liver samples came from two specimens which were removed postmortem from two different subjects.

The mean, maximum, and minimum values of the thermal conductivity, thermal diffusivity, and water content of human liver tissue are as follows

Water Content (%)	Minimum	73.3	Maximum	76.8	Mean	74.6
Thermal Conductivity ($Wm^{-1}K^{-1}$)	Minimum	0.438	Maximum	0.592	Mean	0.510
Thermal Diffusivity ($\times 10^{-7}\ m^2 s^{-1}$)	Minimum	1.216	Maximum	1.370	Mean	1.302

The distribution of the measured sample water content is shown in figure 5.36, while the distribution of the measurements of the thermal conductivity and thermal diffusivity are shown in figures 5.37 and 5.38.

As with the animal tissue, the water content of liver tissue is lower than that seen in human skeletal muscle tissue. The results from the two human liver specimens examined are very similar, with both specimens giving similar average thermal conductivity, thermal diffusivity, and water content.

The variation of the thermal diffusivity with the thermal conductivity is shown in figure 5.39. The linear least square fit of the thermal diffusivity against thermal conductivity data is

$$\alpha = (0.284k + 1.157) \times 10^{-7}\ \mathrm{m^2 s^{-1}}: r = 0.417$$

5.13.3 Comparison Between Human and Animal Liver Tissue.

The most noticeable difference between the human liver tissues and the animal liver tissues examined in this study is the difference in water content. The average percentage

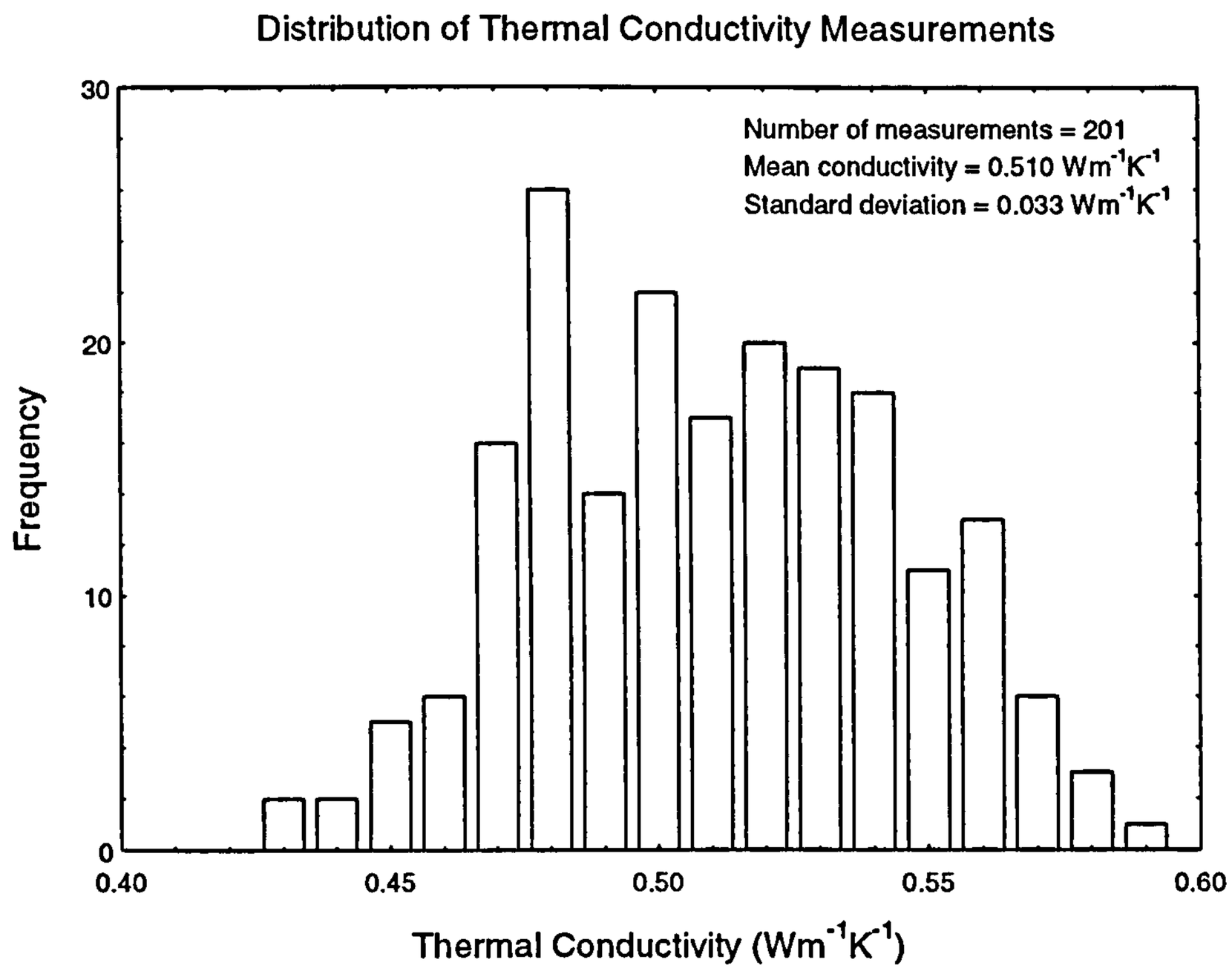

Figure 5.37 Distribution of thermal conductivity for all measurements of human liver.

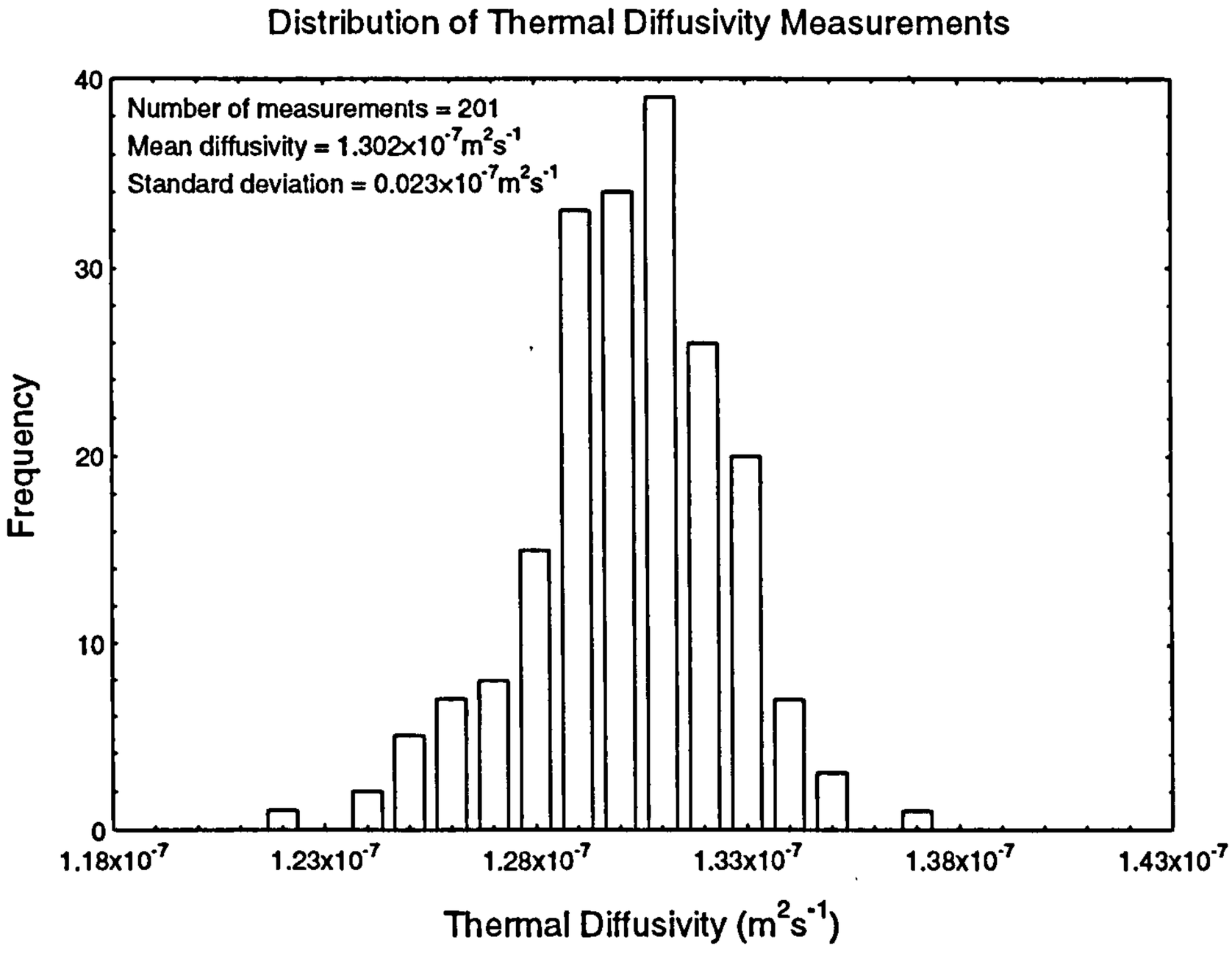

Figure 5.38 Distribution of thermal diffusivity for all measurements of human liver.

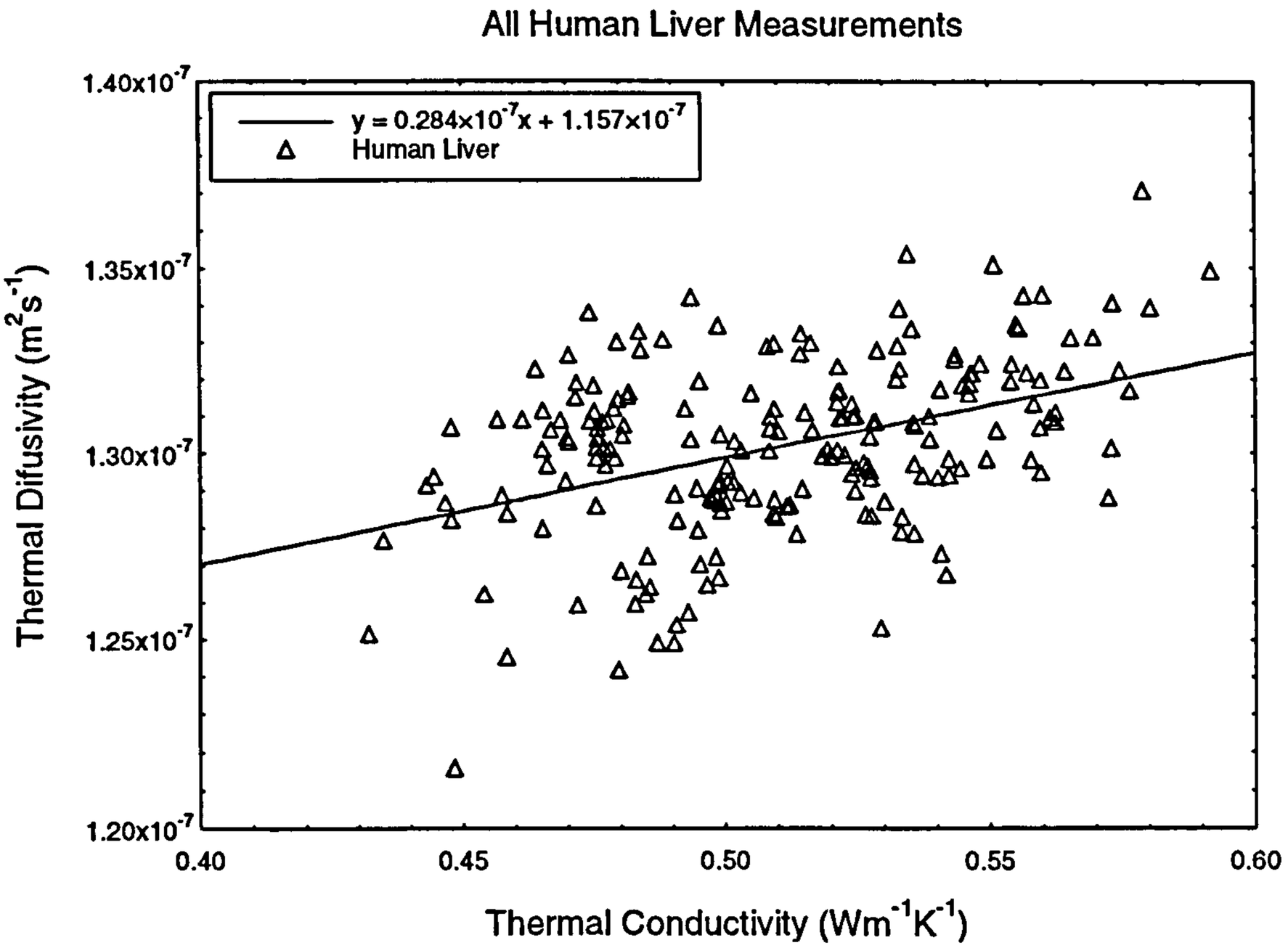

Figure 5.39 The variation of α with k for all measurements on human liver.

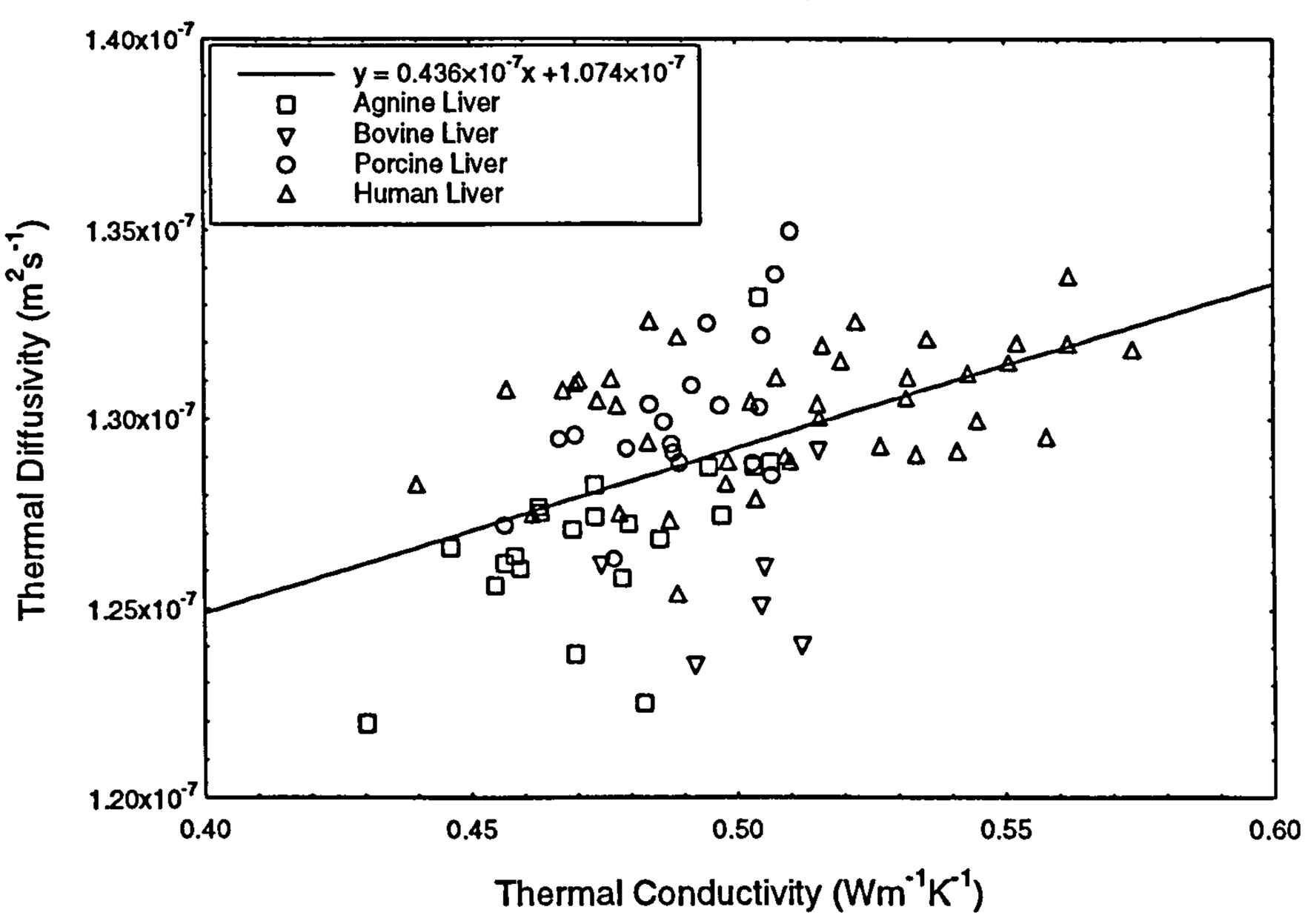

Figure 5.40 The variation of α with k for all liver samples.

water content in animal tissues is 7% lower than that seen in human tissues. The highest measured water content of the animal liver samples is still lower than the lowest measured human liver sample water content. The higher water content of the human tissues is reflected in a higher average thermal conductivity and thermal diffusivity in the human liver than in the animal liver.

The difference in water content is, as with skeletal muscle, probably due to the residual blood being drained from the animal samples. In skeletal muscle, this caused a drop of approximately 3% in water content. In skeletal muscle, the smaller drop in water content and the variability of the human tissues combined to give an average thermal conductivity and thermal diffusivity which varied little from those values seen in animal tissues.

In liver tissues, there was a larger difference in the average water content of human and animal tissues. Also the "quality" of the human liver was similar to that of the animal liver. Liver is a fairly uniform tissue, as shown by the small range of variation in the sample water content. This allows a clear difference between the thermal conductivity and thermal diffusivity of human and animal liver tissues to be seen.

The thermal conductivity and thermal diffusivity of animal and human liver tissues, as stated by other authors, are shown in tables 5.14 and 5.15. It can be seen that the stated thermal conductivities are a closer match to the average thermal conductivity of human liver than animal liver. This is probably due to the fact that the values stated for liver are for specimens which had not been drained of residual blood. The water contents given by Poppendiek (1966) and Cooper and Trezek (1971) are similar to those seen in human liver, which indicates that the values applied to specimens which had not had excess blood removed.

Figure 5.40 shows the variation of thermal diffusivity with thermal conductivity for all the animal and human liver samples examined in this study. It can be seen that the relationship between the thermal diffusivity and thermal conductivity is poorly defined. Howeve,r it appears that both human and animal liver have a similar relationship between the two quantities.

Figure 5.41 shows the variation of the thermal conductivity with sample water content and figure 5.42 shows the variation of the thermal diffusivity with sample water content. There is a general trend apparent, with the higher water content of the human tissues producing higher thermal properties. However, as with skeletal muscle, no definite

Liver Tissue Type	Thermal Conductivity ($Wm^{-1}K^{-1}$)	Reference
Agnine (21°C)	0.507-0.576	Bowman et al (1975)
Agnine (21°C)	0.495	Balasubramaniam and Bowman (1977)
Bovine (72.7% water)	0.488	Poppendiek et al (1966)
Porcine (24.1°C)	0.418	Tanasawa and Katsuda (1972)
Porcine (25°C)	0.518	Valvano et al (1985)
Porcine (15°C)	0.507	Liang et al (1991)
Human (77% water)	0.565	Cooper and Trezek (1971)
Human (37°C)	0.508	Bowman (1981)
Human (25°C)	0.499	Valvano et al (1985)

Table 5.14 Thermal conductivity of various liver tissues.

Liver Tissue Type	Thermal Diffusivity (m^2s^{-1})	Reference
Agnine (21°C)	$(1.14\text{-}1.94)\times10^{-7}$	Bowman et al (1975)
Agnine (21°C)	1.63×10^{-7}	Balasubramaniam and Bowman (1977)
Porcine (24.1°C)	1.73×10^{-7}	Tanasawa and Katsuda (1972)
Porcine (25°C)	1.37×10^{-7}	Valvano et al (1985)
Human (77% water)	1.37×10^{-7}	Cooper and Trezek (1971)
Human (25°C)	1.49×10^{-7}	Valvano et al (1985)

Table 5.15 Thermal diffusivity of various liver tissues.

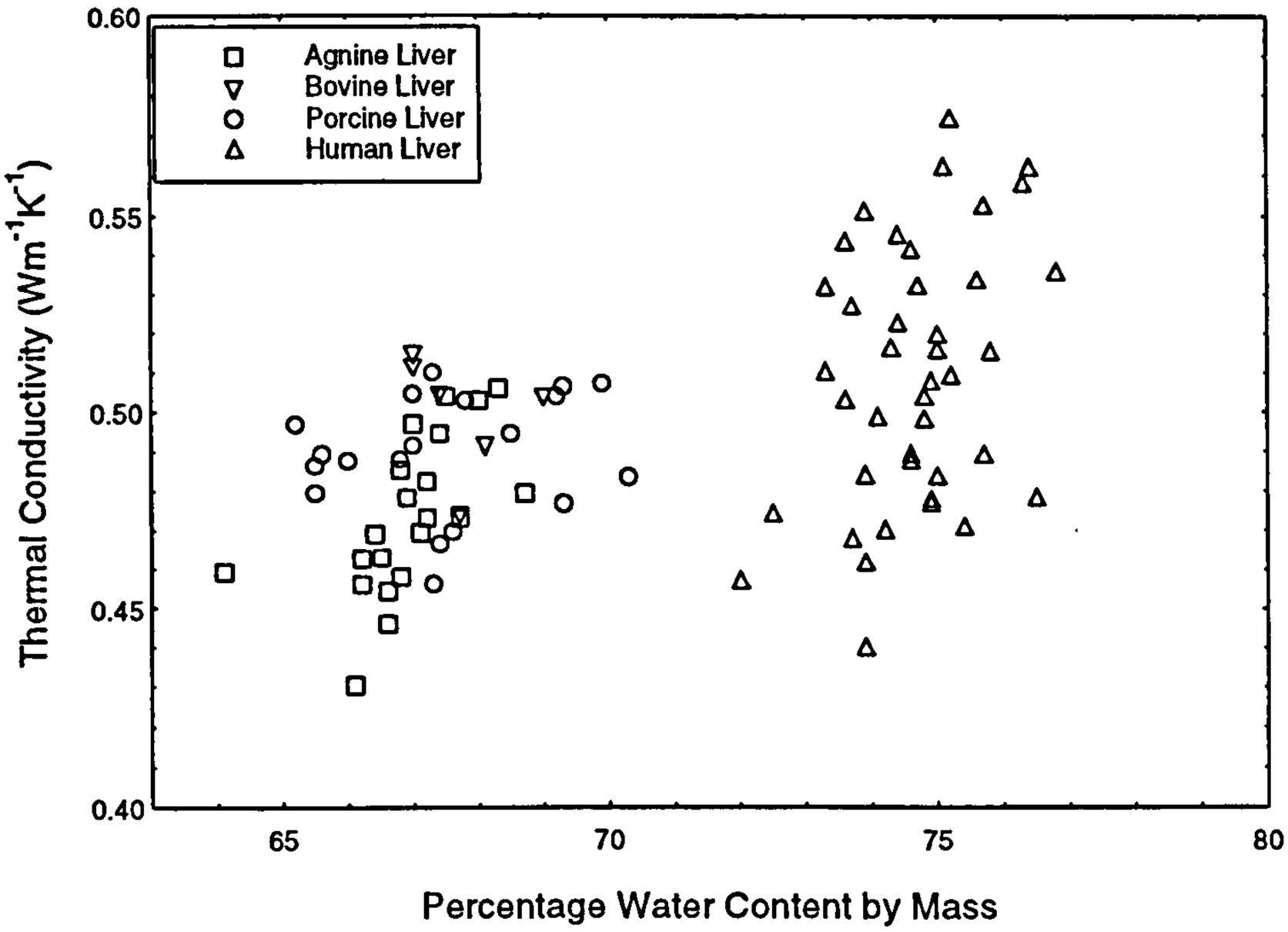

Figure 5.41 Variation in thermal conductivity of liver with sample water content.

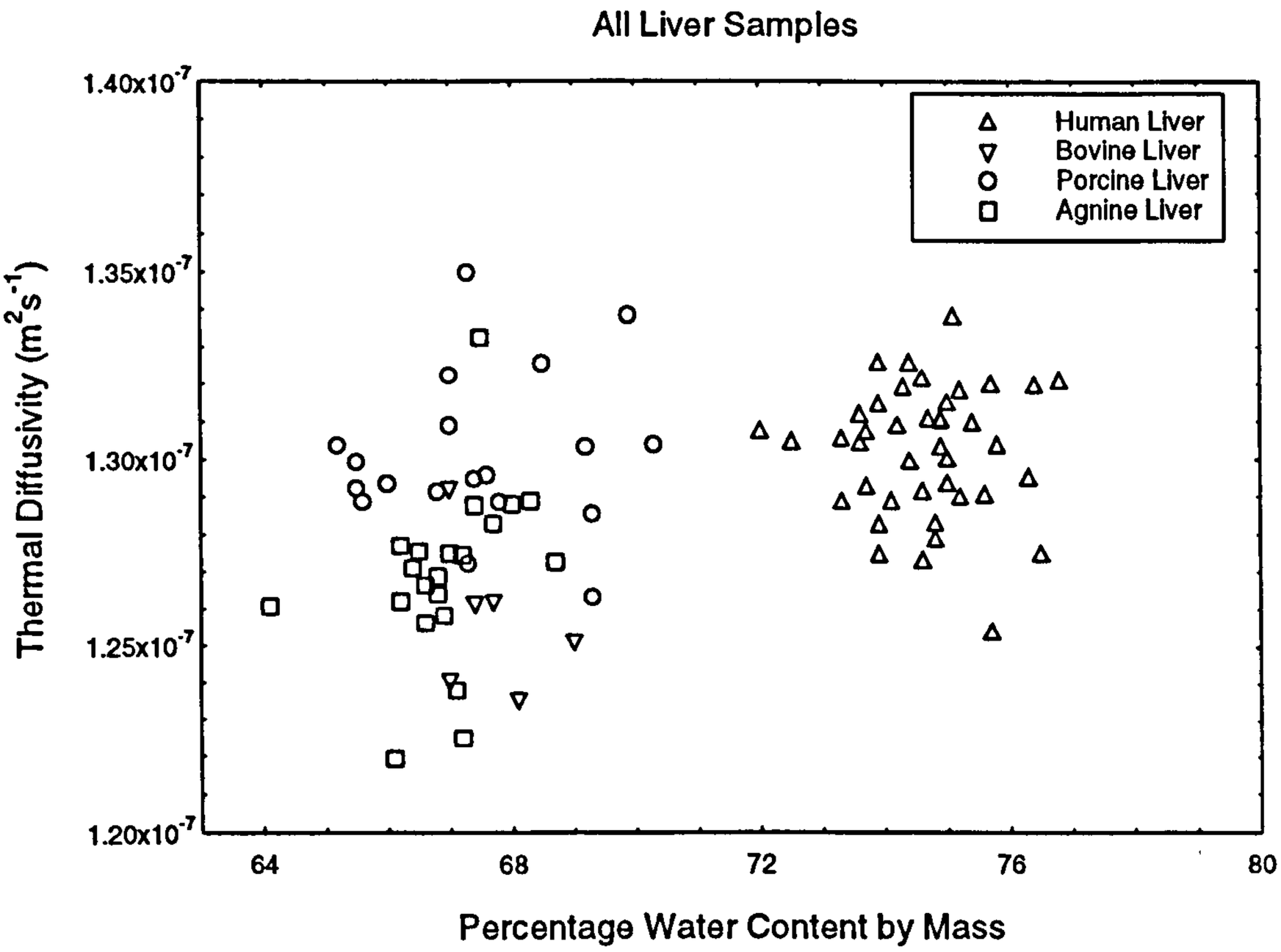

Figure 5.42 Variation in thermal diffusivity of liver with sample water content.

relationship can be discerned between the measured thermal property and the measured sample water content, due to the limited range of water content associated with individual tissues.

5.14 The Kidney.

The kidney is part of the urinary system. The human kidneys are bean shaped organs embedded in the posterior abdominal wall, one on either side of the body. Each kidney will weigh between 120 and 240 grams. When examined in cross section, it can be seen that the human kidney is composed of two regions. The outer part of the kidney, which comprises the majority of the kidney tissue, is known as the cortex, while the smaller inner part of the kidney is known as the medulla. Cup shaped calyces connect to the inner part of the kidney to carry the kidney's waste products into the ureter.
This is also true for the agnine and porcine kidneys, but not the bovine. The bovine kidney differs from the others, being composed of many lobes, each consisting of cortex, medulla, and calyces.

5.14.1 Animal Kidney Tissue.

In total 298 measurements were made on 61 samples of animal kidney. Fifty-five measurements were made on 11 samples of agnine kidney, a further 80 measurements were made on 16 samples of bovine kidney, and 163 measurements were made on 34 samples of porcine kidney. Table 5.16 shows the mean thermal conductivity, thermal diffusivity, and water content of the animal kidney tissues examined in this study.
The distribution of the water content of all the animal kidney samples examined in this study is shown in figure 5.43, while the distribution of thermal conductivity and thermal diffusivity of all the measurements on animal kidney tissue are shown in figures 5.44 and 5.45 respectively.
The range of measurements made on animal kidney cortex of the thermal conductivity, thermal diffusivity, and water content are as follows

Kidney Tissue	No. of Samples	No. of Meas.	Mean Thermal Conductivity ($Wm^{-1}K^{-1}$)	Mean Thermal Diffusivity (m^2s^{-1})	Mean % Water Content by Mass
Cortex:					
Agnine	11	55	0.543	1.357×10^{-7}	77.4
Bovine	14	70	0.524	1.368×10^{-7}	78.0
Porcine	31	148	0.537	1.362×10^{-7}	79.6
Overall	56	273	0.535	1.363×10^{-7}	78.8
Medulla	5	25	0.566	1.397×10^{-7}	82.0

Table 5.16 The mean thermal conductivity, thermal diffusivity and water content of the animal kidney tissues measured in this study.

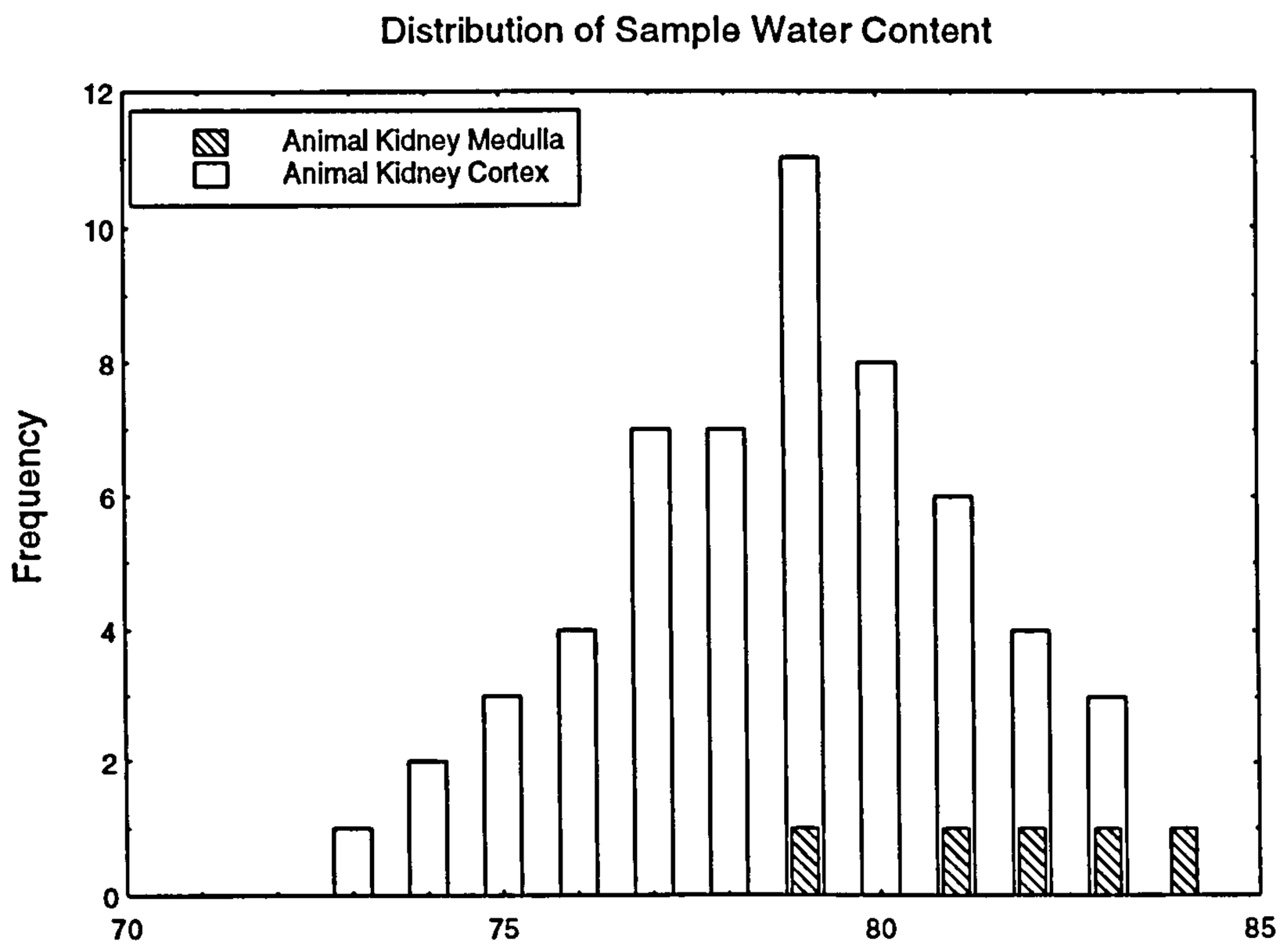

Figure 5.43 The distribution of measured water content for all animal kidney samples.

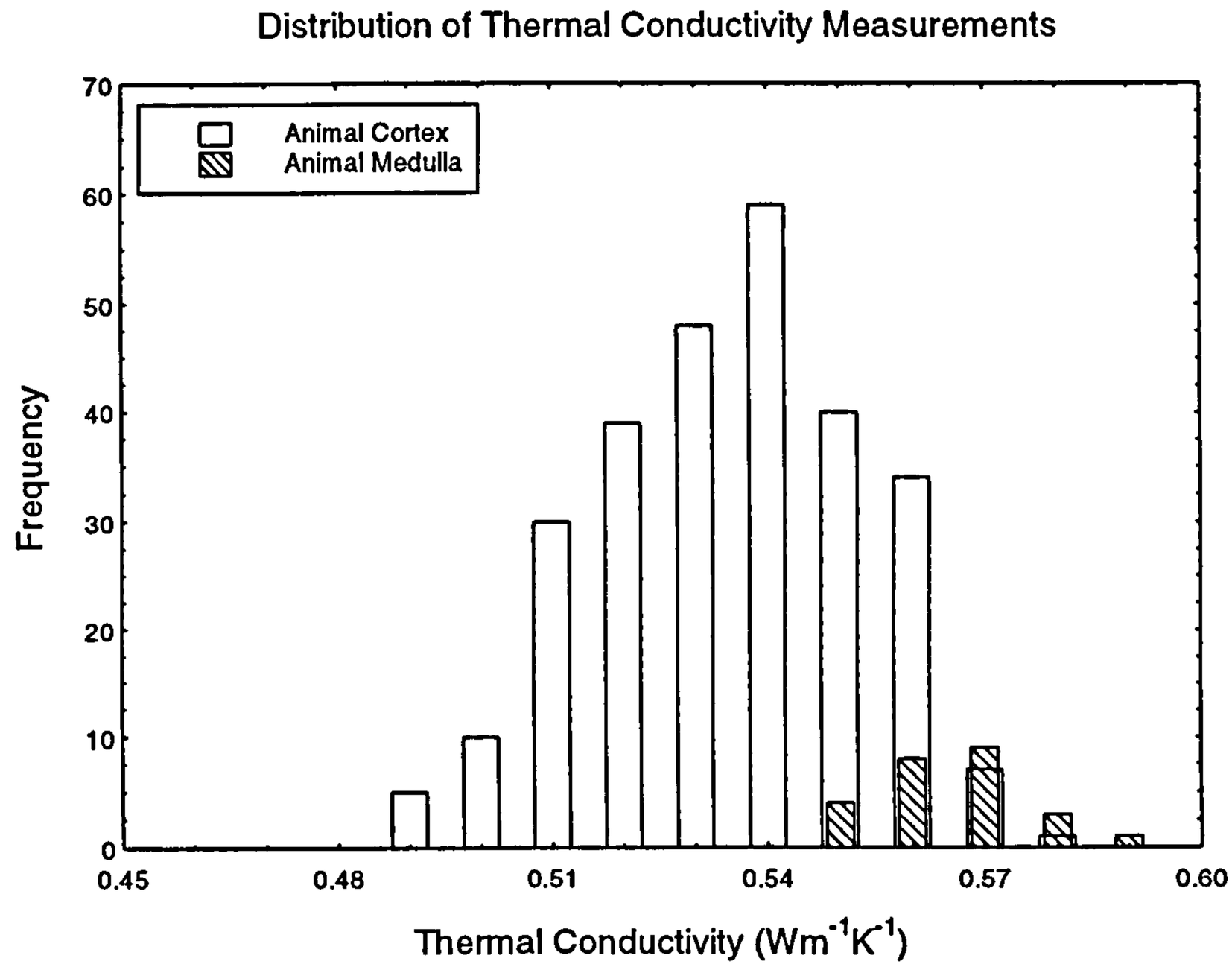

Figure 5.44 Distribution of thermal conductivity measurements on animal kidney.

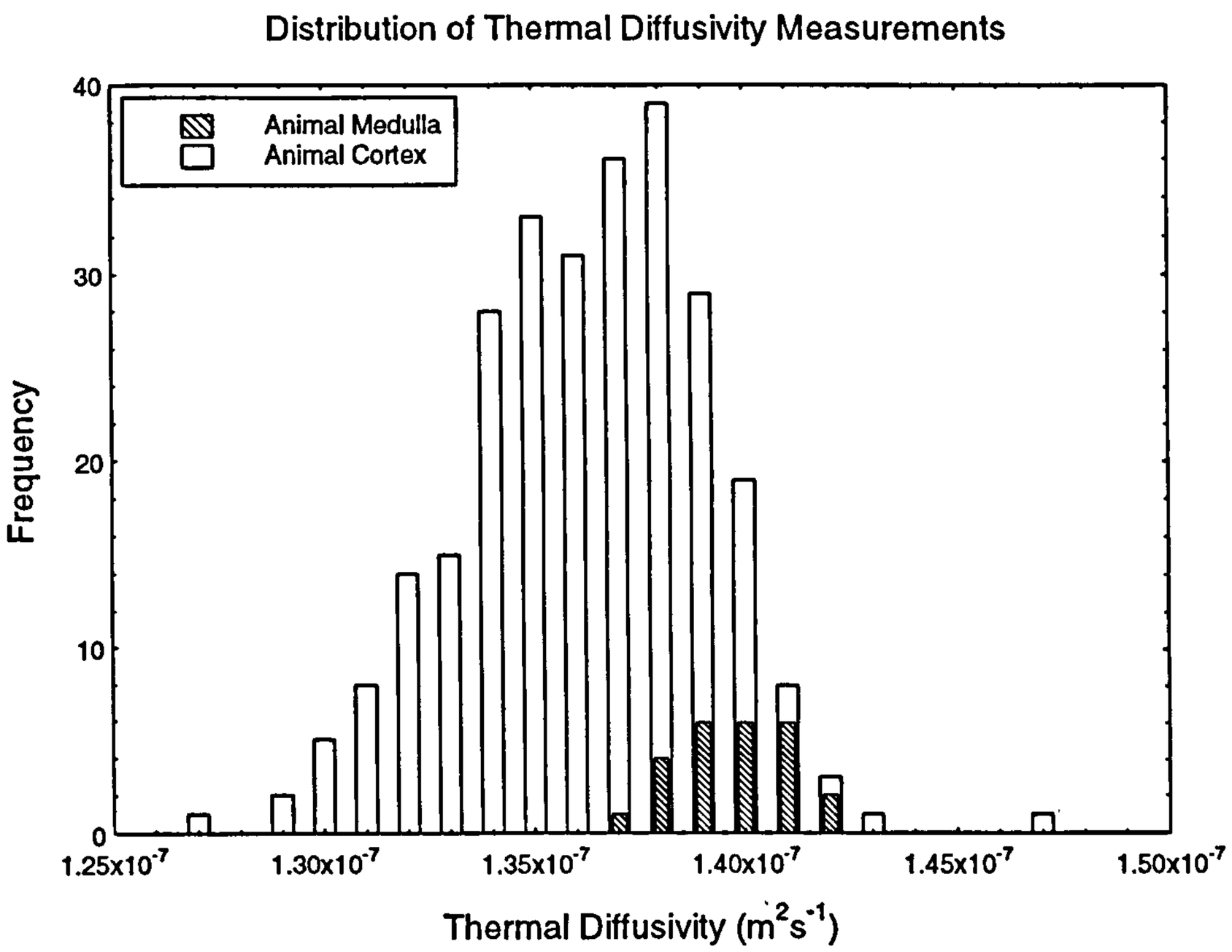

Figure 5.45 Distribution of thermal diffusivity measurements on animal kidney.

Water Content (%)	Minimum	73.2	Maximum	83.2	Mean	78.8
Thermal Conductivity ($Wm^{-1}K^{-1}$)	Minimum	0.487	Maximum	0.576	Mean	0.535
Thermal Diffusivity ($\times 10^{-7}\ m^2s^{-1}$)	Minimum	1.273	Maximum	1.467	Mean	1.363

For the kidney medulla taken from animal specimens, the ranges of the thermal conductivity, thermal diffusivity, and water content are

Water Content (%)	Minimum	79.5	Maximum	84.2	Mean	82.0
Thermal Conductivity ($Wm^{-1}K^{-1}$)	Minimum	0.546	Maximum	0.587	Mean	0.566
Thermal Diffusivity ($\times 10^{-7}\ m^2s^{-1}$)	Minimum	1.371	Maximum	1.422	Mean	1.397

Kidney tissue has the highest water content of all the animal tissues examined so far. Both the kidney cortex and medulla tissue show average thermal conductivities and thermal diffusivites higher than the averages seen in the rest of the tissues, as would be expected given the higher water content.

Kidney medulla tissue has a far higher average water content than the kidney cortex tissue. Thus, it would be expected that the average thermal conductivity and diffusivity of the medulla tissue would be higher than that of cortex tissue, and this is what is seen.

However, the histograms show that there is an overlap between the two tissues. This is mainly due to the fact that there is no fixed boundary between the cortex and medulla tissue. The transition is gradual, so some kidney tissue which was taken to be cortex may actually have the properties of medulla tissue, or a mixture of cortex and medulla tissue.

The variation of the thermal diffusivity with the thermal conductivity is shown in figure 5.46. The linear least square fit of the thermal diffusivity against thermal conductivity data is

$$\alpha = (0.653k + 1.014) \times 10^{-7}\ m^2s^{-1}: r = 0.440$$

5.14.2 Human Kidney Tissue.

Eighty-four measurements were made on nineteen samples of human kidney. The human kidney came from two specimens which were removed postmortem from two different subjects. All the measurements were made on cortex tissue.

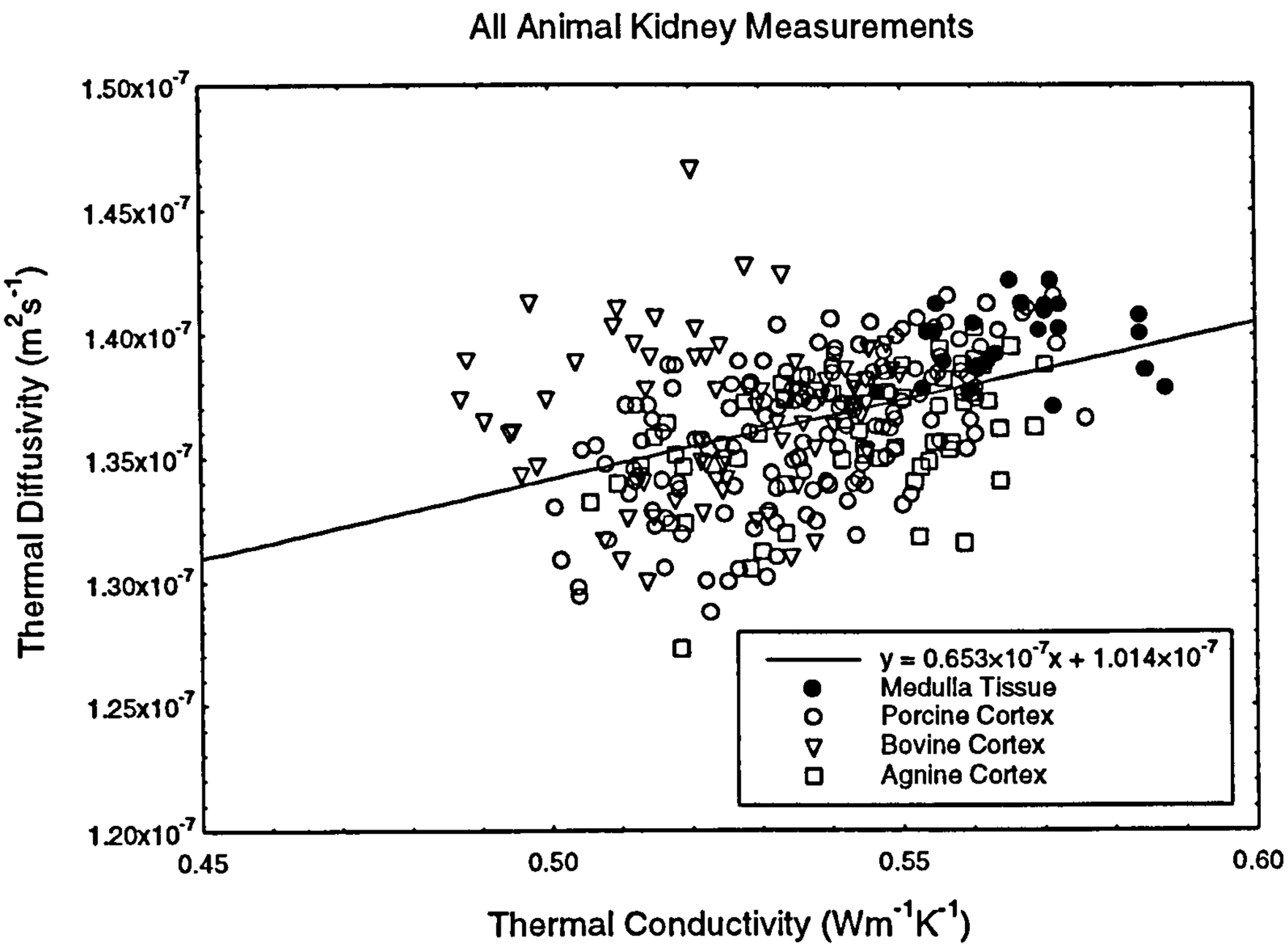

Figure 5.46 The variation of α with k for all measurements on animal kidney.

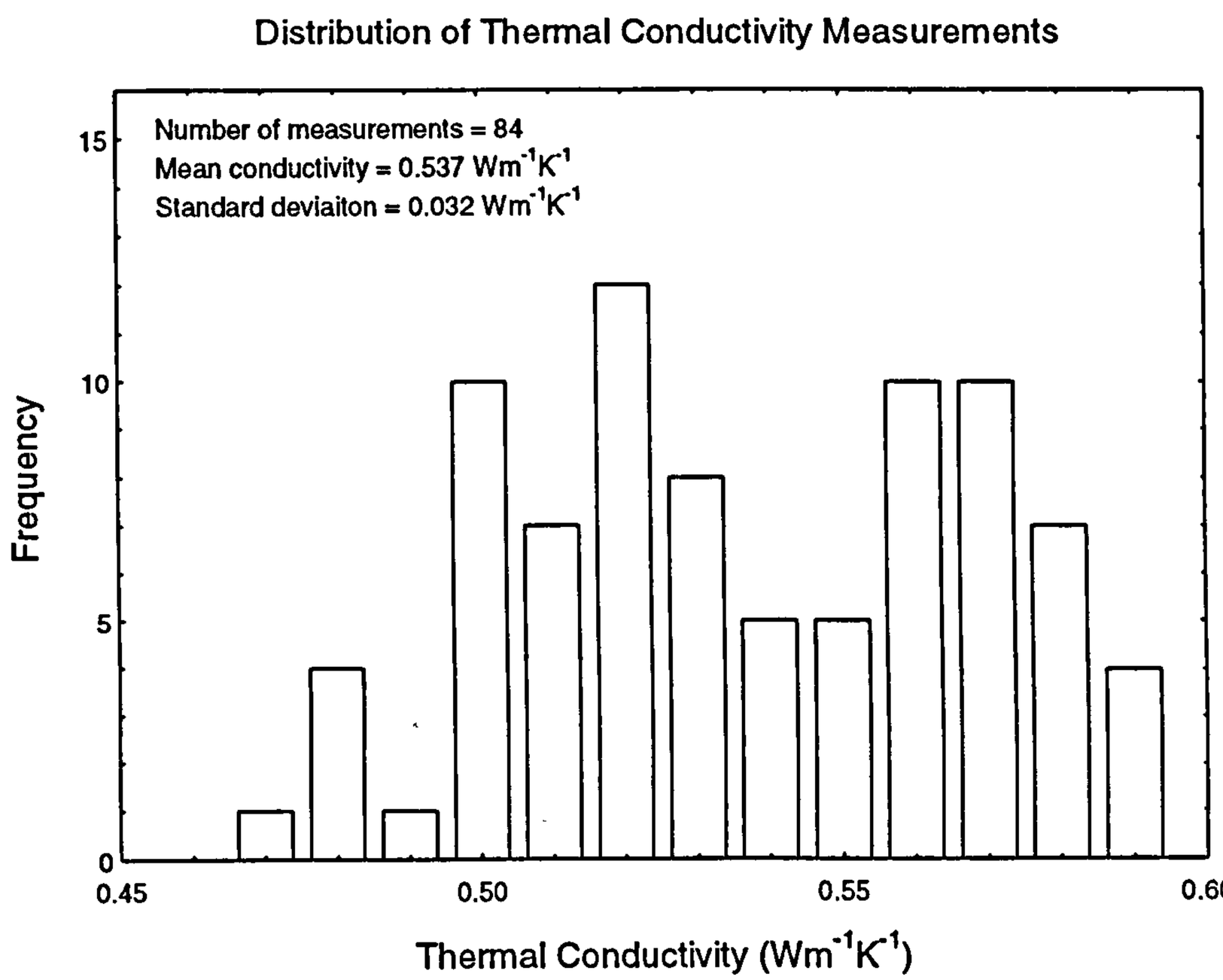

Figure 5.47 Distribution of thermal conductivity for all measurements on human kidney.

The range of measurements made on human kidney tissue of the thermal conductivity, thermal diffusivity, and water content are as follows

Water Content (%)	Minimum	76.8	Maximum	80.4	Mean	79.1
Thermal Conductivity ($Wm^{-1}K^{-1}$)	Minimum	0.417	Maximum	0.590	Mean	0.537
Thermal Diffusivity ($\times 10^{-7}\ m^2s^{-1}$)	Minimum	1.280	Maximum	1.378	Mean	1.333

The distribution of all the measurements of the thermal conductivity and thermal diffusivity of human kidney are shown in figures 5.47 and 5.48. Not enough samples were examined to give a meaningful histogram showing the distribution of sample water content.

As with the animal kidney tissue, human kidney tissue has the highest water content of all the human tissues examined so far. As would be expected from its high water content, human kidney tissue also has the highest average thermal conductivity and thermal diffusivity of all the tissues examined so far.

The variation of the thermal diffusivity with the thermal conductivity is shown in figure 5.49. The linear least square fit of the thermal diffusivity against thermal conductivity data is

$$\alpha = (0.505k + 1.062) \times 10^{-7}\ m^2s^{-1}: r = 0.741$$

5.14.3 Comparison Between Human and Animal Kidney Tissue.

Human and animal kidney are remarkably similar. Unlike the other tissues examined in this study, human kidney has an average water content which lies very close to the average water content of animal kidney. This would suggest that the animal kidneys examined were less affected by the draining of residual blood than the other tissues examined in this study.

The thermal conductivities of human and animal kidney were also remarkably similar. This is as expected, given that the human and animal tissues have such similar water contents. However the thermal diffusivity of the human kidney tissue is roughly 2% lower than that seen in the animal tissue.

The thermal conductivity of kidney tissue as stated by other authors is shown in table 5.17, and the thermal diffusivity of kidney tissue as stated by other authors is shown in

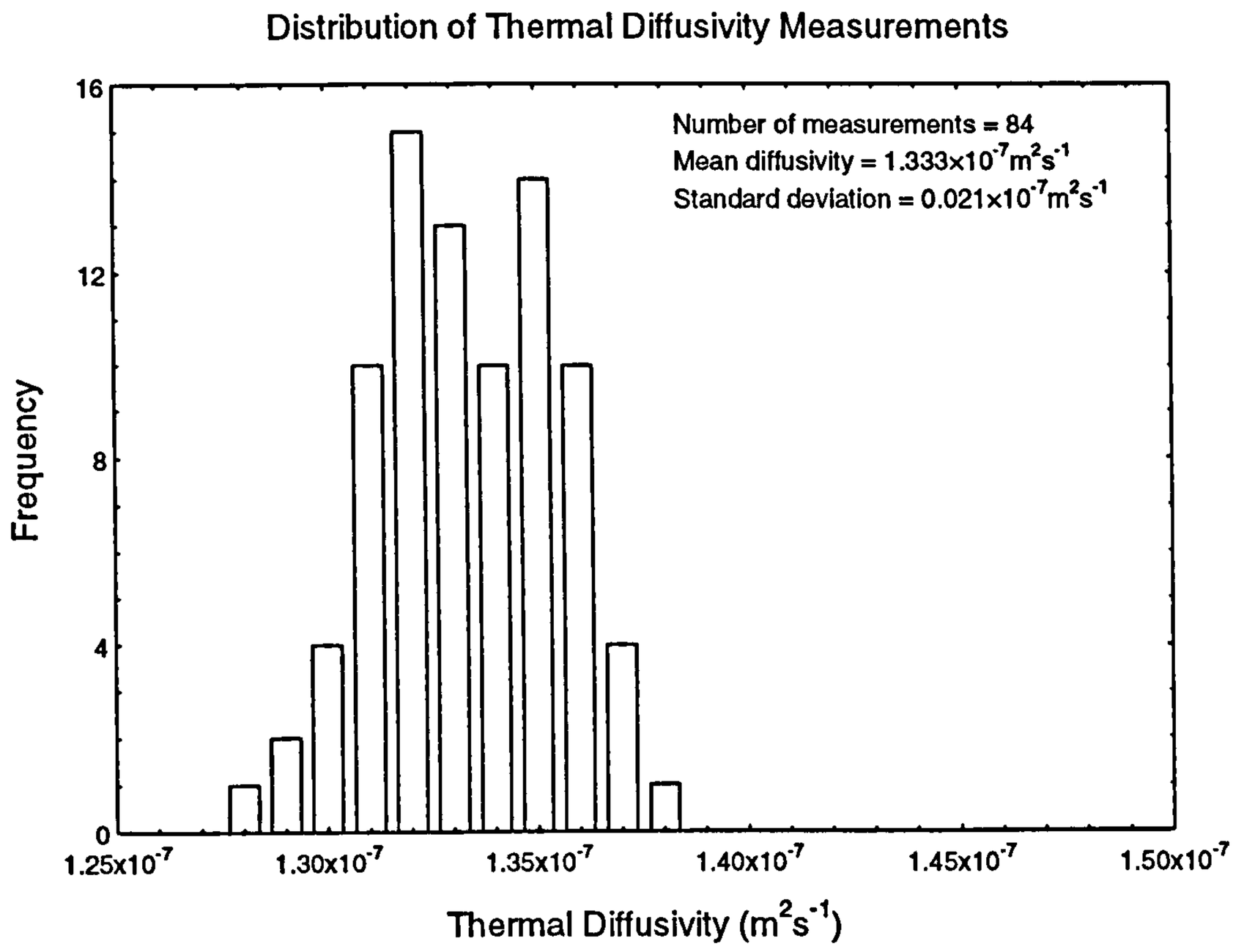

Figure 5.48 Distribution of thermal diffusivity measurements on human kidney.

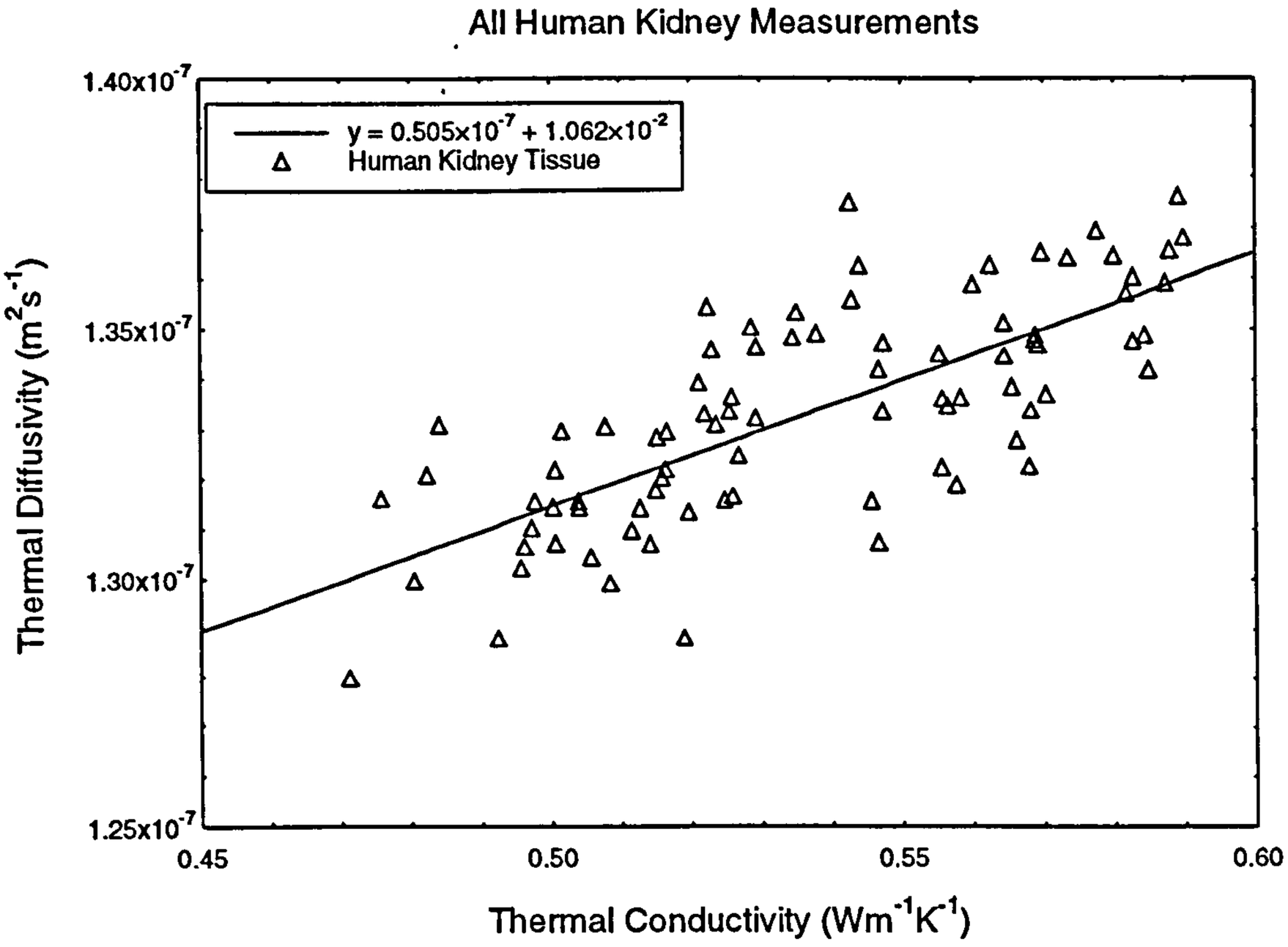

Figure 5.49 The variation of α with k for all measurements on human kidney.

Kidney Tissue Type	Thermal Conductivity ($Wm^{-1}K^{-1}$)	Reference
Agnine (37.8°C)	0.488	Bowman et al (1975)
Bovine (76.4% Water)	0.525	Poppendiek et al (1966)
Porcine Cortex (25°C)	0.526	Valvano et al (1985)
Porcine (15°C)	0.556	Liang et al (1991)
Human (84% Water)	0.544	Cooper and Trezek (1971)
Human (37°C)	0.547	Bowman (1981)
Human Cortex (25°C) Human Medulla (25°C)	0.531 0.527	Valvano et al (1985)
Human	0.547	Strohbehn et al (1986)

Table 5.17 Thermal conductivity of various kidney tissues.

Kidney Tissue Type	Thermal Diffusivity (m^2s^{-1})	Reference
Porcine Cortex (25°C)	1.381×10^{-7}	Valvano et al (1985)
Human (84% Water)	1.32×10^{-7}	Cooper and Trezek (1971)
Human Cortex (25°C) Human Medulla (25°C)	1.404×10^{-7} 1.416×10^{-7}	Valvano et al (1985)
Human	1.381×10^{-7}	Strohbehn et al (1986)

Table 5.18 Thermal diffusivity of various kidney tissues.

table 5.18. The range of values in table 5.17 lies within the range of kidney thermal conductivity measured in this study. There is also little variation in the values of thermal diffusivity, as stated by other authors, which was not the case for the tissues examined previously in this study. The stated thermal diffusivities all lie within a few percent of the mean measured thermal diffusivity.

The variation of the thermal diffusivity with the thermal conductivity for all the kidney samples examined in this study is shown in figure 5.50. As with other tissues, the relationship between the thermal diffusivity and thermal conductivity of kidney is poorly defined. However, it appears that for a given thermal conductivity, human kidney tissue has a lower thermal diffusivity than animal kidney.

Figure 5.51 shows the variation of the thermal conductivity with sample water content, and figure 5.52 shows the variation of the thermal diffusivity with sample water content. As with all the other types of tissue examined, no definite relationship can be determined between the thermal conductivity or thermal diffusivity, and the water content.

5.15 Human Brain Tissue.

The human brain, or encephalon, is a 1.5 kg mass of nervous tissue. It is made up of grey and white nervous matter. The grey matter, which is composed of neuron cell bodies and nerve fibres, is found predominately on the outer surfaces of the brain. The white matter consists of nerve fibres which are surrounded by a white fatty material called myelin.

The brain is different from the other high water contents materials examined. In all other high water content tissues examined, the tissue can be thought of as water and protein. However in brain tissue, there is a significant amount of fat in the white matter. This can be seen in the density of the human brain. The density of pure dry fat is roughly 890 kgm^{-3}, while the density of pure dry protein is near 1300 kgm^{-3}. Cooper and Trezek (1971) gave the water content of white brain tissue as 71% and density as 1040 kgm^{-3}. If solid matter was pure protein, a density in the range 1060-1070 kgm^{-3} would be expected. This lower value is due to the fat present in the white matter. However for grey brain matter, Cooper and Trezek gave the water content as 83% and the density as

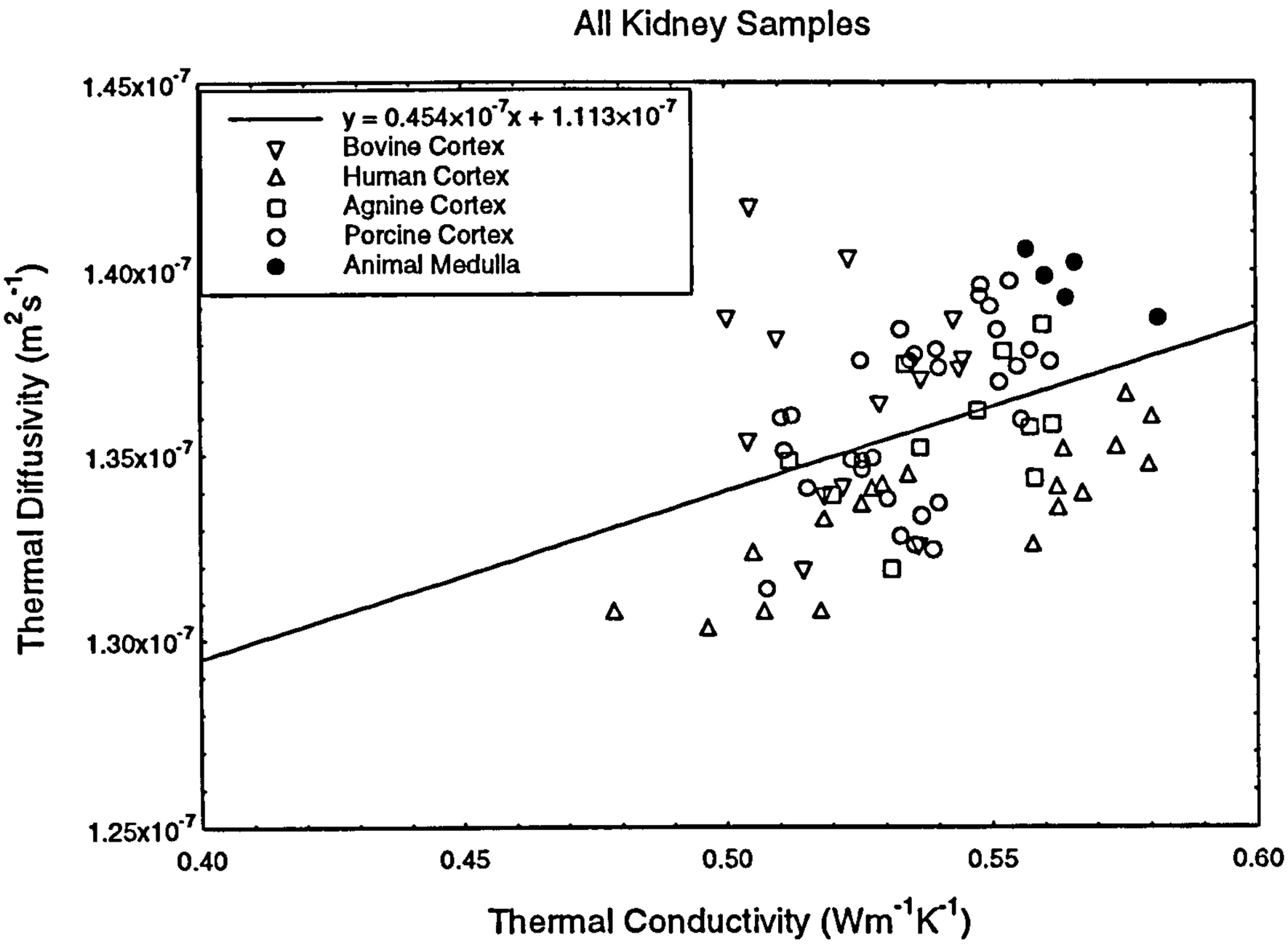

Figure 5.50 The variation of α with k for all animal and human kidney samples.

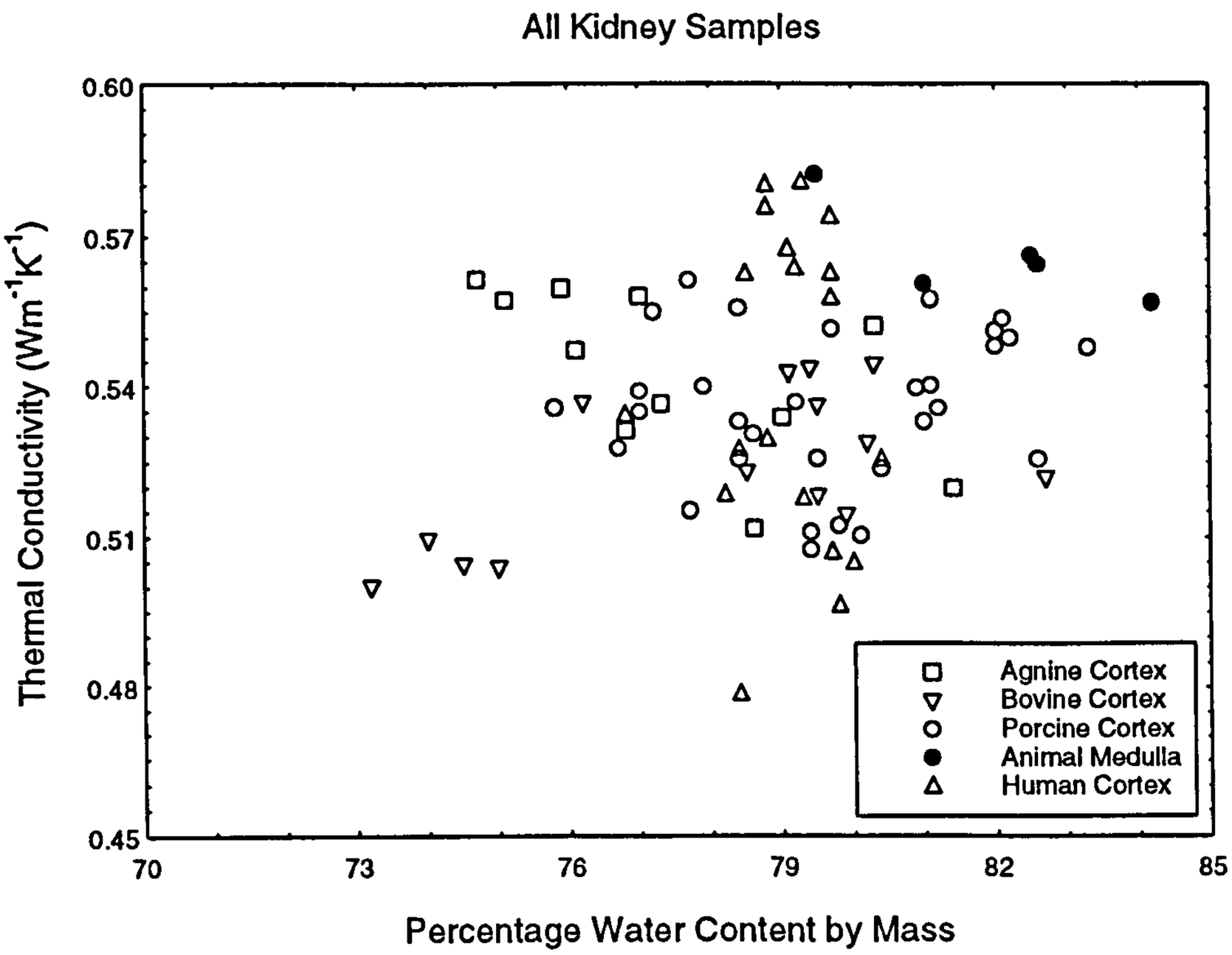

Figure 5.51 The variation of thermal conductivity with sample water content.

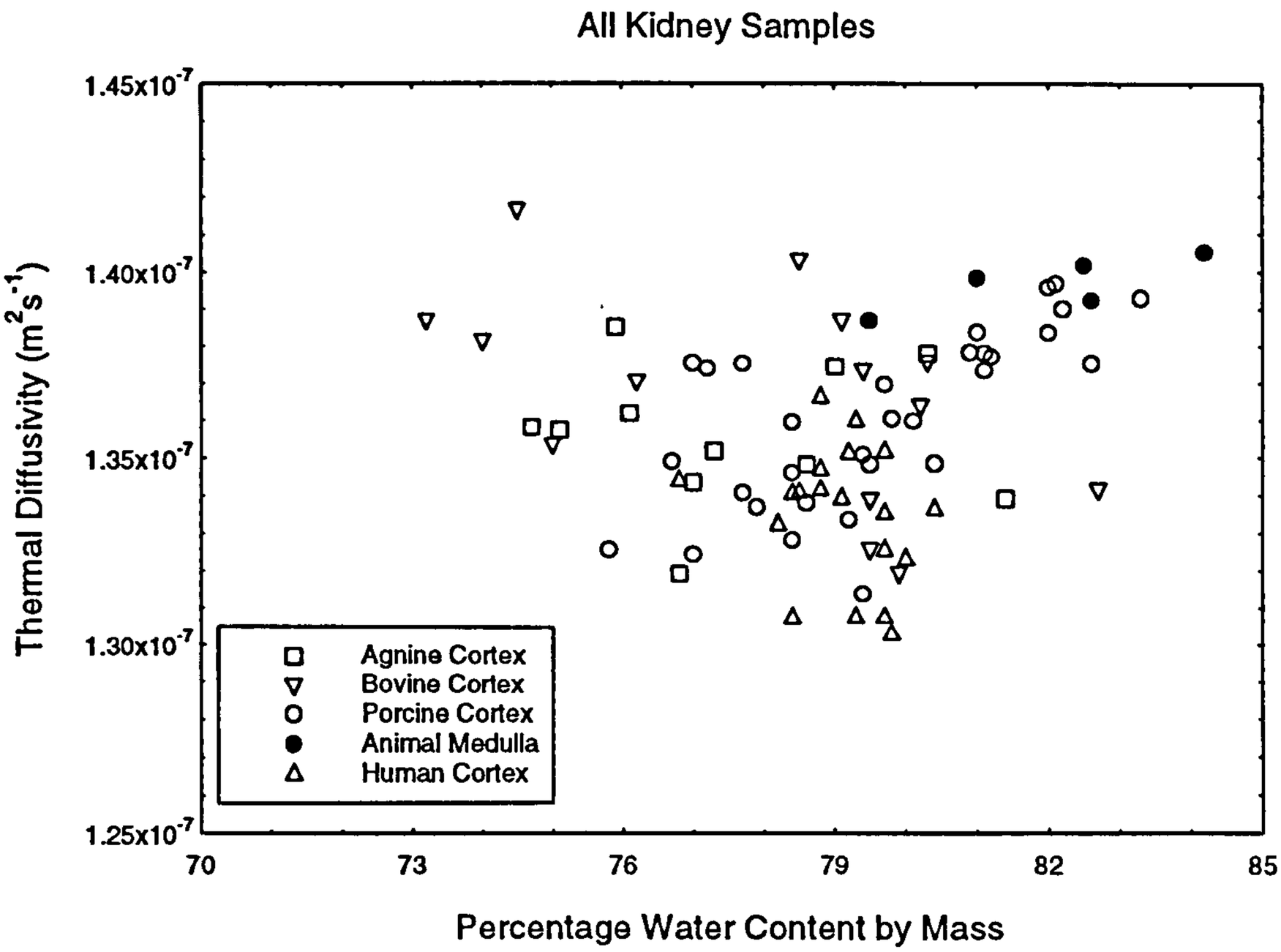

Figure 5.52 The variation of thermal diffusivity with sample water content.

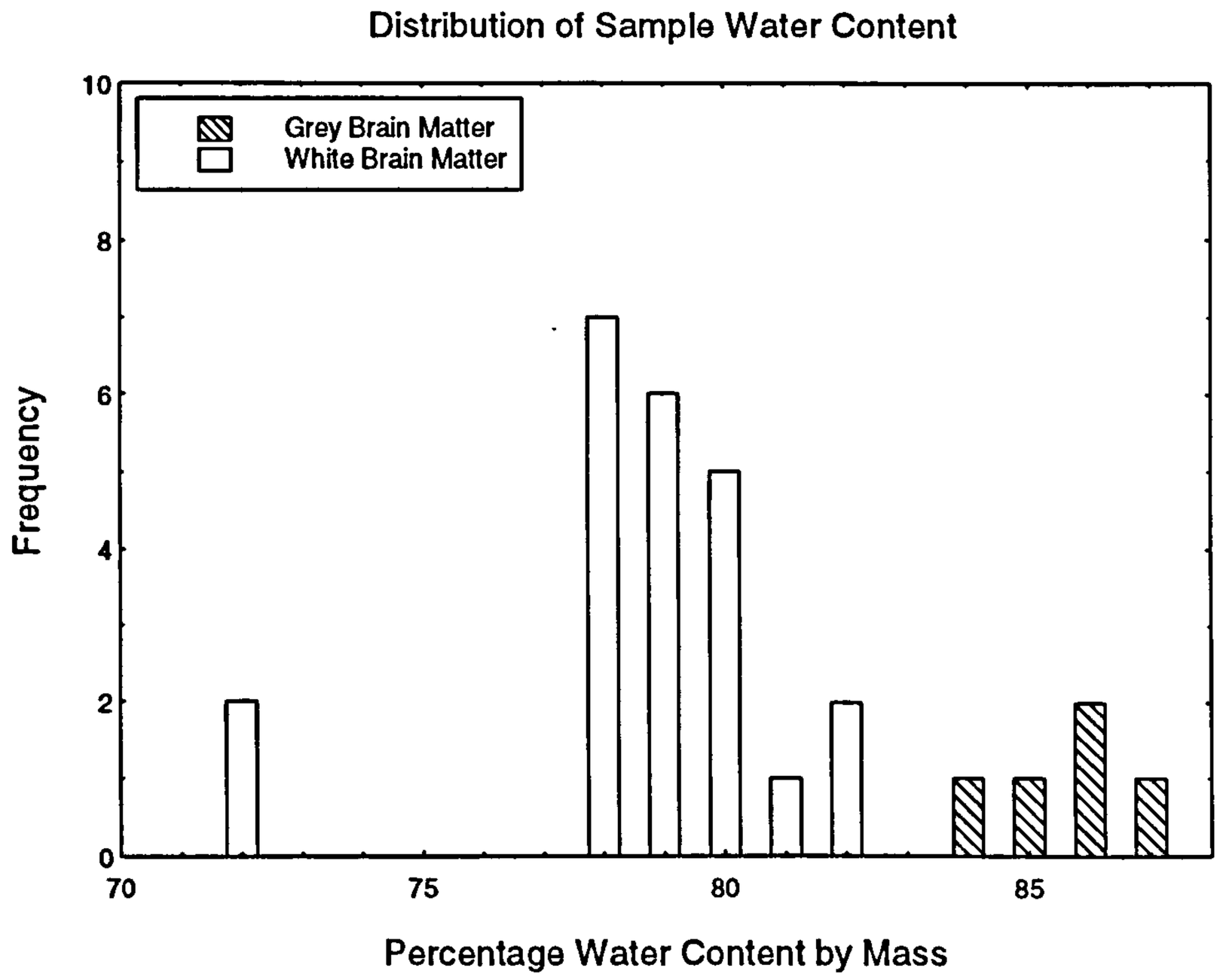

Figure 5.53 The distribution of sample water content of human brain.

1050 kgm^{-3}. This density value is in line with the value expected if the non-water fraction was mainly protein.

One specimen of human brain tissue was obtained, taken from the upper cerebrum. A total of 139 measurements were made on 28 samples taken from the specimen. Five of the 28 samples were of purely grey matter, while the rest of the samples were composed of mostly white matter.

The human brain is extremely delicate. It is barely able to support its own weight once removed from the cranium, and it is also prone to rapid degradation. In order to preserve the brain tissue, it was necessary to store the brain in water. This may have an effect on the water content of the brain tissue and hence its thermal conductivity and thermal diffusivity.

The distribution of the water content of all the human brain samples examined in this study is shown in figure 5.53, while the distribution of thermal conductivity and thermal diffusivity of all the measurements on human brain tissue are shown in figure 5.54 and figure 5.55 respectively.

The range of measurements made on the white brain matter of the thermal conductivity, thermal diffusivity, and water content are as follows

Water Content (%)	Minimum	72.9	Maximum	82.1	Mean	78.7
Thermal Conductivity ($Wm^{-1}K^{-1}$)	Minimum	0.443	Maximum	0.550	Mean	0.489
Thermal Diffusivity ($\times 10^{-7}$ m^2s^{-1})	Minimum	1.221	Maximum	1.399	Mean	1.293

For grey brain matter, the minimum, maximum, and mean values of the thermal conductivity, thermal diffusivity, and water content are

Water Content (%)	Minimum	83.6	Maximum	86.8	Mean	85.7
Thermal Conductivity ($Wm^{-1}K^{-1}$)	Minimum	0.529	Maximum	0.574	Mean	0.554
Thermal Diffusivity ($\times 10^{-7}$ m^2s^{-1})	Minimum	1.331	Maximum	1.400	Mean	1.374

The Biology Data Book (1972) gives the water content of white matter as 70% and the water content of grey matter as 84%. While the water content of grey matter measured in this study is only slightly higher than the stated value, there is a significant difference between stated value and the water content found in white matter. However, this difference in water content may be overstated. Some of the white matter samples had

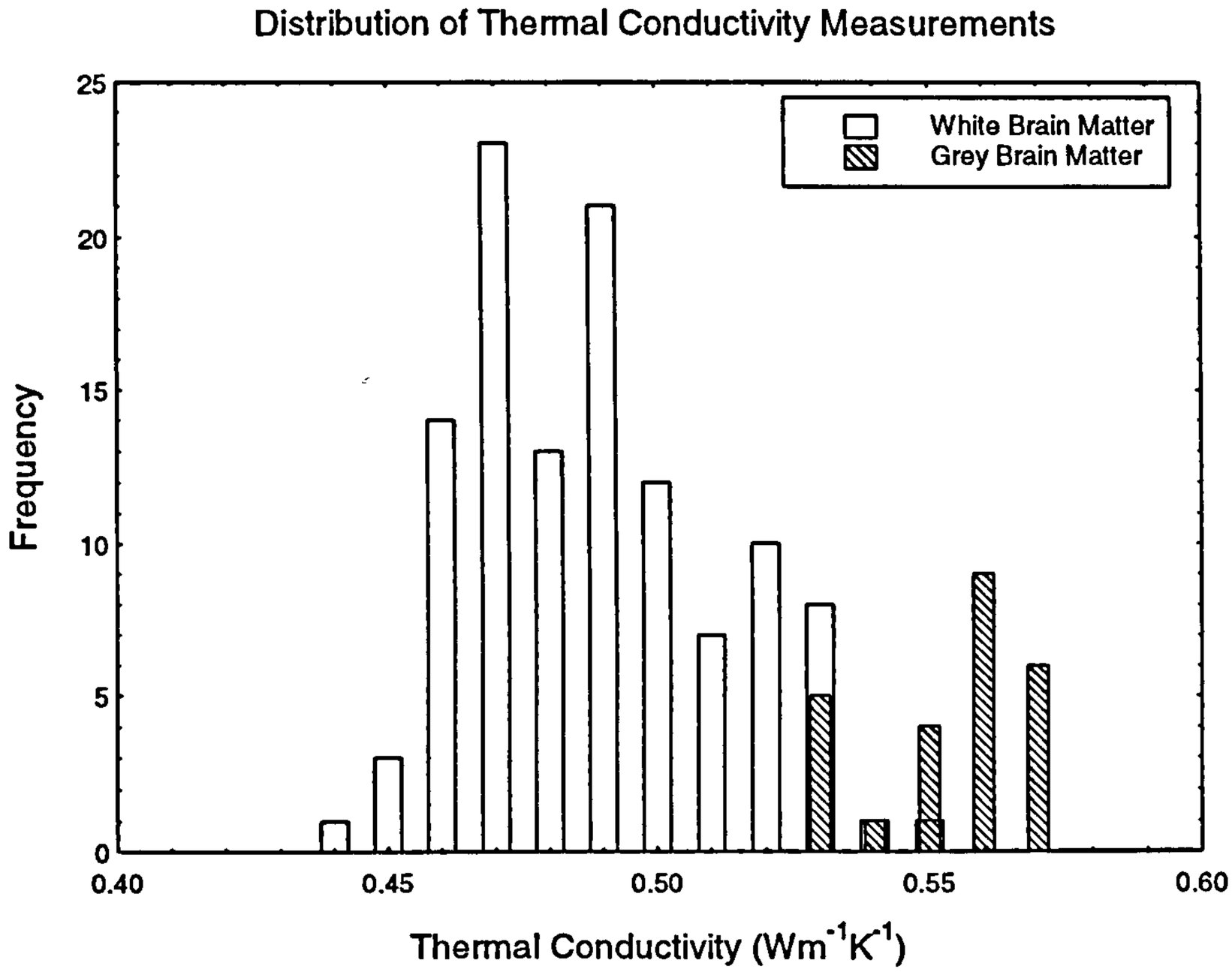

Figure 5.54 Distribution of thermal conductivity for all measurements on human brain.

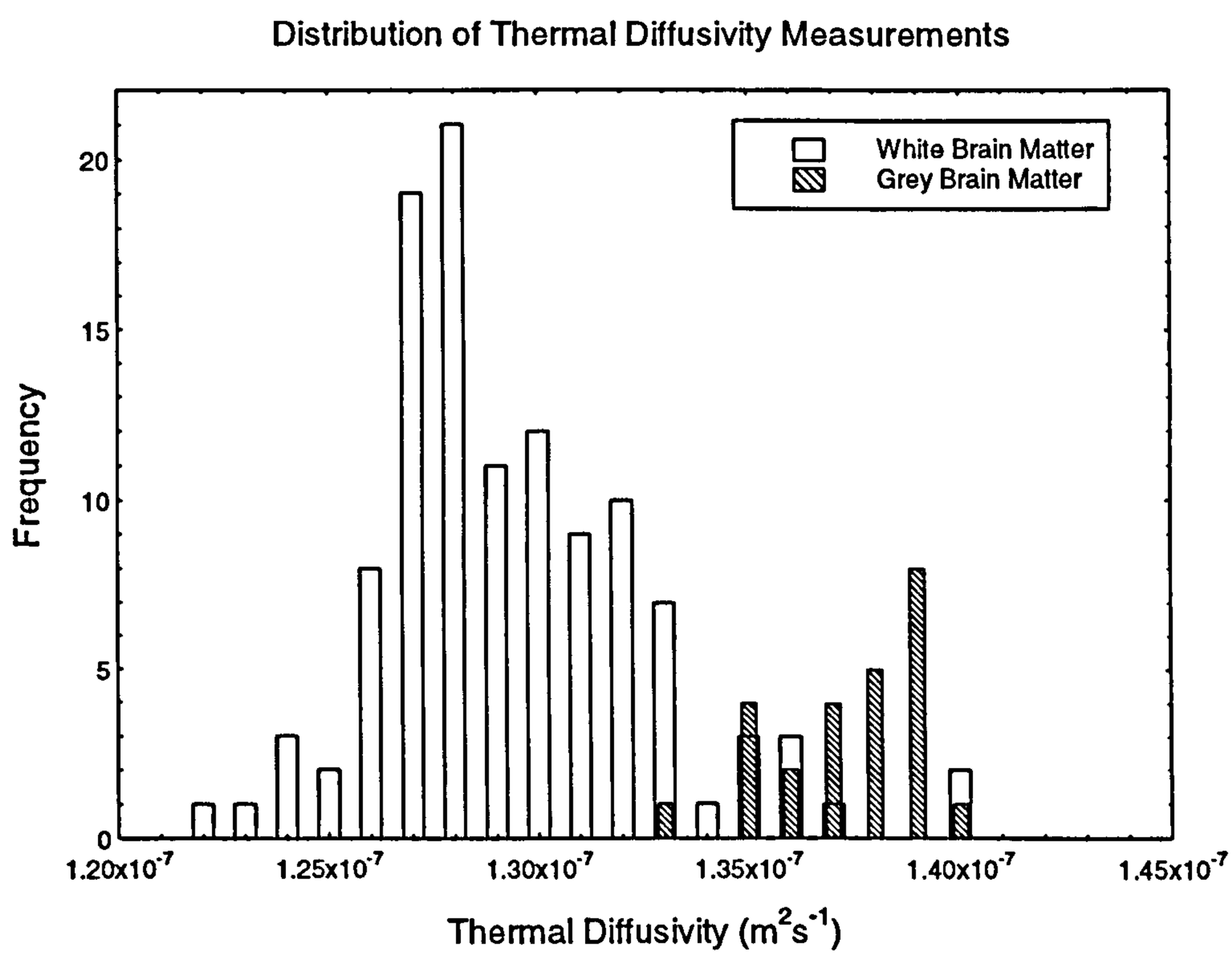

Figure 5.55 Distribution of thermal diffusivity for all measurements on human brain.

small amounts of grey matter in them. So while the measurements were made in pure white matter, the sample water content would not reflect this.

The grey matter had a higher water content than the white matter. As would be expected, the grey matter also had a higher mean thermal conductivity and thermal diffusivity. However, when compared to other high water content tissues, the difference between white brain tissue and the other tissues becomes clear. The thermal conductivity of white brain tissue is lower than would be expected for its water content when compared to other high water content tissues. This is due to the large amount of fat present in the brain. As discussed earlier in this thesis, the thermal conductivity of pure dry protein is higher than that of fat. This gives white matter a lower thermal conductivity and diffusivity than would be the case if the non-water fraction was nearly pure protein, as in the other high water content tissues.

The thermal conductivity and thermal diffusivity of brain tissue as stated by other authors, is shown in table 5.19. There is a reasonable amount of agreement about the thermal properties. Bowman (1981) stated that the lowest measured values were obtained from white tissue while the highest values came from grey tissue. The results of Cooper and Trezek (1972) also agree with the pattern observed in this study.

The variation in the thermal diffusivity with thermal conductivity of the human brain is shown in figure 5.56. The straight line fit of α against k data is

$$\alpha = (1.097k + 0.759) \times 10^{-7}\ \mathrm{m^2 s^{-1}}: r = 0.843$$

It can be seen that the relationship between the thermal diffusivity and thermal conductivity is well defined for human brain tissue and that both the grey and white tissue follow the same relationship.

The variation of thermal conductivity with sample water content for human brain is shown in figure 5.57, while the variation of thermal diffusivity with water content is shown in figure 5.58. A trend is apparent with the higher water content grey matter tissues having higher thermal conductivity and thermal diffusivity values. However, as with all the different tissues examined previously, there is no definite relationship between the sample water content and measured thermal property.

Brain Tissue Type	Thermal Conductivity ($Wm^{-1}K^{-1}$)	Thermal Diffusivity (m^2s^{-1})	Reference
Bovine (77.7% Water)	0.497	-	Poppendiek et al (1966)
White (71% Water) Grey (83% Water) Whole Brain (77% Water)	0.502 0.565 0.527	1.35×10^{-7} 1.43×10^{-7} 1.37×10^{-7}	Cooper and Trezek (1971)
Whole Brain	0.503-0.576	-	Bowman (1981)
Cortex (25°C)	0.512	1.408×10^{-7}	Valvano et al (1985)

Table 5.19 Thermal conductivity of various brain tissues. Human brain tissue unless otherwise stated.

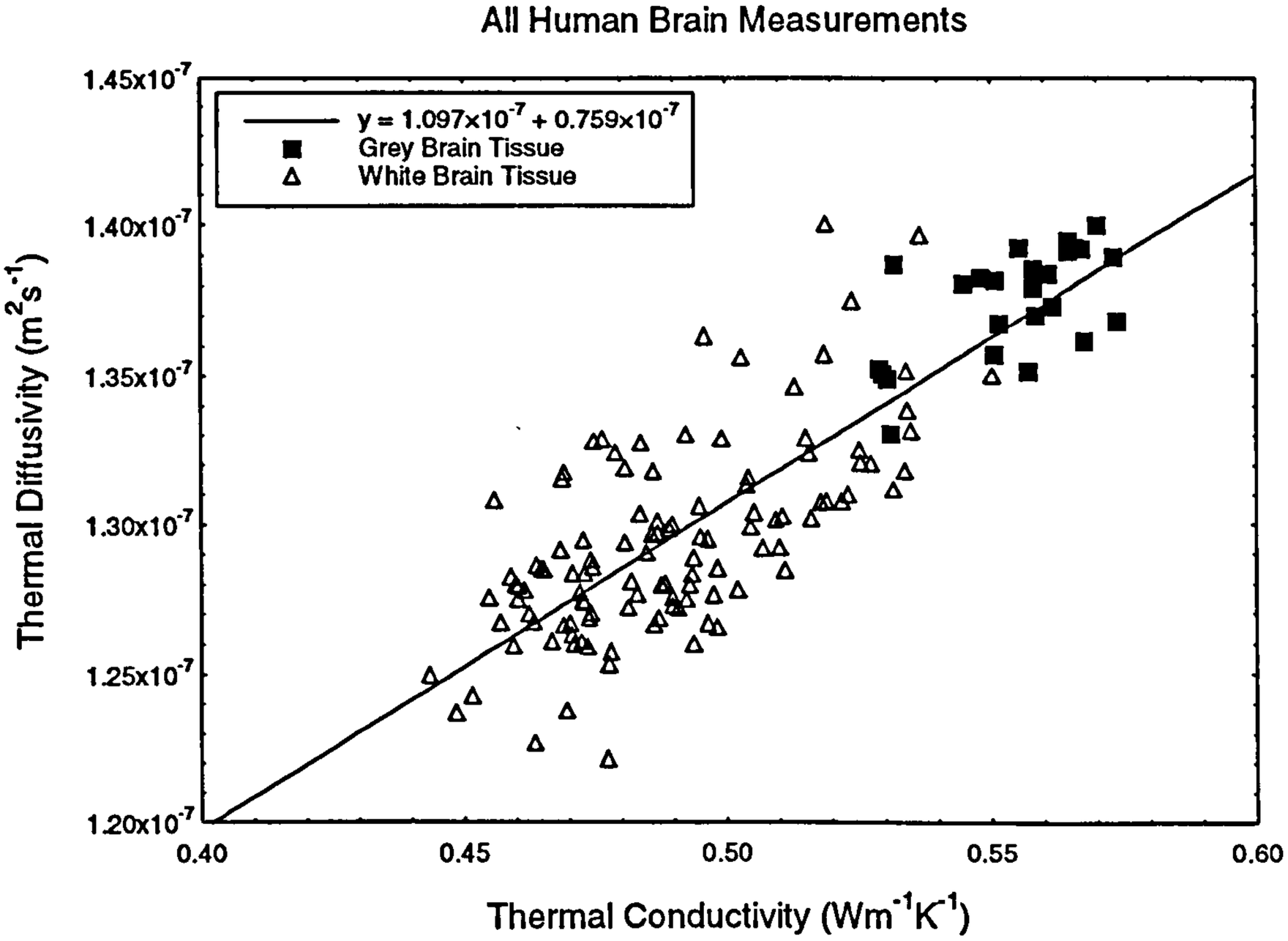

Figure 5.56 The variation of thermal conductivity with thermal diffusivity for all measurements on human brain.

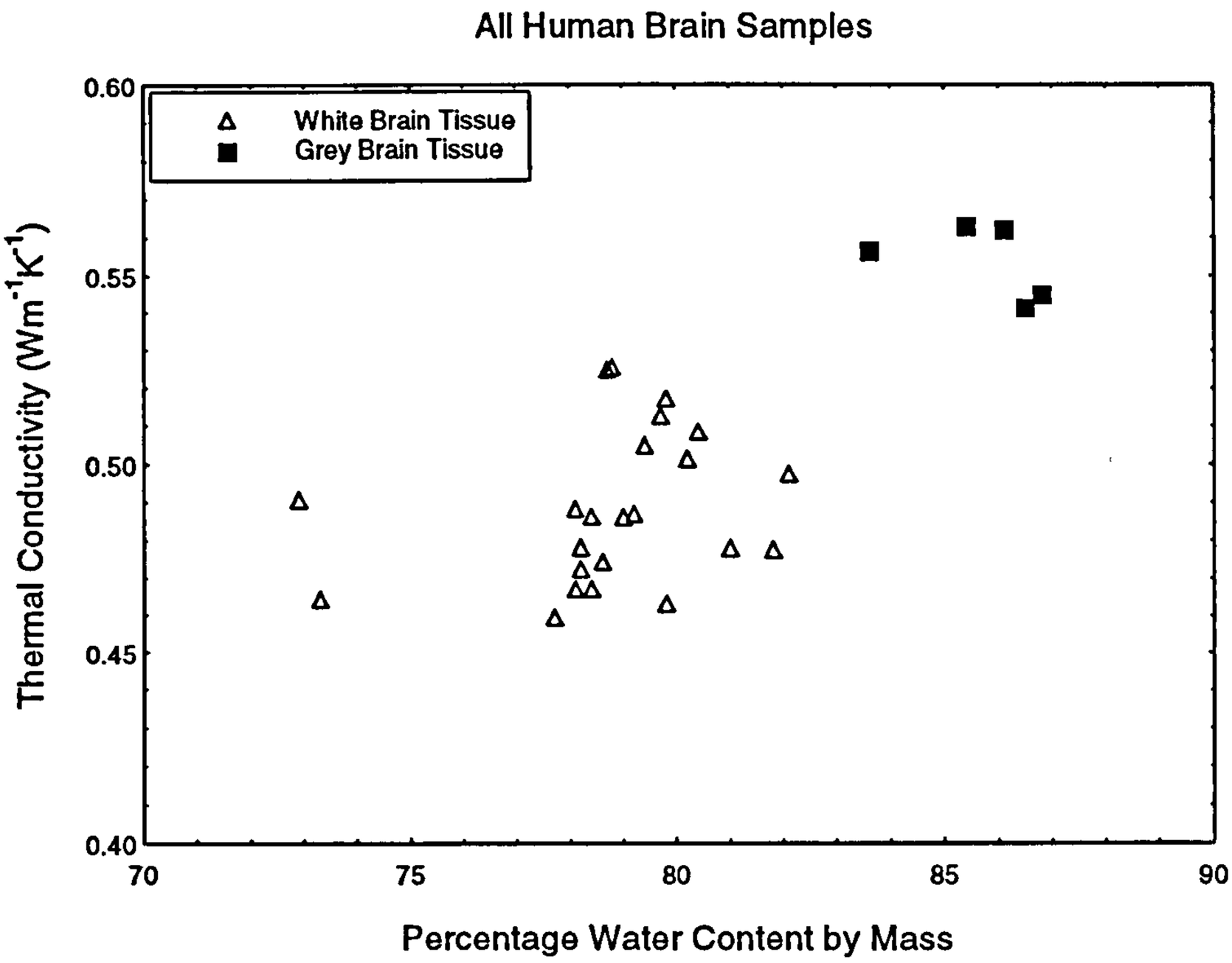

Figure 5.57 Thermal conductivity compared to sample water content for human brain.

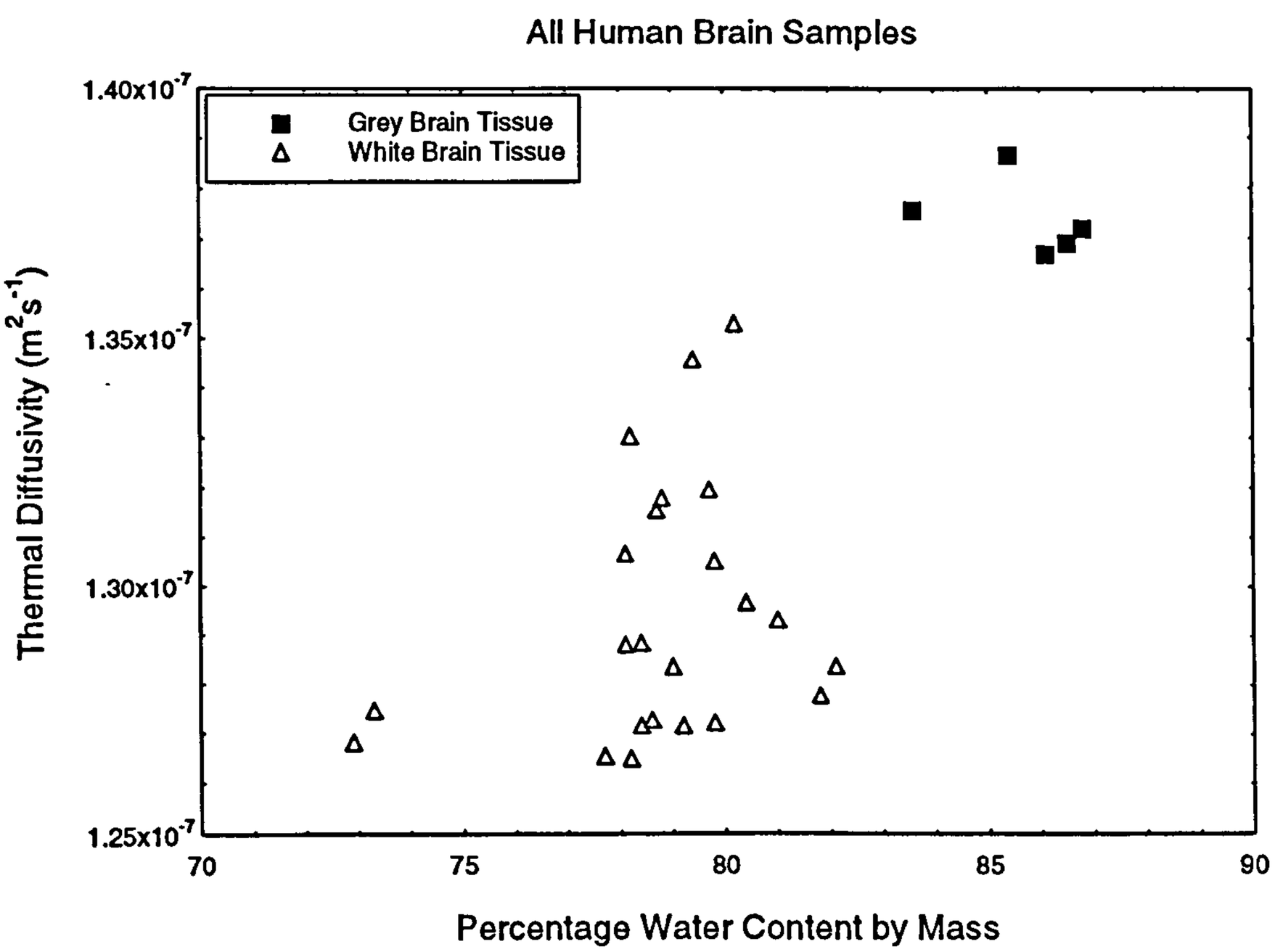

Figure 5.58 Thermal diffusivity compared to sample water content for human brain.

5.16 Human Pancreas Tissue.

The pancreas is a fish shaped gland running behind the stomach. It is about 33 cm long and weighs approximately 88 grams, and it is part of the digestive system. A total of 75 measurements were made on 15 samples from one specimen of human pancreas.
The distributions of measurements of the thermal conductivity and thermal diffusivity of pancreas tissue are shown in figures 5.59 and 5.60, while the distribution of sample water content is shown in figure 5.61.
The minimum, maximum, and mean values of the thermal conductivity, thermal diffusivity and water content of pancreas tissue are as follows

Water Content (%)	Minimum	50.4	Maximum	73.6	Mean	66.7
Thermal Conductivity ($Wm^{-1}K^{-1}$)	Minimum	0.325	Maximum	0.523	Mean	0.452
Thermal Diffusivity ($\times 10^{-7}\ m^2s^{-1}$)	Minimum	1.033	Maximum	1.353	Mean	1.261

There is a large variation in the values of all the measured quantities. This is due to the fact that the pancreas was covered in a layer of fat. There was, however, no clear boundary between the pancreas and the fat with some of the fat having entered the pancreas tissue. This meant that virtually all the samples examined had a small amount of fat in them, if only on the surface of the sample. Hence the average water content of pancreas tissue is much lower than the excepted water content of 75% (Biology Data Book, 1972).
As can be seen in figure 5.59, one sample has a water content significantly lower than the other measured water contents. The measurements of the thermal conductivity and thermal diffusivity made on this sample were lower than any other measurements made on pancreas samples. This sample clearly had a significant amount of fat present in it.
When the distribution of the thermal conductivity is examined, we see that there are several small peaks at lower conductivities, with the main peak located in the upper range of measured values. A similar pattern is seen in the thermal diffusivity. The lower peaks correspond to measurements which were made in measurement volumes which contain fat. The highest peak corresponds to measurements which were made on purer pancreas tissue. Thus it can be seen that the true thermal conductivity of pancreas is

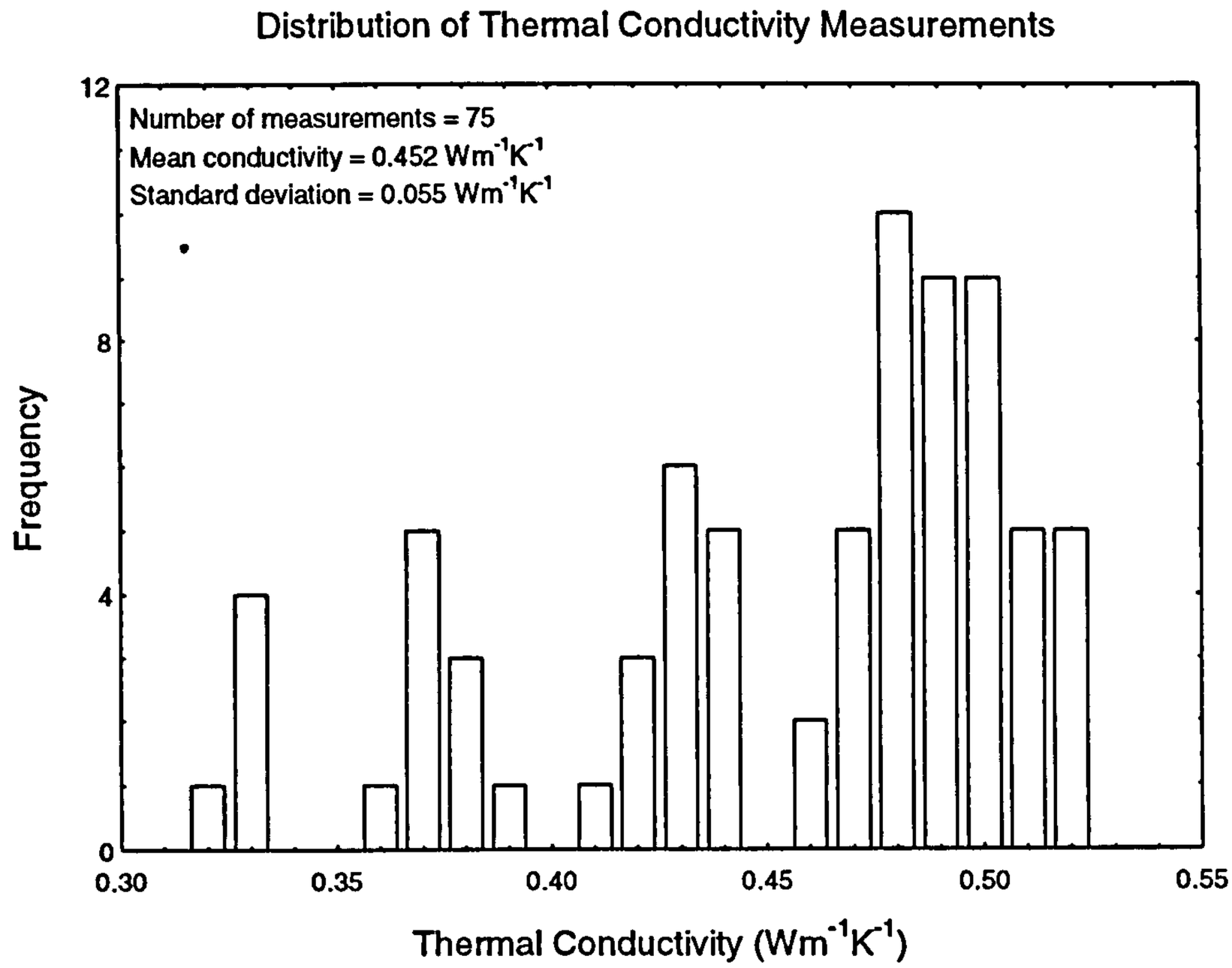

Figure 5.59 Distribution of thermal conductivity measurements on human pancreas.

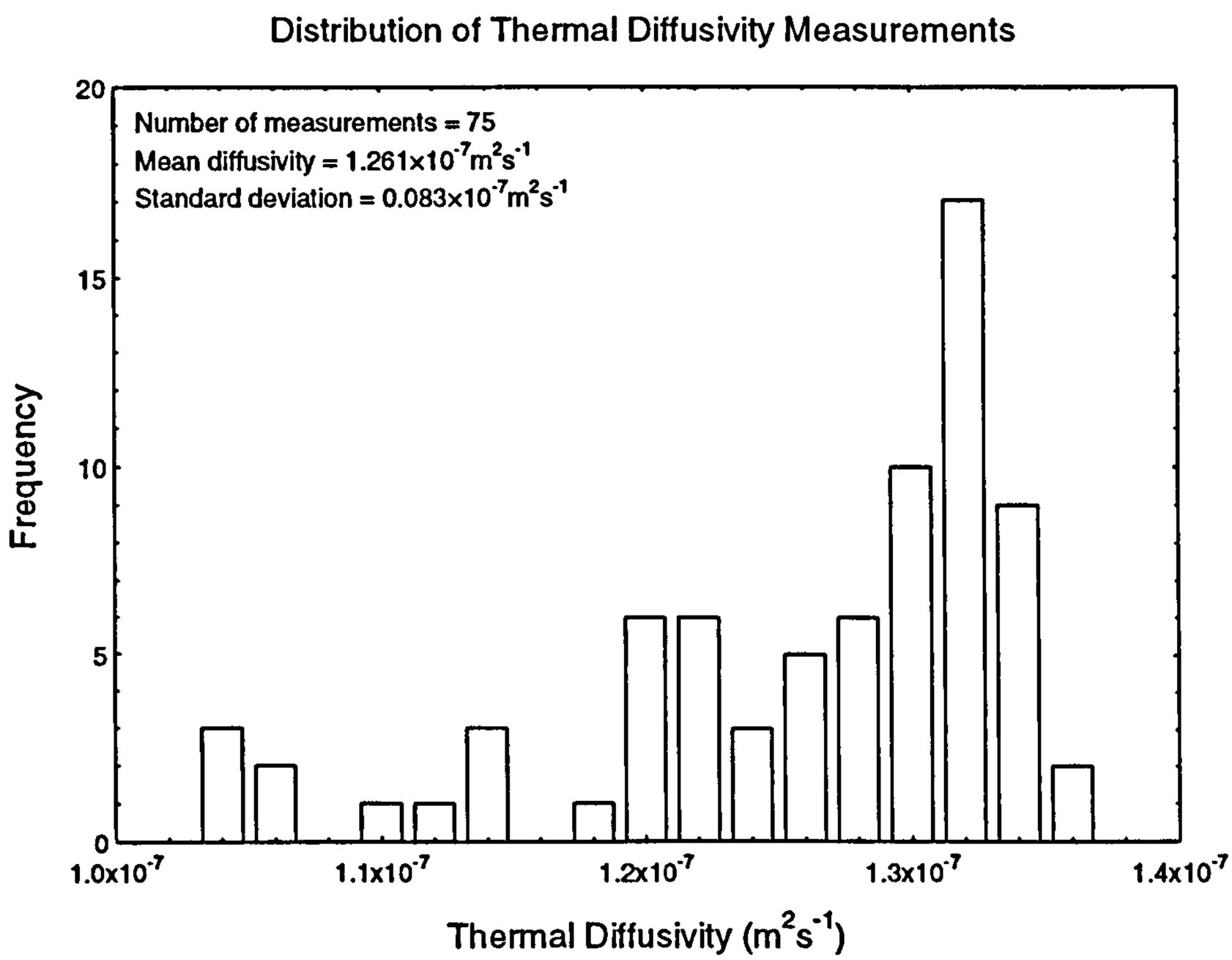

Figure 5.60 Distribution of thermal diffusivity measurements on human pancreas.

higher than mean value. This would give a thermal conductivity of about 0.49 $Wm^{-1}K^{-1}$ and a thermal diffusivity of approximately 1.32×10^{-7} m^2s^{-1} for pancreas tissue.

Few other authors have reported the thermal conductivity of pancreas tissue. Bowman (1981) also found that there was a large variation in the thermal conductivity of human pancreas tissue, finding a range of 0.294-0.588 $Wm^{-1}K^{-1}$. Valvano et al (1985) gave the thermal conductivity of porcine pancreas at 25°C as 0.475 $Wm^{-1}K^{-1}$, and that of human pancreas as 0.508 $Wm^{-1}K^{-1}$.

The variation of the thermal diffusivity with the thermal conductivity is shown in figure 5.62. The least squares linear fit of thermal diffusivity against the thermal conductivity data is

$$\alpha = (1.419k + 0.619)\times10^{-7}\ m^2s^{-1}: r = 0.943$$

The relationship between the thermal diffusivity and thermal conductivity of human pancreas tissue is extremely well defined. It is interesting to note that in tissues with large amounts of fat, such as the brain, the pancreas, and fat tissue itself, there is a good correlation between the thermal conductivity and the thermal diffusivity. This is not so true of the materials with small amounts of fat.

5.17 Other Tissues.

This section considers, in less detail than for the tissues examined in previous sections, the results of measurements on the remaining tissues examined in this study. This is either because there was not enough measurements made on the tissue type to allow more conclusions to be drawn, or that it was felt that the tissue being examined was, for some reason, not a true reflection of the tissues natural properties.

5.17.1 Human Heart Muscle.

The heart is a muscular pump composed mainly of cardiac muscle tissue. Cardiac muscle is broadly similar to skeletal muscle, but has a different cellular construction. One hundred measurements were made on 20 samples from one specimen of human heart tissue. However, there were problems with the heart muscle specimen. The specimen was stored in water for over three days before probing. By this time there was an

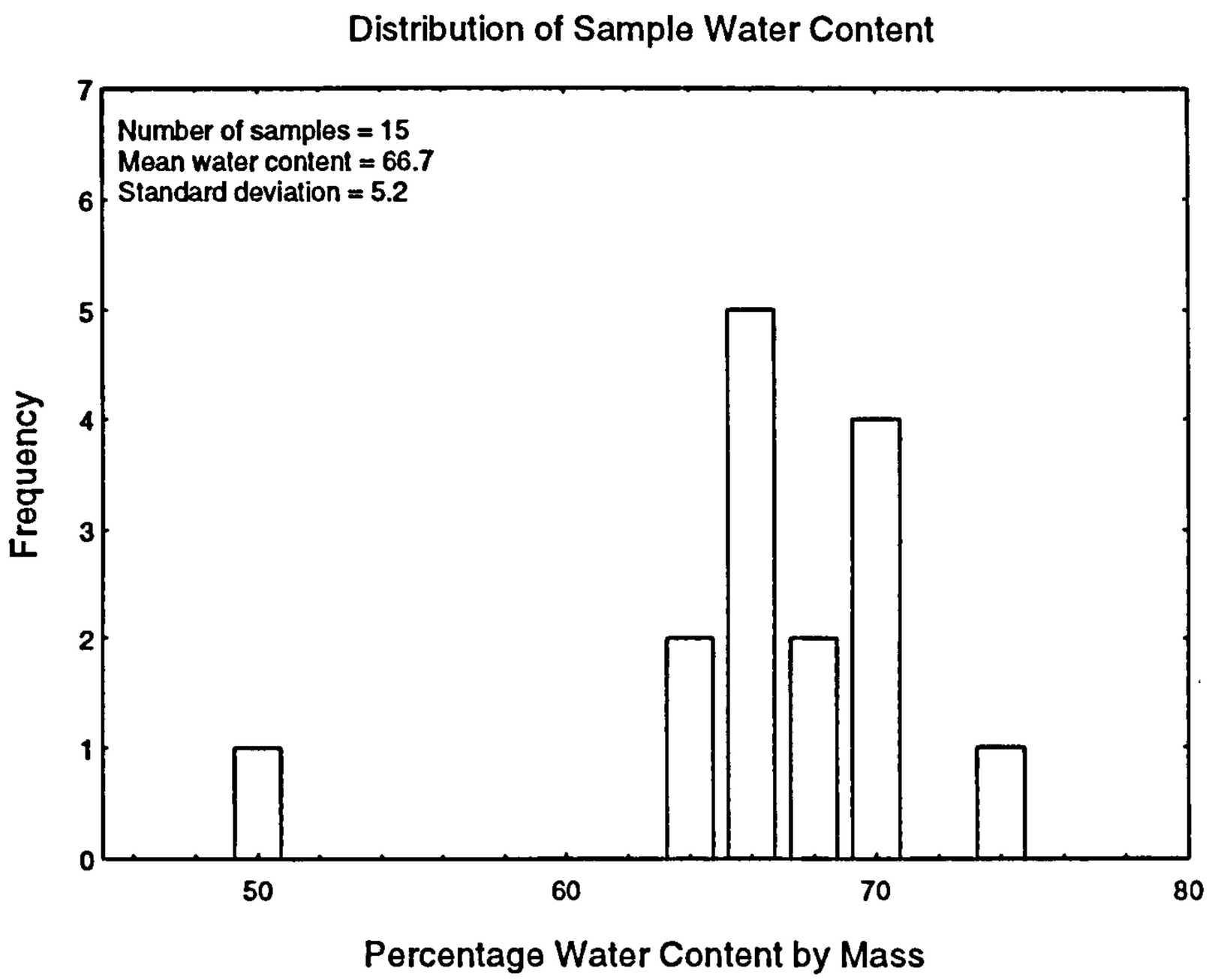

Figure 5.61 The distribution of sample water content for human pancreas tissue.

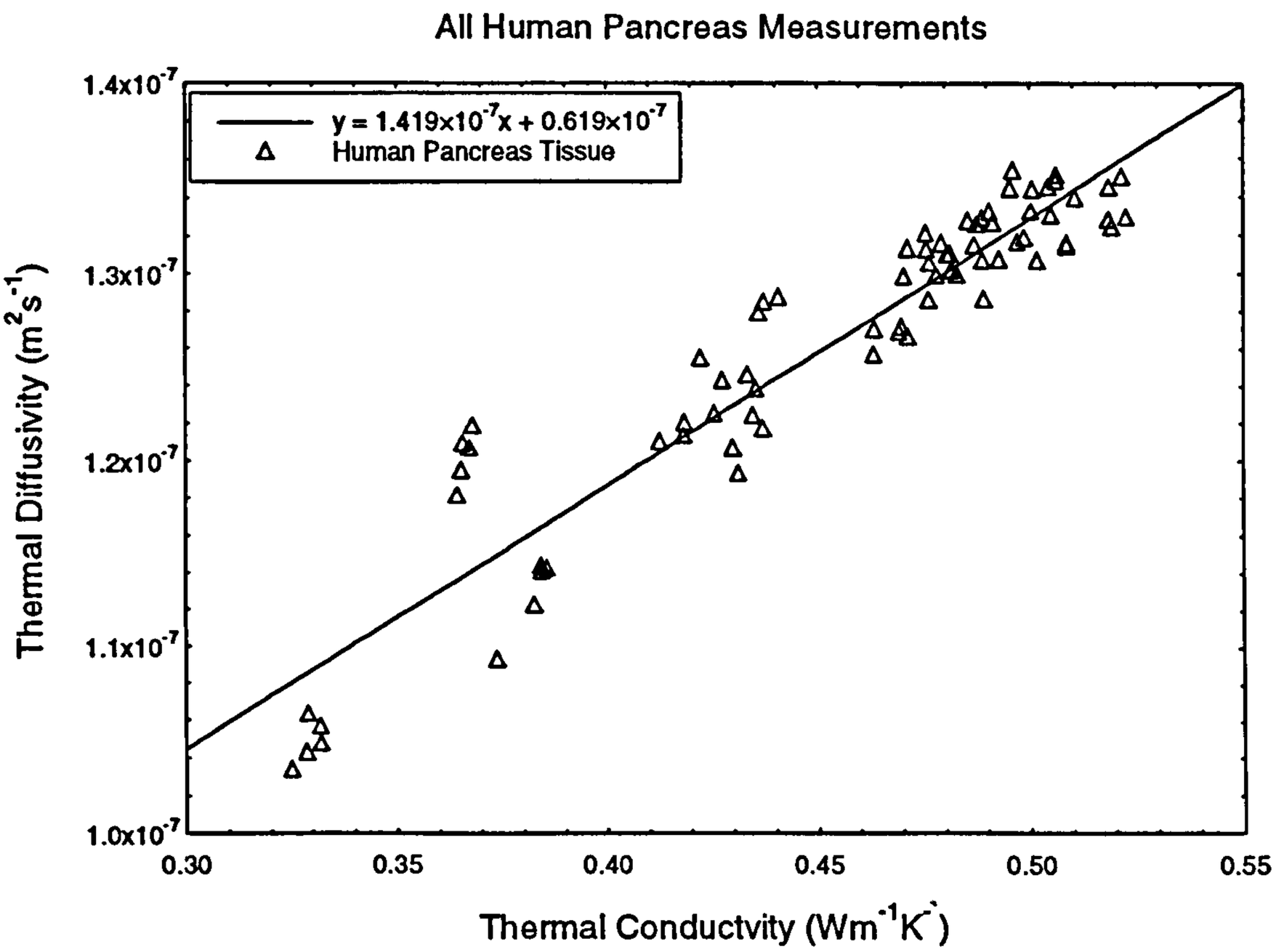

Figure 5.62 The variation of α with k for all measurements on human pancreas.

indication that the heart muscle tissue had began to degrade. The length of storage in water and the period of time before the heart muscle was probed means that it is unlikely that the human heart data accurately reflects the thermal properties of human heart.

The minimum, maximum and mean values measured of the thermal conductivity, thermal diffusivity and water content of human heart are as follows

Water Content (%)	Minimum	80.5	Maximum	83.7	Mean	82.5
Thermal Conductivity ($Wm^{-1}K^{-1}$)	Minimum	0.431	Maximum	0.574	Mean	0.497
Thermal Diffusivity ($\times 10^{-7}\ m^2s^{-1}$)	Minimum	1.265	Maximum	1.403	Mean	1.333

The properties of heart tissue should be similar to that of skeletal muscle tissue (Duck, 1990). However, the extended storage in water had caused the water content of the heart muscle tissue to be far higher than that seen in human or animal skeletal muscle tissue. Given that the tissue has a higher water content, it would be expected that the thermal conductivity and the thermal diffusivity would be higher than the values seen in skeletal muscle. This is true for the thermal diffusivity, but not for the thermal conductivity. The thermal conductivity is identical to that seen in animal skeletal muscle. It is unclear why this should be so, but it is probable that this was due to the degradation of the heart tissue.

5.17.2 Bovine Digestive Track Tissue.

Tissue of the digestive track was originally studied because it was found to have one of the highest water contents of biological tissue. The commercially available tissue from digestive tracts is a bovine tissue, commonly known as *tripe*. However, in order for the tripe to be fit for human consumption, it is boiled prior to sale. Hence the values found for tripe cannot be considered as indicative of the water content, or the thermal properties of digestive track tissue.

One hundred and ten measurements were made on 23 samples of tripe tissue. The minimum, maximum, and mean values measured of the thermal conductivity, thermal diffusivity, and water content of tripe are as follows

Water Content (%)	Minimum	86.9	Maximum	93.0	Mean	90.8
Thermal Conductivity ($Wm^{-1}K^{-1}$)	Minimum	0.493	Maximum	0.596	Mean	0.556
Thermal Diffusivity ($\times 10^{-7}\ m^2s^{-1}$)	Minimum	1.300	Maximum	1.487	Mean	1.395

The water content of the tripe is significantly higher than the accepted range of water contents for digestive track tissue. The Biology Data Book (1972) gives the range of water content as 77% - 83%. This difference in water content is almost certainly caused by the boiling of the tripe.

5.17.3 Human Spleen Tissue.

The spleen is an ovoid shaped organ located on the left hand side of the body, below the diaphragm. It serves as a reservoir for blood and produces many chemicals required by the body. Twenty measurements were made on 4 samples which came from one specimen of human spleen.

The minimum, maximum, and mean values measured of the thermal conductivity, thermal diffusivity, and water content of human spleen are as follows

Water Content (%)	Minimum	82.7	Maximum	83.9	Mean	83.4
Thermal Conductivity ($Wm^{-1}K^{-1}$)	Minimum	0.493	Maximum	0.559	Mean	0.522
Thermal Diffusivity ($\times 10^{-7}\ m^2s^{-1}$)	Minimum	1.297	Maximum	1.386	Mean	1.355

The Biology Data Book (1972) gives the water content of spleen as 78.7%. The spleen specimen contained large amounts of blood, as would be expected given that one of the organs functions is to store blood, and it is possible that this raised the water content to the values seem in this study.

5.17.4 Human Uterus Tissue.

The uterus is part of the female reproductive system and it is composed of smooth muscle tissue. Three specimens of uterine tissue were obtained, all from surgery rather than postmortem sources. A total of fifteen measurements were made on the three specimens of uterus tissue.

The minimum, maximum, and mean values measured of the thermal conductivity and thermal diffusivity of human spleen are as follows

Thermal Conductivity ($Wm^{-1}K^{-1}$)	Minimum	0.541	Maximum	0.587	Mean	0.558
Thermal Diffusivity ($\times 10^{-7}\ m^2s^{-1}$)	Minimum	1.319	Maximum	1.407	Mean	1.363

Given that the mean water content of the three samples of uterus tissue was 78.4, the mean thermal conductivity and thermal diffusivity are far higher than expected. However far more measurements would need to be made on more samples of uterus before more conclusions could be drawn.

5.18 Summary of the Results.

Table 5.20 displays the mean thermal conductivity, thermal diffusivity, and water content of the animal tissues examined in this study, while table 5.21 displays the mean thermal conductivity, thermal diffusivity, and water content of the human tissues examined in this study.

Animal Tissue Type	Thermal Conductivity ($Wm^{-1}K^{-1}$)		Thermal Diffusivity ($\times 10^{-7}$ m^2s^{-1})		Mean Percentage Water Content by Mass
	Mean	Std. Dev.	Mean	Std. Dev.	
Subcutnaeous Fat	0.244	0.035	0.839	0.092	14.1
Kidney Fat	0.150	0.035	0.599	0.123	9.0
Skeletal Muscle	0.497	0.029	1.306	0.036	74.2
Liver	0.485	0.022	1.281	0.033	67.3
Kidney Cortex	0.535	0.018	1.363	0.029	78.8
Kidney Medulla	0.566	0.011	1.397	0.015	82.0

Table 5.20 The mean and standard deviaition of the thermal conductivity and thermal diffusivity and the mean water content for all the animal tissues examined in this study.

Human Tissue Type	Thermal Conductivity ($Wm^{-1}K^{-1}$)		Thermal Diffusivity ($\times 10^{-7}$ m^2s^{-1})		Mean Percentage Water Content by Mass
	Mean	Std. Dev.	Mean	Std. Dev.	
Breast fat	0.209	0.022	0.727	0.066	14.8
Skeletal Muscle	0.513	0.021	1.297	0.040	77.3
Liver	0.510	0.033	1.302	0.023	74.6
Kidney Cortex	0.537	0.032	1.333	0.021	79.1
White Brain Matter	0.489	0.023	1.293	0.032	78.7
Grey Brain Matter	0.554	0.014	1.374	0.018	85.7
Pancreas	0.452	0.055	1.261	0.083	66.7
Spleen	0.522	0.017	1.355	0.023	83.4

Table 5.21 The mean and standard deviaition of the thermal conductivity and thermal diffusivity and the mean water content for all the human tissues examined in this study.

Chapter 6: Analysis of Results.

6.1 Introduction.

In the previous chapter, the thermal conductivity and thermal diffusivity of biological tissues were examined individually. In this chapter the collective results of the main tissues are examined to find patterns in the thermal conductivity and thermal diffusivity data. First, the variation of the thermal diffusivity with the thermal conductivity is examined by species. Next, the variation in the thermal diffusivity and the thermal conductivity are examined with respect to water content, and the thermal properties of protein are estimated. Finally the thermal properties of tissues examined in this study are compared to microwave complex permittivity measurements made on the same tissue samples by a colleague (Gorton, 1996).

6.2 The Variation in Thermal Diffusivity with Thermal Conductivity.

In chapter 5, the relationship between the thermal diffusivity and thermal conductivity was examined for each of the individual tissue types. In this section, the variation of these quantities is examined for all the tissues examined in this study to indicate if the behaviour seen in individual tissue types is partly due to system behaviour.

Figure 6.1 shows the variation of the thermal diffusivity with the thermal conductivity for all the agnine tissue samples examined in this study, while figure 6.2 shows the variation of ρc_p with the thermal conductivity for the same samples. Figure 6.3 shows the variation of the thermal diffusivity with the thermal conductivity for all the bovine tissue samples examined in this study, while figure 6.4 shows the same for all the porcine samples.

The curve fit of the data shown in figures 6.1, 6.3 and 6.4 is of the form

$$\alpha = {k}/{(ak+b)} \tag{6.2.1}$$

This equation assumes that there is a linear relationship between ρc_p and the thermal conductivity. As can be seen in figure 6.2, this is a reasonable assumption. For the animal tissues, the relationship between ρc_p and the thermal conductivity, k, is given by

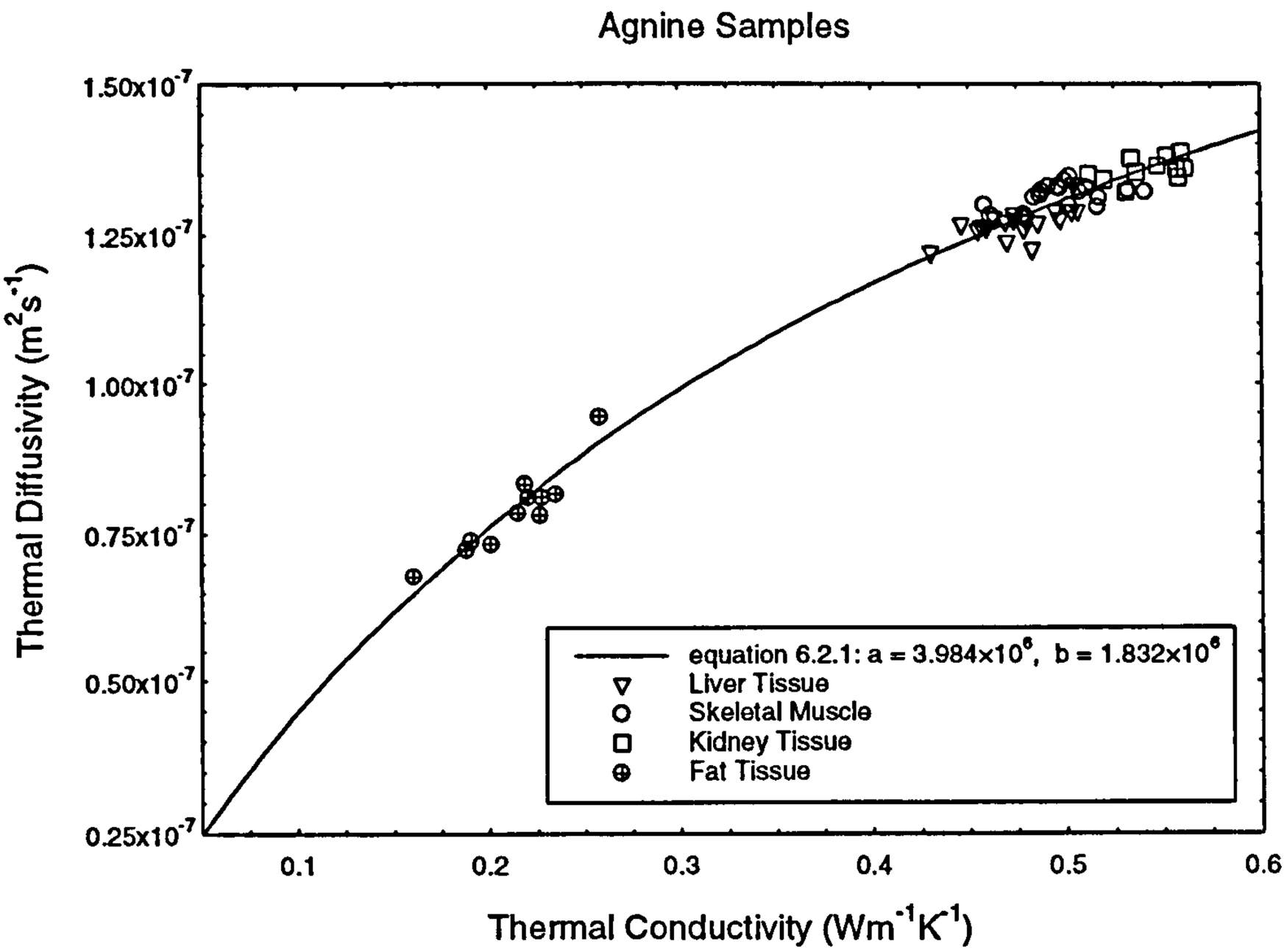

Figure 6.1 The variation of α with k for agnine tissue samples.

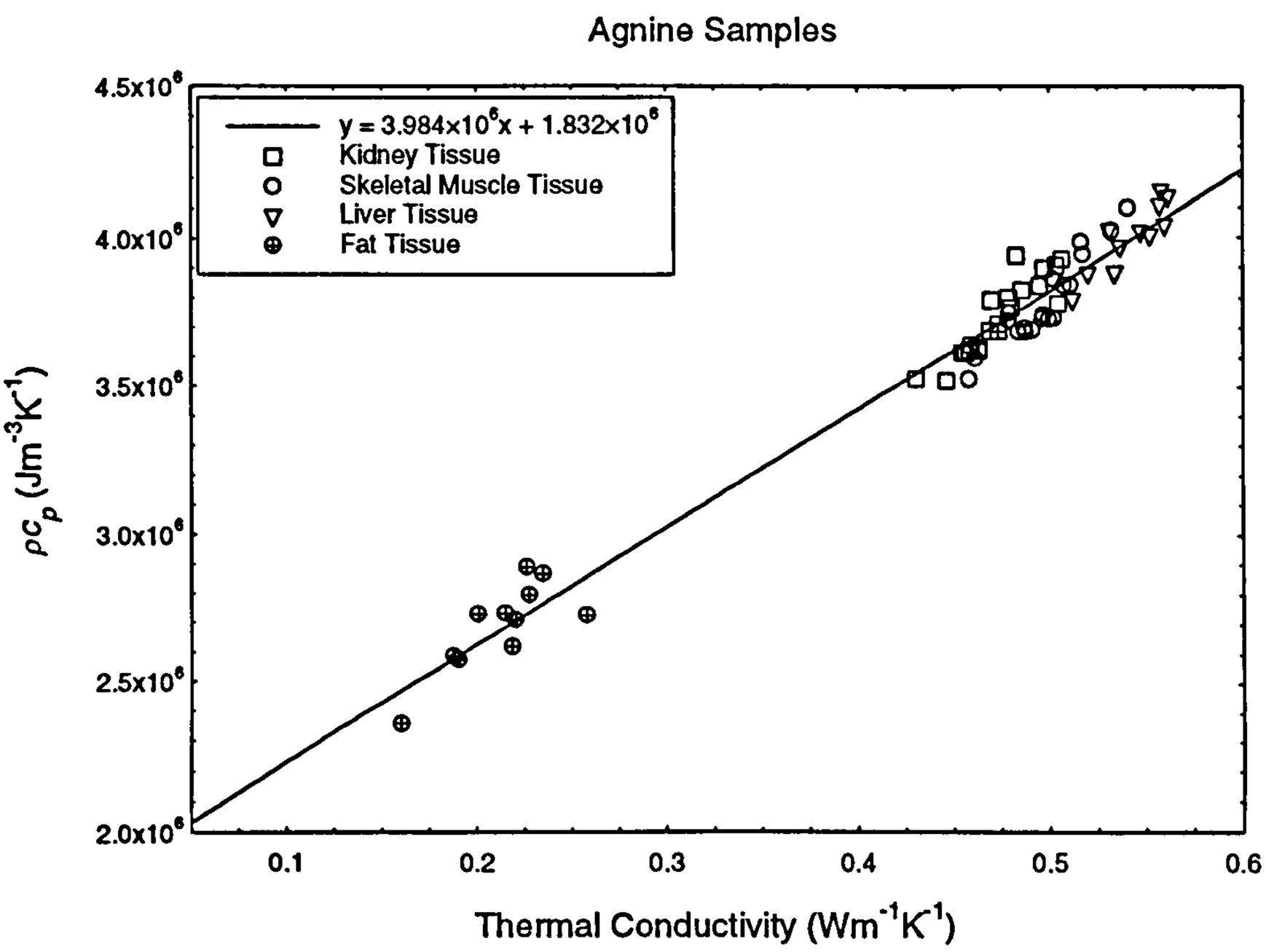

Figure 6.2 The variation of ρc_p with k for agnine tissue samples .

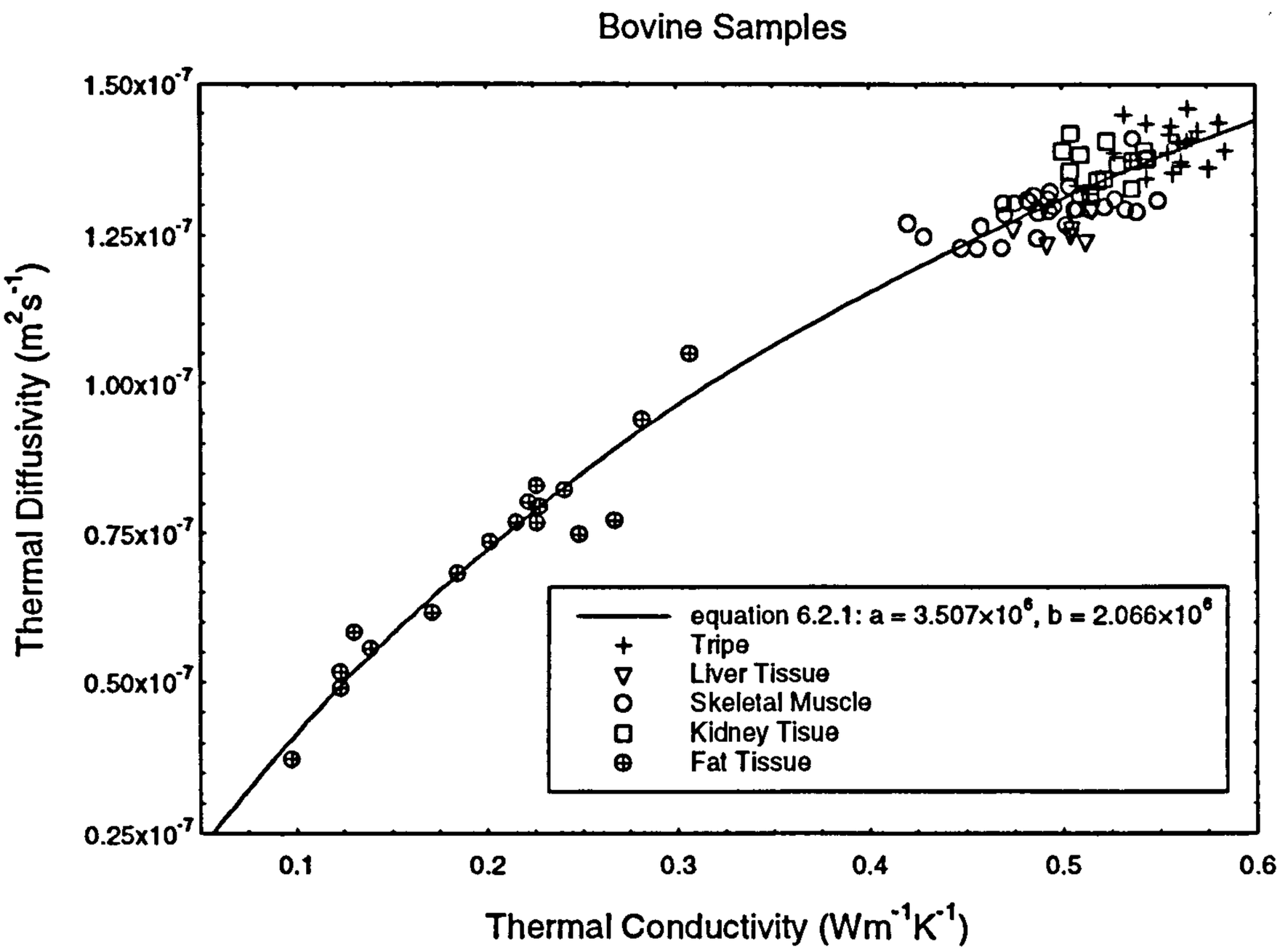

Figure 6.3 Variation of α with k for bovine tissue samples.

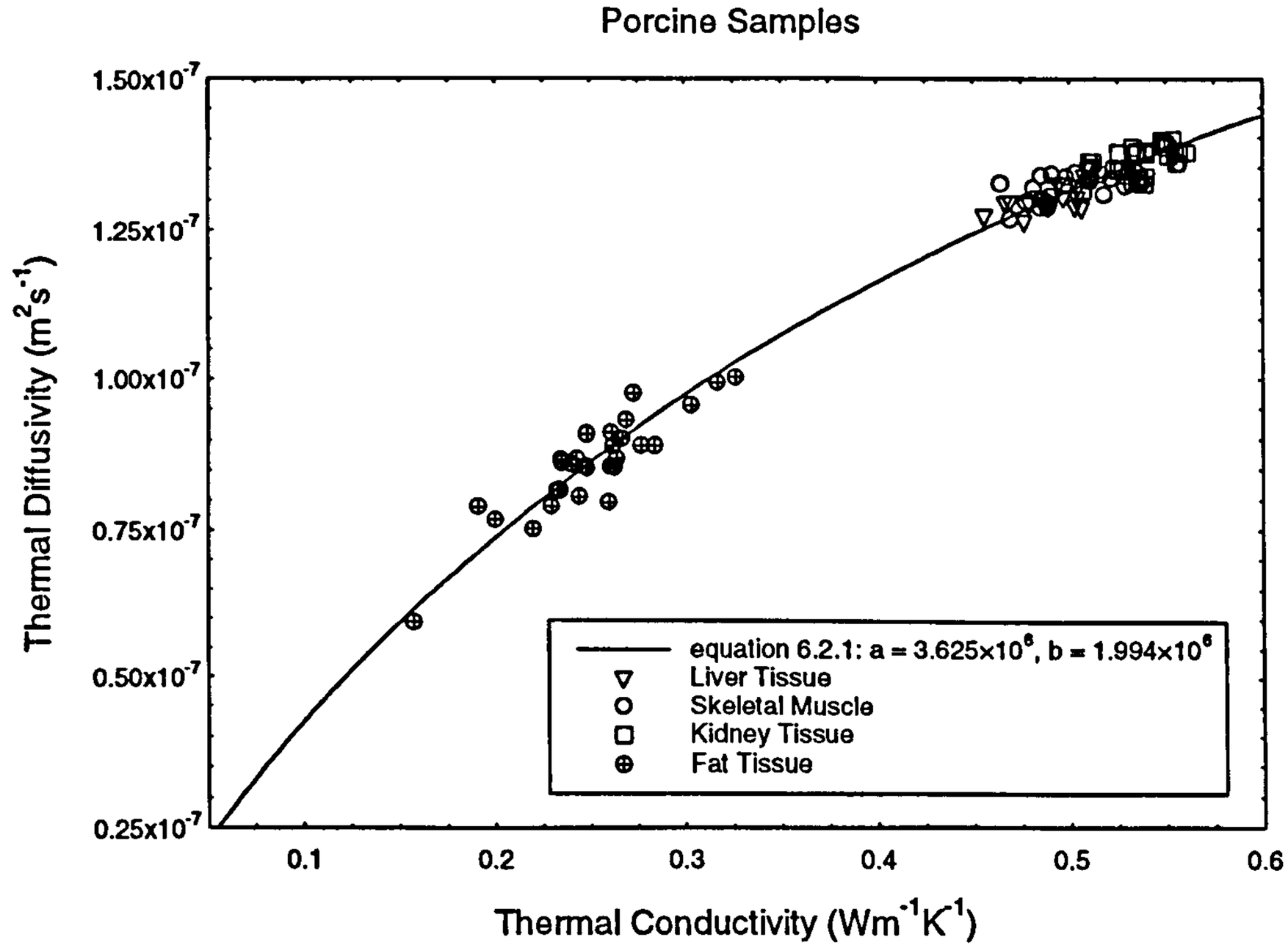

Figure 6.4 Variation of α with k for porcine tissue samples.

Agnine samples: $\rho c_p = (3.984k + 1.832) \times 10^6\ \mathrm{Jm^{-3}K^{-1}}$, $r = 0.987$

Bovine samples: $\rho c_p = (3.507k + 2.006) \times 10^6\ \mathrm{Jm^{-3}K^{-1}}$, $r = 0.962$

Porcine samples: $\rho c_p = (3.625k + 1.994) \times 10^6\ \mathrm{Jm^{-3}K^{-1}}$, $r = 0.982$

All Animal samples: $\rho c_p = (3.653k + 1.998) \times 10^6\ \mathrm{Jm^{-3}K^{-1}}$, $r = 0.975$

Figure 6.5 shows the variation between ρc_p and thermal conductivity for selected human tissues. The graph appears to show different relationships in the behaviour of high water content tissues and fat tissues. However, when the behaviour of the high water content samples is examined, it can be seen that the response is very similar to the behaviour of the measurement system in the calibration materials. As discussed in section 4.15, there is a linear short range variation of ρc_p with thermal conductivity which is generated by the measurement system. The relationship between ρc_p and k for the high water content human tissues is similar to the measurement system generated relationship for agar gelled water. Since the relationship seen in the high water content tissues for individual measurements was partly due to the behaviour of the measurement system, the mean values of the high water content human tissues samples were examined.

Figure 6.6 shows the thermal diffusivity compared to the thermal conductivity for all the human fat samples, along with mean values of the all the high water content human tissue samples. For the human tissue, the relationship between ρc_p and the thermal conductivity is given by $\rho c_p = (3.385k + 2.170) \times 10^6\ \mathrm{Jm^{-3}K^{-1}}$, $r = 0.975$

When these curve fits are compared with the behaviour seen in the individual tissues, as investigated in chapter 5, it becomes clear that in some of the tissues the relationships seen were due to the measurement system, rather than being an intrinsic property of the tissue. Most of the high water content tissues have curve fits of the thermal diffusivity versus thermal conductivity data which are dependant on the probe as well as the tissue. However the pancreas, brain tissue and human skeletal muscle tissues have behaviours which approximately match the expected behaviour of the tissue in that region. The low water content fat tissue also has behaviour which fits the pattern. The curve fits of the thermal diffusivity against thermal conductivity data has a high correlation for these tissues while the correlation for the other tissues is far lower. Thus it can be seen that a

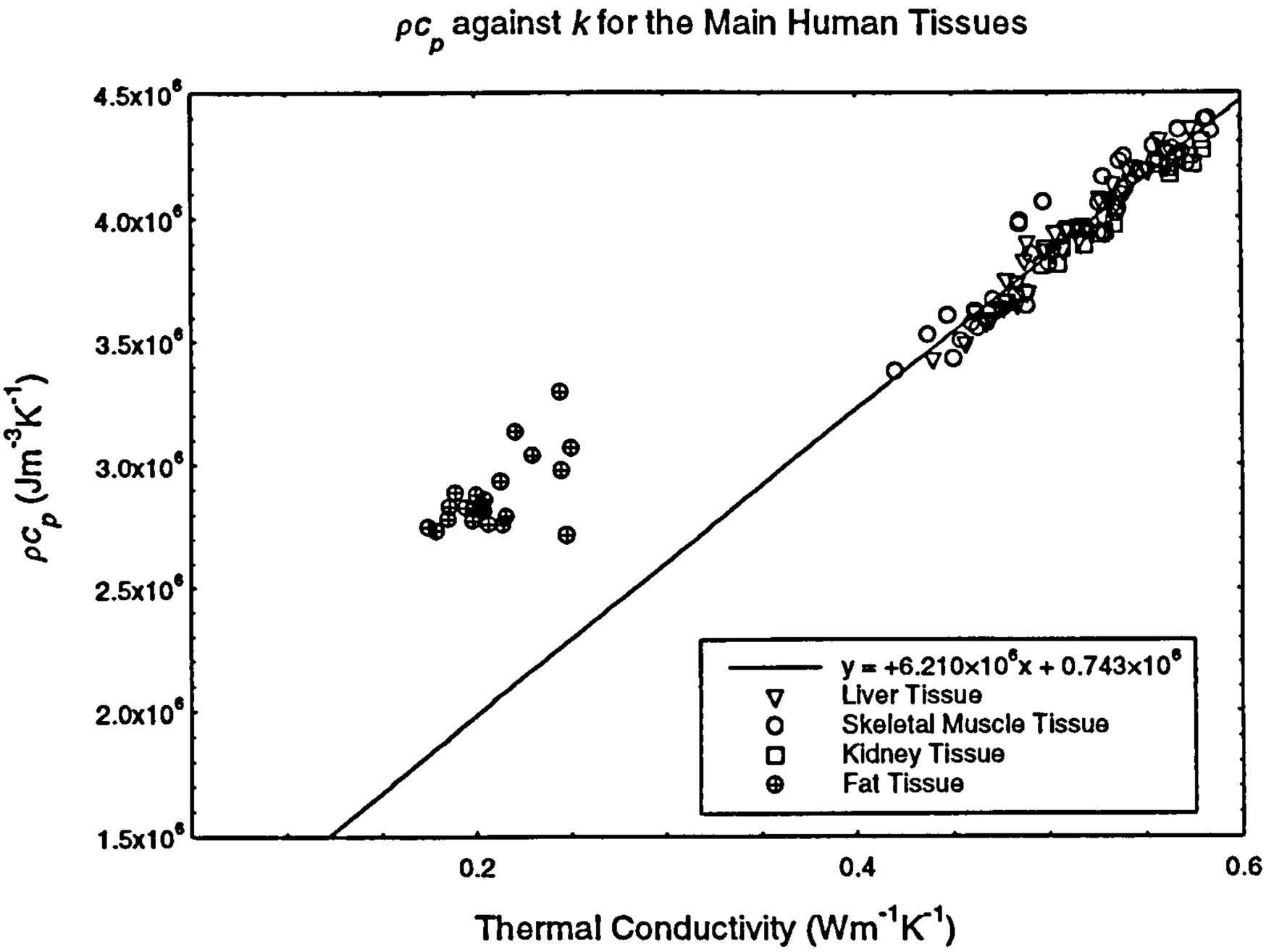

Figure 6.5 Variation of ρc_p with the thermal conductivity for human tissue samples.

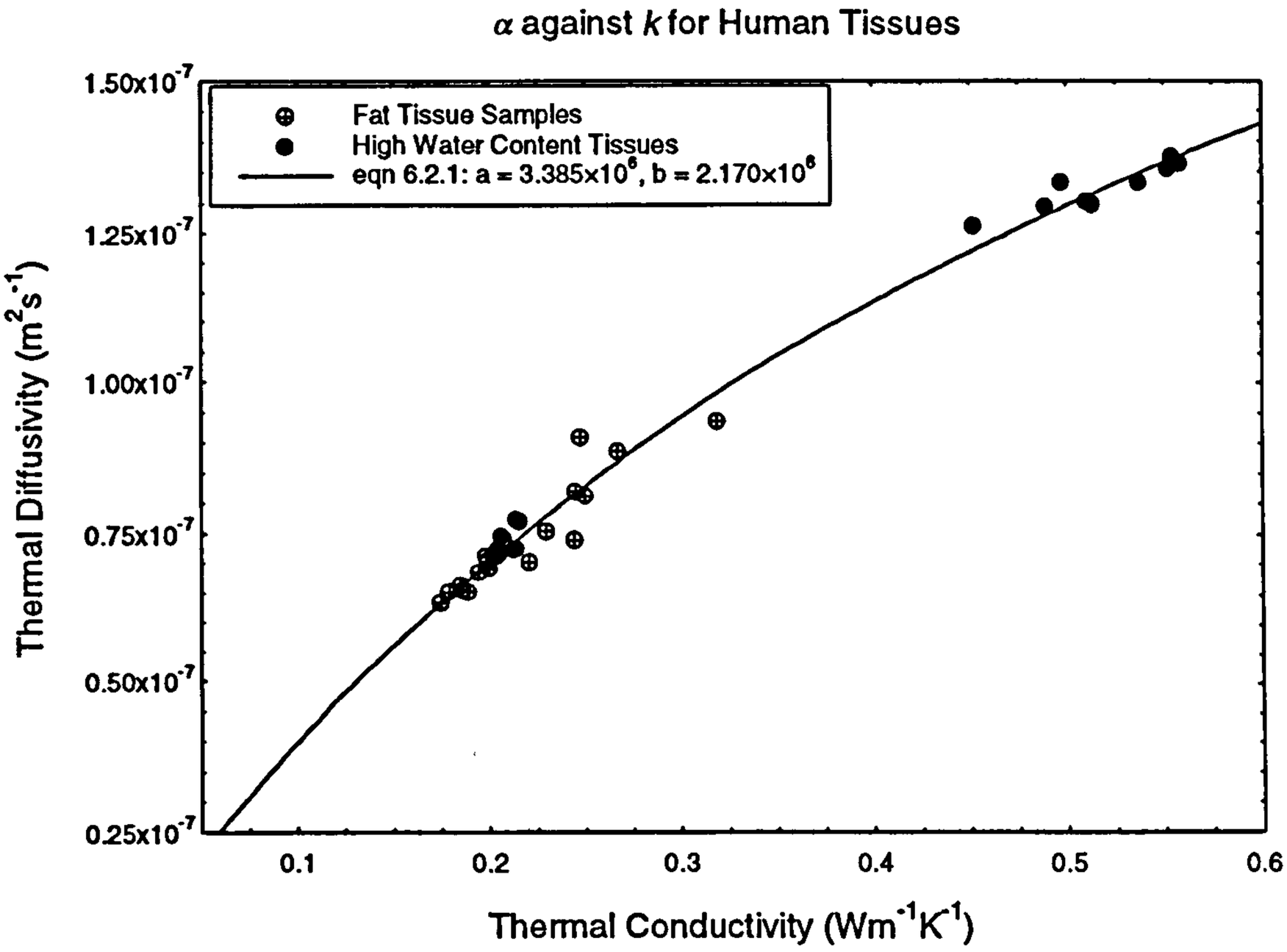

Figure 6.6 Variation of thermal diffusivity with thermal conductivity for human tissue.

high correlation is an indication that the thermal diffusivity against thermal conductivity behaviour seen in individual tissues is dependant on the tissue rather than the probe.

6.3 The Density of Biological Tissues.

For the purposes of modelling the thermal conductivity and thermal diffusivity, high water content biological material can be considered as a two phase medium. The majority phase of such tissue is water, while the minority phase is protein. Thus the thermal conductivity or thermal diffusivity of high water content samples can be modelled by the mixture equations discussed in chapter 3.

However in order to use the mixture equations, the volume fraction of each component of the mixture must be known. The oven dehydration of tissue samples only gave the mass fraction of the water component. In order to determine the volume fraction of the each of the components, the densities of the components must also be known. However no measurements were made to determine the density of the samples, and hence assumptions must be made in order to find the volume fraction.

One technique which can be used to estimate the density of biological tissues is to assume that the density of the entire non-water fraction is given by the density of protein. The density of protein is examined in chapter 3 and it can be seen that protein has a density of about 1300 kgm^{-3}. The volume fraction of water in the tissue, ϕ, is then given by

$$\phi = \frac{p_w \rho_p}{p_w \rho_p + (1 - p_w)\rho_w} \tag{6.3.1}$$

where p_w is the mass fraction of water and ρ_p and ρ_w are the densities of protein and water respectively. However, the density of the non-water fraction will not be constant; it will vary for different tissue types.

Alternatively, tables of density values for common tissues can be used. These tables are found in many of the texts on ultrasonic imaging for which tissue density is an important parameter in establishing the sonic propagation velocity. The density values for this study are taken from Rose and Goldberg (1979). Using these values the volume fraction of water is given by

$$\phi = \frac{\rho p_w}{\rho_w} \tag{6.3.2}$$

where ρ is the density of the tissue as given in tables, such as those in Rose and Goldberg. This technique allows for variations in the density non-water fraction for the different types of material. However this technique makes no allowances for the condition of the sample being examined. The density values given in Rose and Goldberg are the densities of the tissues as they would be in-vivo, as would be required when being used to establish the sonic propagation velocity. However this density will not accurately describe the density of many of the tissues examined in this study. The animal tissues have had excess blood drained which has a significant effect on the water content and hence the density.

Table 6.1 shows the variation of the values of the water content by volume using the two different methods. The density of protein is assumed to be 1300 kgm^{-3}. As can be seen there is a maximum difference of 2% between the water content estimated by setting the density of the dried protein and using the tissue density values as given by Rose and Goldberg.

Given that there is a degree of uncertainty in the density of protein, and there also degree of uncertainty about the density of high water content tissue, the value found for the percentage water content by volume must also have a degree of uncertainty associated with it. In this study, generally the first method was used to find the percentage water content by volume. The uncertainty introduced into the water content by volume by using different protein densities is discussed in detail later in the chapter.

6.4 The Variation of the Thermal Properties of Tissue with Water Content.

In this section, the variation in the thermal conductivity or thermal diffusivity with water content for the main high water content tissues is examined.

In this section the non-water fraction will generally be referred to as protein. It will normally be the case that protein will make up the majority of the non-water fraction. However it must be remembered that there will be amounts of fat, salt and other biological substances present. This section will deal first with the liver, kidney and skeletal muscle tissues. For these tissues it assumed that the majority of the non-water

Tissue Type	No. of Samples	k ($Wm^{-1}K^{-1}$)	α ($\times 10^{-7} m^2 s^{-1}$)	Percentage Water Content by Mass	ρ (kgm^{-3})	ϕ Estimated using $k_p = 1300\ kgm^{-3}$	ϕ Estimated using ρ
Muscle: All Animal Tissues	70	0.497	1.306	74.2	1080	0.789	0.803
Agnine	19	0.498	1.314	75.4		0.800	0.816
Bovine	30	0.492	1.290	73.9		0.787	0.800
Porcine	21	0.504	1.322	73.7		0.785	0.797
Human	39	0.513	1.297	77.3		0.816	0.836
Liver: All Animal Tissues	46	0.485	1.281	67.3	1060	0.728	0.715
Agnine	21	0.475	1.269	66.9		0.725	0.710
Bovine	6	0.501	1.257	67.7		0.732	0.719
Porcine	19	0.490	1.301	67.5		0.730	0.717
Human	41	0.510	1.302	74.6		0.793	0.792
Kidney: All Animal Cortex	56	0.535	1.363	78.8	1040	0.829	0.821
Agnine	11	0.543	1.357	77.4		0.817	0.807
Bovine	14	0.524	1.368	78.0		0.822	0.813
Porcine	31	0.537	1.362	79.6		0.836	0.829
Human Cortex	19	0.537	1.333	79.1		0.832	0.824
Animal Medulla	5	0.566	1.397	82.0		0.856	0.855

Table 6.1 The water content by volume of skeletal muscle, liver and kidney tissue. Tissue densities from Rose and Goldberg (1979).

fraction is protein. The thermal properties of the non-water fraction of brain tissue are then examined separately since, as discussed in chapter 5, brain tissue has a significant amount of fat present in the non-water fraction.

As seen in the previous chapter, when analysing the individual tissues, no pattern could be observed between the thermal conductivity, or thermal diffusivity, and the sample water content. For a single type of tissue there is only a limited range of water content. This limited range of water content will produce a restricted range of thermal property values compared to the total range of values seen in biological tissues. The restricted range of values allows the errors associated with the probe, and the error introduced by the water content in the measurement volume not matching the water content in the sample, to swamp any relationship between the thermal property and water content.

The errors discussed above also serve to partially mask any relationship between thermal properties and water content when examining the behaviour across a range of tissues. The errors will also mask any slight variances in the behaviour of different types compared to the other tissue types. Thus, the mean thermal conductivity, thermal diffusivity and water content of each of the different tissue types will be used.

6.4.1 Limits.

In chapter 3, the limit of the thermal conductivity or thermal diffusivity of a mixture of two phases is discussed. For a high water content sample, Wiener (1912) found the upper, k^+, and the lower, k^-, limits of the thermal conductivity, were given by the series and parallel limits. That is

$$k^+ = \phi k_w + (1-\phi)k_p \qquad \text{Series} \qquad (6.4.1)$$

and

$$\frac{1}{k^-} = \frac{\phi}{k_w} + \frac{(1-\phi)}{k_p} \qquad \text{Parallel} \qquad (6.4.2)$$

where ϕ is the *volume* fraction of water, k_w is the thermal conductivity of water, and k_p is the thermal conductivity of the non-water fraction, which is generally protein. The limits for a high water content sample as given by Hashin and Shtrikman (1961) are

$$\frac{k^+ - k_w}{k^+ + 2k_w} = \frac{k_p - k_w}{k_p + 2k_w}(1-\phi) \qquad (6.4.3)$$

a)

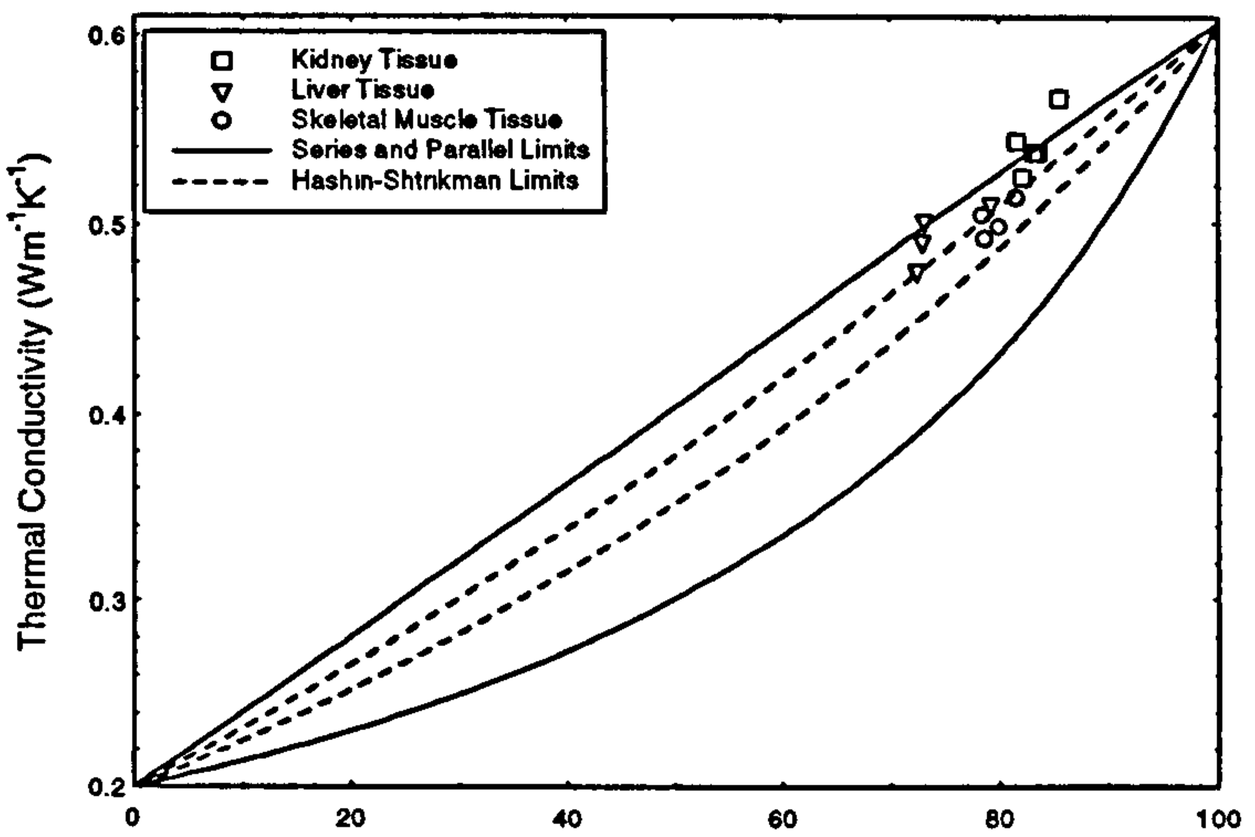

b)

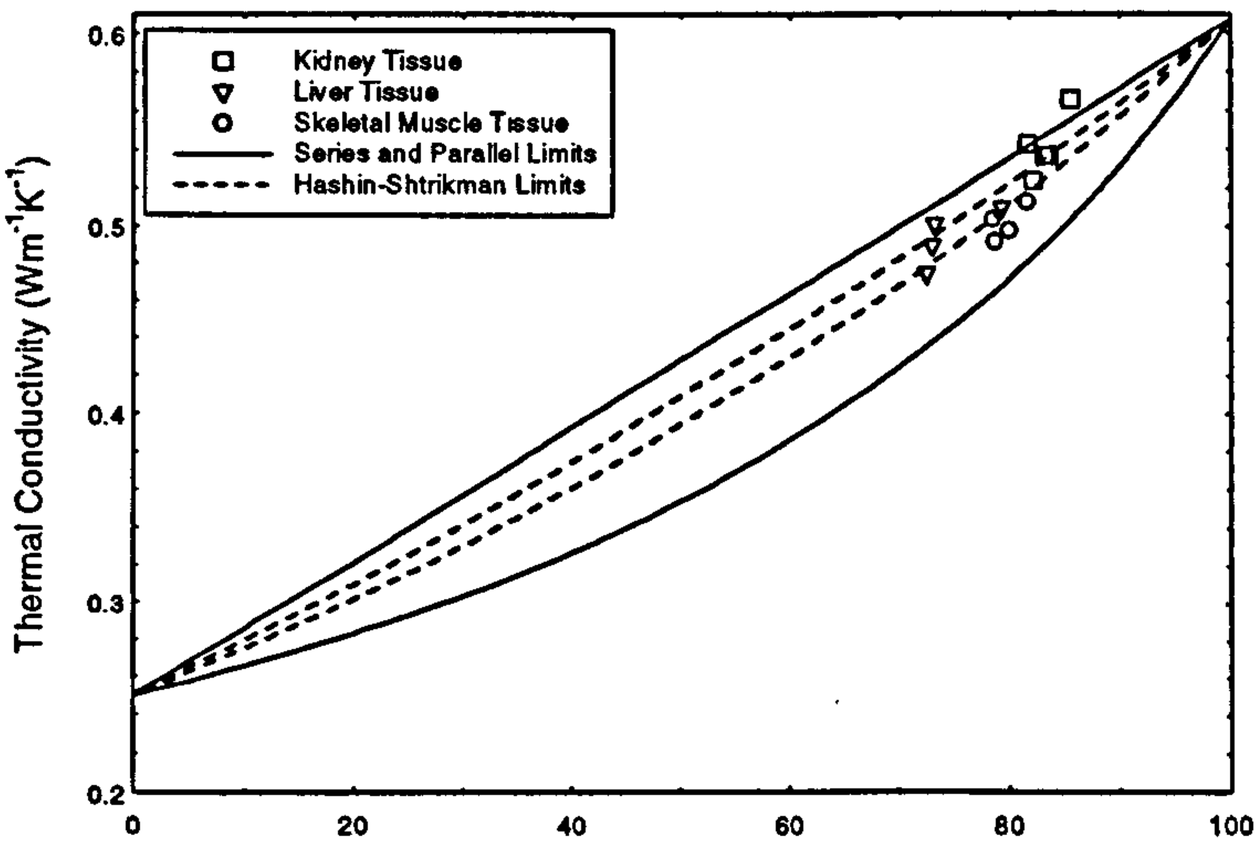

c)

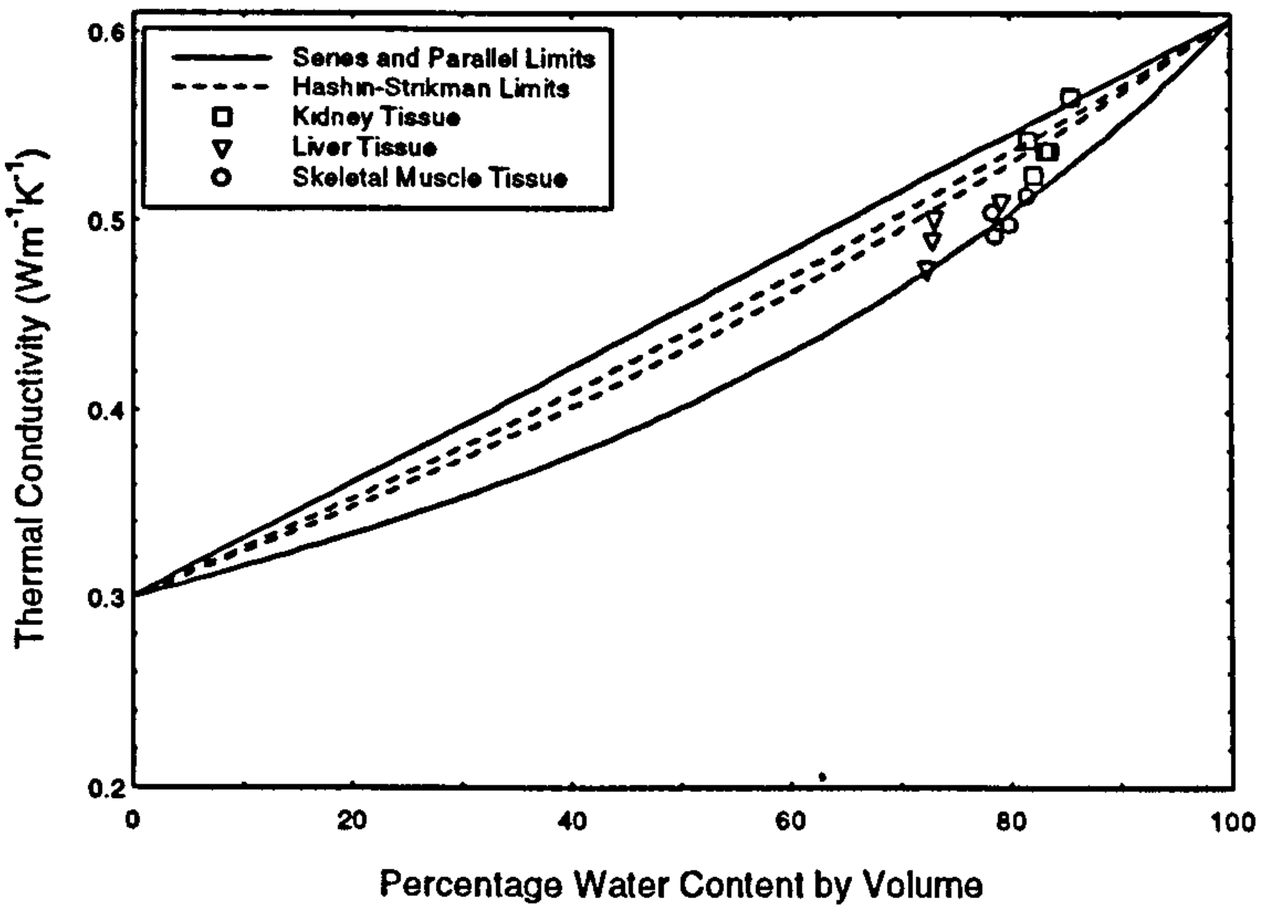

Figure 6.7 Measured thermal conductivity and limits for k_p = 0.20 $Wm^{-1}K^{-1}$ (a), 0.25 $Wm^{-1}K^{-1}$ (b) and 0.30 $Wm^{-1}K^{-1}$ (c).

and $$\frac{k^- - k_p}{k^- + 2k_p} = \frac{k_w - k_p}{k_w + 2k_p}\phi \qquad (6.4.4)$$

There are a similar set of equations for the limits of the thermal diffusivity, α^+ and α^-, of a high water content sample with k_p and k_w being replaced by α_p and α_w, which are the thermal diffusivities of protein and water respectively.

Figure 6.7 shows the variation of the mean thermal conductivity with water content for liver, kidney and skeletal muscle tissues, with the measured values being compared with the theoretical limits for $k_p = 0.20$ $Wm^{-1}K^{-1}$, $k_p = 0.25$ $Wm^{-1}K^{-1}$ and $k_p = 0.30$ $Wm^{-1}K^{-1}$. These values of the thermal conductivity of protein were chosen because they were representative of the range of values found by other authors, as discussed in section 3.11. Similarly, figure 6.8 shows the variation of the mean thermal diffusivity with water content for liver, kidney and skeletal muscle tissues, with the measured diffusivity values being compared with the theoretical limits for $\alpha_p = 0.8\times10^{-7}$ m^2s^{-1}, $\alpha_p = 0.9\times10^{-7}$ m^2s^{-1} and $\alpha_p = 1.0\times10^{-7}$ m^2s^{-1}. For both figure 6.7 and figure 6.8, the percentage water content by volume was found by setting $\rho_p = 1300$ kgm^{-3}.

Figure 6.7 shows that the thermal conductivity value that best describes the measured data out of the values examined is $k_p = 0.25$ $Wm^{-1}K^{-1}$, while figure 6.8 shows that the thermal diffusivity value which best described the data was $\alpha_p = 0.9\times10^{-7}$ m^2s^{-1}. Both figures show that the spread of data in the is rather larger than that of the Hashin and Shtrikman limits. The spread of data is better described by the parallel and series limits. However, it is noticeable that the for each of the individual tissues, the spread in the data is less than the spread in the whole. For example, in figure 6.7, when comparing the measured thermal conductivity data against the that predicted by $k_p = 0.25$ $Wm^{-1}K^{-1}$, it can be seen that while the liver tissue data is spread about the Hashin and Shtrikman limits, the skeletal muscle data is generally lower than the Hashin and Shtrikman lower limit, while the kidney data is generally nearer the Hashin and Shtrikman upper limit. This suggests that there is a difference in the thermal conductivity and the thermal diffusivity of the protein present in the different types of tissue.

a)

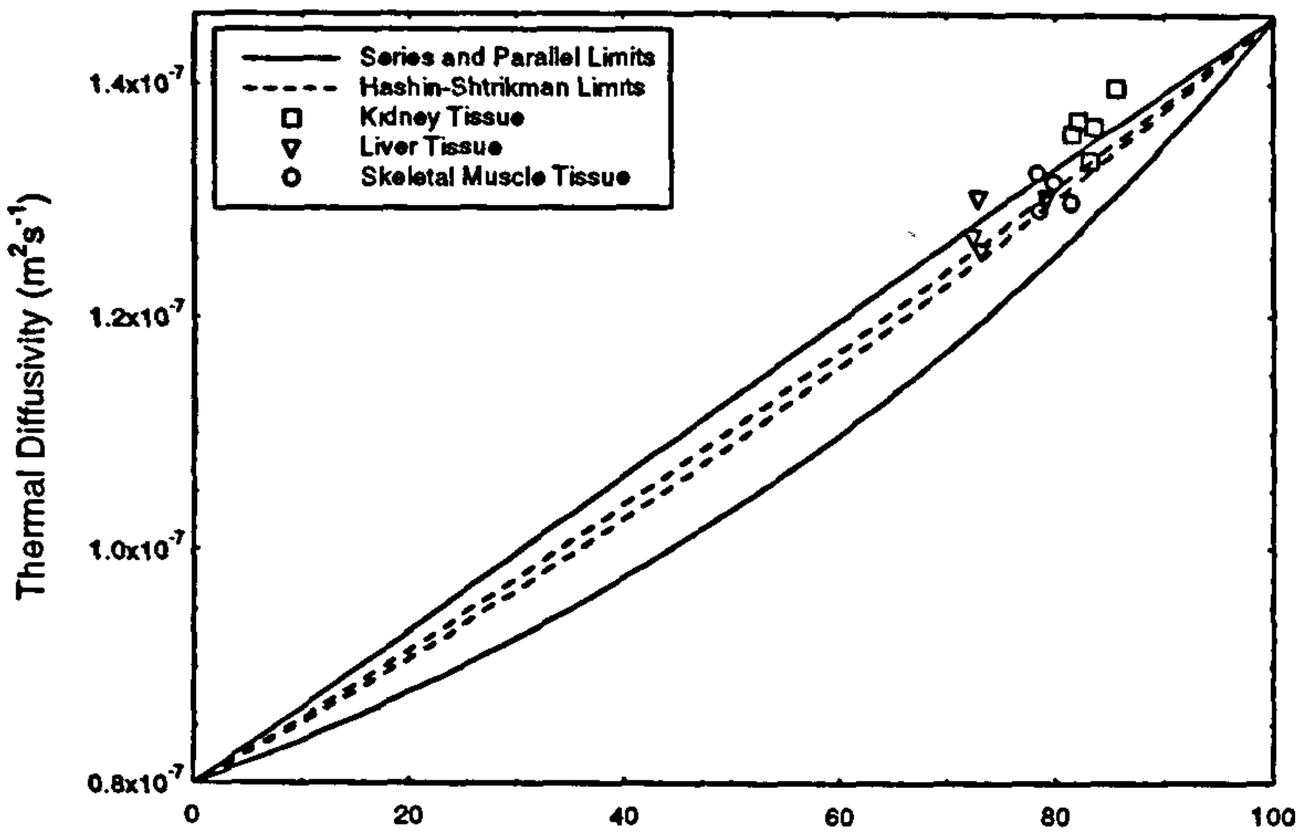

b)

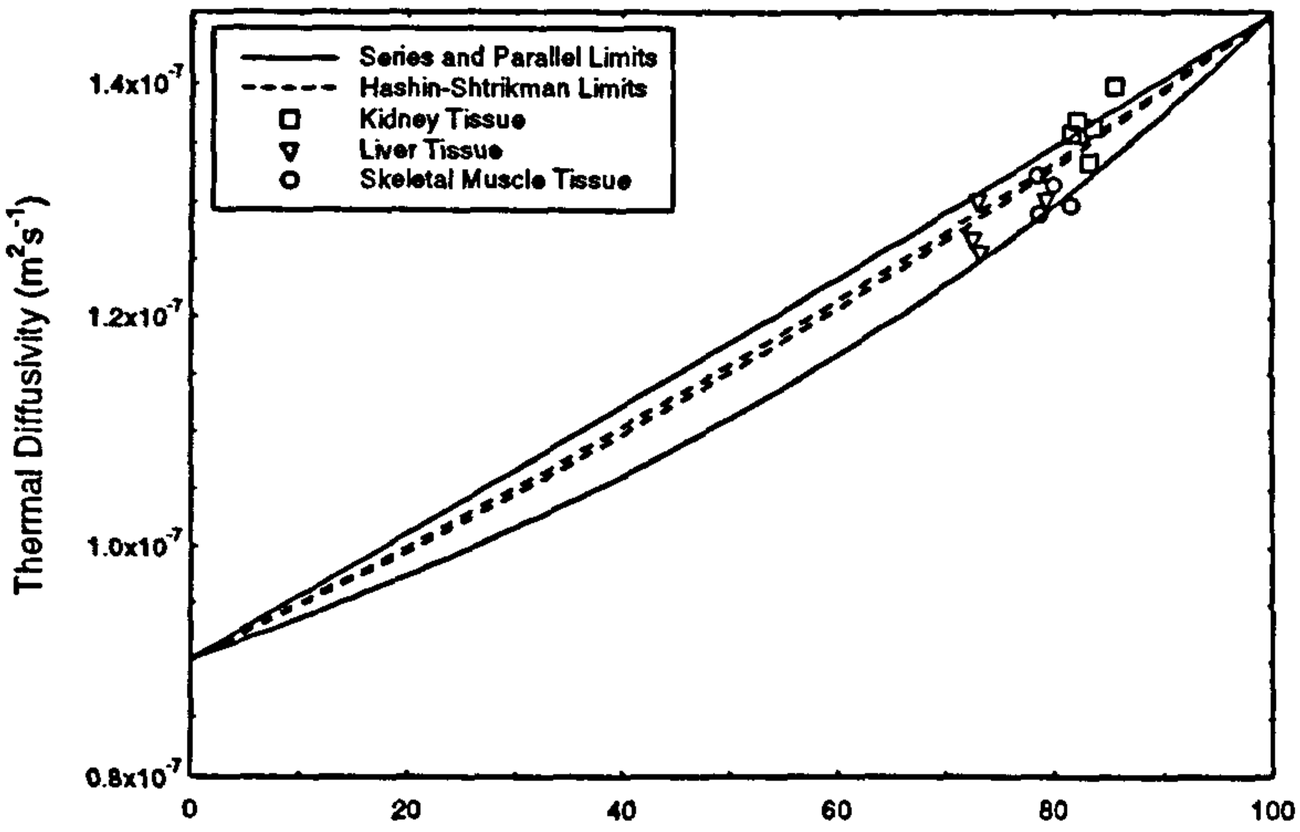

c)

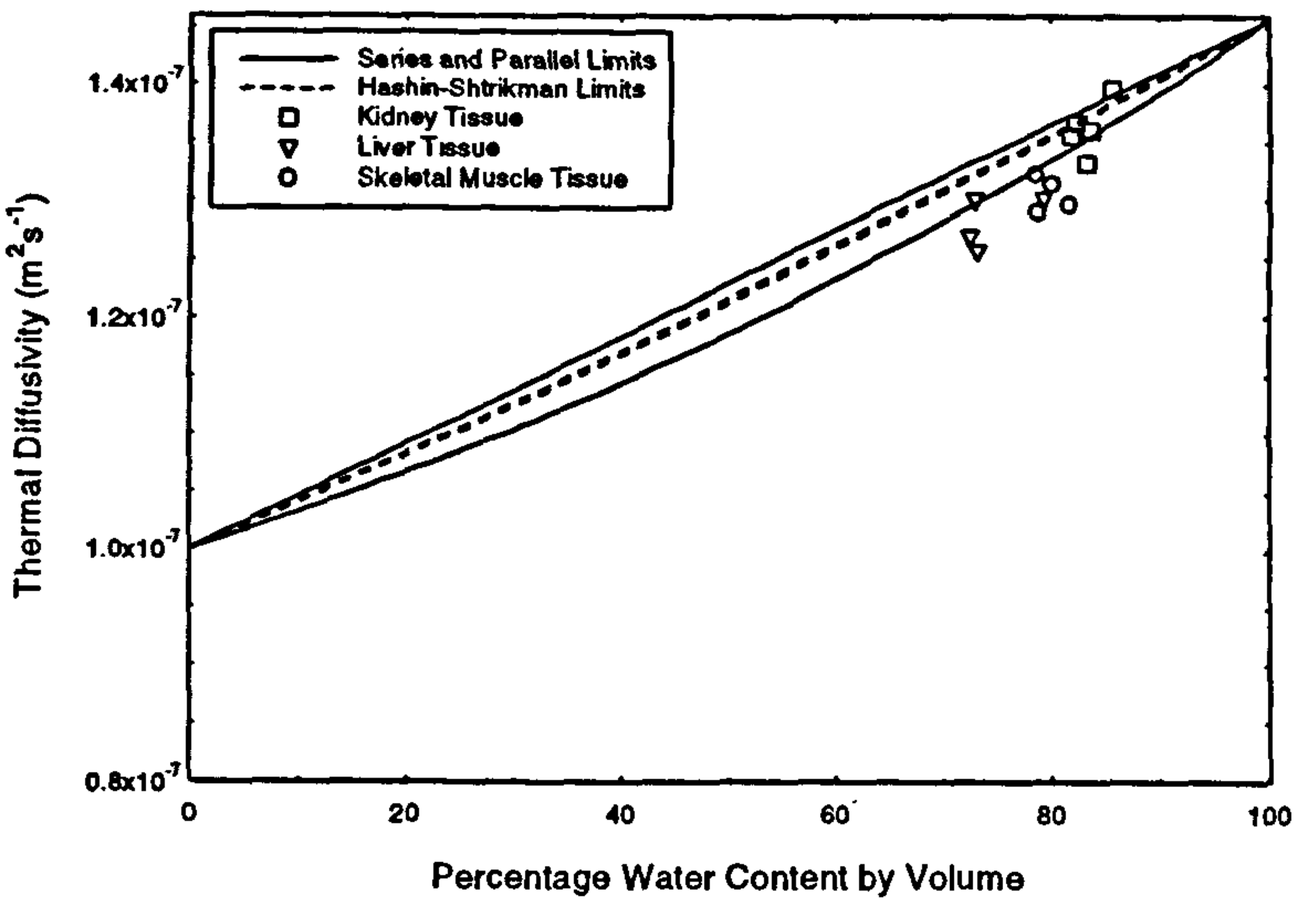

Figure 6.8 Measured thermal diffusivity and limits for $\alpha_p = 0.8\times10^{-7}$ m^2s^{-1} (a), 0.9×10^{-7} m^2s^{-1} (b) and 1.0×10^{-7} m^2s^{-1} (c).

6.4.2 Estimating the Thermal Properties of Protein.

In this section, two of the mixture equations given in chapter 3, Maxwell's mixture equation and Bruggeman's equation, are used to estimate the thermal conductivity of protein found in tissue samples.

The thermal conductivity of high water content biological tissues, as given by Maxwell's mixture equation, is

$$\frac{k-k_w}{k+2k_w}=\frac{k_p-k_w}{k_p+2k_w}(1-\phi) \tag{6.4.5}$$

while the thermal conductivity of high water content tissue, as given by Bruggeman's equation is

$$\left(\frac{k_w}{k}\right)^{\frac{1}{3}}\left(\frac{k_p-k}{k_p-k_w}\right)=\phi \tag{6.4.6}$$

As with the limiting equations, there are a similar set of equations for the thermal diffusivity of a high water content sample, with k_p and k_w being replaced by α_p and α_w.

Firstly the thermal conductivity and thermal diffusivity of protein is estimated by curve fitting the mixture equations to the mean values of the tissues shown in table 6.1. Since the thermal properties of water are well known, the curve fit is only dependant on the thermal properties of protein.

Figure 6.9 shows the thermal conductivity curve fits produced by Maxwell's mixture equation, and Bruggeman's equation. The percentage water content by volume was estimated using ρ_p = 1300 kgm^{-3}. Maxwell's mixture equation estimates the thermal conductivity of protein as k_p = 0.227 Wm^{-1}K^{-1}, while Bruggeman's equation gives the thermal conductivity of protein as k_p = 0.225 Wm^{-1}K^{-1}.

Figure 6.10 shows the thermal diffusivity curve fits produced by Maxwell's mixture equation and Bruggeman's equation. The water content by volume was again estimated by setting ρ_p = 1300 kgm^{-3}. Maxwell's mixture equation estimates the thermal diffusivity of protein as $\alpha_p = 0.858\times10^{-7}$ m^{2}s^{-1}, while Bruggeman's equation gives the thermal diffusivity of protein as $\alpha_p = 0.844\times10^{-7}$ m^{2}s^{-1}.

It must be remembered that these figures are produced by a large extrapolation of the data and the errors associated with these values are large. However, the actual values

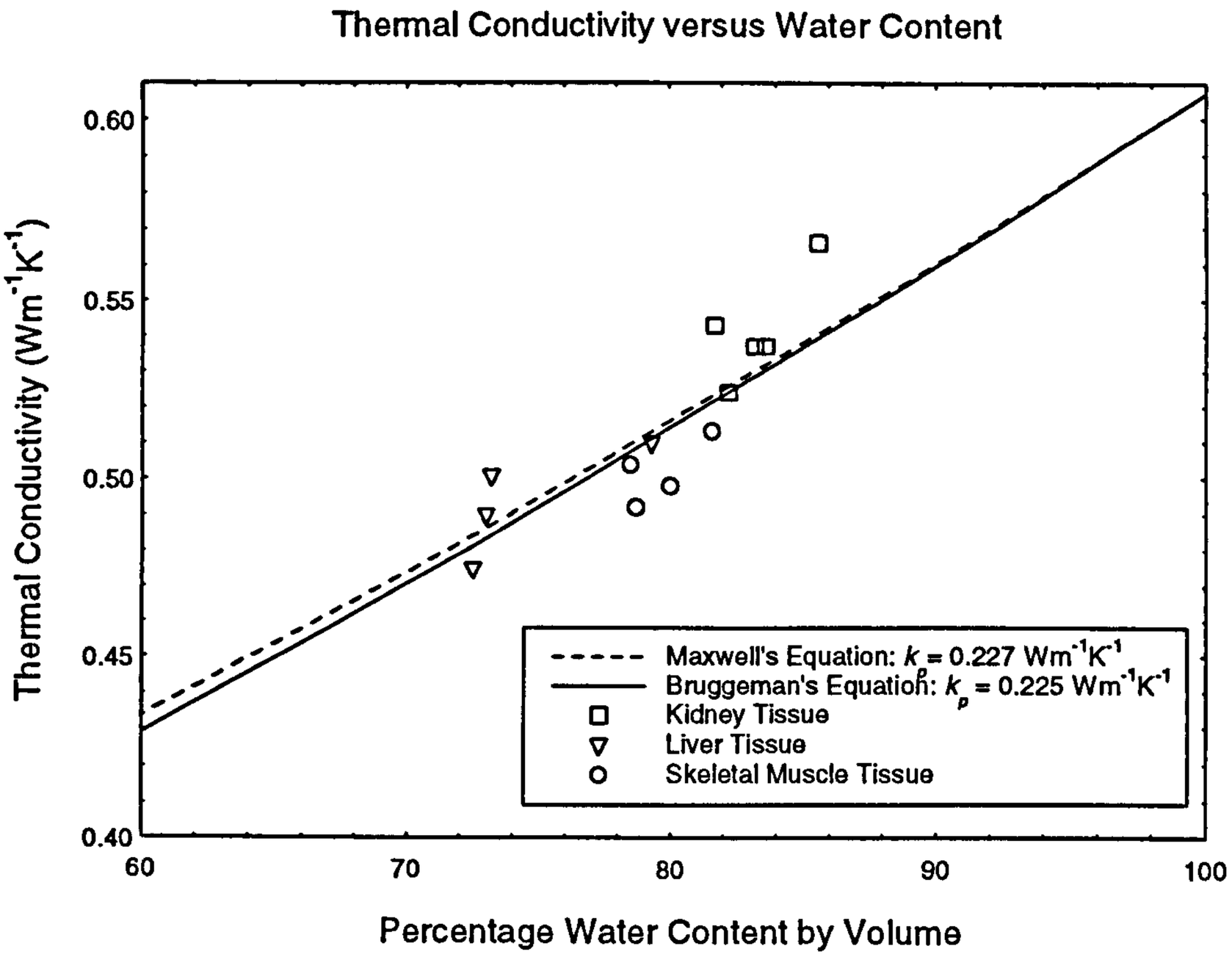

Figure 6.9 Curve fits of the thermal conductivity against water content data.

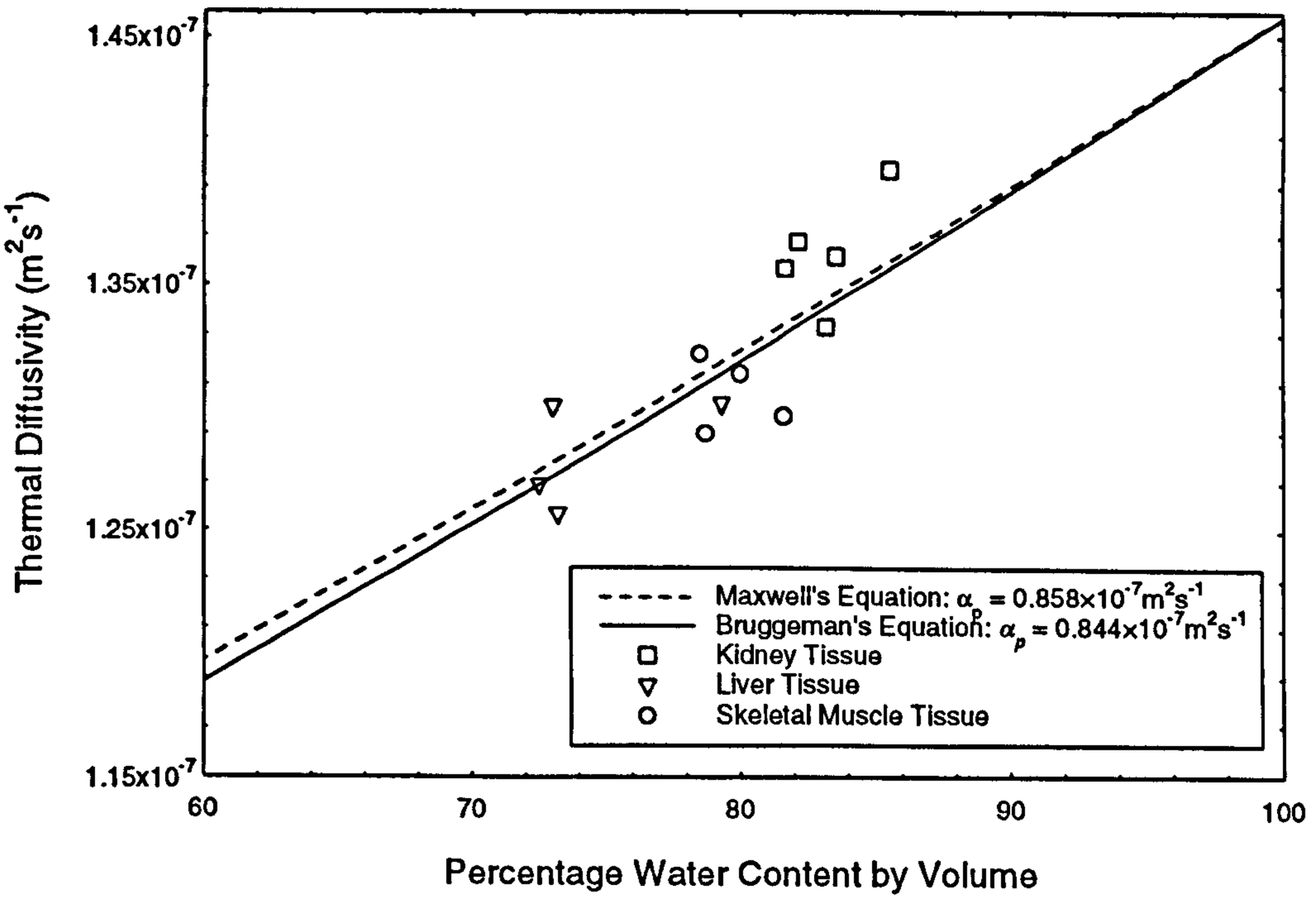

Figure 6.10 Curve fits of the thermal diffusivity against water content data.

themselves are of less interest than the behaviour which becomes apparent when the behaviour of the each of the individual types of tissue is compared to the curve fit.

For both the thermal conductivity and thermal diffusivity, the two values estimated by the two curves are very similar. However, it is noticeable that while the measured liver values are roughly distributed about the expected curve, the thermal properties of the skeletal muscle are generally lower than the values predicted by the curve fits, and those of the kidney tissues are generally higher than the values predicted by the curve fits.

To examine the differing behaviour of the thermal properties of the tissues, the thermal properties of protein estimated by each of the mean values will be examined. Table 6.2 shows the estimated thermal properties of protein as calculated using Bruggeman's and Maxwell's equations. The water content by volume is estimated using $\rho_p = 1300\ kgm^{-3}$.

The differing behaviours in each of the tissues is clear. The lowest protein thermal conductivity and thermal diffusivity is seen in skeletal muscle tissue. The thermal properties of protein found in liver are similar to mean values found earlier in this section, while the protein in kidney tissue has the highest thermal conductivity and thermal diffusivity.

While the thermal conductivity of protein is not much different for animal and human tissues, the thermal diffusivity of human tissue is always lower than that seen in the animal tissues. This was not immediately obvious from the results in chapter 5 since the high water content of human tissues, compared to the animal equivalent, caused the overall thermal diffusivity of human tissue to generally be similar or higher than that seen in the same type of animal tissue. As examined in chapter 5, there are a number of significant differences between human tissue and animal tissue. The animal tissue samples came from the young of the species which were in a fit state to provide meat which was fit for human consumption. The animal tissues also had their excess blood drained. None of this is true in the case of the human tissue samples. Thus it is reasonable to expect that the thermal properties of the non-water fraction may be different in animal and human tissue for the types of samples investigated.

Estimates of the thermal properties of protein are dependant on the way the water content by volume is calculated. The thermal properties of protein were estimated again, using protein density values other than 1300 kgm^{-3}, or using tissue density tables. As seen in table 6.2, the variation in the thermal properties of tissue calculated by Maxwell's

Tissue Type	ϕ	Maxwell's Equation		Bruggeman's Equation	
		k_p ($Wm^{-1}K^{-1}$)	α_p (m^2s^{-1})	k_p ($Wm^{-1}K^{-1}$)	α_p (m^2s^{-1})
Skeletal Muscle:					
All Animal Tissues	0.789	0.181	0.820×10^{-7}	0.186	0.822×10^{-7}
Agnine	0.800	0.167	0.823×10^{-7}	0.173	0.825×10^{-7}
Bovine	0.787	0.169	0.768×10^{-7}	0.175	0.772×10^{-7}
Porcine	0.785	0.209	0.890×10^{-7}	0.214	0.892×10^{-7}
Human	0.816	0.190	0.706×10^{-7}	0.195	0.710×10^{-7}
Liver:					
All Animal Tissues	0.728	0.226	0.870×10^{-7}	0.230	0.873×10^{-7}
Agnine	0.725	0.204	0.842×10^{-7}	0.209	0.844×10^{-7}
Bovine	0.732	0.265	0.792×10^{-7}	0.268	0.795×10^{-7}
Porcine	0.730	0.237	0.928×10^{-7}	0.241	0.930×10^{-7}
Human	0.793	0.217	0.795×10^{-7}	0.221	0.799×10^{-7}
Kidney:					
All Animal Cortex	0.829	0.253	0.956×10^{-7}	0.255	0.957×10^{-7}
Agnine	0.817	0.302	0.958×10^{-7}	0.305	0.959×10^{-7}
Bovine	0.822	0.221	0.996×10^{-7}	0.224	0.997×10^{-7}
Porcine	0.836	0.250	0.933×10^{-7}	0.252	0.934×10^{-7}
Human Cortex	0.832	0.257	0.808×10^{-7}	0.259	0.811×10^{-7}
Animal Medulla	0.856	0.355	1.067×10^{-7}	0.356	1.068×10^{-7}

Table 6.2 The thermal conductivity of protein estimated using Maxwell's and Bruggeman's equations with the water content by volume given by $\rho_p = 1300\ kgm^{-3}$.

mixture equation, and the thermal properties of tissue calculated using Bruggeman's equation, are small when compared to the variation between species. So it is sufficient to calculate the thermal properties of protein using only Maxwell's mixture equation. Table 6.3 shows the thermal conductivity and thermal diffusivity of protein, estimated using ρ_p = 1250 kgm^{-3}, ρ_p = 1350 kgm^{-3}, and the tables of tissue data in Rose and Goldberg.

It can be seen that lowering the assumed density of the protein raises the resultant thermal conductivity and thermal diffusivity estimates. The difference between the thermal conductivity estimated ρ_p = 1250 kgm^{-3} and the thermal conductivity estimated by ρ_p = 1350 kgm^{-3} is roughly 0.02 Wm^{-1}K^{-1} or 10%.

Given that the protein density affects the estimates of the thermal properties of protein, it is possible that the variation in the protein thermal conductivity and diffusivity seen between the different tissues is partly due the differing protein density. If this was the case, it would be expected that the thermal conductivity and thermal diffusivity obtained using tissue density tables, would be closer in value. However the difference between the thermal properties of protein present in each of the types of tissues are similar or greater than when the density was fixed at ρ_p = 1300 kgm^{-3}. This tends to indicate that the difference in the estimated thermal properties of protein between tissues is true, rather than a result of the wrong estimate of the density.

6.4.3 Brain Tissue.

As discussed in the previous chapter, brain tissue has lower thermal conductivity than would be expected given the water content by mass. It was hypothesised that this was due there being a large amount of fat present in brain. This was also supported by the density of brain tissue. This will now be examined in greater detail.

Rose and Goldberg gave the density of human brain tissue as ρ_p = 1033 kgm^{-3}. This is lower than any of the densities seen in any of the other tissues examined. Using this value, the thermal conductivity of the non-water fraction of white matter from the human brain is 0.111 Wm^{-1}K^{-1}, while the thermal diffusivity of the non-water fraction is 0.695×10^{-7} m^{2}s^{-1}. For the grey brain tissue, the thermal conductivity of the non-water

Tissue Type	$\rho_p = 1250$ kgm^{-3}			$\rho_p = 1350$ kgm^{-3}			Rose and Goldberg (1979)		
	ϕ	k_p (Wm^{-1}K^{-1})	α_p (m^{2}s^{-1})	ϕ	k_p (Wm^{-1}K^{-1})	α_p (m^{2}s^{-1})	ϕ	k_p (Wm^{-1}K^{-1})	α_p (m^{2}s^{-1})
Skeletal Muscle:									
All Animal Tissues	0.783	0.191	0.836×10^{-7}	0.796	0.171	0.803×10^{-7}	0.802	0.158	0.782×10^{-7}
Agnine	0.793	0.177	0.839×10^{-7}	0.806	0.157	0.806×10^{-7}	0.815	0.138	0.775×10^{-7}
Bovine	0.780	0.179	0.786×10^{-7}	0.792	0.159	0.751×10^{-7}	0.800	0.148	0.731×10^{-7}
Porcine	0.778	0.219	0.905×10^{-7}	0.791	0.200	0.875×10^{-7}	0.798	0.190	0.860×10^{-7}
Human	0.810	0.201	0.725×10^{-7}	0.822	0.180	0.686×10^{-7}	0.837	0.151	0.630×10^{-7}
Liver:									
All Animal Tissues	0.720	0.234	0.885×10^{-7}	0.736	0.217	0.856×10^{-7}	0.715	0.240	0.895×10^{-7}
Agnine	0.717	0.213	0.856×10^{-7}	0.732	0.195	0.827×10^{-7}	0.711	0.219	0.868×10^{-7}
Bovine	0.724	0.273	0.808×10^{-7}	0.739	0.257	0.776×10^{-7}	0.719	0.278	0.818×10^{-7}
Porcine	0.722	0.245	0.941×10^{-7}	0.737	0.229	0.915×10^{-7}	0.717	0.251	0.950×10^{-7}
Human	0.786	0.227	0.813×10^{-7}	0.799	0.208	0.779×10^{-7}	0.792	0.218	0.797×10^{-7}
Kidney:									
All Animal Cortex	0.823	0.262	0.970×10^{-7}	0.834	0.244	0.942×10^{-7}	0.821	0.265	0.975×10^{-7}
Agnine	0.811	0.312	0.972×10^{-7}	0.822	0.296	0.944×10^{-7}	0.807	0.318	0.982×10^{-7}
Bovine	0.816	0.231	1.009×10^{-7}	0.827	0.211	0.983×10^{-7}	0.813	0.236	1.017×10^{-7}
Porcine	0.830	0.259	0.948×10^{-7}	0.841	0.241	0.918×10^{-7}	0.829	0.260	0.949×10^{-7}
Human	0.826	0.266	0.826×10^{-7}	0.837	0.248	0.791×10^{-7}	0.824	0.269	0.831×10^{-7}
Animal Medulla	0.851	0.362	1.079×10^{-7}	0.860	0.348	1.056×10^{-7}	0.855	0.357	1.070×10^{-7}

Table 6.3 The thermal properties of protein calculated using different ways of estimating the water content by volume.

fraction is 0.225 $Wm^{-1}K^{-1}$, while the thermal diffusivity of the non-water fraction is $0.812\times10^{-7}\ m^2s^{-1}$.

This gives the non-water fraction of white and grey brain matter very different thermal properties. The thermal properties of the non-water fraction in grey brain tissue are only slightly higher than the thermal properties of the non-water fraction of human liver tissue. Thus it is probably reasonable to assume that the non-water fraction of the grey matter in human brain is mainly protein.

The white matter in the human brain has a non-water fraction which has a thermal conductivity and thermal diffusivity which are far lower than the values seen in any other tissue. This is due to the presence of a fatty substance called myelin which is not present in grey brain matter (Brooks and Brooks, 1981). The mass fraction of fat in white brain matter is roughly 18%, whereas it is only roughly 5% in grey brain matter (Geigy Scientific Tables, 1970). When the estimates of the thermal properties of protein are compared to the estimates for the thermal properties of fat, as investigated in chapter 5, it can be seen that fat has a far lower thermal conductivity and thermal diffusivity than protein. It is the myelin present which gives the non-water fraction of the white matter of the human brain a thermal conductivity and thermal diffusivity which lies between that of protein and fat.

6.5 Comparison Between the Thermal and Dielectric Properties of Tissue.

As discussed in chapter 1, the effective microwave temperature for planar thermal radiation propagating normal to the surface of a semi-infinite uniform material, as seen by a perfectly matched radiometer system, is

$$T_{mw} = 2\alpha_\varepsilon \int_0^\infty \exp(-2\alpha_\varepsilon z)T(z)dz \qquad (6.6.1)$$

where T_{mw} is the effective microwave temperature, $T(z)$ is the temperature at depth z, and $2\alpha_\varepsilon$ is the power attenuation constant which is given by

$$2\alpha_\varepsilon = \frac{2\pi}{\lambda_0}\sqrt{2\varepsilon'}\left[\left(1+\left(\frac{\varepsilon''}{\varepsilon'}\right)^2\right)^{1/2}-1\right]^{1/2} \qquad (6.6.2)$$

where λ_0 is the wavelength of the radiation in free space. As discussed in chapter 2, the

temperature distribution in tissue is given by the conventional bio-heat equation

$$\rho c\frac{dT}{dt} = k\nabla^2 T - w_b c_b (T - T_{art}) + Q \qquad (6.6.3)$$

where T_{art} is the arterial blood temperature, ρ and c are the density and specific heat of the tissue, and c_b is the specific heat of the blood. The blood perfusion is given by w_b, and Q is the metabolic heat production in the tissue. These equations show that the effective microwave temperature is dependant on both the thermal and dielectric properties of the tissue. For example, as discussed in section 2.8, if the conventional bio-heat equation is used to model a one dimensional temperature variation, the effective microwave temperature is given by

$$T_{mw} = T_{art} - \frac{h(T_s - T_{amb})}{\left(\sqrt{w_b c_b k} + {w_b c_b}/{2\alpha_\varepsilon}\right)} \qquad (6.6.4)$$

where h is the heat loss coefficient from the surface at temperature T_s to surroundings at T_{amb}. In this section the relationship between the thermal and microwave properties of biological tissues is examined.

The vast majority of the samples which had their thermal properties measured also had their microwave dielectric properties examined. The complex permittivity of the samples was measured at a frequency of 3 GHz by a colleague, who measured the dielectric properties after the thermal properties were measured.

The method used to measure the microwave dielectric properties of biological tissue was the open ended coaxial probe technique. The coaxial line is terminated by a significant volume of the sample material with dimensions comparable to a least a fraction of a wavelength. An input signal of the desired frequency is applied to the coaxial line, and is partly reflected by sample material at the end of the coaxial line, with the electric field between the conductors penetrating a short distance into the sample. This "fringing field" region acts as a small capacitance across the end of the line, with values of capacitance and loss dependant on the material properties. This causes the phase and magnitude of the reflected signal to be dependant on the dielectric properties of the sample material. Thus, examining the profile of the resultant standing wave pattern along the line will give information about the material dielectric properties. For details of

Tissue Type	ϕ	k ($Wm^{-1}K^{-1}$)	α (m^2s^{-1})	Dielectric Constant	Loss Factor
Fat:					
All Animal Tissues	0.118	0.229	0.802×10^{-7}	5.0	1.0
Agnine	0.112	0.213	0.788×10^{-7}	6.7	1.6
Bovine	0.113	0.202	0.715×10^{-7}	3.7	0.5
Porcine	0.123	0.253	0.861×10^{-7}	5.2	1.0
Human	0.130	0.209	0.727×10^{-7}	6.0	0.8
Skeletal Muscle:					
All Animal Tissues	0.789	0.497	1.306×10^{-7}	46.7	16.0
Agnine	0.800	0.498	1.314×10^{-7}	47.2	16.5
Bovine	0.787	0.501	1.290×10^{-7}	46.1	15.6
Porcine	0.785	0.490	1.322×10^{-7}	47.1	16.1
Human	0.816	0.513	1.297×10^{-7}	49.9	16.7
Liver:					
All Animal Tissues	0.728	0.485	1.281×10^{-7}	39.9	13.8
Agnine	0.725	0.475	1.269×10^{-7}	39.0	13.6
Bovine	0.732	0.501	1.257×10^{-7}	41.5	14.2
Porcine	0.730	0.490	1.301×10^{-7}	40.5	14.0
Human	0.793	0.510	1.302×10^{-7}	42.5	14.0
Kidney:					
All Animal Cortex	0.829	0.535	1.363×10^{-7}	50.1	16.6
Agnine	0.817	0.543	1.357×10^{-7}	49.5	16.7
Bovine	0.822	0.524	1.368×10^{-7}	51.6	17.2
Porcine	0.836	0.537	1.362×10^{-7}	49.5	16.2
Human Cortex	0.832	0.537	1.333×10^{-7}	50.1	17.2
Animal Medulla	0.856	0.566	1.397×10^{-7}	53.4	18.6
Brain:					
White Matter	0.814	0.489	1.293×10^{-7}	37.0	8.0
Grey Matter	0.887	0.554	1.374×10^{-7}	54.5	12.3

Table 6.4 The mean thermal properties compared to the mean microwave dielectric properties and mean water content by volume. (Dielectric properties from Gorton, 1996).

this method used to measure the microwave complex permittivity of human and animal tissues, and the results obtained, see Gorton (1996).

It is found to be uninformative to compare the thermal and microwave dielectric properties measured of individual samples. The problems experienced when comparing the water content and thermal properties of individual samples are experienced to an even greater degree when comparing the thermal and dielectric properties of individual samples. The volume of tissue significant for measuring the microwave properties with the coaxial probe, is different from the volume of tissue significant in measuring the thermal properties with the thermistor probe, which is, in turn, different from the volume used to find the water content. This is due to the fundamental spatial response characteristics of the two probes. Since the probes measure in different volumes of tissue, there is likely to be limited correlation between the thermal and microwave property measurements made on individual samples. Thus, the mean thermal and microwave properties of each of the different tissue types must be used when comparing the thermal and dielectric properties.

Table 6.4 shows the mean microwave dielectric properties of liver, kidney, skeletal muscle, brain and fat tissues, along with the mean water content by volume and the mean thermal properties. The water content by volume was calculated by setting the density of protein as 1300 kgm^{-3} for the high water content samples, except brain tissue which used the tissue density value given in Rose and Goldberg. The water content by volume for the low water content fat samples was found by setting the density of pure dry fat as 860 kgm^{-3} (Schepps and Foster, 1980).

The values stated in table 6.4 differ slightly from the values stated in Gorton (1996). This was because Gorton measured the microwave dielectric properties of a number of samples which were not examined to find their thermal conductivity and thermal diffusivity. It was felt that only using measurements that had been made on samples which had been thermally probed would give a better comparison between the thermal and microwave properties.

Figure 6.11 show the variation of the mean dielectric constant and loss factor with water content for all the liver, kidney and skeletal muscle tissues. For dielectric modelling purposes, high water content biological tissue is assumed to consist of physiological saline and protein. The water present in the human body has many dissolved ions but it

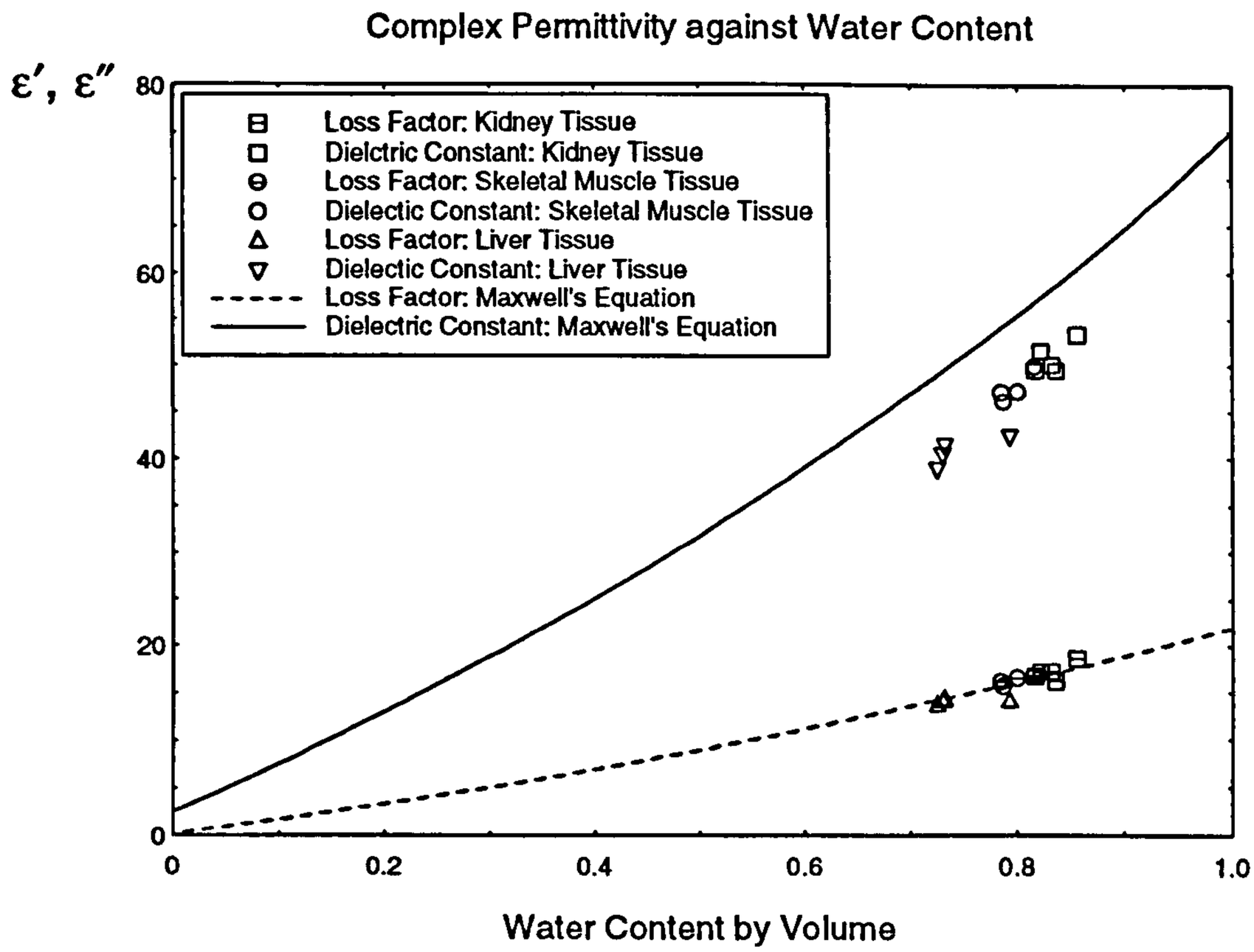

Figure 6.11 Comparison between complex permittivity and water content by volume.

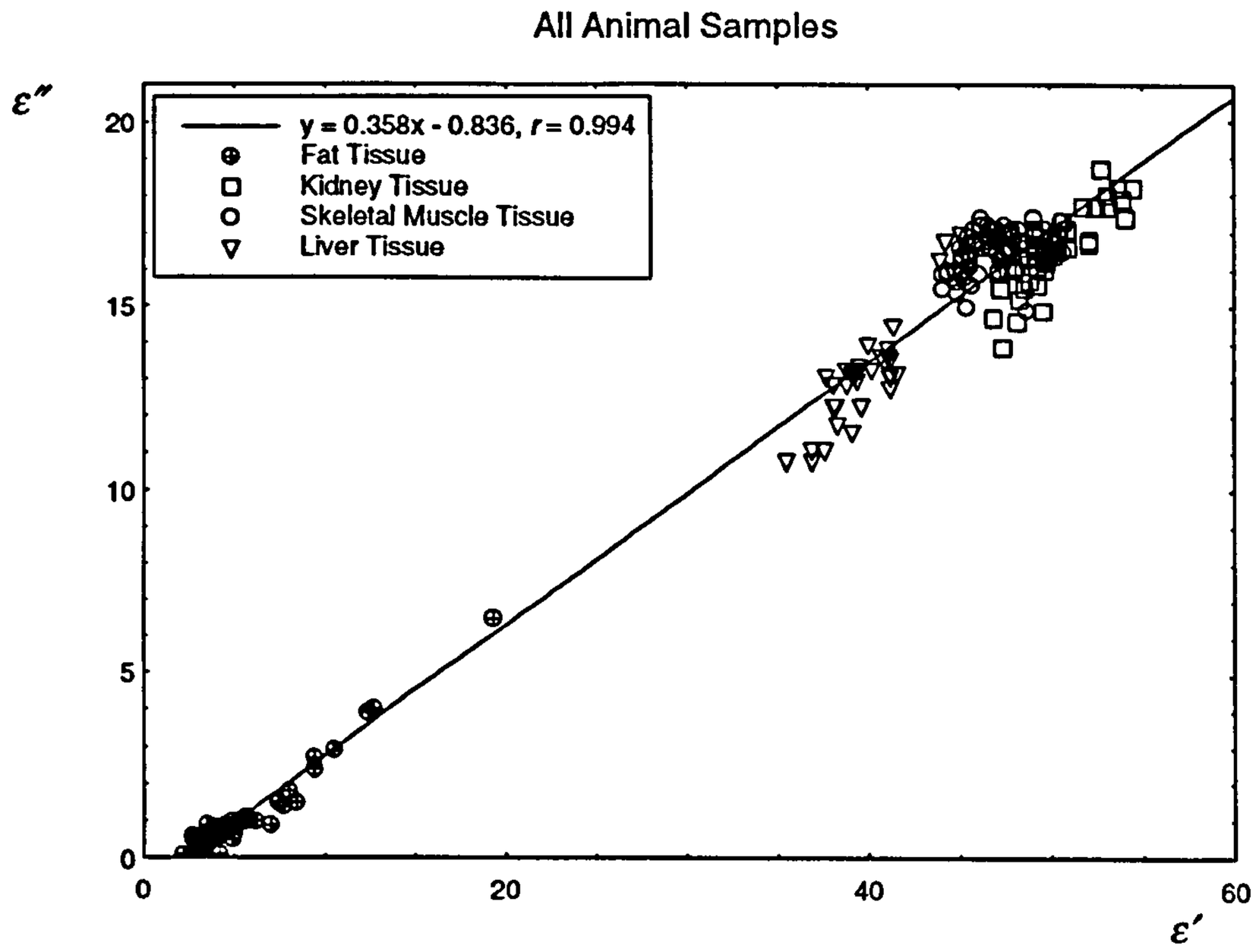

Figure 6.12 Comparison between ε'' and ε' for all the animal samples considered.

has been found that physiological saline, that is 0.15 molar aqueous NaCl solution, well represents the behaviour of the electrolytic water present in the body. Physiological saline has a complex permittivity of $75 - 22j$ at room temperature, while it is assumed that the protein has a complex permittivity of $2.5 - 0.2j$.

Figure 6.11 shows that the dielectric constant of the tissues lies below the values predicted by Maxwell's mixture equation, while the loss factor of the tissues correspond to the values predicted by the Maxwell's mixture equation. This is due to the water bonding to the protein molecules. As discussed in chapter 3, a fraction of the water in biological tissues is bonded to the protein molecules. Although bound water is believed to have the thermal properties of free water, it has different and varying microwave dielectric properties.

Examining figure 3.4, it can be seen that the dielectric constant of bound water at 3 GHz is significantly lower than the dielectric constant of free water at the same frequency. However the loss factor of bound water at 3 GHz is similar if not higher to the loss factor of free water at the same frequency. Thus, the dielectric constant of biological tissue is lower than would be expected for a non-interacting mixture of physiological saline and protein, while the loss factor is similar or slightly higher than that given by Maxwell's equation. For a full discussion of the effect of bound water on the complex permittivity of biological tissue, see Gorton (1996).

Figure 6.12 compares the loss factor with the dielectric constant for all the animal kidney, skeletal muscle, liver and fat samples examined in this study. It can be seen that while the relationship is approximately linear, each tissue has its own variation from that predicted from the curve fit. This is possibly due to slight variations in properties of the electrolytic water present in each of the different types of tissue. A small change in the ionic profile of the water would not affect the dielectric constant but it would affect the loss factor.

Since the loss factor is affected by factors such as the ionic concentration, it is less informative to compare the loss factor to the thermal properties of tissue than it is to compare the dielectric constant to the thermal properties of tissue.

Figure 6.13 compares the mean thermal conductivity with the mean dielectric constant for all liver, kidney, fat, and skeletal muscle tissues, while figure 6.14 compares the mean thermal diffusivity with the mean dielectric constant for the same tissues.

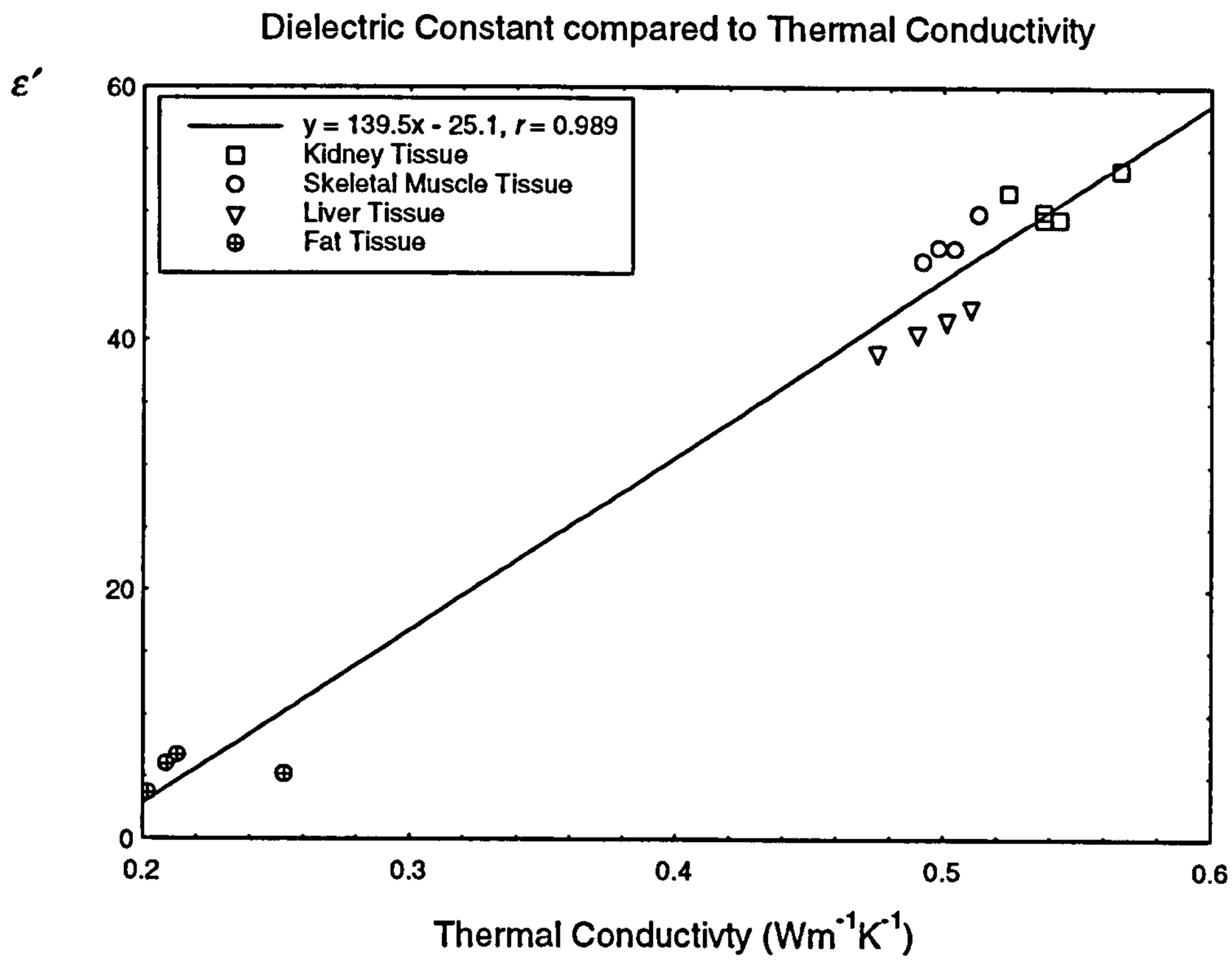

Figure 6.13 Mean thermal conductivity compared with mean dielectric constant.

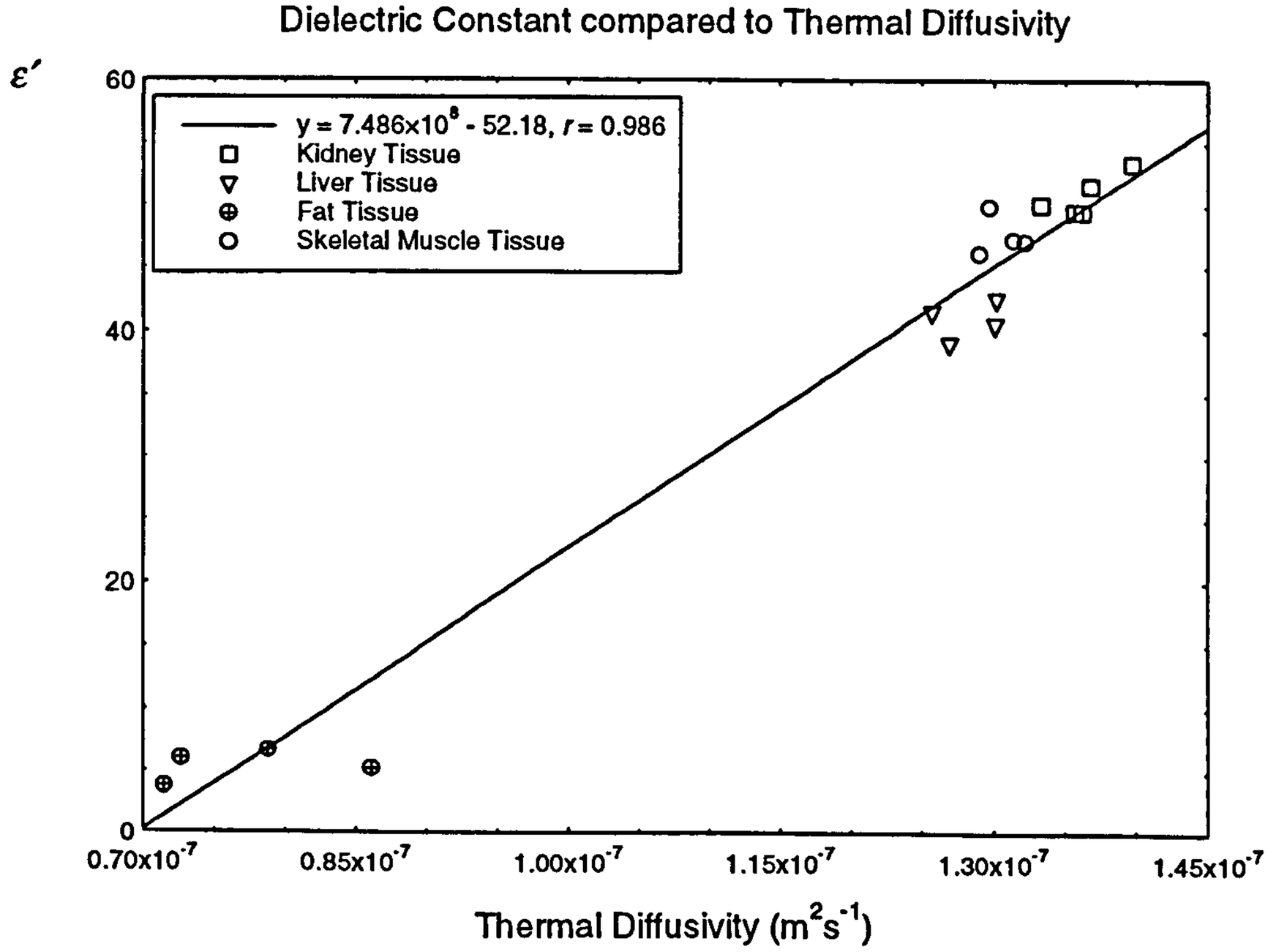

Figure 6.14 Mean thermal diffusivity compared with mean dielectric constant.

These curves both show a reasonable straight line fit, but with noticeable deviation from the mean line by each type of tissue. This can probably be ascribed to the variations in the thermal properties of protein. This is demonstrated in figures 6.15 and 6.16. Figure 6.15 compares the mean thermal conductivity with the mean dielectric constant for liver, kidney, and skeletal muscle. In figure 6.16, the thermal conductivity of the same tissues is estimated by assuming that all these tissues have the same protein thermal conductivity. The value of the protein thermal conductivity is the same as that found in figure 6.7. Using this value, the water content of each of the tissues are used to calculate the thermal conductivity, using Maxwell's mixture equation, and compared to the measured mean dielectric constant.

When figures 6.15 and 6.16 are compared, the difference is clear. While there is only modest evidence of a definite relationship between the two tissue properties in figure 6.15, there is a far clearer relationship between the two properties in figure 6.16. The correlation of the linear curve fit is far higher for the data shown in figure 6.16 than for the data shown in figure 6.15. Thus, it can be seen that if the tissues all had the same protein thermal conductivity, then there would a definite relationship between the thermal conductivity and dielectric constant. Figures 6.17 and 6.18 show the same for the thermal diffusivity and dielectric constant.

Figures 6.15-6.18 suggest that the variation in the thermal properties of protein are significant, while the variation in the dielectric properties of protein are far less so. This is because the thermal properties of protein are significant when compared to the thermal properties of water. The dielectric constant of water is roughly 30 times that of protein. This means that doubling the dielectric constant of protein from $\varepsilon = 2.5$ to $\varepsilon = 5.0$ only causes the dielectric properties of water protein mixtures to increase by roughly 2%, at water content values associated with meat. However, since the thermal conductivity of water is only about 3 times the thermal conductivity of water, the same 2% rise can be brought about by increasing the thermal conductivity of protein by approximately 15%. The same is true of the thermal diffusivity, where the thermal diffusivity of water is only double that of protein. So while the dielectric properties of protein will vary from tissue type to tissue type, the large dielectric constant of water in comparison means, that these variations will not be significant.

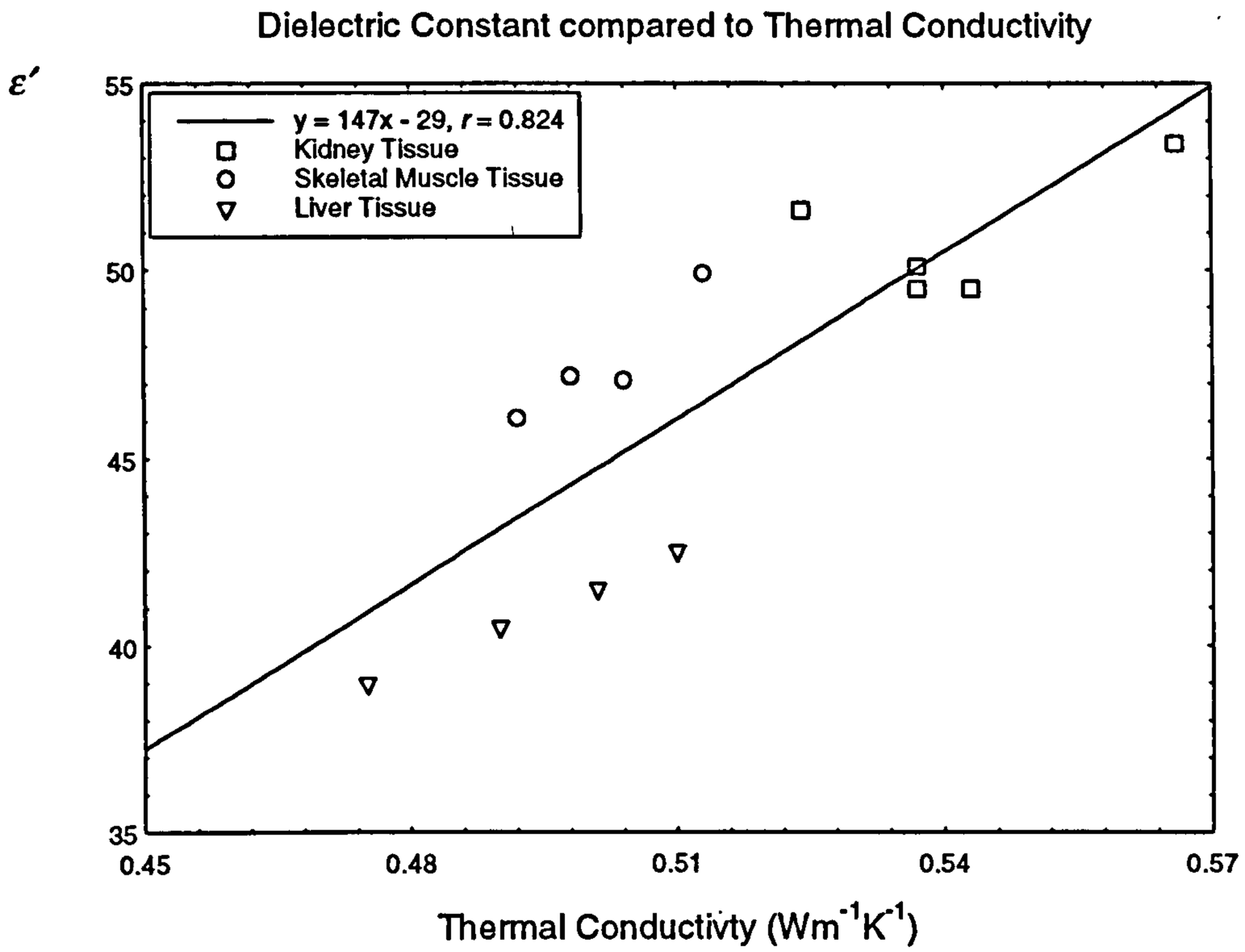

Figure 6.15 ε` compared to k for the main high water content tissues.

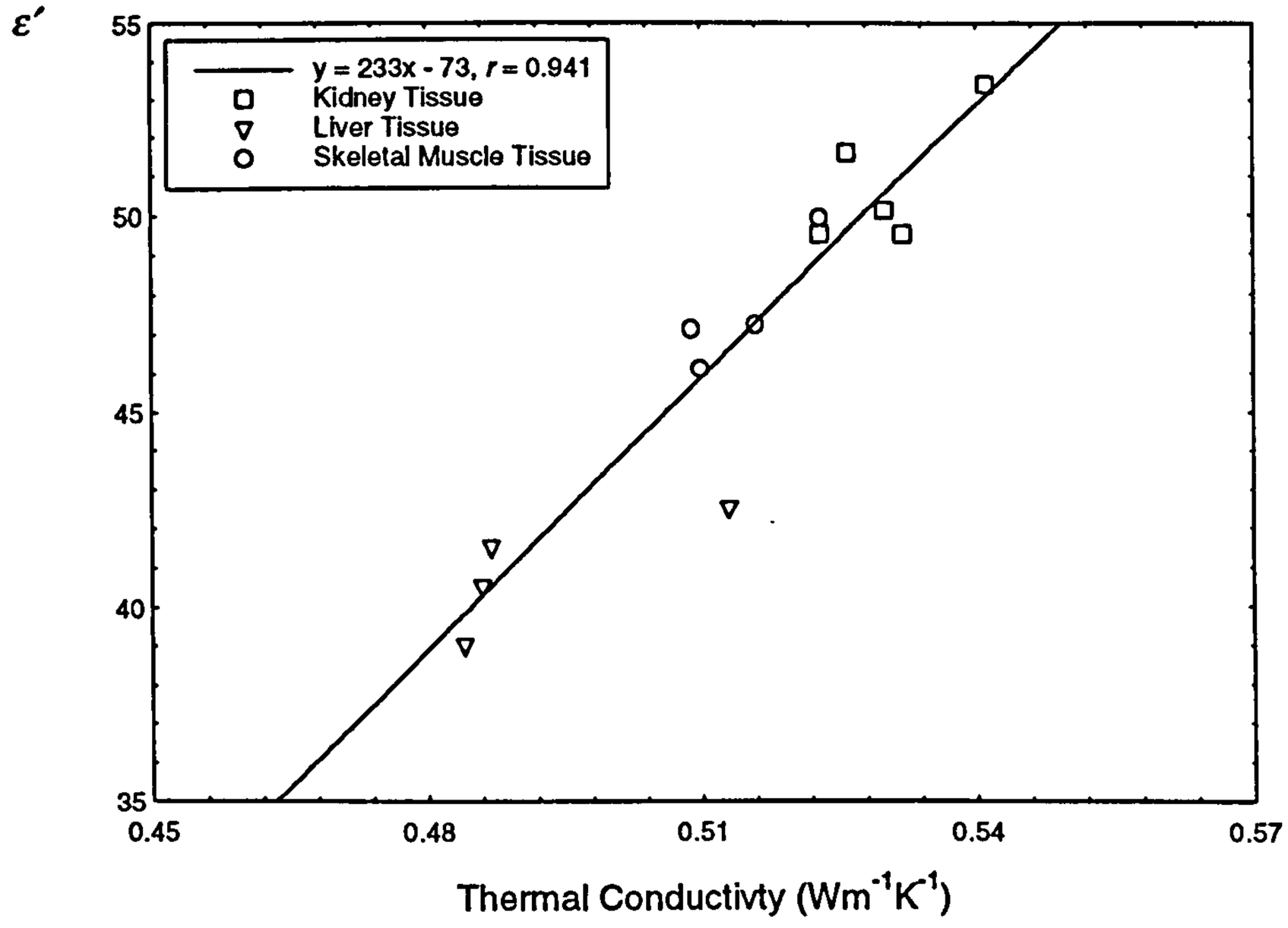

Figure 6.16 ε` compared to the thermal conductivity estimated using the water content for the main high water content tissues.

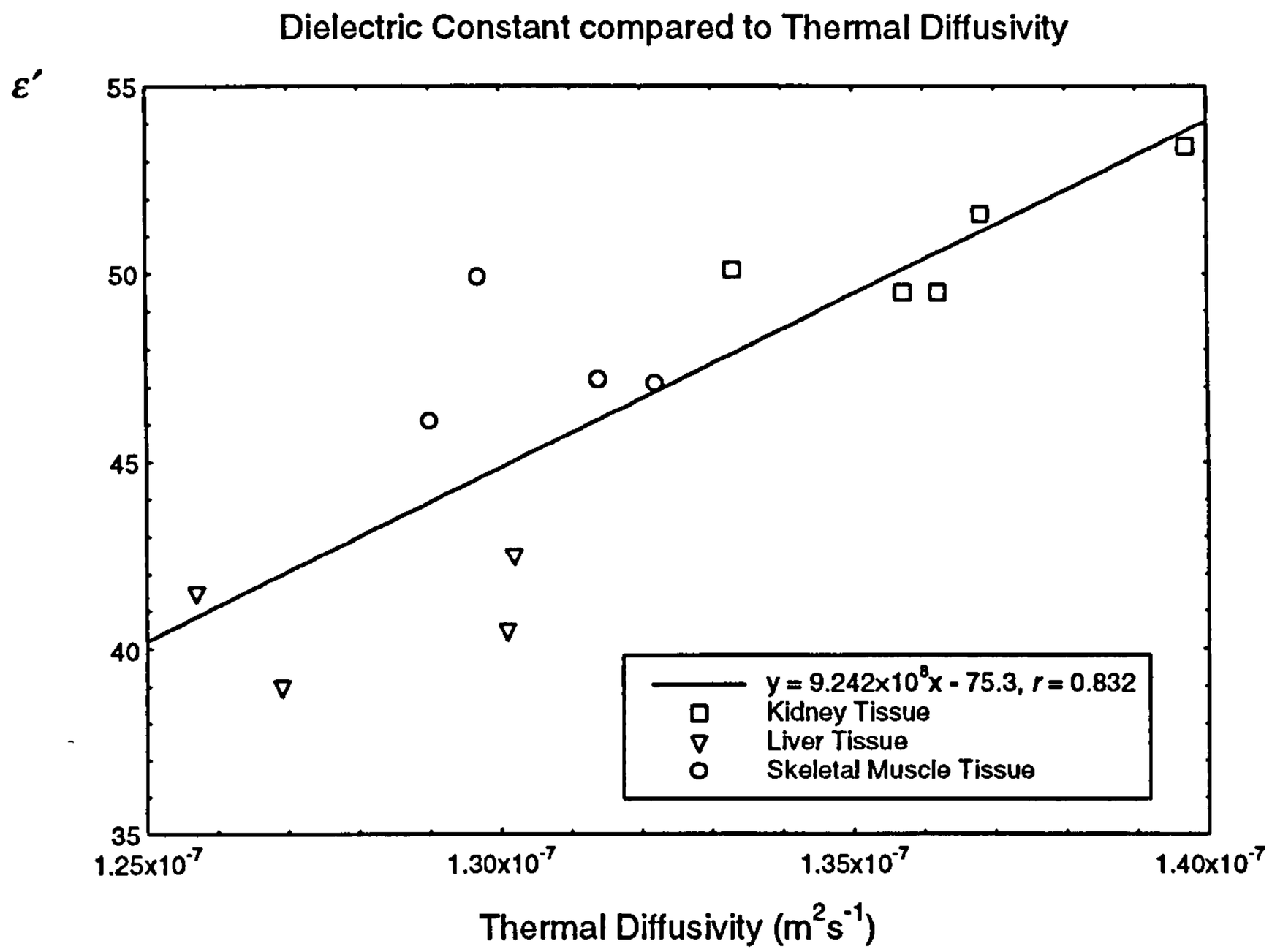

Figure 6.17 ε` compared to α for the main high water content tissues.

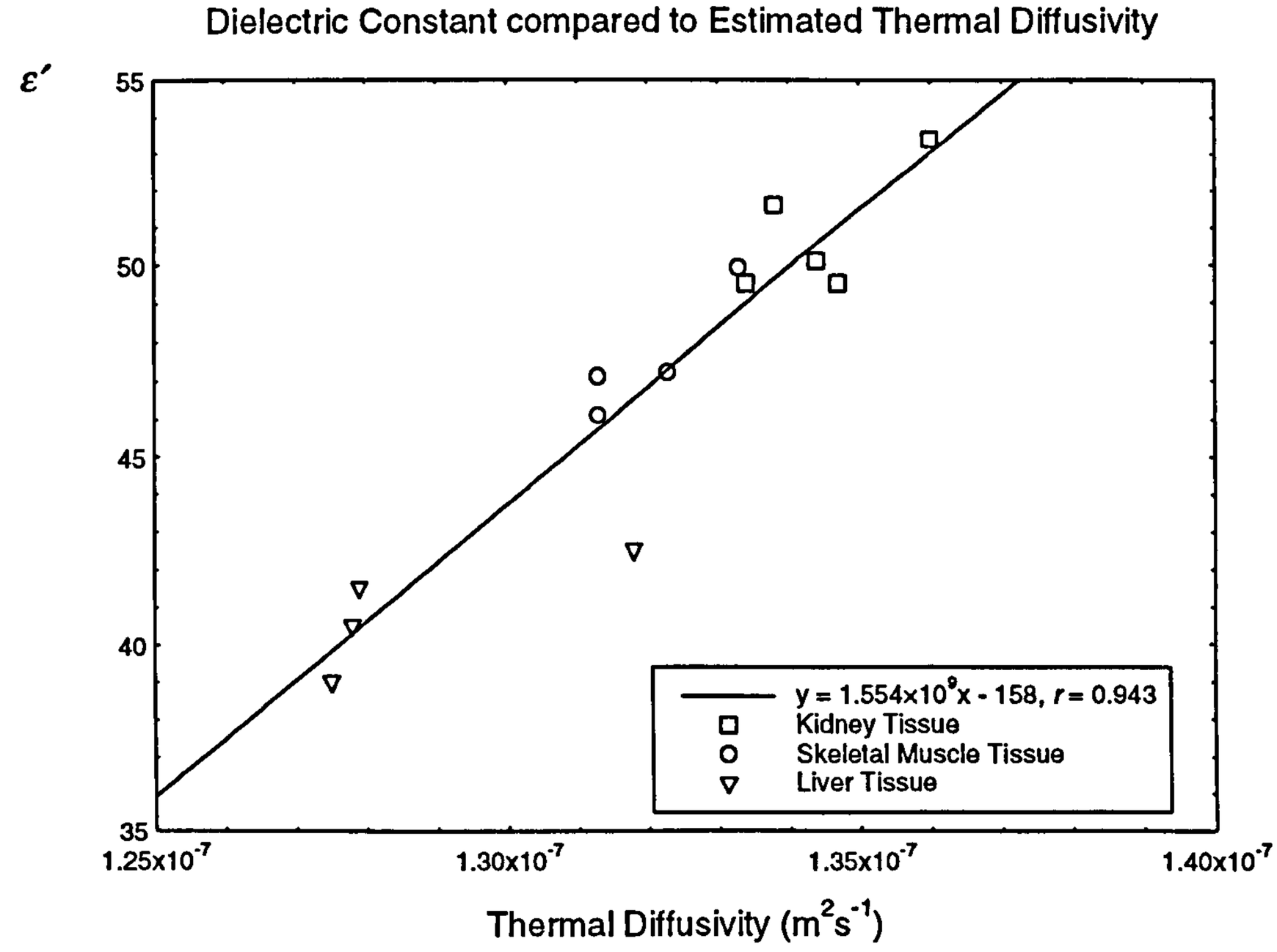

Figure 6.18 ε` compared to the thermal diffusivity estimated using the water content for the main high water content tissues.

For microwave radiometry, it is of special interest to compare the power attenuation constant against the thermal conductivity. Figure 6.19 compares $2\alpha_\varepsilon$ with k for the liver, kidney, fat, and skeletal muscle tissues. From low to high water content tissues there is a general trend, but within the high water content tissues there is no definite relationship between the two properties.

The power attenuation constant is a function of both the dielectric constant and the loss factor. Therefore the amount of bound water and the electrolyte concentration will have a major effect on the attenuation constant. However, the amount of bound water and the electrolyte concentration have little effect on the thermal conductivity. Also, as discussed previously, the dielectric properties of tissue are relatively unaffected by variations in the dielectric properties of protein, whereas the thermal properties are far more affected by variations in the thermal conductivity of protein. These factors combine to remove any definite relationship between the power attenuation constant and the thermal conductivity for the high water content tissues.

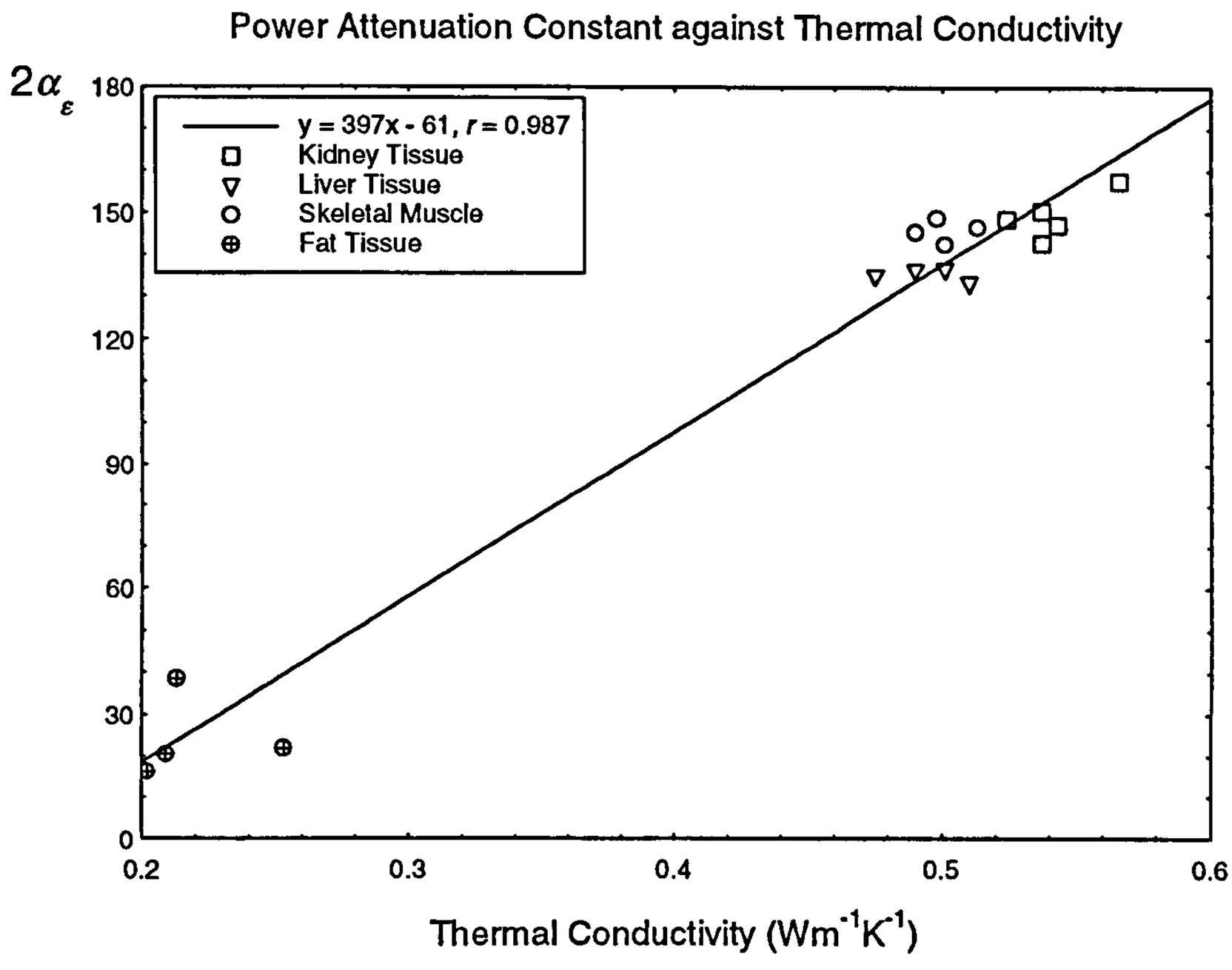

Figure 6.19 Comparison between the power attenuation constant and the thermal conductivity for all liver, kidney, fat and skeletal muscle tissues.

Conclusion.

Knowledge of the thermal properties of biological tissues are required in several areas of clinical research, such as hyperthermia induction, tomographic temperature measurement and microwave thermography. The thermal conductivity and thermal diffusivity of tissues are required to produce realistic computational simulations which will model temperature patterns in regions of interest of the human body. In both microwave thermography and tomographic temperature measurement, these models are required to fully analyse the temperature patterns observed. In hyperthermia, accurate computer models are vital in planning a treatment regime and controlling the applied radio frequency power to produce therapeutic temperatures without causing tissue damage.

To compute the temperature distribution within a tissue volume, a bio-heat equation is required to model the effect of the blood perfusion on the supply of heat within the region. The Pennes conventional bio-heat equation assumes all the heat transfer takes place in the capillaries. Though this hypothesis is theoretically invalid, the conventional bio-heat equation has proven itself in practical situations. In conjunction with microwave radiation modelling, the conventional bio-heat equation suffices for microwave thermography data interpretation.

The thermal properties of biological tissue are dependant on the water content of the tissue. Water is the majority component of the normal human body, and water has a significantly higher thermal conductivity and thermal diffusivity than the other main constituents of the soft tissues, protein and fat. Mixture equations can describe the behaviour of a two constituent non-interacting system, given the properties of the individual constituents and their relative abundance. However, the two main constituents in biological tissues, water and protein, do interact. In the human body, a fraction of the water molecules present will hydrogen bond to the protein macromolecules. This has little effect on the thermal properties of tissue, since the thermal properties of this bound water are similar to unbound water, but it does have a major effect on the dielectric properties of biological tissues. Further, mixture equations require that the properties of the individual materials, must be known. While the thermal properties of water are well known, there is no single value for the thermal conductivity or thermal diffusivity of tissue protein.

A self-heated thermistor probe system was used to measure the in-vitro thermal conductivity and thermal diffusivity of wide range of human and animal soft tissues. The thermistor probe was connected to a computer interface card, which supplied both the voltage and monitored the resistance of the thermistor, allowing the power supplied to the thermistor to be accurately controlled by software. This system did not require excessively large samples and allowed measurement of the thermal properties in reasonable time and to a useful accuracy.

The system was calibrated using glycerol and agar gelled water. These two substances were chosen because the thermal behaviour of the materials and mixtures of the materials is well known and was similar to the range of thermal behaviour seen in soft tissue. Further, the consistency of these materials allowed easy probe insertion and ensured good thermal contact.

Once the system was calibrated, the calibration data was re-examined to determine the accuracy of the probe technique. It was determined that the standard error for the measurement of the thermal conductivity was 3-4%. It was found that the measurement of the thermal diffusivity was more accurate with a standard error lying between 1.3% and 1.7%.

The calibration data was then examined to determine if there was a relationship generated by the system between the two quantities measured. There was no apparent relationship between the thermal conductivity and the thermal diffusivity. However, further analysis revealed a linear relationship between the thermal conductivity and ρc_p, where ρ is the density and c_p is the specific heat capacity of the tissue. This behaviour is considered to dominate when there is only small amount of variation in the thermal conductivity of the samples being examined, as when examining the behaviour of individual tissue types. However, it was found that if there was large variations in the thermal conductivity of the samples being examined, as when examining different tissue types, the behaviour of the tissue will become dominant over the behaviour of the probe. Any relationship seen between the thermal diffusivity or ρc_p and the thermal conductivity over the range of tissues examined will be independent of the probe.

The thermal diffusivity and thermal conductivity of a wide range of human and animal tissues samples were measured using the self heated thermistor technique. In collaboration with a colleague the complex permittivity of the tissue samples was also

measured using a open-ended coaxial probe (Gorton, 1996). Finally, the water content by mass of the tissues was measured by dehydration.

The measured data was first analysed for each of the individual tissue types. When analysing an individual tissue type, no definite relationship could be observed between the thermal conductivity, or thermal diffusivity, and the sample water content. For a single type of tissue there is only a limited range of water content variation. This limited range of water content will produce a restricted range of thermal property values compared to the total range of values seen in biological tissues. Thus for an individual tissue type, the restricted range of values allowed the error associated with the probe, and the error produced by the volume significant for thermal property measurement being different from the volume used to measure the water content, to mask any relationship between the thermal property and the water content. However, when examining the behaviour of the range of tissues studied, there will be a wide range of water content variation, and this limitation will no longer apply.

Fat tissue has the lowest thermal conductivity and thermal diffusivity, which would be expected given that mean water content by mass of fat tissue was measured as 13.4%, with a range of water content values from 5.0% to 33.8%. The thermal conductivity of internal fat from the region around the kidney varied from $k = 0.097$ to 0.201 $Wm^{-1}K^{-1}$, with a mean thermal conductivity of $k = 0.209$ $Wm^{-1}K^{-1}$, while the thermal diffusivity varied from $\alpha = 0.361\times10^{-7}$ to 0.761×10^{-7} m^2s^{-1} with a mean thermal diffusivity of $\alpha = 0.599\times10^{-7}$ m^2s^{-1}. These values are lower than those seen in subcutaneous fat with the range of measured thermal properties being given by $k = 0.152$ - 0.338 $Wm^{-1}K^{-1}$ and $\alpha = 0.572\times10^{-7}$ - 1.070×10^{-7} m^2s^{-1}, and the mean thermal properties being given by $k = 0.244$ $Wm^{-1}K^{-1}$ and $\alpha = 0.839\times10^{-7}$ m^2s^{-1}. Human breast fat was also examined and it was found to its thermal property values varied from $k = 0.171$ to 0.253 $Wm^{-1}K^{-1}$ and from $\alpha = 0.601\times10^{-7}$ to 0.923×10^{-7} m^2s^{-1}, and the mean thermal properties were $k = 0.209$ $Wm^{-1}K^{-1}$ and $\alpha = 0.727\times10^{-7}$ m^2s^{-1}, which are slightly lower values than that seen in subcutaneous animal fat.

As stated above, it proved impossible to define a definite relationship between the thermal conductivity or diffusivity, and water content within a single tissue type, such as fat tissue. However, there was a clear relationship between the thermal diffusivity and

thermal conductivity for fat tissues. This relationship was used to determine the thermal properties of dehydrated fat tissue. The Maxwell mixture equations for the thermal conductivity and thermal diffusivity of fat tissue were combined to produce an equation which was independent of water content. This gave the dehydrated fat thermal conductivity in the range 0.06 - 0.15 $Wm^{-1}K^{-1}$, and dehydrated fat thermal diffusivity in the range 3×10^{-8} - 6×10^{-8} m^2s^{-1}. For animal fat, the mean thermal properties for dehydrated fat were $k = 0.099$ $Wm^{-1}K^{-1}$ and $\alpha = 0.451\times10^{-7}$ m^2s^{-1}.

All the other tissues examined were high water content tissues. Measurements on animal skeletal muscle gave mean thermal properties of $k = 0.497$ $Wm^{-1}K^{-1}$ and $\alpha = 1.306\times10^{-7}$ m^2s^{-1}, and a range of thermal properties of $k = 0.411$ - 0.575 $Wm^{-1}K^{-1}$ and $\alpha = 1.201\times10^{-7}$ - 1.418×10^{-7} m^2s^{-1}. The mean water content by mass was 74.2%, with a range of water content values from 68.6% to 77.0%. Human skeletal muscle had slightly different properties with mean thermal properties given by $k = 0.513$ $Wm^{-1}K^{-1}$ and $\alpha = 1.297\times10^{-7}$ m^2s^{-1} and a range of thermal properties of $k = 0.408$ - 0.590 $Wm^{-1}K^{-1}$ and $\alpha = 1.189\times10^{-7}$ - 1.390×10^{-7} m^2s^{-1}. The mean water content by mass was 77.3%, with a range of water content values from 69.8% to 81.4%. Animal skeletal muscle was found to have a lower water content than human tissues, this possibly being because animal tissues are "hung" and drained of blood to prepare them for human consumption. This lower water content in animal muscle tissues produced a lower thermal conductivity than that for human muscle tissues.

The difference that the draining of blood made to the thermal properties of animal tissues was clearer in liver tissue. Measurements on human liver tissue gave mean thermal properties of $k = 0.510$ $Wm^{-1}K^{-1}$ and $\alpha = 1.302\times10^{-7}$ m^2s^{-1}, and a range of thermal properties of $k = 0.438$ - 0.592 $Wm^{-1}K^{-1}$ and $\alpha = 1.216\times10^{-7}$ - 1.370×10^{-7} m^2s^{-1}. The mean water content by mass was 74.6%, with a range of water content values from 73.3% to 76.8%. Animal liver tissue had a lower mean water content by mass of 67.3%, with a range of water content values from 64.1% to 70.3%. This gave lower mean thermal property values of $k = 0.485$ $Wm^{-1}K^{-1}$ and $\alpha = 1.281\times10^{-7}$ m^2s^{-1} and a lower range of thermal properties of $k = 0.419$ - 0.534 $Wm^{-1}K^{-1}$ and $\alpha = 1.199\times10^{-7}$ - 1.383×10^{-7} m^2s^{-1}.

Surprisingly, the draining of blood did not appear to have a major effect on the thermal properties of animal kidney tissue since the thermal conductivity, thermal diffusivity, and water content of animal tissue was similar to that of human tissue. However, different parts of the kidney did have different properties. Animal kidney medulla tissue had a mean water content of 82%, and a range of water content of 79.5% - 84.2%. This compared to a mean water content of 78.8%, and a range of water content of 73.2% - 83.2% for animal kidney cortex tissue. This gave kidney medulla tissue mean thermal properties of $k = 0.566$ $Wm^{-1}K^{-1}$ and $\alpha = 1.397\times10^{-7}$ m^2s^{-1}, and a range of thermal property values of $k = 0.546$ - 0.587 $Wm^{-1}K^{-1}$ and $\alpha = 1.371\times10^{-7}$ - 1.422×10^{-7} m^2s^{-1}. This compared to mean thermal properties for kidney cortex tissue of $k = 0.535$ $Wm^{-1}K^{-1}$ and $\alpha = 1.363\times10^{-7}$ m^2s^{-1} and a range of thermal properties of $k = 0.487$ - 0.576 $Wm^{-1}K^{-1}$ and $\alpha = 1.273\times10^{-7}$ - 1.467×10^{-7} m^2s^{-1}.

Brain tissue was also found to have different behaviours for different tissue types. Grey brain tissue has a mean water content by mass of 85.7%, and a range of water content of 83.6% - 86.8%. The mean thermal property values were $k = 0.554$ $Wm^{-1}K^{-1}$ and $\alpha = 1.374\times10^{-7}$ m^2s^{-1}, and the range of thermal property values were $k = 0.529$ - 0.574 $Wm^{-1}K^{-1}$ and $\alpha = 1.331\times10^{-7}$ - 1.400×10^{-7} m^2s^{-1}. White brain tissue has a mean water content of 78.7%, and a range of water content of 72.9% - 82.1%. The mean thermal property values were $k = 0.489$ $Wm^{-1}K^{-1}$ and $\alpha = 1.293\times10^{-7}$ m^2s^{-1}, and the range of thermal property values were $k = 0.443$ - 0.550 $Wm^{-1}K^{-1}$ and $\alpha = 1.221\times10^{-7}$ - 1.399×10^{-7} m^2s^{-1}. While grey brain matter had the high thermal properties which would be expected considering its a high water content, white brain matter had a far lower thermal conductivity and thermal diffusivity than would be expected given its water content. White brain matter is different from the other high water content tissues since the majority of its non-water fraction is fat.

Once the properties of individual tissue types were studied, the measured properties were examined across a range of tissue types. First the variation of thermal diffusivity with thermal conductivity was examined for each species type. It was found that there was a linear relationship between ρc_p and the thermal conductivity. Further, it was found that most of the relationships found between the thermal diffusivity and the thermal conductivity for individual tissues were affected by system generated behaviour. The

only tissues for which the α against k behaviour matched that seen over the range of tissues was the pancreas, brain, fat, and human skeletal muscle tissues.

The variation in the thermal properties with water content was then examined using mixture equations. As discussed previously, no definite relationship was discerned between the thermal *conductivity, or diffusivity,* and water content of individual tissues for individual sample measurements. The errors discussed above will also serve to mask any slight variances in the behaviour of a tissue type compared to the behaviour of other tissue types. Thus the mean thermal conductivity, thermal diffusivity and water content of each of the different tissue types were used when examining the variation of the thermal conductivity with water content.

To use mixture equations, the volume fraction of each of the components must be known. However, only the mass fraction of water was measured. In order to determine the volume fraction, the density must be known. However, the density of tissues samples were not measured and so assumptions were made about the density of the sample. One technique assumed the density of the non-water fraction was given by the density of protein. Since the density of water is well known, the density of the tissue could be found. However, the density of the non-water fraction will not be constant and it will vary for different tissue types. The other technique used tables of tissue density values, as provided in texts on ultrasonic imaging. However these tables provide the in-vivo density of tissues which may not accurately describe the density of the tissues examined in the study. Generally, the first method was used to calculate the density in this study.

The thermal conductivity and thermal diffusivity of protein were estimated by curve fitting the liver, kidney and skeletal muscle tissue data, using Maxwell's mixture equation and Bruggeman's equation. It was assumed that the protein density, ρ_p, was 1300 kgm^{-3}. For both the thermal conductivity and thermal diffusivity, the two estimated curves are very similar. However, it was noticeable that the spread in the data for each of the individual tissues was less than the spread of all the data. That is, the measured liver values were roughly distributed about the expected curve, while the thermal properties of the skeletal muscle were generally lower than the values predicted by the curve fits, and those of the kidney tissues were generally higher than the values predicted by the curve fits. This suggested that there was a difference in the thermal conductivity and the thermal diffusivity of the protein present in the different types of tissue.

The thermal properties of the non-water fraction of the main high water content tissues were estimated using Maxwell's mixture equation, and Bruggeman's equation. It was again assumed that $\rho_p = 1300\ \text{kgm}^{-3}$. The difference between the values produced by the equations were far smaller than the differences seen in the tissue, so it was felt sufficient just to use Maxwell's mixture equation to analyse the data.

It was found that different tissues produced different estimates of the thermal properties of the non-water fraction. For animal skeletal muscle tissue, the thermal conductivity of non-water fraction, k_p, was 0.181 $\text{Wm}^{-1}\text{K}^{-1}$, while the thermal diffusivity of non-water fraction, α_p, was $0.822\times10^{-7}\ \text{m}^2\text{s}^{-1}$. For human skeletal muscle the estimated values were similar with $k_p = 0.190\ \text{Wm}^{-1}\text{K}^{-1}$ and $\alpha_p = 0.706\times10^{-7}\ \text{m}^2\text{s}^{-1}$. For animal liver tissue, the estimated thermal properties were $k_p = 0.226\ \text{Wm}^{-1}\text{K}^{-1}$ and $\alpha_p = 0.870\times10^{-7}\ \text{m}^2\text{s}^{-1}$ while for human liver tissue the values were $k_p = 0.217\ \text{Wm}^{-1}\text{K}^{-1}$ and $\alpha_p = 0.795\times10^{-7}\ \text{m}^2\text{s}^{-1}$. Finally, for animal kidney cortex tissue, the estimated thermal properties were $k_p = 0.253\ \text{Wm}^{-1}\text{K}^{-1}$ and $\alpha_p = 0.956\times10^{-7}\ \text{m}^2\text{s}^{-1}$, while for human kidney cortex tissue, the estimated thermal properties were $k_p = 0.257\ \text{Wm}^{-1}\text{K}^{-1}$ and $\alpha_p = 0.808\times10^{-7}\ \text{m}^2\text{s}^{-1}$.

The differing behaviour of the non-water fraction of the different tissue types is clear. The lowest protein thermal conductivity and thermal diffusivity is seen in skeletal muscle tissue. The thermal properties of protein found in liver are higher than in skeletal muscle, while the protein in kidney tissue has the highest thermal conductivity and thermal diffusivity. Examining the difference between human and animal tissues it becomes clear that while the estimates of the thermal properties of protein are very similar, the thermal diffusivity of protein in human tissues is always lower than the thermal diffusivity seen in its animal counterpart.

Given that the protein density affects the estimate of the thermal properties of protein, it is possible that the variation in the protein thermal conductivity and diffusivity seen between the different tissues is partly due the differing protein density. The thermal properties of protein were calculated again using $\rho_p = 1250\ \text{kgm}^{-3}$, $\rho_p = 1350\ \text{kgm}^{-3}$, and using the tissue density values provided by the ultrasonic imaging texts. The difference between the thermal properties calculated for $\rho_p = 1250\ \text{kgm}^{-3}$, and those calculated for $\rho_p = 1350\ \text{kgm}^{-3}$, was insufficient to account for the variation seen between individual tissues. Further, if the variation in the density of protein was affecting the estimated

thermal properties, it would be expected that the thermal conductivity and thermal diffusivity obtained using tissue density tables would be closer in value. However, the difference between the thermal properties of protein for each of the tissues types was similar or greater when estimated using tissue density tables than it was when the density was fixed at $\rho_p = 1300$ kgm^{-3}. This tends to indicate that the difference in the estimated thermal properties of protein between tissues is genuine, rather than a result of a wrong estimate of the protein density.

The thermal properties of the non-water fraction of brain tissue was also estimated. For the non-water fraction of grey brain tissue, the thermal conductivity was 0.225 Wm^{-1}K^{-1}, while the thermal diffusivity was 0.812×10^{-7} m^{2}s^{-1}. However, for white brain matter, the thermal conductivity of the non-water fraction was 0.111 Wm^{-1}K^{-1} while the thermal diffusivity of the non-water fraction was 0.695×10^{-7} m^{2}s^{-1}. This was due to the amount of fat in white brain tissue. Unlike the other high water content tissues, white brain matter has a large amount of fat in its non water fraction. The estimates of the thermal properties of dehydrated fat are significantly lower than the estimates of the thermal properties of protein. This gave the non-water fraction of white brain matter thermal properties far lower than those seen in other high water content tissues.

Finally, the behaviour of the thermal properties of the tissues examined in this study were compared to the dielectric properties at 3 GHz of the same tissues, as measured by a colleague (Gorton, 1996). It is found to be uninformative to compare the thermal and microwave dielectric properties measured on individual samples since both probes measure in different volumes of tissue. Instead, the mean thermal and microwave properties of each of the different tissue types were used when comparing the thermal and dielectric properties.

For dielectric modelling purposes, high water content biological tissue is assumed to consist of physiological saline and protein. Physiological saline has a complex permittivity of $75 - 22j$, while it is assumed that the protein has a complex permittivity of $2.5 - 0.2j$. When the mean dielectric properties of the main high water content tissues were compared to the expected curve produced by Maxwell's mixture equation, the dielectric constant of the tissues lay below the values predicted by Maxwell's mixture equation, while the loss factor of the tissues lie about the values predicted by the Maxwell's mixture equation. This is due to the water bonding to the protein molecules.

A fraction of the water in biological tissues is bonded to the protein molecules, and although bound water is believed to have the thermal properties of free water, it has different and varying microwave dielectric properties. At 3 GHz, the dielectric constant of bound water is much lower than that of free water, but the loss factor of bound water is similar to that of free water.

When the loss factor is compared to the dielectric constant for all the kidney, skeletal muscle, liver, and fat samples examined in this study, it can be seen that while the relationship is approximately linear, each tissue has its own variation from that predicted from the curve fit. This is possibly due to slight variations in properties of the electrolyte present in each of the different types of tissue, or the degree of water bonding. A small change in the ionic profile of the water would not affect the dielectric constant but it would affect the loss factor. Since the loss factor is affected by factors such as the ionic concentration, it is less informative to compare the loss factor to the thermal properties of tissue than it is to compare the dielectric constant to the thermal properties of tissue.

When the thermal properties are compared to the dielectric constant there is a reasonable linear relationship, but with there being noticeable deviation from the mean line by each type of tissue. This can probably be ascribed to the variations in the thermal properties of protein. To examine if this was true, Maxwell's mixture equation was used to estimate what the thermal properties of liver, kidney, and skeletal muscle would be if they had the same protein thermal properties. While there was only modest evidence of a relationship between the measured thermal properties and dielectric constant, there was a far clearer relationship between the estimated thermal property and the dielectric constant. Thus it can be seen that if all the tissues had the same protein thermal properties, there would be a definite relationship between the thermal properties and the dielectric constant of biological tissue.

Finally, for microwave radiometry it is of interest to compare the power attenuation constant against the thermal conductivity. While there is a apparent trend with the higher water content tissues having far higher attenuation constants, there is no definite relationship between the two properties. Since the attenuation constant is dependant on the loss factor as well as the dielectric constant, it is unsurprising, for the reason discussed above, that there is a lack of correlation between the thermal conductivity and the attenuation constant.

References.

Abdul-Razzak, M.M., Hardwick, B.A., Hey-Shipton, G.L., Kester, R.C., Matthews, P.A. and Monson, J.R., "Microwave Thermography for Medical Applications", *IEE Proceedings*, Vol. 134, Pt. A, pp. 171-174, (1987).

al-Alousi, L.M. et al, "A Non-invasive Method for Post-mortem Temperature Measurements using a Microwave Probe", *Forensic Science International*, Vol. 64, pp. 35-46, (1994).

Andrieu, J., Gonnet, E. and Laurent, M., "Pulse Method Applied to Foodstuffs: Thermal Diffusivity Determination", *Food Engineering and Process Applications*, edited by LeMaguer, M. and Jelen. P., Elsevier Applied Science Publishing, London, pp. 103-122, (1986).

Arkin, H., Holmes, K.R. and Chen, M.M., " A Sensitivity Analysis of the Thermal Pulse Decay Method for Measurement of Local Tissue Conductivity and Blood Perfusion", *Journal of Biomechanical Engineering*, Vol. 108, pp. 54-58, (1986a).

Arkin, H., Holmes, K.R., Chen, M.M. and Bottje, W.G., "Thermal Pulse Decay Method for Simultaneous Measurement of Local Thermal Conductivity and Blood Perfusion: A Theoretical Analysis", *Journal of Biomechanical Engineering*, Vol. 108, pp. 208-213, (1986b).

Atkinson, R.E., "Hyperthermia Techniques and Instrumentation", in *Hyperthermia in Cancer Therapy*, edited by Storm, F.K., G.K. Hall Medical Publishers, Boston, Massachusetts, pp. 233-255, (1983).

Baish, J.W., Foster, K.R. and Ayyaswamy, P.S., "Perfused Phantom Models of Microwave Irradiated Tissue", *Journal of Biomechanical Engineering*, Vol. 108, pp. 239-245, (1986).

Balasubramaniam, T.A. and Bowman, H.F., "Temperature Field Due to a Time Dependant Heat Source Of Spherical Geometry in an Infinite Medium", *Journal Of Heat Transfer*, Vol. 96, pp. 296-299, (1974).

Balasubramaniam, T.A. and Bowman, H.F., "Thermal Conductivity and Thermal Diffusivity of Biomaterials: A Simultaneous Measurement Technique", *Journal Of Biomechanical Engineering*, Vol. 99, pp. 148-154, (1977).

Bardati, F. and Tognolatti, P., "Multifrequency Microwave Radiometry Imaging", *Proceedings of IEEE / URSI Conference "Microwaves in Medicine 1993"*, Rome, Oct. 11-14, pp. 217-220, (1993).

Barford, N.C. "Experimental Measurements: Precision Error and Truth", John Wiley and Sons Ltd., 2nd Edition, (1985).

Barrett, A.H., Myers, P.C. and Sadowsky, N.L., "Microwave Thermography in the Detection of Breast Cancer", *American Journal of Roentology*, Vol. 134, pp. 365-368, (1980).

Batchelor, G.K., "Transport Properties of Two-Phase Materials with Random Structures"; *Annual Review of Fluid Mechanics*, Vol. 6, pp. 227-255, (1974).

Bates. O.K., "Thermal Conductivity of Liquids", *Industrial and Engineering Chemistry*, Vol. 28, pp. 494, (1936).

Biology Data Book, edited by Altman, P.L. and Dittmer, D.S., Federation of American Societies for Experimental Biology, Bethesda, Maryland, Second Edition, Vol. 1, pp. 392-398, (1972).

Bligh, J., "Regulation of Body Temperature", in *Heat Transfer in Medicine and Biology*, edited by Shitzer, A. and Eberhart, R.C., Plenum Press, New York, Vol. 1, pp. 15-51, (1985).

Bocquet, B., Mamouni, A., Hochedez, M., Van de Velde, J.C. and Leroy, L., "Visibility of Local Thermal Structures and Temperature Retrieval by Microwave Radiometry", *Electronics Letters*, Vol. 22, pp. 120-122, (1986).

Bocquet, B., Van de Velde, J.C., Mamouni, A., Leroy, Y., Giaux, G., Delannoy, J. and Delvalee, D., "Microwave Radiometric Imaging at 3 GHz for the Exploration of Breast Tumours", *IEEE Transactions on Microwave Theory and Techniques*, Vol. 38, pp. 791-793, (1990).

Boned, C. and Peyrelasse, J., "Some Comments on the Complex Permittivity of Ellipsoids Dispersed in Continuum Media", *Journal of Physics D*, Vol. 16, pp. 1777-1784, (1983).

Böttcher, C.F.J., "The Dielectric Constant of Crystalline Powders", *Recueil des Travaux Chimiques des Pays-Bas*, Vol. 64, pp. 47-51, (1945).

Bowman, H.F., Cravalho, E.G. and Woods, M., "Theory, Measurement and Application of Thermal Properties of Biomaterials", *Annual Review of Biophysics and Bioengineering*, Vol. 4, (1975).

Bowman, H.F., "Heat Transfer and Thermal Dosimetry", *Journal of Microwave Power*, Vol. 16, pp. 121-133, (1981).

Brooks, S.M. and Brooks, N.P, "The Human Body, Structure and Function in Health and Disease", The C.V. Mosby Company, St. Louis, (1980).

Broquetas, A., Romeu, J., Rius, J.M., Elias-Fuste, A.M., Cardama, A. and Jofre, L., "Cylindrical Geometry: A Further Step in Active Tomography", *IEEE Transactions on Microwave Theory and Techniques*, Vol. 39, pp. 836-844, (1991).

Brown, V.J., "Development of Computer Modelling Techniques for Microwave Thermography", Ph.D. Thesis, University of Glasgow, (1989).

Bruer, H., "The Thermal Conductivity of Muscle and Fat", Archiv für die Gesamte Physiologie, Vol. 204, pp. 442-447, (1924); cited in Bowman et al (1975).

Bruggeman, D.A.G., "Berechnung Verschiedener Physikalischer Konstanten von Heterogenen Substanzen", *Annalen der Physik*, Vol. 24, pp. 636-679, (1935).

Bull, H.B. and Breese, K., "Protein Hydration II. Specific Heat of Egg Albumin", *Archives of Biochemistry and Biophysics*, Vol. 128, pp. 497-502, (1968).

Camart, J.C., Despretz, D., Chive, M. and Pritbetich, J., "Modelling of Various Kinds of Applicators Used for Microwave Hyperthermia Based on the FDTD Method, "*IEEE Transactions on Microwave Theory and Techniques*", Vol. 44, pp. 1287-1298, (1996).

Caorsi, S. and Gragnani, G.L, "Thermal Distribution Simulation by Using a Multifrequency Digital Radiometer", *Proceedings of IEEE/URSI Conference "Microwaves in Medicine 1993"*, Rome, Oct. 11-14, pp. 217-220, (1993).

Carslaw, H.S. and Jaeger, J.C., "Conduction of Heat in Solids", Oxford University Press, (1947).

Cetas, T.C., "Temperature Measurement" in *Heat Transfer in Medicine and Biology*, edited by Shitzer, A. and Eberhart, R.C., Plenum Press, New York, Vol. 2, pp. 373-392, (1985).

Chandrasekhar, S., "An Introduction to the Study of Stellar Structure", Dover Publications, New York, (1957).

Chandrasekhar, S., "Radiative Transfer", Clarendon Press, Oxford, (1950).

Chato, J.C., "A Method of the Measurement of the Thermal Properties of Biological Materials", *Thermal Problems in Biotechnology*, ASME, New York, pp. 16-25, (1968).

Chen, M.M. and Holmes, K.R., "Microvascular Contributions in Tissue Heat Transfer", *Annals of the New York Academy of Sciences*, Vol. 335, pp 133-150, (1980).

Cherneeva, L.I., "Study of the Thermal Properties of Foodstuffs", Report of VKIKHI, Gostorgisdat, Moscow, USSR, (1956); cited in Duck (1990).

Chiew, Y.C. and Glandt, E.D., "The Effect of Structure on the Conductivity of a Dispersion", *Journal of Colloid and Interface Science*, Vol. 94, pp. 90-104, (1983).

Choi, Y. and Okos, M.R., "Effects of Temperature and Composition on the Thermal Properties of Food" in *Food Engineering and Process Applications*, edited by Le Maguer, M. and Jelen P., Elsevier Applied Science Publishers, Vol. 1, pp. 93-101, (1986).

Christensen, D.A., "Thermometry and Thermography", in *Hyperthermia in Cancer Therapy*, edited by Storm, F.K., G.K. Hall Medical Publishers, Boston, Massachusetts, pp. 223-232, (1983).

Colin, J. and Houdas, Y., "Experimental Determination of Coefficient of Heat Exchanges by Convection of Human Body", *Journal of Applied Physiology*, Vol. 22, pp. 31-38, (1967).

Conway, J., Hawley, M.S., Seagar, A.D., Brown, B.H and Barber, D.C., "Applied Potential Tomography (APT) for Noninvasive Thermal Imaging During Hyperthermia Treatment", *Electronics Letters*, Vol. 21, pp. 836-838, (1985).

Cooper, T.E. and Trezek, G.J., "Correlation of Thermal Properties of Some Human Tissue with Water Content", *Aerospace Medicine*, Vol. 42, pp. 24-27, (1971).

Cooper, T.E. and Trezek, G.J., "A Probe Technique for Determining the Thermal Conductivity of Tissue", *Journal of Heat Transfer*, Vol. 94, pp. 133-140, (1972)

Cornillion, P., Andrieu, J., Duplan, J.-C. and Laurent, M., "Use of Nuclear Magnetic Resonance to Model Thermophysical Properties of Frozen and Unfrozen Model Food Gels", *Journal of Food Engineering*, Vol. 25, pp. 1-19, (1995).

CRC Handbook of Chemistry and Physics, 74th edition, CRC Press, Boca Raton, Florida, (1993).

Croft D.R and Lilley, D.G., "Heat Transfer Calculations Using Finite Difference Equations.", Applied Science Publishers Ltd., London, (1977).

Cui, Z.F. and Barbenel, J.C., "The Influence of Model Parameter Values on the Prediction of Skin Surface Temperature: II. Contact Problems", *Physics in Medicine and Biology*, Vol. 36, pp. 1607-1620, (1991).

Derksen, W.L., Murtha, T.D. and Monahan, T.I., "Thermal Conductivity and Diathermancy of Human Skin for Sources of Intense Thermal Radiation Employed in Flash Burn Studies", *Journal of Applied Physiology*, Vol. 11, pp. 205-210, (1957).

Draper, J.W. and Boag, J.W., "The Calculation of Skin Temperature Distributions in Thermography", *Physics and Medicine in Biology*, Vol. 16, pp. 201-211, (1971).

Duck, F.A., "Physical Properties of Tissue", Academic Press, London (1990).

Dukhin, S.S., "Dielectric Properties of Disperse Systems", *Surface and Colloid Science*, Vol. 3, pp. 83-165, (1971).

Einstein, A., "Eine Neue Bestimmungder Molekül-dimensionen", *Annalen der Physik*, Vol. 19, pp. 289, (1906).

Enander, B. and Larson, G., "Microwave Radiometric Measurements of the Temperature Inside a Body", *Electronics Letters*, Vol. 10, pp. 317, (1974).

Enel, L., Leroy, Y., Van de Velde, J.C. and Mamouni, A., "Improved Recognition of Thermal Structures by Microwave Radiometry", *Electronics Letters*, Vol. 20, pp. 293-294, (1984).

European Society for Hyperthermic Oncology Task Group, "Treatment Planning and Modelling in Hyperthermia", *Tor Vergata Medical Physics Monographs*, Rome, (1992).

Foster, K.R. and Cheever, E.A., "Microwave Radiometry in Biomedicine: A Reappraisal", *Bioelectromagnetics*, Vol. 13, pp. 567-579, (1992).

Foster, K.R, Cheever, E., Leonard, J.B. and Blum, F.D., "Transport Properties of Polymer Solutions", *Biophysics Journal*, Vol. 45, pp. 975-984, (1984).

Fraser, S.M., Land, D.V. and Sturrock, R.D., "Microwave Thermography in Rheumatic Disease", *Engineering in Medicine*, Vol. 16, pp. 209-212, (1987).

Fricke, H., "The Mathematical Treatment of the Electric Conductivity and Capacity of Disperse Systems", *Physical Review*, Vol. 24, pp. 575-587, (1924).

Fricke, H., "The Electrical Capacity of Suspensions of Red Corpuscles of a Dog", *Physical Review*, Vol. 25, pp. 682-687, (1925).

Fricke, H. and Morse, S., "An Experimental Study of the Electrical Conductivity of Disperse Systems. 1. Cream", *Physical Review*, Vol. 25, pp. 361-367, (1925).

Gagge, A.P., Stolwijk, J.A.J. and Hardy, J.D., "A Novel Approach to Measurement of Man's Heat Exchanges with a Complex Radiant Environment", *Journal of Aerospace Medicine*, Vol. 36, pp. 431-435, (1965).

Gauthrie, M., Edrich, J., Zimmer, R., Guerguin-Kern, J.L and Robert, J., "Millimetre-wave Thermography - Application to Breast Cancer", *Journal of Microwave Power*, Vol. 14, pp 123-129, (1979).

Geigy Scientific Tables, 7th Edition, JR Geigy S.A., Basle, Switzerland, (1970)

Gibbs, F.A., "A Thermoelectric Blood Flow Recorder in the Form of a Needle", *Proceedings of the Society for Experimental Biology and Medicine*, Vol. 31, pp. 141-146, (1933).

Giese, A.C., "Cell Physiology", W.B. Saunders Company, Philadelphia, (1979).

Gordon, R.G., Roemer, R.B. and Horvath, S.M., " A Mathematical Model of the Human Temperature Regulatory System - Transient Cold Exposure Response", *IEEE Transactions on Biomedical Engineering*, Vol. 23, pp 434-444, (1976).

Gorton, A.J., "Measurements and Analysis of the Microwave Dielectric Properties of Human and Animal Tissues", Ph.D. Thesis, University of Glasgow, (1996).

Grayson, J., Coulson, R.L. and Winchester, B., "Internal Calorimetry - Assessment of Myocardial Blood Flow and Heat Production", Vol. 30, pp. 251-257, (1971).

Hale, D.K., "The Physical Properties of Composite Materials", *Journal of Materials Science*, Vol. 11, pp. 2105-2141, (1976).

Hamamoto, K., Andreas, B., Shiina, T. and Ito, M., "Basic Investigation on Reflection Mode Ultrasonic Attenuation Tomography", *Japanese Journal of Applied Physics*, Vol. 34, Pt. 1, pp. 2812- 2816, (1995).

Hampton, W.F. and Mennie, J.H., "Heat Capacity Measurements on Gelatin Gels", *Canadian Journal of Research*, Vol. 10, pp. 452-462, (1934).

Hanai, T. and Koizumi, N., "Dielectric Relaxation of W/O Emulsions in Particular Reference to Theories of Interfacial Polarization", *Bulletin of the Institute of Chemical Research, Kyoto University*, Vol. 53, pp. 153-160, (1975).

Hand, J.W., "The Current Status of Microwave Induced Hyperthermia and Radiotherapy for the Treatment of Recurrent Breast Cancer", in *IEE Colloquium "The Application of Microwaves in Medicine"*, Digest No: 1995/041, (1995).

Hand, J.W., Ledda, J.L. and Evans, N.T.S., "Temperature Distribution in Tissues Subjected to Local Hyperthermia by RF Induction Heating", *British Journal of Cancer*, Vol. 45, Suppl. V, pp. 31-35, (1982).

Hand, J.W. and James, J.R., "Physical Techniques in Clinical Hyperthermia", Research Studies Press, Letchworth, pp. 1-64, (1986).

Hansen, W.P., Greenwald, R.J. and Bowman, H.F., "Applications of the CO_2 Laser to Thermal Properties Measurements in Biomaterials", *Journal of Engineering Materials and Technology*, Vol. 95, pp. 138-141, (1974).

Hardy, J.D. and Soderstrom, G.F., "Heat Loss from the Nude Body and Peripheral Blood Flow at 22-35°C", *Journal of Nutrition*, Vol. 16, pp. 493-509, (1938).

Harness, P.C. and Land, D.V., "Finite Element Analysis of Microwave Thermographic Images", *Royal Photographic Society Conference on "The Thermal Image"*, Bath, 11-12 October, (1994).

Harris, R.A., Follett, D.H., Halliwell, M. and Wells, P.N.T., "Ultimate Limits in Ultrasonic Imaging Resolution", *Ultrasound in Medicine and Biology*, Vol. 17, pp. 547-558, (1991).

Harvey, A.F., "Microwave Engineering", Academic Press, p780-781, (1963).

Hashin, Z. and Shtrikman, S., "Note on the Effective Constants of Composite Materials", *Journal of the Franklin Institute*, Vol. 271, pp. 423-426, (1961).

Hatfield, H.S. and Pugh, L.G.C., "Thermal Conductivity of Human Fat and Muscle", *Nature*, Vol. 168, pp. 918-919, (1951).

Hatfield, H.S., "Measurement of the Thermal Conductivity of Animal Tissue", *Journal of Physiology*, Vol. 120, pp. 35P-38P, (1953).

Hayes, L.J. and Valvano, J.W., "Steady-State Analysis of Self-Heated Thermistors Using Finite Elements", *Journal of Biomechanical Engineering*, Vol. 107, pp. 77-80, (1985).

Henriques, F.C. and Moritz, A.R., "Studies of Thermal Injury I. The Conduction of Heat to and Through skin and the Temperatures Attained Therein. A Theoretical and an Experimental Investigation", *American Journal of Pathology*, Vol. 23, pp. 531-549, (1947).

Hill, J.E., Leitman, J.D. and Sunderland, J.E., "Thermal Conductivity of Various Meats", *Food Technology*, Vol. 21, pp. 1143-1148, (1967).

Jain, R.E., "Bioheat Transfer: Mathematical Models of Thermal Systems", in *Hyperthermia in Cancer Therapy*, edited by Storm, F.K., G.K. Hall Medical Publishers, Boston, Massachusetts, pp. 9-46, (1983).

Jofre, L., Hawley, M.S., Broquetas, A., De Los Reyes, E., Ferrando, M. and Elias-Fuste, A.R., "Medical Imaging with a Microwave Tomographic Scanner", *IEEE Transactions on Biomedical Engineering*, Vol. 37, pp. 303-312, (1990).

Johnson, R.H., Preece, A.W. and Green, J.L., "Capabilities and Limitations of Electromagnetic Hyperthermia Applicators", in *IEE Colloquium "The Application of Microwaves in Medicine"*, Digest No: 1995/041, (1995).

Jones, C.H., "Methods of Breast Imaging", *Physics in Medicine and Biology*, Vol. 27, pp. 463-499, (1982).

Jones, C.H., "Medical Thermography", *IEE Proceedings*, Vol. 134, Pt. A, No. 2, pp. 225-236, (1987).

Kelso, M.B., "A Study of the Use of Combined Thermal and Microwave Modelling of Body Regions for Microwave Thermography", Ph.D. Thesis, University of Glasgow, (1995).

Kent, M., Christiansen, K., van Hanegham, I.A. et al, "Cost 90 Collaborative Measurements of Thermal Properties of Food", *Journal of Food Engineering*, Vol. 3, pp. 117-150, (1984).

Kong, J.-Y., Miyawaki, O., Nakamura, K. and Yano, T., "The Intrinsic Thermal Conductivity of Some Wet Proteins in Relation to Their Hydrophobicity: Analysis on Gelatin Gel", *Agricultural and Biological Science*, Vol. 46, pp. 783-788, (1982a).

Kong, J.-Y., Miyawaki, O., Nakamura, K. and Yano, T., "The Intrinsic Thermal Conductivity of Some Wet Proteins in Relation to Their Hydrophobicity: Analyses on Gels of Egg-albumin, Wheat Gluten and Milk Casein", *Agricultural and Biological Science*, Vol. 46, pp. 789-794, (1982b).

Kulios, M.C., Sherar, M.D. and Hunt, M.J., " Large Blood Vessel Cooling in Heated Tissues - A Numerical Study", *Physics in Medicine and Biology*, Vol. 40, pp. 477-494, (1995).

Kvadsheim, P.H., Folkow, L.P. and Blix, S.P., "Thermal Conductivity of Minke Whale Blubber", *Journal of Thermal Biology*, Vol. 21, pp. 123-128, (1996).

Lagendijk, J.J.W., "The Influence of Bloodflow in Large Vessels on the Temperature Distribution in Hyperthermia", *Physics in Medicine and Biology*, Vol. 27., pp 17-23, (1982).

Land, D.V., "Radiometer Receivers for Microwave Thermography", *Microwave Journal*, Vol. 26, pp. 196-201, (1983)

Land, D.V., "Measurement of Radio Frequency and Microwave Fields by Nonresonant Perturbation", *IEE Proceedings*, Vol. 131, Pt. H, pp. 1-8, (1984).

Land, D.V., "Application of the Nonresonant Perturbation Technique to the Measurement of High-Frequency Fields in Biological Phantom Materials", *Electronics Letters*, Vol. 24, pp. 70-71, (1988).

Land, D.V., "Simplified Nonresonant Perturbation Method of Measuring Aspects of Performance of UHF and Microwave Antenna for Biomedical Applications", *Electronics Letters*, Vol. 28, pp. 1190-1192, (1992).

Land, D.V., "Medical microwave radiometry and its clinical applications", in *IEE Colloquium "The Application of Microwaves in Medicine"*, Digest No: 1995/041, (1995).

Landau, L.D. and Lifshitz, E.M., "Electrodynamics of Continuous Media", Pergamon Press, London, (1960).

Lapshin, A., "Heat and Temperature Conduction of Raw Fat Material and Molten Fat", *Myasnaya Industriya S.S.S.R.*, Vol. 25., pp. 55-56, (1954); cited in Duck (1990).

Levy, L., Graichen, H., Stolwijk, J.A.J and Calabresi, M., "Evaluation of the Local Tissue Blood Flow by Continuous Direct Measurement of Thermal Conductivity", *Journal of Applied Physiology*, Vol. 22, pp. 1026-1029, (1967).

Lewin, L., "The Electrical Constants of a Material Loaded with Spherical Particles" *Journal of the Institute of Electrical Engineers*, Vol. 94, pp. 65-68, (1947).

Liang, X.G., Ge, X.S., Zhang, Y.P. and Wang, G.J., "A Convenient Method of Measuring the Thermal Conductivity of Biological Tissue", *Physics in Medicine and Biology*, Vol. 36, pp. 1599-1605, (1991).

Lichtenecker, K, "Mischköropertheorie als Wahrscheinlichkeits-problem", *Physikalische Zeitschrift*, Vol. 30, pp. 805-809, (1929).

Lipkin, M., and Hardy, J.D., "Measurement of Some Thermal Properties of Human Tissue", *Journal of Applied Physiology*, Vol. 7, pp. 212-217, (1954).

Lipton, J.M., "Thermoregulation in Pathological States" in *Heat Transfer in Medicine and Biology*, edited by Shitzer, A. and Eberhart, R.C., Plenum Press, New York, Vol. 1, pp. 79- 105, (1985).

Looyenga, H, "Dielectric Constants of Heterogeneous Mixtures", *Physica*, Vol. 31, pp. 401-406, (1965).

Lowry, O.H., "Extracellular material in animal tissues", *Biol. Symp*, Vol. 10, pp. 239, (1943).

MacDonald, A.G., Land, D.V. and Sturrock, R.D., "Microwave Thermography as a Noninvasive Assessment of Disease Activity in Inflammatory Arthritis", *Clinical Rhuematology*, Vol. 13, pp. 589-592, (1994).

Mamouni, A., Leroy, Y., Van de Velde, J.C. and Bellarbi, L., "Introduction to Correlation Microwave Thermography', *Journal of Microwave Power*, Vol. 18, pp. 285-293, (1983).

Mamouni, A., Leroy, Y., Bocquet, B., Van de Velde, J.C. and Gelin, P., "Computation of Near-Field Microwave Radiometric Signals: Definition and Experimental Verification", *IEEE Transactions on Microwave Theory and Techniques*, Vol. 39, pp. 124-132, (1991).

Marr, C.M., "Microwave Thermography: a Non-invasive Technique for Investigation of Injury of the Superficial Digital Flexor Tendon in the Horse", *Equine Veterinary Journal*, Vol. 24, pp. 269-273, (1992).

Martin, J., Broquetas, A. and Jofre, L., "Dynamic Active Microwave Thermography Applied to Hyperthermia Monitoring", *Journal of Photographic Science*, Vol. 39, pp. 146-148, (1991).

Maxwell, J.C., "A Treatise on Electricity and Magnetism", Claredon Press, London, (1881).

Miles, C.A., Van Beek, G. and Veerkamp, C.H., "Calculation of the Thermophysical Properties of Food" in *Physical Properties of Food*, edited by Jowitt, R., Escher, F., Hallström, B., Meffert, H.F.Th., Spiess, W.E.L. and Vos, G., Applied Science Publishers, London, (1983).

Mimi, M., "An Investigation of Radiometer and Antenna Properties for Microwave Thermography", Ph.D. Thesis, University of Glasgow, (1990).

Miner, C.S. and Dalton, N.N., "Glycerol", Reinhold Publishing Corporation, New York, (1953).

Miyawaki, O., Abe, T. and Yano, T., "Theoretical Model for Freezing of Food Gels with Temperature depending on the Fraction of Frozen Water", *Agricultural and Biological Chemistry*, Vol. 52, pp. 2995-3000, (1988).

Miyawaki, O. and Pongsawatmanit, R., "Mathematical Analysis of the Effective Thermal Conductivity of Food Materials in the Frozen State", *Bioscience Biotechnology and Biochemistry*, Vol. 58, pp. 1222-1225, (1994).

Morley, M.J., "Thermal Conductivities of Muscles, Fat and Bones", *Journal of Food Technology*, Vol. 1, pp. 303-311, (1966).

Moskowitz, M., Milbrath, J., Gartside, P., Zermeno, A. and Mandel, D., "Lack of Efficacy of Thermography as a Screening Tool for Minimal and Stage 1 Breast Cancer", *The New England Journal of Medicine*, Vol. 295, pp. 249-252, (1976).

Moskowitz, M.J., Paulsen, K.D., Ryan, T.P. and Pang, D, "Temperature Field Estimation Using Electrical Impedance Profiling Methods", *International Journal of Hyperthermia*, Vol. 10, pp. 229-245, (1994).

Parker, D.L., "Applications of NMR Imaging in Hyperthermia: An Evaluation of the Potential for Localised Tissue Heating and Noninvasive Temperature Monitoring", *IEEE Transactions on Biomedical Engineering*, Vol. 31, pp. 161-167, (1984).

Patel, P.A., Valvano, J.W., Pearce, J.A., Prahl, S.A. and Denham C.R., "A Self-Heated Thermistor Technique to Measure Effective Thermal Properties from the Tissue Surface", *Journal of Biomechanical Engineering*, Vol. 109, (1987)

Pennes, H.H., "Analysis of Tissue and Arterial Blood Temperatures in the Resting Human Forearm", *Journal of Applied Physiology*, Vol. 1, pp. 93-122, (1948).

Pichot, C., Jofre, L., Peronnet, G. and Bolomey, J.C., "Active Microwave Imaging of Inhomogenous Bodies", *IEEE Transactions on Antennas and Propagation*, Vol. 33, pp. 416-425, (1985).

Polder, D. and Van Santen, J.H., "The Effective Permeability of Mixtures of Solids", *Physica*, Vol. 12, pp. 257-271, (1946).

Pongsawatmanit, R., Miyawaki, O. and Yano, T., "Measurement of the Thermal Conductivity of Unfrozen and Frozen Food Materials by a Steady State Method with Coaxial Dual-cylinder Apparatus", *Bioscience Biotechnology and Biochemistry*, Vol. 57, pp. 1072-1076, (1993).

Poppendiek, H.F., Randall, R., Breeden, J.A., Chambers, J.E. and Murhy J.R., "Thermal Conductivity Measurements and Predictions for Biological Fluids and Tissues", *Crybiology*, Vol. 3, pp. 318-327, (1966).

Ramo, S., Whinnery, J.R. and Van Duzer, T., "Fields and Waves in Communication Electronics", John Wiley and Sons Inc., New York, (1965).

Rastorguev, Y.L. and Ganiev, Y.A., "Thermal Conductivity of Aqueous Solutions of Organic Liquids", *Russian Journal of Physical Chemistry*, Vol. 40, pp. 869-871, (1966).

Rayleigh, Lord, "On the Influence of Obstacles Arranged in Rectangular Order Upon the Properties of a Medium", *Philosophical Magazine*, Vol. 34, pp. 481, (1892).

Renaud , T., Briery, P., Andrieu, J. and Laurent, M., "Thermal Properties of Model Foods in the Frozen State", *Journal of Food Engineering*, Vol. 15, pp 83-97, (1992).

Rice, C.W., "Free and Forced Convection of Heat from Bodies of Simple Shape in Gases and Liquids", *International Critical Tables*, Vol. 5, pp. 234-236, (1926).

Riedel, L, "Wärmeleitfähigkeitsmessungen an Mischungen Verschiedener Organischer Verbindungen mit Wasser", *Chemie-Ingenieur-Technik*, Vol. 19, pp. 465-469, (1951).

Ring, E.F.J., "Quantitative Thermal Imaging", *Clinical Physics and Physiological Measurement*, Vol. 11, Suppl. A, pp. 87-95, (1990).

Ring, E.F.J., "The Historical Development of Temperature Measurement in Western Europe", *Biomedical Thermology*, Vol. 13, No. 4, pp. 83-97, (1993).

Ring, E.F.J., "Quantitative Thermal Imaging in Rheumatology", *Biomedical Thermology*, Vol. 15, No. 2, pp. 69-71, (1995).

Rose, J.L, and Goldberg, B.B., "Basic Physics in Diagnostic Ultrasound", Wiley, New York, (1979).

Runge, I., "Zur elektrischen Leitfahigkeit Metallischer Aggregate", *Zeitschrift Fur Technische Physik*, Vol. 6, pp. 61-68, (1925).

Sakiyama, T., Han, S., Torii, A., Mikawaki, O. and Yano, T., "Intrinsic Thermal Conductivity Estimated Independently of Heat Conduction Models", *Agricultural and Biological Science*, Vol. 55, pp. 487-492, (1991).

Schawb, (1988) cited in European Society for Hyperthermic Oncology Task Group (1992).

Schawn, H.P., "Electrical Properties of Bound Water", *Annals of the New York Academy of Science*, Vol. 125, pp. 344-354, (1965).

Schepps, J.L. and Foster, K.R. "The UHF and Microwave Dielectric Properties of Normal and Tumour Tissues: Variation on the Dielectric Properties with Tissue Water Content", *Physics in Medicine and Biology*, Vol. 25, pp. 1149, (1980).

Shitzer, A. and Eberhart, C., "Heat Transfer in Medicine and Biology", Plenum Press, New York, Vol. 1, pp. 137-152, (1985).

Storm, F.K., "Hyperthermia in Cancer Therapy", G.K. Hall Medical Publishers, Boston, Massachusetts, (1983).

Straube, W.L. and Arthur, R.M., "Theoretical Estimation of the Temperature Dependence of Backscattered Ultrasonic Power for Noninvasive Thermometry", *Ultrasound in Medicine and Biology*, Vol. 20, pp. 915-922, (1994).

Strobhehn, J.W. and Mechling, J.A., "Interstitial Techniques for Clinical Hyperthermia", in *Physical Techniques in Clinical Hyperthermia*, edited by Hand, J.W. and James, J.R., Research Studies Press, Letchworth, pp. 210-287, (1986).

Swindell, W., "Ultrasonic Hyperthermia", in *Physical Techniques in Clinical Hyperthermia*, edited by Hand, J.W. and James, J.R., Research Studies Press, Letchworth, pp. 288-326, (1986).

Tanasawa, I. and Katsuda, T., *Siesan Kenyku*, Vol. 24, pp. 440-443, (1972); cited in Bowman et al (1975).

Taylor, G.I., "Viscosity of a Fluid Containing Small Drops of Another Fluid", *Proceedings of the Royal Society of London Series A*, Vol. 138, pp. 41, (1932).

Touloukian, Y.S., Liley, P.E. and Saxena, S.C., "The Thermophysical Properties of Matter: The TPRC Data Series", Vol. 3, (1970a).

Touloukian, Y.S., Powell, R.W., Ho, C.Y. and Nicolaou, M.C., "The Thermophysical Properties of Matter: The TPRC Data Series", Vol. 10, (1970b).

Touloukian, Y.S. and Makita, T., "The Thermophysical Properties of Matter: The TPRC Data Series", Vol. 6, (1970).

Turner, J.C.R, "Two Phase Conductivity: The Electrical Conductance of Liquid-Fluidized Beds of Spheres" *Chemical Engineering Science*, Vol. 31, pp. 487-492, (1976).

Valvano, J.W., Allen, J.T. and Bowman, H.F., "The Simultaneous Measurement of Thermal Conductivity, Thermal Diffusivity, and Perfusion in Small Volumes of Tissue", *Journal of Biomechanical Engineering*, Vol. 106, pp. 192-197, (1984).

Valvano, J.W., Cochran, J.R. and Diller, K.R., "Thermal Conductivity and Diffusivity of Biomaterials Measured with Self-Heated Thermistors", *International Journal Of Thermophysics*, Vol. 6, pp. 301-311, (1985).

Velick, S. and Gorin, M., "The Electrical Conductance of Suspensions of Ellipsoids and its Relation to the Study of Avian Erythrocytes", *Journal of General Physiology*, Vol. 23, pp. 753-771, (1940).

Vendrick, A.J.H and Vos, J.J., "A Method for the Measurement of the Thermal Conductivity of Human Skin", *Journal of Applied Physiology*, Vol. 11, pp. 211-215, (1957).

Wagner, K.W, "Erklarung der Dielektrischen Nachwirkungsvorgange auf Grund Maxwellscher Vortstellungen, *Archiv Electrotechnik*, Vol. 2, pp. 371, (1914).

Weinbaum, S., Jiji, L.M. and Lemons, D.E., "Theory and Experiment for the Effect of Vascular Microstructure on Surface Tissue Heat Transfer - Part 1: Anatomical Foundation and Model Conceptualisation", *Journal of Biomedical Engineering*, Vol. 106, pp. 321-320, (1984).

Weinbaum, S. and Jiji, L.M., "A New Simplified Bioheat Equation for the Effect of Blood Flow on Local Tissue Temperature", *Journal of Biomechanical Engineering*, Vol. 107, pp. 131-139, (1985).

Wiener, O., "Herkunft und Stellung der Aufgabe", *Abhandleinger Sachsischen Akademie Wissensehaften Math-Phys. Kl*, Vol. 32, pp. 509-604, (1912).

Wissler, E.H, "Comments on Weinbaum and Jiji's Discussion of Their Proposed Bioheat Equation", *Journal of Biomechanical Engineering*, Vol. 109, pp. 355-356, (1987).

Wulff, W., "The Energy Conservation Equation for Living Tissue", *IEEE Transactions on Biomedical Engineering*, Vol. 21, pp. 494-495, (1974).